

# **Protein-Polysaccharide Conjugates as Food Emulsifiers and Steric Stabilizers**

**Thesis**

Rui Ding

Submitted in accordance with the requirements for the degree of  
Doctor of Philosophy

The University of Leeds  
School of Food Science and Nutrition

September 2018

The candidate confirms that the work submitted is his own, except where work which has formed part of jointly authored publications has been included. The contribution of the candidate and the other authors to this work has been explicitly indicated below. The candidate confirms that appropriate credit has been given within the thesis where reference has been made to the work of others.

The work in Chapter 1 of the thesis has appeared in publication as follows:

Covalently cross-linked proteins & polysaccharides: Formation, characterisation and potential applications, 2017, Akhtar, M. & Ding, R.

I was responsible for Introduction, Preparation of protein-polysaccharide conjugates, Characterisation of protein-polysaccharide conjugates, and Functional properties of protein-polysaccharide conjugates.

The contribution of the other author was Title, Abstract, Site-specific conjugates, Conclusion, Acknowledgements, and References. Moreover, the other author contributed valuable comments on other parts of this review paper.

The work in Chapter 4 of the thesis has appeared in publication as follows:

Insignificant impact of the presence of lactose impurity on formation, 2017, Ding, R., Volicka, E., Akhtar, M., and Ettelaie, R.

I was responsible for Introduction, Materials and methods, Results and discussion (3.1-3.3), Conclusion, and References.

The contribution of the other authors was Title, Abstract, Results and discussion (3.4), and Acknowledgements.

This copy has been supplied on the understanding that it is copyright material and that no quotation from the thesis may be published without proper acknowledgement.

© 2018 The University of Leeds and Rui Ding

## **Acknowledgements**

I would love to acknowledge colleagues from University of Leeds (UK) and Zhejiang Gongshang University (China) and my family for their encouragement and support for the past four years. First of all, I acknowledge my primary supervisor Dr. Rammile Ettelaie who introduced me into the field of food colloids. Moreover, he guided me through the whole PhD stages from research plan to the final thesis. I learnt essential research philosophy and theoretical calculations in detail from him. He is always supportive and encouraging to me to challenge difficulties in experiments and theories. Secondly, I would like to acknowledge my secondary supervisor Dr. Mahmood Akhtar. He had a great influence on me through discussing experiments and valuable research suggestions. I had an enjoyable experience with him in my project and learnt various analytical techniques and experimental designs. I also thank all of the professors and MSc students from School of Food Biotechnology and Science, Zhejiang Gongshang University, Hangzhou, China. They offered me a precious opportunity to conduct part of my 2<sup>nd</sup>-year research in their brand new laboratory. I, especially wish to thank Professor Jianshe Chen from Zhejiang Gongshang University, previously in School of Food Science and Nutrition, University of Leeds, who provided me with many stimulating ideas and constructive suggestions during my exchange visit to China. Additionally, I appreciate all technical supports from technicians and PhD students in both University of Leeds and Zhejiang Gongshang University. Finally, I would like to take this opportunity to thank my wife Yu Gu, daughter Jiayin (Esther) Ding and son Jiaxin (Paul) Ding for being extremely patient with me when I was fully involved in the research. Last but not the least, I am

grateful to my parents and parents-in-law for their unconditional love and care while I have been far away from China.

## Publications from thesis

**Ding, R.**, Volicka, E., Akhtar, M., & Ettelaie, R. (2017). Insignificant impact of the presence of lactose impurity on formation and colloid stabilising properties of whey protein–maltodextrin conjugates prepared via Maillard reactions. *Food Structure*, 43-53. doi:10.1016/j.foostr.2017.02.004

Akhtar, M., & **Ding, R.** (2017). Covalently cross-linked proteins & polysaccharides: Formation, characterisation and potential applications. *Current Opinion in Colloid & Interface Science*, 28, 31-36. doi:10.1016/j.cocis.2017.01.002

Manuscripts in progress:

**Ding, R.**, Ettelaie, R., Akhtar, M., & Chen, J. (2018). Competitive adsorption and stabilizing properties of WPI and WPI-MD19 conjugates on oil-water interface. *Colloids and Surfaces B: Biointerfaces*, in progress.

**Ding, R.**, Akhtar, M., & Ettelaie, R. (2018). A Novel preparation method of protein-polysaccharide conjugates by Spinning Disc Reactor (SDR). *Colloids and Surfaces A: Physicochemical and Engineering Aspects*, in progress.

## Accepted conference abstracts

- Ding, R.**, Akhtar, M., & Ettelaie, R. Stabilising properties of whey protein covalently bonded with lactose via the Maillard reactions. *The 2<sup>nd</sup> Annual Food Science & Nutrition PhD Conference* – University of Leeds, Leeds, UK, November 16, 2015
- Ding, R.**, Volicka, E., Akhtar, M., Ettelaie, R., & Chen, J. Influence of the presence of lactose and unconjugated whey protein isolate impurity on colloidal stabilising properties of whey protein isolate – maltodextrin conjugates prepared via the Maillard reactions. *The 16<sup>th</sup> Food Colloids Conference* – University of Wageningen, Wageningen, the Netherlands, April 10-13, 2016
- Ding, R.**, Akhtar, M., Ettelaie, R., & Chen, J. Competitive adsorption to oil-water interface between WPI and WPI-MD19 conjugates. *The 4<sup>th</sup> Annual Food Science & Nutrition PhD Conference* – University of Leeds, Leeds, UK, November 22, 2017
- Ding, R.**, Akhtar, M., Ettelaie, R., & Chen, J. Competitive adsorption to oil-water interface between WPI and WPI-MD19 conjugates. *The 2<sup>nd</sup> Physics in Food Manufacturing Conference* – University of Edinburgh, Edinburgh, UK, January 10-11, 2018
- Ding, R.**, Akhtar, M., Ettelaie, R., & Chen, J. Protein-polysaccharide conjugates as food emulsifiers and stabilizers in emulsion systems. *The 17<sup>th</sup> Food Colloids Conference* – University of Leeds, Leeds, UK, April 8-11, 2018

## **Abstract**

Protein-based emulsifiers and stabilizers are important in food colloids. The potential of protein-polysaccharide conjugates prepared through the Maillard reaction as food emulsifiers and stabilizers has been well established and reported in the literature. In this work, following a review of previous studies, a preliminary investigation on the conjugates between whey protein isolate (WPI) and maltodextrins (MD) was conducted. The conjugates were prepared through two methods: dry-heating approach and wet-heating method, using the Spinning Disc Reactor (SDR), and their performance compared. The formation of these conjugates was confirmed by the spectrophotometric technique. Furthermore, the physicochemical properties of conjugates such as solubility, emulsifying activity and stability in oil-in-water system were also studied. The results show that WPI-MD conjugates prepared by dry-heating method exhibit enhanced solubility and emulsifying properties compared to native WPI. This improvement is most likely due to the enhanced steric stabilisation provided by the hydrophilic polysaccharide moiety.

In the study of competitive adsorption between WPI-MD and unmodified WPI on oil-water interface (Chapter 3), both theoretical calculations from Self-Consistent-Field (SCF) model and results from surface pressures suggest that WPI-MD conjugate can adsorb onto the oil-water interface in the presence of unmodified WPI and not be easily displaced by unmodified WPI.

The nature of polysaccharides can significantly influence the stabilizing properties of WPI-MD conjugates prepared via Maillard reactions.

Experimental results from Chapter 4 suggest that longer polysaccharides attached to proteins have stronger steric stability than shorter ones in O/W emulsions. Furthermore, when lactose is present in WPI and MD mixtures as an impurity before dry-heat treatment, the stabilizing properties of Maillard-type products are not significantly affected even when the molar ratio between MD and lactose is at 1:10. This interesting finding shows a potential to lower the cost of preparing whey protein based conjugates in large scale by using less pure whey protein from cheese manufacturing.

The major obstacles for large-scale manufacturing of protein-polysaccharide conjugates are long preparation time (from a couple of days to a few weeks) and dry processing conditions for Maillard reactions. In this PhD project, a novel processing method to prepare protein-polysaccharide conjugates was explored by using Spinning Disc Reactor (SDR). This method can successfully combine WPI and MD in less than 20 mins under controlled processing conditions in an aqueous medium. The SDR-processed conjugates have similar stabilizing properties as the ones prepared through traditional dry-heat treatment. The details can be found in Chapter 5.

Protein-polysaccharide conjugates have a promising future in food applications as new emulsifiers and stabilizers based on these studies.

## Table of Contents

<b>Acknowledgements.....</b>	<b>iv</b>
<b>Publications from thesis.....</b>	<b>vi</b>
<b>Accepted conference abstracts .....</b>	<b>vii</b>
<b>Abstract.....</b>	<b>viii</b>
<b>Table of Contents .....</b>	<b>x</b>
<b>List of Tables .....</b>	<b>xiv</b>
<b>List of Figures .....</b>	<b>xv</b>
<b>Chapter 1 Foundations of Research.....</b>	<b>1</b>
1.1 Introduction .....	1
1.2 Colloidal systems .....	3
1.2.1 Significance of colloid science.....	4
1.2.2 Classification of colloidal systems .....	5
1.2.3 The preparation of colloidal systems.....	6
1.3 Stability of colloidal dispersions.....	8
1.3.1 The definition of colloidal stability and instability .....	8
1.3.2 The mechanism of colloidal stability .....	9
1.3.3 Other effects of polymers on colloidal stability .....	14
1.4 Emulsifiers and stabilizers.....	16
1.4.1 Definition and examples of emulsifiers .....	17
1.4.2 Definition and examples of stabilizers .....	18
1.5 Interfacial Activity .....	20
1.5.1 Liquid-liquid interfaces.....	21
1.5.2 Measurement of interfacial tension .....	23
1.5.3 Adsorption of macromolecules at interfaces.....	24
1.6 Proteins, polysaccharides and conjugates .....	28
1.6.1 Background of proteins and polysaccharides.....	28
1.6.2 Stabilizing mechanism of protein-polysaccharide conjugates.....	30
1.6.3 Preparation methods of conjugates.....	32
1.6.4 Functional properties of conjugates .....	35

<b>Chapter 2 Theoretical and Experimental Methods .....</b>	<b>40</b>
2.1 Introduction .....	40
2.2 Theoretical calculations.....	41
2.2.1 Thermal and statistical physics .....	42
2.2.2 Self-consistent-field theory .....	47
2.2.3 SCF calculation procedure .....	55
2.3 Experimental Methods.....	56
2.3.1 Introduction .....	56
2.3.2 Particle sizing methods .....	57
2.3.3 Rheological methods.....	59
2.3.4 Interfacial tension methods .....	63
2.3.5 Other experimental methods .....	64
<b>Chapter 3 Competitive Adsorption and Stabilizing Properties of WPI and WPI-MD19 Conjugates on Oil-water Interface.....</b>	<b>68</b>
3.1 Introduction .....	68
3.2 Materials and Methods.....	68
3.2.1 Theoretical calculations.....	68
3.2.2 Key materials for experiments.....	72
3.2.3 Preparation of WPI-MD19 conjugates .....	72
3.2.4 Confirmation of successful conjugation .....	73
3.2.5 Interfacial properties of WPI-MD19 conjugates .....	74
3.2.6 O/W emulsion preparation.....	75
3.2.7 Emulsion stability monitoring.....	76
3.2.8 Statistical analysis .....	77
3.3 Results and Discussions .....	77
3.3.1 Predictions of theoretical model .....	77
3.3.2 Appearance of WPI-MD19 conjugates after the Maillard reactions .....	90
3.3.3 Confirmation of conjugates by SDS-PAGE and OPA tests .....	92
3.3.4 Interfacial properties of dry-heating WPI-MD19 conjugates.....	95
3.3.5 Stability analysis of O/W emulsions with the mixture of WPI and WPI-MD19.....	99

3.4 Conclusions.....	115
<b>Chapter 4 Influence of Reducing Polysaccharides on Protein-polysaccharide Conjugates via the Maillard Reactions.....</b>	<b>117</b>
4.1 Introduction .....	117
4.2 Materials and Methods.....	118
4.2.1 Preparation of WPI-MD conjugates.....	118
4.2.2 Preparation of WPI-MD19 conjugates with lactose .....	120
4.2.3 Degree of conjugation .....	121
4.2.4 Preparation of emulsions.....	121
4.2.5 Emulsion stability monitoring.....	121
4.2.6 Statistic analysis.....	122
4.3 Results and Discussions .....	122
4.3.1 Appearance of conjugates.....	122
4.3.2 Solubility of conjugates.....	124
4.3.3 Degree of conjugation .....	126
4.3.4 Emulsion stability by visual assessment.....	131
4.3.5 Emulsion stability by average droplet size.....	135
4.3.6 Emulsion stability by droplet size distribution .....	140
4.3.7 Emulsion stability studied via rheological properties .....	147
4.3.8 Emulsion stability by images from CLSM .....	151
4.4 Conclusions.....	156
<b>Chapter 5 A Novel Approach for Preparing Protein-polysaccharide Conjugates via Spinning Disc Reactor (SDR).....</b>	<b>158</b>
5.1 Introduction .....	158
5.2 Materials and Methods.....	162
5.2.1 Preparation of WPI-MD conjugates.....	162
5.2.2 Confirmation of successful conjugation .....	163
5.2.3 Preparation of emulsions.....	165
5.2.4 Interfacial properties of SDR-processed WPI-MD19 conjugates.....	165
5.2.5 Stabilizing properties of SDR-processed WPI-MD19 conjugates.....	167
5.2.6 Statistic analysis.....	167
5.3 Results and Discussions .....	167

5.3.1 Visual assessment of SDR-processed conjugates.....	167
5.3.2 Degree of conjugation for SDR-processed conjugates ....	168
5.3.3 Spectra scanning of SDR-processed conjugates .....	171
5.3.4 Hydrophobicity change of WPI-MD19 from SDR by HPLC .....	174
5.3.5 Adsorption behaviour of SDR-processed WPI-MD19 conjugates.....	176
5.3.6 Stabilizing properties of SDR-processed WPI-MD19 conjugates.....	181
5.4 Conclusions.....	185
<b>Chapter 6 General Discussion and Conclusions.....</b>	<b>187</b>
6.1 Introduction .....	187
6.2 Improved colloidal stability by protein-polysaccharide conjugates.....	187
6.3 Interfacial properties of protein-polysaccharide conjugates.....	188
6.4 Influence of polysaccharides on the properties of protein- polysaccharide conjugates .....	189
6.5 Novel preparation method of protein-polysaccharide conjugates.....	190
6.6 Conclusions and outlook .....	191
<b>Bibliography .....</b>	<b>194</b>
<b>List of Abbreviations.....</b>	<b>204</b>
<b>Appendix A .....</b>	<b>205</b>

## List of Tables

<b>Table 1.1 The Different Types of Colloidal Dispersions.....</b>	<b>4</b>
<b>Table 3.1 Flory-Huggins Interaction Parameters (<math>K_B T</math>) between Monomer Types and <math>pK_a</math> Values for Charged Amino Acid Residues .....</b>	<b>71</b>
<b>Table 3.2 Stabilizers of WPI and WPI-MD19 at Different Weight and Molar Ratios to be Utilized in O/W Emulsions .....</b>	<b>76</b>
<b>Table 4.1 Conjugates WPI-MD Prepared with Different DE Values at Various WPI to MD Ratios .....</b>	<b>119</b>
<b>Table 4.2 Conjugates WPI-MD with Different DE Values at Various Ratios of MD19 to Lactose .....</b>	<b>120</b>

## List of Figures

Figure 1.1 A schematic illustration of two types of stabilisation in O/W emulsions (A) electrostatic stabilisation; (B) steric stabilisation. Red dots represent hydrophobic moieties in proteins.....	11
Figure 1.2 A schematic model of electrical double layer.....	12
Figure 1.3 A schematic illustration of depletion flocculation induced by unadsorbed polymers in bulk phase.....	15
Figure 1.4 A schematic illustration of bridging flocculation induced by polymers in bulk phase.....	16
Figure 1.5 A schematic illustration of Pickering stabilization in an O/W emulsion .....	19
Figure 1.6 Attractions between molecules in bulk phase and at the liquid-liquid interface.....	22
Figure 1.7 2-D configurations of macromolecules adsorbed on the interface .....	25
Figure 1.8 Three stages of protein adsorption from the bulk phase to the interface. ....	28
Figure 1.9 (A) Basic chemical mechanism for the formation of protein-polysaccharide conjugates via Maillard reaction (B) the overview structure of the conjugate. ....	30
Figure 1.10 Comparison between protein- and conjugate-stabilised oil droplet in O/W system. The red blocks represent proteins; the blue branches represent polysaccharides.....	32
Figure 1.11 Preparation of protein-polysaccharide conjugates via dry-heating and wet-heating pathways: (A) dry-heating pathway; (B) wet-heating pathway.....	33
Figure 2.1 Schematic illustration of theoretical and experimental methods cooperatively applied to research cycle. ....	41
Figure 2.2 Binary model with different magnetic spins. ....	43
Figure 2.3 Lattice model separating the space between two flat plates into basic cubes.....	50
Figure 2.4 Density profile of a hydrophilic model polymer (bulk volume fraction 0.001) between two hydrophobic surfaces calculated via SCF model.....	55
Figure 2.5 Schematic illustration of light travelling from the homogenous medium to a droplet.....	57
Figure 2.6 Schematic illustration of Mastersizer 3000 for particle sizing.....	58

Figure 2.7 Schematic illustration of Rheometer with cone geometry in shearing experiment. ....	62
Figure 2.8 Schematic illustration of OCA for interfacial tension analysis of oil-in-water system. ....	63
Figure 2.9 A schematic illustration of reaction between TNBS and amino groups. ....	65
Figure 2.10 A chemical reaction of OPA with SH- and NH <sub>2</sub> - groups to form detectable compound at 340nm. ....	66
Figure 3.1 Primary structure of $\beta$ -lactoglobulin without disulphide bonds under five different groups, according to the physical properties of each amino acids. ....	70
Figure 3.2 Colloidal interaction potential between two droplets (d=1 $\mu$ m) mediated by systems consisting of a single type of polymer for $\beta$ -lactoglobulin (Beta-LG), $\alpha$ -lactalbumin (Alpha-LA), $\beta$ -lactoglobulin-MD19 conjugate (Beta-LG-MD19) and $\alpha$ -lactalbumin-MD19 (Alpha-LA-MD19) respectively. ....	78
Figure 3.3 Interactions induced between two droplets (d=1 $\mu$ m) by polymers in a system containing both $\beta$ -lactoglobulin (Beta-LG) and $\beta$ -lactoglobulin-MD19 conjugate (Beta-LG-MD19). ....	79
Figure 3.4 Interaction potential between two droplets mediated by polymers in a mixed system of $\alpha$ -lactalbumin (Alpha-LA) and $\alpha$ -lactalbumin-MD19 conjugate (Alpha-LA-MD19). ....	81
Figure 3.5 Interaction potential between two droplets mediated by polymers in a mixed system of $\beta$ -lactoglobulin (Beta-LG) and $\alpha$ -lactalbumin-MD19 conjugate (Alpha-LA-MD19). ....	82
Figure 3.6 Interaction potential between two droplets mediated by polymers in a mixed system of $\alpha$ -lactalbumin (Alpha-LA) and $\beta$ -lactoglobulin-MD19 conjugate (Beta-LG-MD19). ....	83
Figure 3.7 Interaction potential curve for forces induced in a mixed three-polymer system containing $\alpha$ -lactalbumin (Alpha-LA), $\beta$ -lactoglobulin-MD19 conjugate (Beta-LG-MD19) and $\alpha$ -lactalbumin-MD19 conjugate (Alpha-LA-MD19). ....	84
Figure 3.8 Colloidal interaction potential plotted as a function of particle-particle separation distance, induced between droplets in mixed solutions of $\beta$ -lactoglobulin (Beta-LG) + $\beta$ -lactoglobulin-MD19 conjugate (Beta-LG-MD19) + $\alpha$ -lactalbumin-MD19 conjugate (Alpha-LA-MD19). ....	85
Figure 3.9 Interaction potential between two droplets mediated by polymers in a system containing $\beta$ -lactoglobulin (Beta-LG), $\alpha$ -lactalbumin (Alpha-LA), and $\alpha$ -lactalbumin-MD19 conjugate (Alpha-LA-MD19). ....	86

<b>Figure 3.10 Interaction potential graph in a mixed three-polymer system involving <math>\beta</math>-lactoglobulin (Beta-LG) + <math>\alpha</math>-lactalbumin (Alpha-LA) + <math>\beta</math>-lactoglobulin-MD19 conjugate (Beta-LG-MD19).</b> .....	<b>87</b>
<b>Figure 3.11 Colloidal interaction induced between a pair of droplets in systems consisting of four types of polymer: <math>\beta</math>-lactoglobulin (Beta-LG), <math>\alpha</math>-lactalbumin (Alpha-LA), <math>\beta</math>-lactoglobulin-MD19 conjugate (Beta-LG-MD19), and <math>\alpha</math>-lactalbumin-MD19 conjugate (Alpha-LA-MD19).</b> .....	<b>88</b>
<b>Figure 3.12 Appearance of WPI-MD19 conjugates prepared via dry-heat treatments (sample 2, 3, 4) and wet-heat treatments (sample 6, 7, 8); sample 1 and 5 are controls (heated WPI only)</b> .....	<b>91</b>
<b>Figure 3.13 SDS-PAGE results of WPI, WPI-lactose conjugates, and WPI-MD19 conjugates prepared via dry-heat treatments.</b> .....	<b>92</b>
<b>Figure 3.14 Degree of conjugation analysis of different protein and protein/polysaccharide systems via OPA tests.</b> .....	<b>94</b>
<b>Figure 3.15 Interfacial tensions of WPI, dry-heated WPI, and WPI-MD19 conjugates at various protein concentrations, measured for oil-water interfaces.</b> .....	<b>95</b>
<b>Figure 3.16 Interfacial pressures of WPI, dry-heated WPI, and WPI-MD19 conjugates at different adsorption time on the oil-water interface. Total protein content was the same for all systems at 0.1 w/v %.</b> .....	<b>98</b>
<b>Figure 3.17 Average droplet size (ADS) of O/W emulsions stabilized by the mixture of WPI and WPI-MD19 conjugates at various weight ratios under different environmental pH.</b> .....	<b>100</b>
<b>Figure 3.18 Average droplet size (ADS) of O/W emulsions stabilized by the mixture of WPI and WPI-MD19 conjugates at various weight ratios under different concentrations of CaCl<sub>2</sub>.</b> ...	<b>102</b>
<b>Figure 3.19 Average droplet size <math>d[4,3]</math> of O/W emulsions (pH 4.6) stabilized by the mixture of WPI and WPI-MD19 conjugates at various mix weight ratios, following different storage time.</b> .....	<b>104</b>
<b>Figure 3.20 Droplet size distribution (DSD) of O/W emulsions (pH 4.6) stabilized by the mixture of WPI and WPI-MD19 conjugates at three weight ratios (0, 60, and 100%) at storage time Day 0.</b> .....	<b>106</b>
<b>Figure 3.21 Droplet size distribution (DSD) of O/W emulsions (pH 4.6) stabilized by the mixture of WPI and WPI-MD19 conjugates at three weight ratios (0, 60, and 100%) at storage time Day 28.</b> .....	<b>108</b>

<b>Figure 3.22 Viscosity profiles of the emulsion stabilized by WPI-MD19 conjugates only in 85 °C water bath for 2 hours and gradually cooled down to room temperature under different shear rates.....</b>	<b>110</b>
<b>Figure 3.23 Viscosity profiles of the emulsion stabilized by native WPI only in 85 °C water bath for 2 hours and gradually cooled down to room temperature under different shear rates.....</b>	<b>111</b>
<b>Figure 3.24 Viscosity profiles of the emulsion stabilized by the mixture of WPI-MD19 conjugates (60 w/w %) and WPI (40 w/w %) in 85 °C water bath for 2 hours and gradually cooled down to room temperature under different shear rates.....</b>	<b>113</b>
<b>Figure 3.25 Viscosity profiles of the emulsions stabilized by different systems in 85 °C water bath after 2 hours and gradually cooled down to room temperature under different shear rates.....</b>	<b>114</b>
<b>Figure 4.1 Appearance of the whey protein isolate and maltodextrin mixture in the dry state before (Left) and after (Right) following heat treatments at 80 °C for 3 hours.....</b>	<b>123</b>
<b>Figure 4.2 An illustration of WPI and MD19 mixture combining various proportions of lactose before (Left) and after (Right) the Maillard reactions; (1) MD19 : lactose (molar) = 1:1; (2) MD19 : lactose (molar) = 1:2; (3) MD19 : lactose (molar) = 1:4; (4) MD19 : lactose (molar) = 1:6; (5) MD19 : lactose (molar) = 1:10.....</b>	<b>124</b>
<b>Figure 4.3 Solubility tests of WPI and WPI-MD19 conjugates at different pH values from 3 to 10, including the pl of WPI pH 4.6; (1) 1 w/v % WPI at pH 3, 4.6, 6, 7, and 10; (2) 1 w/v % (on protein basis) WPI-MD19 at pH 3, 4.6, 6, 7, and 10.....</b>	<b>125</b>
<b>Figure 4.4 Degree of conjugation for WPI and maltodextrin (DE 2) at various weight ratios between WPI and maltodextrin based on the protein concentration 1 w/v %.....</b>	<b>126</b>
<b>Figure 4.5 Degree of conjugation for WPI and maltodextrin (DE 19), at various weight ratios between WPI and maltodextrin, based on the protein concentration of 1 w/v %.....</b>	<b>127</b>
<b>Figure 4.6 Degree of conjugation for WPI and maltodextrin (DE 47) at various weight ratios between WPI and maltodextrin based on the protein concentration 1 w/v %.....</b>	<b>128</b>
<b>Figure 4.7 Degree of conjugation for WPI and maltodextrin (DE 19) at weight ratio of 1:2 with different molar ratios of MD19 to lactose during the Maillard reactions based on the protein concentration 1 w/v %.....</b>	<b>130</b>

<b>Figure 4.8 Photograph of O/W emulsions stabilized by WPI-MD2 at different weight ratios between WPI and MD2 from storage day 0 to day 28; (1) WPI : MD2 = 2:1; (2) WPI : MD2 = 1:1; (3) WPI : MD2 = 1:2; (4) WPI : MD2 = 1:3; (5) WPI : MD2 = 1:4.....</b>	<b>132</b>
<b>Figure 4.9 Photograph of O/W emulsions stabilized by WPI-MD47 at three different weight ratios between WPI and MD47 from storage day 0 to day 28; (1) WPI : MD47 = 2:1; (2) WPI : MD47 = 1:1; (3) WPI : MD47 = 1:2.....</b>	<b>133</b>
<b>Figure 4.10 Photograph of O/W emulsions stabilized by different complexes after 28 days; in each case the emulsifier was synthesized as follows: (1) WPI-MD19 (1: 2 w/w) without lactose contamination; (2) WPI-MD19 with lactose impurity present at the molar ratio of 1:10 (MD19 : lactose); (3) WPI-lactose (2:1 w/w) with no maltodextrin present; (4) a mixture of WPI and MD19 (1:2 w/w) without any heat treatment; in sample 3, the position of cream layer is indicated by an arrow. ....</b>	<b>134</b>
<b>Figure 4.11 Average droplet size of emulsions stabilized by WPI-MD2 at different weight ratios between WPI and MD2 from storage day 0 to day 28.....</b>	<b>136</b>
<b>Figure 4.12 Average droplet size of emulsions stabilized by WPI-MD47, synthesized at different weight ratios between WPI and MD47, throughout storage from day 0 to day 28.....</b>	<b>137</b>
<b>Figure 4.13 Average droplet size of emulsions stabilized by WPI-MD19 containing lactose as impurity at different molar ratios between MD19 and lactose for 28 days.....</b>	<b>139</b>
<b>Figure 4.14 Droplet size distribution of the emulsion stabilized by WPI-MD2, formed at a weight ratio of 2:1, on day 0 and day 28.....</b>	<b>141</b>
<b>Figure 4.15 Droplet size distribution of the emulsion stabilized by WPI-MD2 at the weight ratio of 1:4 at day 0 and day 28.....</b>	<b>142</b>
<b>Figure 4.16 Droplet size distribution of the emulsion stabilized by WPI-MD47 at the weight ratio of 2:1 at day 0 and day 28.....</b>	<b>143</b>
<b>Figure 4.17 Droplet size distribution of the emulsion stabilized by WPI-MD47 at the weight ratio of 1:2 at day 0 and day 28.....</b>	<b>144</b>
<b>Figure 4.18 The comparison of droplet size distribution (DSD) of the emulsions stabilized by WPI-MD19 with the impurity of lactose at molar ratio of 1:10 (MD19 : lactose) at day 0 and day 28.....</b>	<b>145</b>
<b>Figure 4.19 The relationship between viscosities and shear rates for two emulsions stabilized by WPI-MD2 (2:1 w/w) and WPI-MD2 (1:4 w/w), immediately after preparation and after 28 days of storage.....</b>	<b>147</b>

<b>Figure 4.20 The relationship between viscosities and shear rates for two emulsions stabilized by WPI-MD47 (2:1 w/w) and WPI-MD47 (1:2 w/w), at day 0 and day 28 following emulsion preparation. ....</b>	<b>149</b>
<b>Figure 4.21 The relationship between viscosities and shear rates for two emulsions stabilized by WPI-MD19 (1:2 w/w), WPI-MD19 (1:2 w/w) with lactose at molar ratio 1:10 (MD19 : lactose) and WPI-lactose (2:1 w/w). ....</b>	<b>150</b>
<b>Figure 4.22 Images obtained from CLSM of emulsions stabilized by WPI-MD2 (2:1 w/w): (1) &amp; (2) and WPI-MD2 (1:4 w/w): (3) &amp; (4), respectively at day 0 and day 28, post preparation of emulsions. ....</b>	<b>152</b>
<b>Figure 4.23 Images from CLSM of emulsions stabilized by WPI-MD47 (2:1 w/w): (1) &amp; (2) and WPI-MD47 (1:2 w/w): (3) &amp; (4) initially and following 28 days of storage. ....</b>	<b>154</b>
<b>Figure 4.24 Images from CLSM of emulsions stabilized by WPI-MD19 (1:2 w/w): (1) &amp; (2), WPI-MD19 (1:2 w/w), formed in the presence of lactose contamination, at the molar ratio of 1:10 (MD : lactose): (3) &amp; (4), and WPI-lactose (2:1 w/w): (5) &amp; (6), immediately post emulsion preparation and after 28 days of storage. ....</b>	<b>155</b>
<b>Figure 5.1 A schematic diagram of main reactor showing various components in SDR during process. ....</b>	<b>160</b>
<b>Figure 5.2 The SDR system in the School of Food Science and Nutrition University of Leeds. ....</b>	<b>161</b>
<b>Figure 5.3 Photographs of WPI-MD12 (1:3 w/w) conjugates prepared by using the SDR at different reaction time for 14 mins. ....</b>	<b>168</b>
<b>Figure 5.4 Degree of conjugations for WPI-MD conjugates with different chain length of MD prepared via dry-heating method and SDR processing (10 mins). ....</b>	<b>169</b>
<b>Figure 5.5 Degree of conjugations for WPI-MD12 (1:3 w/w) prepared via SDR at different process time. ....</b>	<b>170</b>
<b>Figure 5.6 Absorbance spectra of WPI-MD12 conjugates prepared by SDR (110 °C for 10 minutes): (1) 10 g/L MD12; (2) 10 g/L WPI alone; (3) 10 g/L WPI-MD12 (1:3 w/w) mixture. ....</b>	<b>171</b>
<b>Figure 5.7 Absorbance at 280 nm of WPI-MD12 mixture subjected to wet-heating method using the SDR (110 °C) at various reaction time: (1) 10 g/L WPI alone; (2) 10 g/L WPI-MD12 (1:3 w/w). ....</b>	<b>173</b>
<b>Figure 5.8 The relationship between retention time and absorbance at wavelength 280 nm of WPI and WPI-MD19 prepared by SDR or dry-heating (DH) method. ....</b>	<b>175</b>

<b>Figure 5.9 The relationship between the concentration of WPI-MD19 in serum layer and the absorbance of complex formed via the Biuret method at wavelength 540nm.....</b>	<b>177</b>
<b>Figure 5.10 The adsorption of WPI-MD19 at the oil-water interface in emulsions (O/W 20:80 v/v) at various concentrations. ....</b>	<b>178</b>
<b>Figure 5.11 The surface area of oil droplets of oil-in-water emulsions containing various WPI-MD19 concentrations.....</b>	<b>179</b>
<b>Figure 5.12 The surface concentration of WPI-MD19 in emulsions with different total conjugates concentrations.....</b>	<b>180</b>
<b>Figure 5.13 Average droplet size, <math>d[4,3]</math>, of emulsions stabilized by WPI-MD19 conjugates prepared by dry heating (DH) and SDR processing at different weight ratios for a storage period of 28 days.....</b>	<b>181</b>
<b>Figure 5.14 Droplet size distribution of freshly made emulsions stabilized by WPI-MD19 prepared by dry heating (DH) and SDR processing at different weight ratios.....</b>	<b>183</b>
<b>Figure 5.15 Droplet size distribution of emulsions stabilized by WPI-MD19 prepared by dry heating (DH) and SDR at different weight ratios at storage day 28.....</b>	<b>184</b>

## Chapter 1 Foundations of Research

### 1.1 Introduction

We are familiar with the colloidal state of matter when drinking a cup of milk tea or cappuccino every morning. The word *colloid* is from the Greek *`kolla`* which means glue (Dickinson, 1982a). However, the colloidal state is difficult to understand when we study it carefully. First of all, the colloidal state of matter cannot be simply categorized into the classic states of matter: solid, liquid and gas (Shaw, 1991a). The colloidal state can be thought of as an intermediate class of materials between any two states. Gel, for example, is a colloidal system which has both solid and liquid characters. Secondly, there are often more than one component in a colloidal system, which makes the system complicated owing to the interactions among all these constituents. In order to understand the mysterious state of colloids, scientific methods were adopted to the field of colloids. Colloid science concentrates on systems in which at least one large component is dispersed through a dispersion medium. Generally, the size of dispersed material is from nanometre to tens of micrometres, and can include protein solutions and emulsions (Shaw, 1991a).

In a colloidal system, there are a number of important features which interest to colloid scientists (Everett, 1988a). Kinetic properties, i.e., the movements of colloidal particles in a colloidal system plays a major part in all these features. For example, particles can diffuse according to a concentration gradient (Dickinson, 1992a). However, if the particles are charged in an

electric field (i.e., electrophoresis), the diffusion pattern can vary significantly (Everett, 1988a). The kinetic properties of a colloidal system can also be affected by other external fields such as gravity and centrifuging, which may lead to the phenomena of creaming in oil-in-water emulsions (Dickinson, 1992a). Apart from kinetical properties, colloidal systems can exhibit various optical properties. When light passes through the system, the light can be scattered because the refractive indexes of light in different medium vary (Everett, 1988d). That is the main reason why milk is opaque instead of being transparent. Other features of a colloid are their unique rheological properties. For example, when a shear force is applied to a hard gel, the gel may show more elastic behaviours than fluid characteristics; but upon sufficient application of shears, the behaviour of gel reverts to that displayed by fluids (Dickinson, 1992c). All these interesting properties of colloids can to some extent be understood by knowledge from other fundamental subjects e.g. thermodynamics, interfacial chemistry and physical chemistry. The useful application of concepts and models from these origins establish a solid foundation for colloid science.

In the field of colloid science, there is an inevitable concept of a colloidal stability (Dickinson, 1982a & 1992a). A stable system is usually desirable when a dispersion is prepared, such as an oil-in-water emulsion. On the other hand, a colloidal state of matter is undesirable in some other areas e.g. air or water pollution. The fundamental question about the two above scenarios is why a colloidal system can remain in the dispersed state. In order to answer this question, thermodynamics and physical chemistry can be used to provide us with some insights into the colloidal stability. In section 1.3, the mechanisms of colloidal stability will be discussed in detail.

Another key feature of a colloidal dispersed system is the large contact area (i.e. interface or surface) between dispersed phase and dispersion medium (Hunter, 2001). The physico-chemical properties of the interface such as structural, electrical, and rheological properties of the system are significantly influenced by the presence of a large interface. Therefore, not surprisingly, surface chemistry plays a critical role in colloid science. This project focuses on liquid-liquid interfaces and will involve a discussion of interfacial tension and the adsorption of macromolecules on the interface. Therefore, an introduction to this is given in section 1.5.

The aim of this chapter is going to establish a foundation for this PhD research project. The principle and methodology of this project are rooted in the foundation of colloid science.

## **1.2 Colloidal systems**

Colloidal systems are often the mixture of various components with domains of the dispersed phase in the range of colloidal scale (i.e.  $10^{-9} \sim 10^{-6}$  m) (Shaw, 1991a). In a simple colloidal system, one material (*dispersed phase*) is dispersed in another continuous phase (*dispersion medium*). Dispersion medium in food colloids is usually a liquid phase. If the dispersed phase is solid particles smaller than  $10^{-6}$  m, the colloidal system is called *sol* (Dickinson, 1992a). There are several types of colloidal systems based on the nature of dispersed phase and that of dispersion medium as listed in Table 1.1 (Hunter, 2001).

**Table 1.1** The Different Types of Colloidal Dispersions

<b>Dispersed phase</b> \ <b>Medium</b>	<b>Gas</b>	<b>Liquid</b>	<b>Solid</b>
<b>Gas</b>	-	Foam	Solid foam
<b>Liquid</b>	Aerosol	Emulsion	Solid emulsion
<b>Solid</b>	Aerosol	Sol	Solid dispersion

In terms of food colloids, most of the systems of interest are foams and emulsions. For example, foam is an important feature of beer products, and many dairy products such as pasteurised whole milk are typical oil-in-water (O/W) emulsions (Dickinson, 1992a). Moreover, there are a great number of complicated colloidal systems in foods. Ice cream is an excellent example to show the complexity of a colloidal system in real food products. It is a solid foam of air, stabilised partially by emulsified fat and by an ice crystal network, which is dispersed in an aqueous solutions with macromolecules (e.g. proteins) and sweeteners (e.g. sugars) (Dickinson, 1982g).

### **1.2.1 Significance of colloid science**

Colloid science can be considered as a solid foundation for many industrial applications in modern society. Inks, for instance, have their own colloidal properties which become important under different applications such as in high-speed printers and ballpoint pen. Even for the same material, it can exhibit various colloidal characters at different stages of application. For example, paint is stable during storage and needs to have high viscosity post application, while it should shear thin when it is being applied to a surface. Apart from inks and paints, colloid science is also crucial in cosmetics, ceramic products, oil industry and not least in foods (Hunter, 2001).

There are many natural processes in biology that also heavily depend on colloidal systems. One example is blood which can be understood as a dispersion of various cells in a liquid (Dickinson, 1992a). In food science, a large number of modern food products are in the colloidal state, from dairy products (milk, yoghurt, cheese etc.) to baked foods (bread, cake, biscuits, etc.) (Dickinson, 1992a). Therefore, colloid science plays a critical role in explaining the desired behaviour of many food products in designing and guiding research into future foods and in developing new products in food industry.

### **1.2.2 Classification of colloidal systems**

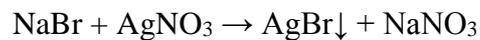
Generally, colloidal systems can be classified into three categories: macromolecular solutions, association colloids and colloidal dispersions (Hunter, 2001). Macromolecular solutions are generally thermodynamically stable systems and easily reconstituted if the separation occurs between solute and solvent. In association colloids, a large number of small molecules associate together to form micelles, which are of colloidal dimensions. The association colloids are also thermodynamically stable and formed spontaneously (Shaw, 1991a).

Colloidal dispersions are different from the other two colloidal systems above. They are thermodynamically unstable because of their large interfacial free energy that exists between the two immiscible components: a dispersed phase (discontinuous phase) and a dispersion medium (continuous phase) in the system (Hunter, 2001). According to the nature of dispersed particles and medium, colloidal dispersions can be further classified into various categories (Table 1) (Hunter, 2001). In terms of food emulsions, there are two basic

types: an oil-in-water (O/W) emulsion such as milk consisting of oil droplets dispersed in water and water-in-oil (W/O) emulsions (e.g. margarine and butter) in which the role of these two phases are reversed (Dickinson, 1992a). In this project, the system of interest will be O/W emulsions.

### 1.2.3 The preparation of colloidal systems

Generally speaking, there are two main methods to form a colloidal system: aggregation of small molecules and degradation of bulk matter (Everett, 1988c). It is possible to prepare a colloidal particle from small molecules by forming complexes which aggregate to increase size to colloidal range. Some chemical reactions can lead to the aggregation of small molecules. For example, a colloidal dispersion can be prepared by the reaction between sodium bromide and silver nitrate.



The aggregation of silver bromide is formed immediately after the reaction. Similarly, sodium chloride can also react with silver nitrate to form a colloidal system by aggregation (Everett, 1988c). Another method to prepare a colloidal system is to break down the bulk matter until colloidal size is reached.

Emulsification is a major technique in methods of reducing the size of bulk matter. One type of liquid is dispersed into another liquid by large force to break down the dispersed liquid to small droplets within the size of colloidal range. Meanwhile, an extremely large interfacial area is also created during emulsification. The large force applied to the two-liquid system is partially used to increase the interface according to the surface tension:

$$dW = \gamma \cdot dA$$

$\gamma$  is surface tension;  $dA$  is the increase of interfaces;  $dW$  is the work required to form new interfaces (Shaw, 1991a; Dickinson, 1992b). These newly formed interfaces exert a significant influence on the stability of emulsions. The stability of emulsions will be discussed in detail in section 1.3.

To form an *OW* emulsion, it is possible to shake the oil-water system with suitable emulsifiers and stabilizers in a closed container by hand. The smallest droplets of this coarse emulsion will tend to be larger than 20  $\mu\text{m}$  (Dickinson, 1982c). In order to prepare fine emulsions, various equipment can be used. High-speed mixer can prepare emulsions with smaller droplet size (5  $\mu\text{m}$ ) than that from hand-shaking method. Oil and water is mixed under turbulent flow generated by the high-speed blades, which is more effective than the method of shaking by hand. However, the droplet size around 5  $\mu\text{m}$  is still not small enough for many systems of practical use (Dickinson, 1982c). To further reduce the size, still more powerful device is required. Colloid mill and high-pressure homogenizer can produce more finely divided dispersions. In a colloid mill, the liquids pass through the narrow gap between rotor and stator surfaces (Dickinson, 1982c). A strong shear force is applied to the liquids to break down the bulk matter. The droplet size of emulsion prepared by colloid mill is around 2  $\mu\text{m}$ . Compared to colloid mill, high-pressure homogenizer not only can reduce droplet size under 1  $\mu\text{m}$  but also leads to a narrow distribution of droplet sizes. In the device used in this project, a high pressure is generated by compressed air to push down two pistons till the bottom of two independent chambers which contains two immiscible liquids. The two liquids pass through a narrow hole ( $d \sim 1 \mu\text{m}$ ) and are mixed together in a short time (i. e.  $\sim 1 \text{ s}$ ). The device is often referred to as high pressure homogenizer (Dickinson, 1982c). Apart from the preparation methods of

colloidal systems discussed above, ultrasonic techniques are also used in emulsification process. For example, ultrasonic jet generator is a high efficiency machine to prepare emulsions compared to high-pressure homogenizer, because the ultrasonic jet generator can reduce the droplet size to smaller than 0.1  $\mu\text{m}$  (Dickinson, 1982c).

### **1.3 Stability of colloidal dispersions**

Colloid scientists and technologists are keen on understanding how to make and destroy a colloidal dispersion due to the importance of colloidal stability in many fields. In food industry, it is critical to produce a stable emulsion under various environmental conditions (e.g. temperature, shelf life etc.) for example during development or storage a new dairy product. However, air or water pollution problems, resulting from unwanted colloidal materials, often requires destabilising the colloidal system. Similar issues can arise in food science during flavour release. Therefore, it is vital to study the stability of colloidal systems.

#### **1.3.1 The definition of colloidal stability and instability**

A colloidal dispersion can be considered as a kinetically stable system if there is no detectable aggregation of particles over a certain period of time (Dickinson, 1982b & 1992a). As mentioned in 1.1, colloidal dispersions are thermodynamically unstable owing to the excess free energy in the interfacial region, but can be made kinetically stable during the observation period, which is said to be *colloidally stable* or *metastable* (Shaw, 1991a; Dickinson, 1982b & 1992a). If a colloidal system is to be in the metastable state over a sufficiently long period, there should be a substantial energy barrier preventing changes to the colloidal state. Thus, in order to prepare a stable colloidal

dispersion, it is critical to control the factors which give rise to this energy barrier having a sufficient height. On the contrary, it is of significant importance to destabilise a colloidal dispersion by lowering the energy barriers adequately.

There are several instabilities in colloidal dispersions. The most common ones are *sedimentation* and *creaming* under gravity depending on the density difference between the dispersed phase and dispersion medium. The kinetical property of creaming process is dependent on the size of droplets, density difference and rheological properties of dispersion medium e.g. viscosity (Dickinson, 1982c). Generally, a group of particles or droplets held together is called an *aggregate*. If the distance between particles or droplets is larger than atomic dimensions, these aggregates are named as flocs. However, if the distance is much smaller, it is called a coagulation aggregate. The structure of flocculation aggregates is more loose than that of coagulation ones (Dickinson, 1992a).

### 1.3.2 The mechanism of colloidal stability

The major driving force for particle aggregation in a colloidal dispersion is the long-range van der Waals attractive forces between particles. In order to avoid the attraction, some equally long-range repulsive forces are required to promote stability.

The long-range attractions between colloidal particles are from the summation of interaction between each individual molecules in two particles. For two molecules *i* and *j*, the attractive energy can be estimated as follows:

$$G_{i,j}^{att}(r) = -\frac{A_{i,j}}{r^6}$$

where  $A_{i,j}$  is a constant determined by molecular polarizabilities;  $r$  is the distance between the mass centres of two molecules (Dickinson, 1982a). When it comes to the sum of these attractions between each molecules in colloidal particles, the Hamaker constant  $A_H$  is necessary to be introduced, which is related to the density and polarizability of two materials:

$$A_H = \pi^2 \rho_i \rho_j A_{i,j}$$

where  $\rho_i \rho_j$  is the density of material  $i$  and  $j$  (Dickinson, 1982a). If the dispersed particles are made of the same material, the net force between particles is always attractive. For example, the net interaction between a pair of oil droplets can be attractive in O/W emulsions when emulsifiers are absent. Furthermore, when the particles are in a solvent, interactions between molecules of the particles and solvent also need to be taken into account. This modifies the value of Hamaker constant. In this case, the Hamaker constant is known as the composition Hamaker constant (Dickinson, 1982a).

In order to counteract the attractive potential between particles in colloidal systems, it is essential to introduce repulsive interactions to stabilize the whole system. There are two major stabilization mechanisms in foods: electrostatic stabilization and steric stabilization (Figure 1.1) (Lam and Nickerson, 2013).

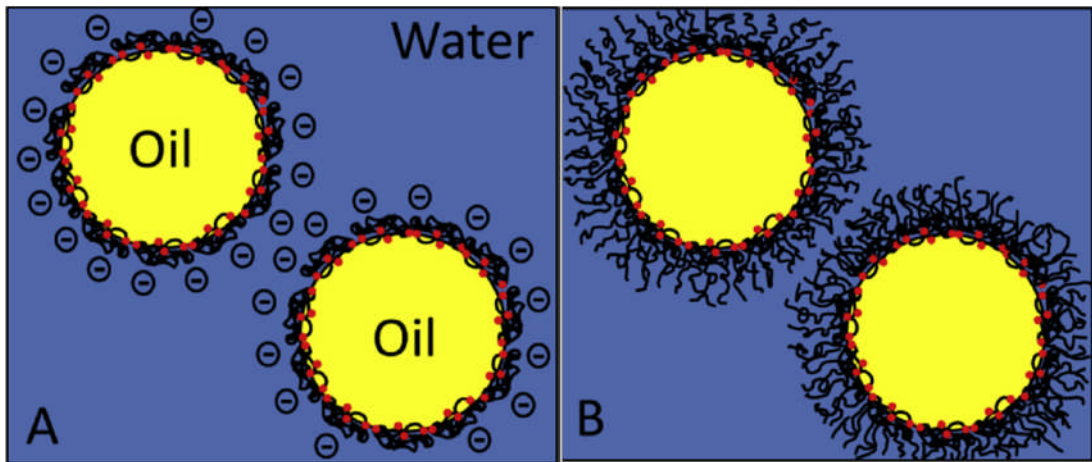


**Figure 1.1** A schematic illustration of two types of stabilisation in O/W emulsions (A) electrostatic stabilisation; (B) steric stabilisation. Red dots represent hydrophobic moieties in proteins.

In order to explain the mechanism of electrostatic stabilization, it is critical to introduce the model of *electrical double layer* (Dickinson, 1992a). The distribution of ions in an aqueous electrolyte solution can be influenced by an electrically charged interface in this solution. The oppositely charged ions are attracted to this interface whilst ions with the same charge are preferably repelled. Consequently, an unequally distributed ions near the interface form the electrical double layer (Figure 1.2) (Dickinson, 1992a). In this model, there are two important regions: the Stern layer which is an inner immobile region and an outer region (the diffuse layer) which is more mobile than the Stern layer (Dickinson, 1992a). It turns out that the electrical potential in the solution decreases exponentially with the distance away from the interface. The thickness of the double layer can be measured by this distance denoted as  $\kappa^{-1}$ . It has been shown that the thickness of the double layer is affected by the bulk ionic strength in the solution significantly. The thickness declines when the ionic strength is increased in the aqueous medium. For example,  $\kappa^{-1}$  is around 1 nm in the 0.1 M NaCl solution while it reduces to 0.3 nm when the ionic strength of the solution is increased to 10 times (1 M NaCl solution)

(Dickinson, 1992a). The reason why food colloids scientists are interested in the thickness of double layer is that  $\kappa^{-1}$  is highly related to the electrostatic stability of a colloidal system.

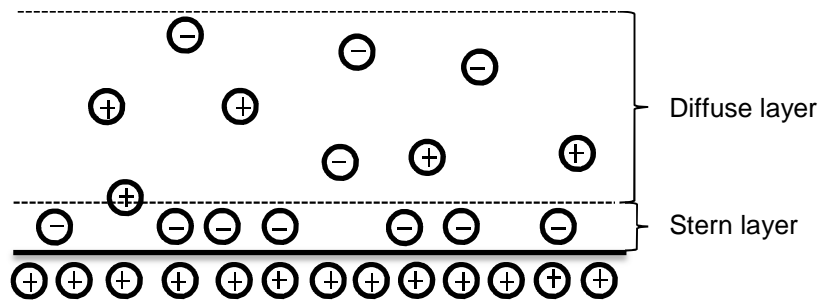


**Figure 1.2** A schematic model of electrical double layer.

We have to consider the interactions of two colloidal particles with electrical double layers when they are approaching each other in order to investigate the electrostatic stability of a colloidal system. When the two colloidal particles with electrical double layers are far away from each other, one particle may see the other as an uncharged entity because of its neutralising double layer (Everett, 1988b). However, at a sufficient close distance between two particles, where the double layers of adjacent particles overlap, they will begin to ‘feel’ one another’s influence. In another words, each particle ‘sees’ the other as a partially charged entity once the electrical double layers overlap. Consequently, the same charged particles will repel each other to avoid further contact which may induce colloidal instability such as flocculation and coalescence (Everett, 1988b).

Based on the discussion above, colloidal particles with thick electrical double layers tend to repel one another at a relatively long separation, which

indicates less probability of coalescence (Everett, 1988b). On the other hand, thin double layer may suggest higher possibility to colloidal instability. That is why a colloidal system, mainly stabilized by electrostatic interactions, can be destroyed by increasing ionic strength in the surrounding environment (Everett, 1988b). Moreover, not only can the ionic strength influence the thickness of double layer, but so can the type of ions (e. g. valency number) and temperature can affect stability of a colloidal system (Everett, 1988b).

Apart from electrostatic stabilizing mechanism, there is another method to stabilize a colloidal system: steric stabilization (Dickinson, 1982b). This kind of stability usually arises from layers of polymers adsorbed onto the surface of colloidal particles. In order to give sufficient steric stability, there are three major requirements for the stabilizers: (i) polymers are strongly anchored to the interface; (ii) interface is fully covered by polymers; (iii) the thickness of adsorbed polymers is sufficient (Dickinson, 1982b).

When two particles coated with polymers approach each other, there are mainly two ways that the adsorbed layers become distorted: compression and interpenetration (Dickinson, 1982a). For compression, losing configurational entropy can lead to an increase ( $\Delta G_E$ ) of the free energy of interaction, owing to the more restricted volume between two approaching surfaces. For interpenetration, there is also a free energy change ( $\Delta G_M$ ) corresponding to the changes in the mixing of polymer segments and solvent, before and after interpenetration (Dickinson, 1982b).  $\Delta G_E$  is always positive due to the reduction in the number of configurations of adsorbed macromolecules. However,  $\Delta G_M$  can be either positive or negative depending on the Flory-Huggins parameter which measures the strength of segment-solvent relative

to the segment-segment and solvent-solvent interactions (Dickinson, 1982a). The total steric free energy change can be obtained by summing the elastic (compression) and mixing (interpenetration) terms.

The total free energy difference between infinite separation and a certain closer distance is summed as follows and give the interaction potential between the particles:

$$\Delta G = \Delta G^{att} (\text{van der Waals}) + \Delta G^{rep} (\text{electrostatic}) + \Delta G^{rep} (\text{steric})$$

The stability of a colloidal system depends greatly on the total interactions between two colloidal particles and the nature of  $\Delta G$  (Everett, 1988a).

### **1.3.3 Other effects of polymers on colloidal stability**

As discussed in 1.3.2, polymers need to be strongly anchored onto the interface in steric stabilization. When two colloidal particles come together, the concentration of polymer segments between two particles increases, which leads to a repulsion owing to the osmotic pressure between the bulk phase and the space in the middle of these two particles. However, if the macromolecules cannot be attached to the interface, the situation is quite different. The density of polymer segments will be lower close to the interface compared to the bulk phase. This space is known as depletion zone around a colloidal particle (Dickinson, 1982b). When two colloidal particles with depletion zones approach each other, the concentration of solute in the gap between the two will be lower than that in bulk phase (Dickinson, 1982b). Therefore, the solvent molecules preferably diffuse out of the interparticle space resulting in an attraction between two particles in a phenomenon not too dissimilar to osmosis . This type of flocculation is called depletion flocculation (Figure 1.3) (Everett, 1988e).

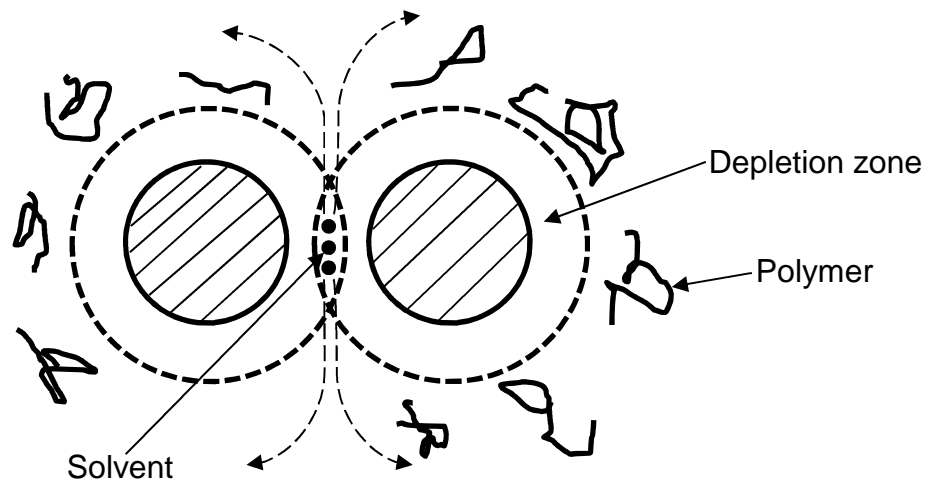


**Figure 1.3** A schematic illustration of depletion flocculation induced by unadsorbed polymers in bulk phase.

Depletion flocculation can be destroyed by diluting the bulk phase with solvent because this type of instability is driven by osmotic pressures. However, there is another kind of flocculation which cannot be easily destroyed upon dilution: so called bridging flocculation (Figure 1.4). Bridging flocculation is also induced by polymers which are adsorbed at the surface of particles, in the dispersion. There are several requirements for bridging flocculation (Dickinson, 1982b):

- Available anchor sites for polymers on the surface
- Available train and loop configurations of polymers on the surface
- Number of trains and loops are sufficient.

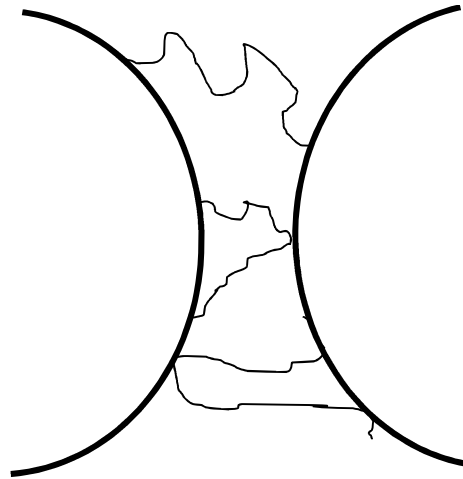


**Figure 1.4** A schematic illustration of bridging flocculation induced by polymers in bulk phase.

In contrast to depletion flocculation, low polymer concentration in bulk phase favours bridging flocculation. In order to avoid bridging flocculation in a colloidal system, it is critical to cover the surface of particle completely and minimize available anchor sites on the surface, when another particle approaches.

It is important to understand the mechanisms of stabilities and instabilities of a colloidal system. For example, it is possible to purify water and mineral waste by mixing certain polymers carefully at critical concentrations resulting in effective aggregation of a colloidal dispersion (Hunter, 2001). In such context, the polymers are often known as flocculants.

## **1.4 Emulsifiers and stabilizers**

In section 1.3 we have discussed the stability of colloidal systems. It is clear that emulsifiers and stabilizers play an important role in production of stable dispersions. In this section, we will focus on these components and their special functions in colloid science.

### **1.4.1 Definition and examples of emulsifiers**

It is essential to add emulsifying or foaming agents to aqueous phase in order to prepare a stable emulsion or foam because two immiscible phases will separate without any emulsifiers, after mixing, in a short period of time (Dickinson, 1982a). Therefore, as an emulsifier, it should possess certain stabilizing capacity in a colloidal system. Moreover, it is critical for emulsifiers to be surface active in order to lower the interfacial tension between two immiscible phases (Dickinson, 1992b; Shaw, 1991b). Lowering the interfacial tension by surface-active emulsifiers facilitates the formation of emulsions because during such a process a considerable amount of interfacial area is formed (Dickinson, 1992b; Shaw, 1991b).

There are generally two categories of emulsifiers in food: low-molecular-weight surfactants such as monoglycerides and macromolecules (e.g. proteins). For low-molecular-weight surfactants, there is a hydrophile-lipophile balance (HLB) value, estimating the emulsifying and stabilizing properties of a material in a colloidal system (Dickinson, 1992b). For example, high HLB value materials are suitable to stabilize an O/W emulsion because they are more hydrophilic and preferentially dissolve in the water containing phase (Dickinson, 1992b). On the other hand, low-HLB-value materials can be used in the W/O systems to confer sufficient stability (Dickinson, 1992b). Nevertheless, HLB system is too simplistic to be applied to complicated food matrix. First of all, HLB is based on a simple colloidal model which assumes stabilization by low-molecular-weight surfactants. Secondly, the interactions between surfactants in the system have not been considered in HLB evaluation system. In real food, colloidal systems are rarely stabilized by a single surfactant. Most food colloids are stabilized by macromolecules such

as proteins and even polysaccharides. However, emulsifiers and stabilizers can interact with each other in real foods. Therefore, HLB values cannot be adapted to real food systems very well.

For macromolecules to act as emulsifiers, these compounds have to be amphiphilic, so that the hydrophobic segments prefer to staying in the oil phase while the hydrophilic parts are located in the aqueous phase (Dickinson, 1992a). For example, proteins from milk are common emulsifiers in food industry. Hydrophilic amino acids such as arginine, lysine and aspartic acid in the primary structure of proteins preferably stay in the aqueous phase in O/W emulsions while amino acids with hydrophobic side chains such as isoleucine, leucine and valine are located just below the oil phase at the interface (Dickinson, 1992a). Once proteins are on the oil-water interface, they can confer relatively long-term stability. Therefore, proteins are not only considered as emulsifiers but also true colloidal stabilizers in food. The amphiphilic structure of proteins is the critical feature of the protein-polysaccharide conjugates as food emulsifiers and stabilizers in this project.

#### **1.4.2 Definition and examples of stabilizers**

Different from emulsifiers, stabilizers are not necessarily surface active. Stabilizers may or may not be adsorbed onto the interface. For example, polysaccharides are often used as food stabilizers by modifying the viscosity of continuous phase or gelation. Xanthan gum is a high-molecular-weight polysaccharide which can be used as a stabilizer only when an emulsion has already been prepared (Dickinson, 1992a). However, there is one type of natural polysaccharide (Gum Arabic) which has certain emulsifying properties owing to a small fraction of hydrophobic segments in its structure (Akhtar and

Dickinson, 2007). Nonetheless, if two droplets are brought into contact with each other, the presence of polysaccharides does not prevent their coalescence. This is what differentiates true colloidal stabilizers like protein from polysaccharides.

Polysaccharides are major components in most food. Generally they are hydrophilic due to presence of carboxyl and hydroxyl groups in their structures. These characteristics are the fundamental features for behaviour of protein-polysaccharide conjugates as stabilizers, especially for steric stabilization in O/W emulsions (Dickinson, 1992a).

In food emulsions, there is another possible means to stabilize a colloidal system, via so called Pickering stabilization (Dickinson, 1992a). Particles are adsorbed on the oil-water interface to form a layer to protect droplets from coalescences. A schematic illustration of Pickering stabilization in O/W emulsions is shown below (Figure 1.5):

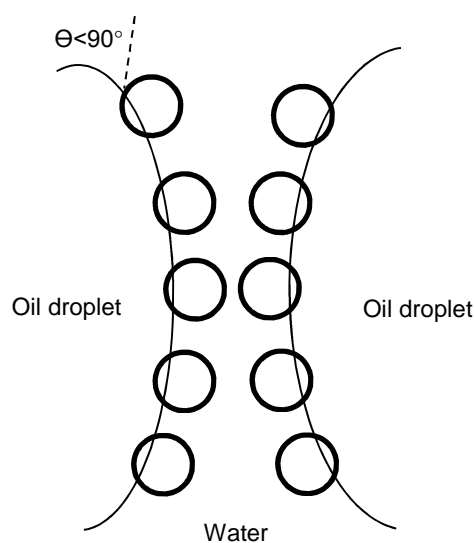


**Figure 1.5** A schematic illustration of Pickering stabilization in an O/W emulsion

In an O/W emulsion, to provide effective Pickering stabilization, the particles on the oil-water interface need to be preferentially wetted by the aqueous phase. In other words, the contact angle  $\Theta$  needs to be smaller than  $90^\circ$  on the oil-water interface. However, if the contact angle is larger than  $90^\circ$ , this type of particle cannot stabilize O/W emulsions, but are suitable for stabilizing W/O emulsions (Dickinson, 1992a).

Even though there are several differences between emulsifiers and stabilizers, the distinction is not entirely clear cut. For food colloid scientists, there are two critical questions to answer:

- What is the chemical structure of this material playing critical role in a colloidal system?
- What is the structure-function relationship of this material in a colloidal system?

Once we obtain the answers to these two questions, we can define with more confidence if the material is an emulsifier or a stabilizer.

## **1.5 Interfacial Activity**

An important feature of a colloidal system is the large area of the interface between two immiscible phases, owing to the extremely small volume of each dispersed particle and their great numbers. This characteristic plays a crucial role in the properties of a colloidal system. For example, the stability of a colloid is highly dependent on the behaviours of emulsifiers and stabilizers on the interface as we discussed in section 1.3. Therefore, it is essential to study the interfacial properties of a colloidal system and

adsorption process of surface-active molecules onto the interface especially at liquid-liquid interfaces.

### **1.5.1 Liquid-liquid interfaces**

Liquid-liquid interfaces are common in food colloids as for example in O/W or W/O emulsions. Molecules in bulk phase are attracted evenly by their neighbours through van der Waals interactions or perhaps hydrogen bonding in water or metal bonding such as in liquid mercury, whilst those molecules at the interface between phases experience unbalanced attractions from different types of surrounding molecules (Figure 1.6). These unbalanced attractive forces lead to a net inward pull in order to minimize the contact area. That is the main reason as to why water droplets or gas bubbles tend to adopt a spherical shape (Shaw, 1991b). Therefore, in order to increase the surface areas in a colloidal system, it is necessary to do extra work on the system. The required amount of work done to increase the interface by one unit area, is often defined as surface tension or surface free energy (Dickinson, 1992b). Surface tension is a key parameter to investigate interfacial properties in colloid science.

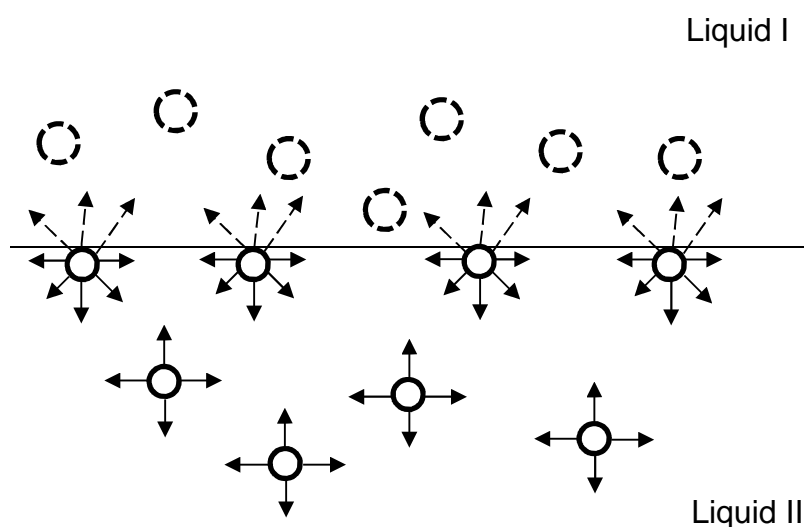


**Figure 1.6** Attractions between molecules in bulk phase and at the liquid-liquid interface

The typical surface tension between water and air is around  $73 \text{ mN}\cdot\text{m}^{-1}$  under room temperature ( $20 \text{ }^\circ\text{C}$ ). Under the same temperature, the interfacial tension between water and benzene is  $35.0 \text{ mN}\cdot\text{m}^{-1}$  which is similar to the surface tension between water and sunflower oil ( $\sim 30 \text{ mN}\cdot\text{m}^{-1}$ ) (Shaw, 1991b). If the hydrophobic phase is replaced with metal instead of organic solvents, the surface tension could be ten times higher. For example, the surface tension between water and mercury is  $375 \text{ mN}\cdot\text{m}^{-1}$  (Shaw, 1991b). The high surface tension between water and metal indicates that it is extremely difficult to increase the contact area between these two phases owing to the strong attraction between metal ions.

In the next section, we are going to study various methods to measure liquid-liquid interfacial tension. It is critical to determine an appropriate method to investigate the interfacial behaviours of proteins and protein-polysaccharide conjugates in this PhD project.

### **1.5.2 Measurement of interfacial tension**

There are many classic methods to determine the liquid-gas and liquid-liquid interfacial tensions including capillary rise method, Wilhelmy plate method, ring method and pendant drop method (Dickinson, 1982d). Some of these methods are static while others are detachment and dynamic. Generally speaking, static methods are more accurate than detachment methods. However, detachment methods are easier to perform than static ones (Shaw, 1991b).

Capillary rise method is a static method to offer accurate results of interfacial tensions (Dickinson, 1982d). It is usually used to measure the surface tensions between liquid and vapour. When a narrow capillary is placed into a liquid, there is a rise of this liquid following the capillary. The surface tension can be calculated by the inner diameter of this capillary tube, the height of rising liquid, the density difference between the liquid and air, and the contact angle (Dickinson, 1982d). The most challenging part of this method is to use a uniform capillary tube.

Different from capillary rise method, Wilhelmy plate method can be used in two different measurements: static model and detachment model (Shaw, 1991b). A microscope slide is partially immersed in the target liquid, and the other end of this slide is suspended from the arm of a balance. For detachment model, the liquid is gradually lowered till the point of detachment. At the same time, the pulling force is recorded by the balance (Dickinson, 1982d). For static model, it is often adopted to measure the change of surface tension especially during adsorption process (Dickinson, 1982d). Similar to Wilhelmy plate method, ring method is another way to measure surface tension by

detachment (Shaw, 1991b). The detachment force is related to the interfacial tension.

In the pendant drop method, a liquid drop is ejected and hung from a tip in air or continuous phase (Dickinson, 1982d). The interfacial tension can be obtained by measuring the projecting image of the shape of the hanging drop. The main advantage of this method is that all these calculations can be conducted by computers. The quality of optical arrangement plays an important role in measuring surface tensions because all the estimations depend on the projecting image of the drop (Dickinson, 1982d). Moreover, pendant drop method can also be used to investigate interfacial rheological properties of polymers such as protein films in dilation tests.

In this PhD project, pendant drop method is the major approach to investigate interfacial behaviours of whey protein isolate and its polysaccharide conjugates especially for studying the competitive adsorption to the oil-water interface.

### **1.5.3 Adsorption of macromolecules at interfaces**

The adsorption of amphiphilic compounds to the interface is critical to the stability of a colloidal system. Surface-active materials containing both polar and non-polar parts prefer to stay at the interface owing to their amphiphilic structures (Shaw, 1991b). The strong adsorption of surfactants at the interface can form a monomolecular layer. However, surfactant molecules are not permanently anchored at the interface. They can exchange with the molecules in the bulk phase under thermal motions. The final state is a result of a dynamic equilibrium at the interface (Shaw, 1991b).

When it comes to macromolecular adsorption, the process is more complicated (Dickinson, 1982e). Firstly, there are several possible positions for adsorption in one macromolecule. Secondly, various configurations may occur on the interface due to the size and flexibility of the polymer chain. When a polymer is adsorbed onto an interface, there are broadly three parts to the adopted configurations: train, loop, and tail (Figure 1.7) (Dickinson, 1982e).

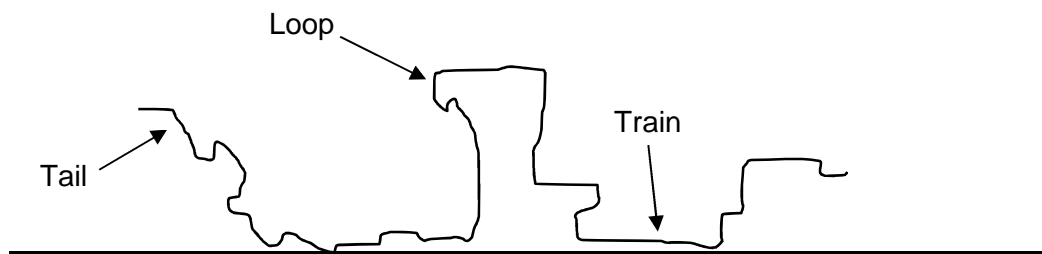


**Figure 1.7** 2-D configurations of macromolecules adsorbed on the interface

Tails, loops and trains on the interface are highly dependent on the interactions among monomers, surface and solvent. In food colloids, the most common macromolecules with surface activities are proteins which will adsorb onto many interfaces (Dickinson, 1982e). The stability relies on protein adsorption process and configurations on the interface significantly in protein-stabilized colloidal systems. Moreover, the protein adsorption and configurations are also affected by environmental conditions such as pH, temperature and ionic strength (Dickinson, 1982e). Apart from external factors, the structures of proteins are critical in adsorption process. Generally, there are two categories of proteins according to their structures: disordered proteins such as caseins and globular proteins (e. g. whey proteins). Caseins

are more flexible than globular proteins as they possess less secondary and tertiary structures. Structure flexibility is another critical element to influence protein adsorption.

Protein adsorption is a complicated process including three stages: diffusion-controlled stage, surface penetration stage and surface rearrangement stage (Dickinson, 1982e). The kinetics of protein adsorption is usually assessed by recording the time-dependent interfacial pressures which are the change of interfacial tensions from clean surface to the final equilibrium state. Furthermore, another parameter also useful to monitor protein adsorption is the surface coverage. Both interfacial tension and surface coverage are usually measured when studying protein adsorptions. In order to further illustrate the protein adsorption process, let us consider a globular protein, lysozyme, to demonstrate the three stages of adsorption.

At the initial stage of adsorption, the surface interfacial pressure is zero indicating no protein on the interface (Dickinson, 1982e). When the surface coverage increases with time, the interfacial pressure increases accordingly. However, at the very beginning of adsorption, the surface concentration increases significantly well before the interfacial pressure is detectable (Dickinson, 1982e). This indicates that there is little interfacial tension change when proteins have already been adsorbed onto the interface. A possible reason for this phenomenon is that it takes a noticeable period for the macromolecules to penetrate and rearrange on the oil-water interfacial region. On the contrary, disordered proteins such as  $\beta$ -casein do not have this delay in their interfacial pressure response at the initial stages (Dickinson, 1982e). The major reason for this adsorption difference is the flexibility of protein

chains. More flexible proteins are faster to adsorb at the oil-water interface and to reduce surface tension than globular proteins. In the first stage of adsorption, the surface is relatively clean, and the surface coverage by proteins is low. Therefore, for these disordered protein, adsorption is a rapid process mainly limited by the rate of molecular diffusion to the surface.

The adsorption rate significantly decreases when proteins are spread at the interface (Dickinson, 1982e). The adsorbed proteins have an inhibiting effect on further adsorption. The adsorbing proteins not only interact with the oil-water interface but also interact with other adsorbed macromolecules. Therefore, the adsorption in this stage is not controlled by diffusion alone.

In the final stage, the surface concentration becomes stabilized, which indicates that the surface is saturated with protein molecules. The interactions between adsorbed proteins become dominant at the last stage of adsorption. Strong intermolecular bonds may be formed in this concentrated protein film. At this stage the protein molecules are largely denatured (Dickinson, 1982e).

The kinetics of protein adsorption onto the oil-water interface is schematically illustrated in Figure 1.8. The properties of protein adsorptions onto the oil-water interfaces especially for globular proteins establish a solid foundation for investigation of interfacial behaviours of protein and protein-polysaccharide conjugates in O/W emulsions in this PhD project.

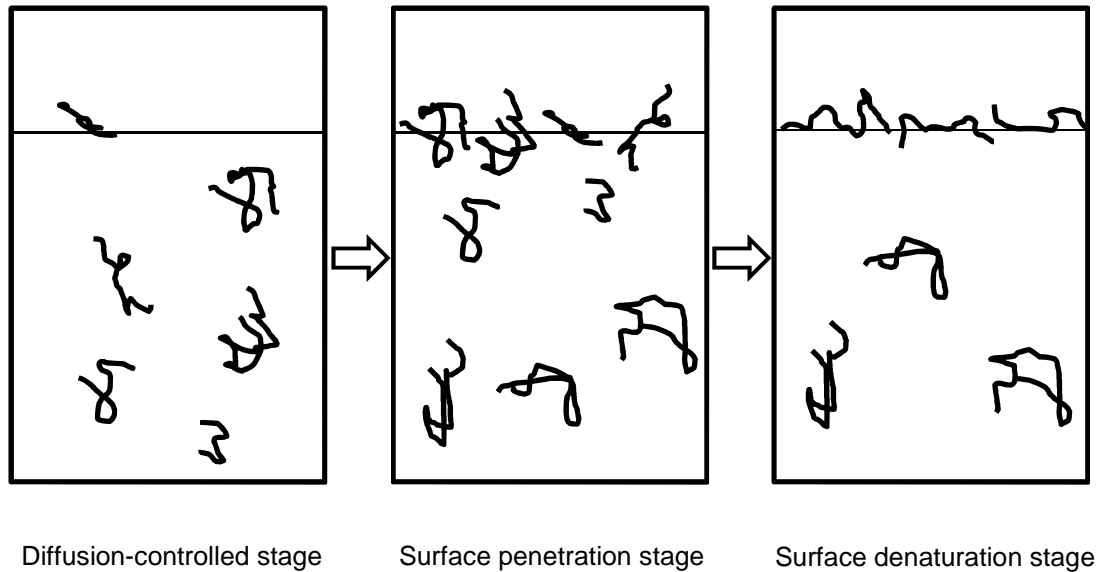


**Figure 1.8** Three stages of protein adsorption from the bulk phase to the interface.

## 1.6 Proteins, polysaccharides and conjugates

According to the scope of this research, it is necessary to concentrate on the proteins and their conjugates as emulsifiers and stabilizers in foods. Many food proteins can be used to emulsify and stabilize emulsions owing to their amphiphilic structures. On the other hand, polysaccharides are generally hydrophilic and less surface active than proteins, but usually utilized as food thickeners and gelling agents. If the emulsifying properties of proteins can be combined with the strong stabilizing properties of polysaccharides, it has a great potential to prepare a new polymer with enhanced functional properties. In this section, the fundamental properties of proteins and polysaccharides and previous researches about protein-polysaccharide conjugates will be reviewed and examined to establish the foundation for further investigations.

### 1.6.1 Background of proteins and polysaccharides

One of the major sources of food proteins is bovine milk which contains ~3.3 % (w/w) proteins (Fox, 2015; Oliver, 2011). Apart from the nutritional

value of milk proteins, they are of vital importance from the physicochemical perspective. Briefly, there are two categories in milk proteins: caseins (~75—85% of the total milk protein) and whey (~ 15—22% of the total milk protein) (Fox, 2015). Caseins comprise four species:  $\alpha_{s1}$ -,  $\alpha_{s2}$ -,  $\beta$ -, and  $\kappa$ -casein with the weight ratio of 4:1:4:1 in milk (Fox, 2015; Belitz, 2004). Moreover, caseins are disordered proteins, which are heat stable, with very few secondary structure whilst whey proteins, which will denature under thermal process over 60 °C, are quite heat-sensitive. The major component in whey proteins is  $\beta$ -lactoglobulin (~ 18.3 kDa) which is over 50% of the total whey in bovine milk. Whey proteins possess more three-dimensional structures including  $\alpha$ -helix and  $\beta$ -sheet than caseins (Fox, 2015).

Polysaccharides, which are high-molecule-weight polymers, in foods are usually used as thickeners to modify the viscosity of aqueous phase in order to stabilise emulsions. Generally, they are not surface active compared to proteins due to the lack of hydrophobic segments. However, natural polysaccharides demonstrate emulsifying properties, such as gum arabic (*Acacia senegal*) (Dickinson, 1992a). Gum arabic is a highly branched carbohydrate polymer comprising ~2% covalent-bonded proteins which are responsible for the surface activity to gum arabic. Furthermore, gum arabic has been already applied in soft drinks industry to emulsify citrus flavour oils (Dickinson, 1992a). Therefore, the example of natural gum arabic points to a direction to synthesise a compound from proteins and polysaccharides to improve emulsifying properties of native proteins.

### 1.6.2 Stabilizing mechanism of protein-polysaccharide conjugates

In order to produce sufficient steric stabilisation there are a couple of requirements for the polymers. First of all, the polymer should be amphiphilic to adsorb and strongly attach at the interface. Secondly, the adsorbed polymers should fully cover the interface to prevent such issues as bridging attraction. Finally, the solvent loving segments such as loops and tails of the adsorbed polymer should protrude into the solvent (Dickinson, 1982b).

Based on the discussion above, the covalent bonding via the Maillard reactions between proteins and polysaccharides may be expected to lead to an enhancement of protein functionality both as emulsifiers and stabilizers. The basic mechanism of the coupling could be illustrated in Figure 1.9 (Kato, 2002).

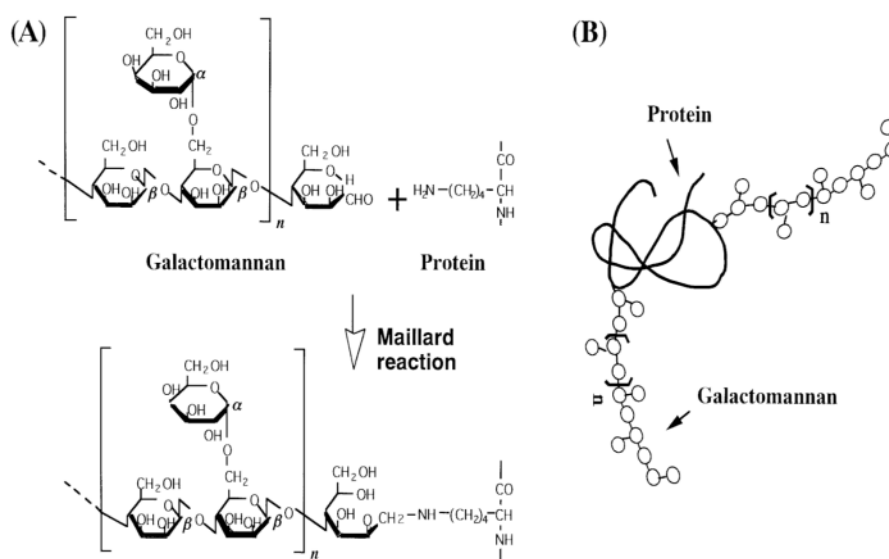


**Figure 1.9** (A) Basic chemical mechanism for the formation of protein-polysaccharide conjugates via Maillard reaction (B) the overview structure of the conjugate.

The major advantage of this linkage is maintenance of solubility and molecular integrity over a wide range of environmental conditions such as low pH and high ionic strength (Dickinson, 1982e). For example, gum arabic is a

natural glycoprotein, which has been applied to emulsification of citrus flavour oil in soft drinks and could be replaced by whey protein-maltodextrin conjugates as emulsifiers and stabilizers (Akhtar and Dickinson, 2007). This research suggests that the well-prepared protein-polysaccharide conjugates have a substantial improvement in emulsifying and stabilising properties compared to native proteins under both low and neutral pH. Furthermore, the conjugates exhibited an effective stabilisation of emulsion with colouring agents even after extensive emulsion dilution over several weeks (Akhtar and Dickinson, 2007).

When the protein-polysaccharide conjugates are formed via Maillard reaction, they can stabilise emulsions better than proteins alone due to the improved steric stabilisation especially under harsh environmental conditions such as low pH, high ionic strength and high temperature. The mechanism of this enhanced stabilisation is illustrated in Figure 3.2. The resilience of emulsions stabilised by such conjugates largely arises from the less dependence on electrostatic repulsion.

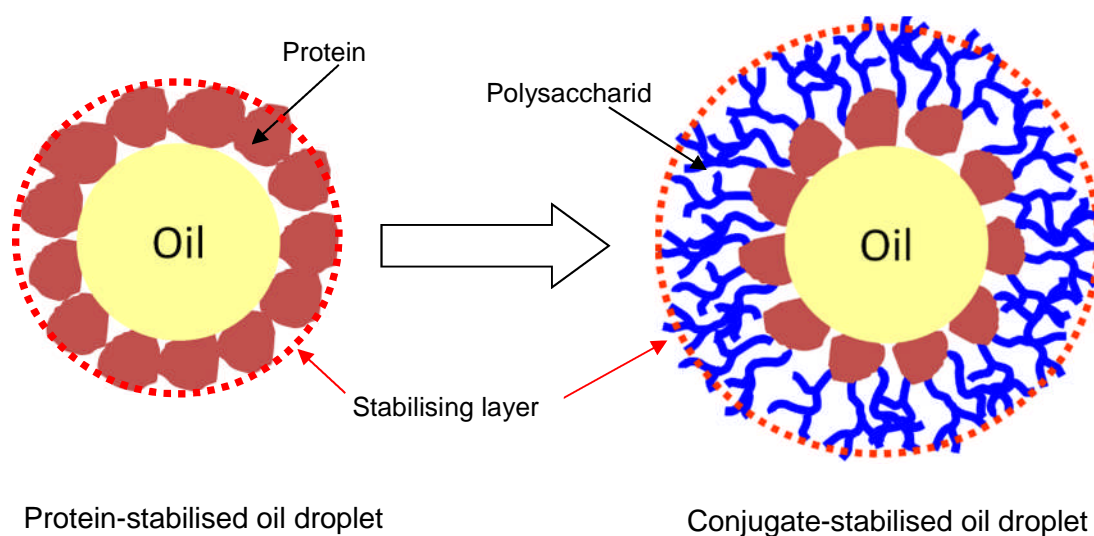


**Figure 1.10** Comparison between protein- and conjugate-stabilised oil droplet in O/W system. The red blocks represent proteins; the blue branches represent polysaccharides.

Also, as can be seen from Figure 1.10, the conjugate-stabilised droplet has thicker stabilising layer than protein-stabilised droplet, when the molecular weight of polysaccharide moiety is sufficiently large. In other words, the molecular weight of polysaccharide determines the thickness of steric stabilising layer.

### 1.6.3 Preparation methods of conjugates

Proteins used as functional ingredients in foods are predominantly from animals or animal products e.g. meat, eggs and milk whilst the other source is plants such as soy protein and pea protein. A large proportion of the research in protein-polysaccharide conjugates has concentrated on animal-derived proteins (caseins, whey, egg white) (Kato et al., 1990 & 1992; Jiménez-Castaño et al., 2007), although there have been some investigations on preparation of conjugates using plant proteins (Usui et al., 2004; Qi et al., 2009; Li et al., 2013). For the polysaccharides, dextran and maltodextrin were

the most popular options in all these experiments (Nakamura et al., 1991; Kato et al., 1992; Wong et al., 2009) while other saccharides were also adopted such as glucose, lactose and chitosan (Medrano et al., 2009; Gu et al., 2010; Usui et al., 2004).

There have been mainly two methods developed to prepare protein-polysaccharide conjugates in the last 25 years: dry-heating method and wet-heating method demonstrated in the following flow chart Figure 1.11.

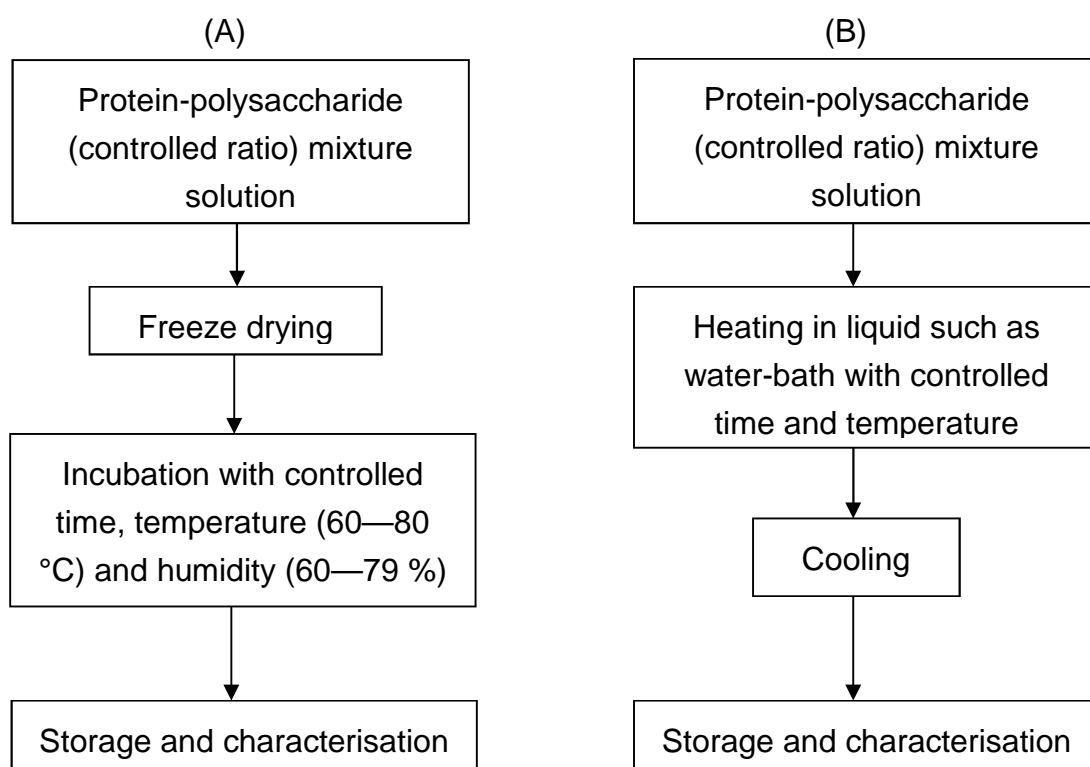


**Figure 1.11** Preparation of protein-polysaccharide conjugates via dry-heating and wet-heating pathways: (A) dry-heating pathway; (B) wet-heating pathway.

In 1990, an ovalbumin-dextran conjugate was prepared under controlled dry-heating method by a group of Japanese researchers (Kato et al., 1990). Two years later, a similar method was adopted to synthesize hybrids between three different proteins (11S globulin *vicia faba*, bovine serum albumin,  $\beta$ -

casein) and dextran in Procter Department of Food Science, University of Leeds (Dickinson and Semenova, 1992). Both of them carefully selected the incubation conditions as follows: temperature 60°C, relative humidity (RH) 65% and reaction time 3 weeks. These key parameters were established in the preparation of conjugates as a reference level for the following investigations. For example, the incubation conditions were changed to temperature 80°C, RH 79% in order to reduce the reaction time to 2 hours (Akhtar and Dickinson, 2003).

Compared to dry-heating method, the coupling between proteins and polysaccharides in aqueous solution through Maillard reaction was not investigated until 2008 (Zhu et al., 2008). Following this research, three more papers have been published using similar wet-heating method to synthesise protein-polysaccharide conjugates (Zhu et al., 2010; Mu et al., 2011; Niu et al., 2011). The main reason for adopting wet-heating method is to avoid the freeze-drying step before incubation because the freeze-drying process is energy- and time-consuming (Zhu et al., 2010; Mu et al., 2011). However, some researchers argued that dry-heating method is more desirable from an industrial point of view than the wet method because of the ease of handling and long-term storage in dry reactions (Oliver et al., 2006). Therefore, there are three major obstacles in preparation of protein-polysaccharide conjugates to delay their industrial application:

- energy-consuming freeze drying
- strict reaction conditions (temperature and RH)
- long reaction time (usually for weeks)

In order to eliminate the freeze-drying process, some other drying techniques could be considered as alternatives such as spray drying and roller drying (Oliver et al., 2006). In Chapter 5, a promising wet-heating method using Spinning Disc Reactor (SDR) to prepare protein-polysaccharide conjugates will be explored to tackle the current obstacles based on its high efficiency of heat transfer and continuous production.

#### **1.6.4 Functional properties of conjugates**

The main aim of synthesising protein-polysaccharide conjugates is to apply them to final products which can be enhanced in physico-chemical quality such as longer shelf-life. In order to achieve this aim, it is necessary to assess the functional properties of protein-polysaccharide conjugates including solubility, thermal stability, emulsifying, gelling and foaming properties before industrial application.

To be effective proteinaceous emulsifiers, sufficient solubility is a critical requirement (Halling, 1981). Nevertheless, the high solubility of proteins is usually difficult to achieve especially when environmental conditions are harsh. For instance, when pH of the aqueous phase is not far from pI, the solubility is markedly lower for most proteins. The conjugation between proteins and polysaccharides can improve the solubility of native proteins due to the hydrophilicity of the saccharide moieties in conjugates. A number of researchers have demonstrated the improvement of solubility of proteins after glycosylation (Akhtar and Dickinson, 2007; Qi et al., 2009; Mu et al., 2011). Akhtar M. and Dickinson E. (2007) reported that the solubility of whey proteins was significantly enhanced after coupling with polysaccharides around pI. The whey protein solution was turbid at pH 4.7, while the conjugate solutions

remained clear from pH 3.0 to 5.5 (Akhtar and Dickinson, 2007). Similarly, a considerable improvement in solubility of soy proteins coupled with acacia gum was observed compared to the mixture of protein-acacia gum without Maillard reaction (Mu et al., 2011). In contrast, the decrease of solubility in egg white protein-pectin conjugates were reported by Al-Hakkak and Al-Hakkak (2010).

Another important test for protein stability is to determine the heat resistance. Thermal treatment is nearly inevitable in food processing such as pasteurisation, which can lead to denaturation of proteins. Previously, many investigations suggested the improvement of protein thermal stability when grafted by polysaccharides (Shu et al., 1996; Jiménez-Castaño et al., 2007). All these observations suggested that a more stable structure was formed during Maillard reaction. It is likely to be the hindrance of denatured protein-protein interactions during heating by attached polysaccharides (Kato, 2002).

Generally, it is expected that protein-polysaccharide conjugates possess better emulsifying activity and stability than native proteins particularly at pH around pI. A large number of studies support this theory (Kato et al., 1990; Dickinson and Semenova, 1992; Shu et al., 1996; Akhtar and Dickinson, 2003; Sun et al., 2011). Furthermore, some critical parameters, which significantly influence the emulsifying properties of protein-polysaccharide conjugates, such as molecular weight of polysaccharide and the ratio between proteins and polysaccharides, have also been studied to a lesser extent.

It has been suggested that the molecular weight of polysaccharide plays an important role in emulsifying properties of protein-polysaccharide conjugates (Dickinson and Semenova, 1992; Shu et al., 1996; Akhtar and

Dickinson, 2007). An investigation by Shu et al. (1996) reported that the emulsifying properties of the conjugates (lysozyme-galactomannan) was enhanced significantly by increasing the molecular weight of the polysaccharide. The optimum molecular weight of the polysaccharide was identified to be 6 kDa. The emulsifying properties may not be improved by grafting polysaccharides of molecular weight less than 6 kDa (Kato, 2002). Similarly, conjugates between whey protein isolate and maltodextrin DE 19 ( $M_w = 8.7$  kDa) prepared by Akhtar and Dickinson, (2007) exhibited better emulsifying properties than conjugates with maltodextrin DE 2 and 47. This optimum molecular weight of polysaccharide (8.7 kDa) was very close to the value (10 kDa) suggested by Kato, (2002). Theoretically, protein-polysaccharide conjugates should possess better stabilising properties than pure proteins because the sugar moieties are fairly hydrophilic, which provide sufficient steric stabilisation. However, if the polysaccharide is too large, compared to proteins, it will affect the adsorption of the conjugates onto the oil-water interface detrimentally owing to the large molecular weight of conjugates. On the other hand, if the polysaccharide chains are too small, it may not be able to confer sufficient steric restriction at long enough droplet-droplet separation. Therefore, an optimum point should exist in the range of different length polysaccharide chains.

Apart from the size of polysaccharides, there is another important factor to affect the emulsifying properties of protein-polysaccharide conjugates: the molar ratio or weight ratio between proteins and polysaccharides. This key parameter was investigated by Dickinson and Semenova (1992), in their study on the protein-dextran hybrids with various molar ratios. Four years later, an investigation of lysozyme attached with 1 and 2 mol galactomannan,

respectively, showed that conjugates synthesised with higher proportion of polysaccharides may have better emulsifying properties than that with relatively low proportion of polysaccharides (Shu et al., 1996). Similarly, an improvement of emulsifying properties by increasing the proportion of polysaccharides from 1:0.5 to 1:3 (whey : maltodextrin, w/w) was studied by Akhtar and Dickinson, (2007). However, if the content of polysaccharides is above certain level, the non-linked polysaccharides may destabilise emulsions due to depletion flocculation (Lam and Nickerson, 2013). Therefore, it is critical to control the molar or the weight ratio between proteins and polysaccharides for the synthesis of effective conjugates.

Similar to emulsifying properties, gelling and foaming properties of protein-polysaccharide conjugates have also been reported to improve, compared to native proteins (Dickinson and Izgi, 1996; Matsudomi et al., 2002; Spotti et al., 2013). For gelling properties, research comparing the gels prepared by egg white protein-galactomannan conjugates and egg white protein alone, respectively, showed the increase of gel strength and water retention capacity (Matsudomi et al., 2002). Moreover, Spotti et al. (2013) reported that WPI-DX conjugate significantly enhanced the mechanical property of gels, which could be subjected to even 80% deformation in uniaxial compression test without fracture, far higher than the gel prepared by WPI-DX mixture without the Maillard reaction. In terms of foaming properties of protein-polysaccharide conjugates, it has been reported that conjugates between lysozyme and dextran lead to a dramatic improvement in foaming properties whilst there is a negative effect with  $\beta$ -casein-dextran conjugates (Dickinson and Izgi, 1996).

A conclusion can be drawn from the literature review that protein-polysaccharide conjugates prepared via Maillard reaction can enhance the functional properties of native proteins. Apart from these advantages, other properties of protein-polysaccharide conjugates have also been investigated such as antimicrobial property and masking allergen structure of proteins (Kato, 2002), but these will not be considered in the present project.

## **Chapter 2**

### **Theoretical and Experimental Methods**

#### **2.1 Introduction**

Many problems in colloid science, including those investigated here, are studied by applications of complementary theoretical and experimental methods. Theoretical methods are established according to physico-chemical theories such as thermal and statistical physics. Moreover, mathematical and statistical calculations are essential for theoretical methods to predict the trend of results. Once the theoretical model is established, it is quite efficient to estimate influence of various parameters on the behaviour of the system by modifying the initial input conditions. Apart from this advantage of theoretical methods, they are helpful to guide design of experiments in the laboratory, by providing convincing predictions in advance. However, theoretical models do have their own limitations, such as the often necessary oversimplification of real systems. Therefore, results from theoretical estimations on their own are normally not sufficient to discover the true and full picture of problems arising in colloid science.

Experimental methods are inevitably important in colloid research. The solid understanding of the colloidal state of matter is heavily dependent on experimental results. These methods are mainly from techniques developed in physics and chemistry. For example, particle sizing is a key technique to investigate the property of dispersions or emulsions. Light-scattering methods are quite popular to measure the particle size due to the reliability and convenience of these techniques. Not only can physico-chemical techniques be used in colloid science, but other experimental methods are also helpful

such as centrifugation in biology (Dickinson, 1982d). Experimental methods are usually time-consuming processes including labour, and in some cases, significant funds. The combination of theoretical and experimental methods is a powerful research toolbox which is illustrated in Figure 2.1.

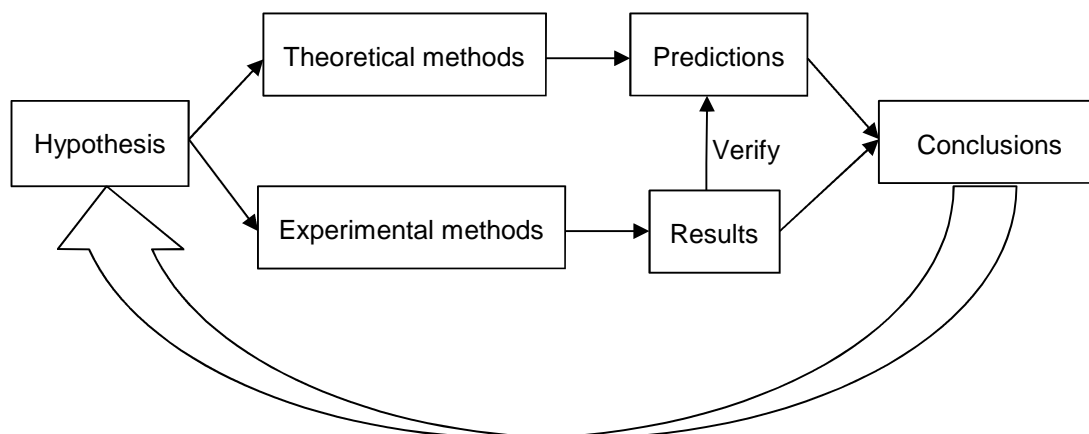


**Figure 2.1** Schematic illustration of theoretical and experimental methods cooperatively applied to research cycle.

In this PhD project, both experimental and theoretical methods were used to study the properties of protein-polysaccharide conjugates. Results from these methods offer an enhanced understanding of the problem. The rest of this chapter will discuss the theoretical model (SCF) and experimental methods used in the current work. These include light-scattering techniques, rheological and microscopic methods. In the last section of this chapter, the relationships between various methods will be discussed, leading to overall project methodology.

## 2.2 Theoretical calculations

In this project, theoretical calculations are established on the principles of thermodynamics. It is first necessary to cover some basic theories and

simple models in thermal physics, before introducing the technique of Self-Consistent-Field (SCF), which is the main theoretical tool used in this project.

### **2.2.1 Thermal and statistical physics**

Thermal physics is a study of the fundamental principles of materials from astronomical objects down to small electronic systems on nanoscales. It bridges the macroscopic and the microscopic worlds. The powerful tool in thermal physics is statistics, due to the large number of moving particles atoms, molecules, etc., in the system. In a system containing an enormous number of objects, thermal physics tries to investigate the macroscopic behaviour of this collection of particles from properties of individual entity. An important concept in doing so is “entropy”, which is defined as proportional to the logarithm of the number of microstates in a system (Kittel, 1980b). Dependent on entropy and the energy of a system, temperature can be defined (Kittel, 1980b). From entropy, temperature, and free energy, other thermodynamic quantities of interest can be obtained, such as pressure and chemical potential.

In order to understand the general statistical properties of a system, a simple binary model system can be used to demonstrate the point. The binary system is widely accepted to apply well to real physical systems. The binary system can be used to mimic the adsorption of monomers on a hydrophobic interface. The binary system is presented as follows (Kittel, 1980a):

In a binary system, there are  $N$  separate sites. Each site has a molecule with a spin which can take two configurations, either pointing up or down with magnetic moment  $-m$  or  $+m$ , respectively.

↓	↑	↓	↑	↓	↓	↑	↓	↓	↑
↓	↓	↑	↓	↑	↓	↓	↓	↓	↓
↑	↑	↓	↑	↑	↑	↓	↑	↑	↓
↓	↑	↓	↑	↑	↓	↑	↓	↓	↑

**Figure 2.2** Binary model with different magnetic spins.

If this system is placed in a magnetic field of which the energy is  $B$  and the direction is up, the net energy of this binary system is

$$U = B \cdot (-m) \cdot (N_{\uparrow} - N_{\downarrow})$$

where  $N_{\uparrow}$  is the number of sites with up conformation and  $N_{\downarrow}$  is the number of cells with down conformation. In order to simplify the calculation, a parameter  $s$  is introduced to represent the number of  $N_{\uparrow}$  and  $N_{\downarrow}$ . Such that

$$\frac{1}{2}N + s = N_{\uparrow} \quad \frac{1}{2}N - s = N_{\downarrow}$$

$$N_{\uparrow} - N_{\downarrow} = \left(\frac{1}{2}N + s\right) - \left(\frac{1}{2}N - s\right) = 2s$$

Therefore, the net energy of the system can be presented as follows:

$$U = B \cdot (-m) \cdot (2s) = -2smB$$

There are many ways of averaging the spins, up or down, that can lead to the same net value of the system energy. At certain system energy, the multiplicity of the system at certain energy level can be calculated by the parameters  $s$  and the total sites number ( $N$ ). The multiplicity function  $g(N, s)$ , which is the number of microstate that all have the same energy value, is

$$g(N, s) = \frac{N!}{\left(\frac{1}{2}N + s\right)! \left(\frac{1}{2}N - s\right)!}$$

When  $N \gg 1$ ,  $\ln N! \cong N \ln N - N$ , according to Sterling approximation (Kittel, 1980a). Therefore,

$$\begin{aligned} \ln[g(N, s)] &= \ln \left[ \frac{N!}{\left(\frac{1}{2}N + s\right)! \left(\frac{1}{2}N - s\right)!} \right] \\ &= [N \ln N - \left(\frac{1}{2}N + s\right) \ln \left(\frac{1}{2}N + s\right) - \left(\frac{1}{2}N - s\right) \ln \left(\frac{1}{2}N - s\right)] \end{aligned}$$

As mentioned above entropy was related to logarithm of the number of microstates. Therefore, entropy  $S$  is

$$S = k_B \cdot \ln[g(N, s)]$$

$k_B$  is Boltzmann constant (Kittel, 1980b).

Based on the definition of Helmholtz free energy (Kittel, 1980c),

$$F = U - TS$$

and the free energy of this binary system can be presented as follows:

$$F = -2smB - k_B T \ln[g(N, s)]$$

When the free energy is at its minimum, the whole system will be at the equilibrium state, at a given temperature  $T$  (Kittel, 1980b). In other word,

$$\frac{\partial F}{\partial s} = 0$$

$$\begin{aligned} \frac{\partial F}{\partial s} &= -2mB - k_B T \left[ -\ln\left(\frac{1}{2}N + s\right) - \left(\frac{1}{2}N + s\right) \cdot \frac{1}{\left(\frac{1}{2}N + s\right)} + \ln\left(\frac{1}{2}N - s\right) \right. \\ &\quad \left. - \left(\frac{1}{2}N - s\right) \cdot \frac{1}{\left(\frac{1}{2}N - s\right)} \cdot (-1) \right] \\ &= -2mB + k_B T \ln \left[ \frac{\left(\frac{1}{2}N + s\right)}{\left(\frac{1}{2}N - s\right)} \right] = 0 \end{aligned}$$

∴

$$s = \frac{e^{\frac{2mB}{k_B T}} - 1}{e^{\frac{2mB}{k_B T}} + 1} \cdot \frac{N}{2}$$

Therefore, for a given number of sites ( $N$ ), this binary system placed in a magnetic field ( $B$ ) under temperature  $T$ , reaches the equilibrium state when:

$$N_{\uparrow} = \frac{1}{2}N + s = \frac{N}{1 + e^{\frac{-2mB}{k_B T}}}$$

$$N_{\downarrow} = \frac{1}{2}N - s = \frac{N}{1 + e^{\frac{2mB}{k_B T}}}$$

From the calculations above, we can make a reliable prediction of the macroscopic properties (in this case the magnetic moment) of our system from the behaviour of individual spins on a microscopic scale, under certain given conditions, temperature  $T$  and field  $B$ . Similarly, we can apply this binary

system to also describe the adsorption of monomers onto a hydrophobic interface, under different conditions.

Again, we assume that there are  $N$  sites available for monomer adsorption on the oil-water interface. The adsorption energy for each monomer is  $\varepsilon$ , while if the monomer is not adsorbed, the energy is 0. When the whole system reaches its equilibrium state, there will be  $n$  sites occupied by monomer. It is  $n$  that we wish to obtain from this model of adsorption. The surface coverage can be defined as

$$\theta = \frac{n}{N}$$

The total energy for adsorbed monomers is

$$U = \varepsilon \cdot n$$

and the total entropy on the surface similarly to the binary system discussed previously, is

$$S = k_B \ln \frac{N!}{n! \cdot (N - n)!}$$

The total free energy of this system is

$$F = U - TS + (G_b - n\mu)$$

where  $G_b$  is the free energy in the bulk phase with no monomer adsorbed, and  $\mu$  is the chemical potential for each monomer in the bulk phase (Kittel, 1980c).

When the whole system attains the equilibrium state,

$$\frac{\partial F}{\partial n} = 0$$

$$F = \varepsilon n - k_B T [N \ln N - n \ln n - (N - n) \ln(N - n)] + G_b - n\mu$$

$$\begin{aligned} \therefore \frac{\partial F}{\partial n} &= \varepsilon + k_B T \left[ \ln n + n \cdot \frac{1}{n} - \ln(N - n) + (N - n) \cdot \frac{1}{(N - n)} \cdot (-1) \right] - \mu \\ &= \varepsilon + k_B T \ln \frac{n}{N - n} - \mu = 0 \end{aligned}$$

Therefore, the surface coverage is calculated to be

$$\theta = \frac{n}{N} = \frac{1}{1 + e^{\frac{\varepsilon - \mu}{k_B T}}}$$

In a diluted system, the chemical potential can be estimated by the bulk concentration  $[c]$  based on Henry's Law (Kittel, 1980c).

$$\mu = \mu^* + k_B T \ln[c]$$

where  $\mu^*$  is the chemical potential of the pure monomer. Therefore, the surface coverage can be calculated from the monomer bulk concentration  $[c]$ .

$$\theta = \frac{n}{N} = \frac{1}{1 + e^{\frac{\varepsilon - \mu}{k_B T}}} = \frac{[c]}{[c] + e^{\frac{\varepsilon - \mu^*}{k_B T}}} = \frac{K_H [c]}{1 + K_H [c]}$$

where  $K_H$  is a constant known as Henry's constant which equals to  $e^{\frac{-\varepsilon + \mu^*}{k_B T}}$ .

All these statistical calculations in thermal physics are helpful for scientists to predict the collective behaviour of an extremely large number of objects in a system. When it comes to real colloidal systems, more conditions are essential to be considered to make a meaningful prediction, such as interactions between monomers. In next section, the Self-Consistent-Field model will be presented to estimate the adsorption of polymers on the interfaces.

### 2.2.2 Self-consistent-field theory

The application of Self-Consistent-Field theoretical calculations to polymer systems, dates back to early sixties when advanced theories of

polymer physics were first being developed (Edwards, 1965). However, for complicated polymers such as co-polymers, or polymers with more complex architectures, those early implementations are not suitable. It was the scheme proposed by Scheutjens and Fleer that allowed such more complex polymers to be applied to systems of interest here, including disordered proteins (Scheutjens and Fleer, 1979 & 1980).

The improved SCF calculations have been successfully applied to various biopolymers such as proteins especially for disordered milk proteins (e.g. caseins) (Akinshina et al., 2008; Ettelaie et al., 2014a). There are various types of amino acids with different side chains that make them hydrophobic, charged and polar uncharged residues. The distribution of these amino acid monomers along the backbone can significantly influence the colloidal stabilizing properties of the chains when adsorbed on hydrophobic interfaces. For example, if the hydrophobic segments are at one end of the polypeptide chain, while the hydrophilic ones are at the other end, this type of polymer can have excellent stabilizing properties, as a diblock polymer (Ettelaie, 2003). In this project, SCF model will be used to estimate the stabilizing properties of protein-polysaccharide conjugates as a complex biopolymer. The model is structured as follows.

The calculation envisages two flat plates immersed in a solution containing polymers. The distance between the two plates is denoted as  $L$ . The concentrations of polymers between these two plates will not be uniform owing to the interactions between polymers and the two flat plates. Furthermore, the concentration profile of polymers will fluctuate around some mean value at any given point in the gap. For each concentration profile, there is a free energy associated accordingly. The free energy is the key indicator

to determine the probability of the occurrence of its associated concentration profile. Based on the thermodynamic principles, the profile with the minimum free energy has the highest probability of occurrence. Indeed given the high number of degrees of freedom, as with other thermodynamic systems, this profile with lowest free energy can be taken to dominate the thermodynamic behaviour of our system.

It must be stressed that SCF is not a simulation but rather numerical calculation performed on a computer. For the purpose of numerical calculations, it is necessary to discretize the gap into grid points. In the scheme proposed by Scheutjens and Fleer (1980) the grid size is taken as the nominal monomer size (typically  $a_0 \sim 0.3$  nm here). This is useful, as it also connects the model to the earlier lattice models of polymers, such as Huggins-Flory model (Huggins, 1941; Flory, 1985). The lattice model as applied to the space between the two plates is shown in Figure 2.3. The space is divided into basic cubes with length of  $a_0$ .

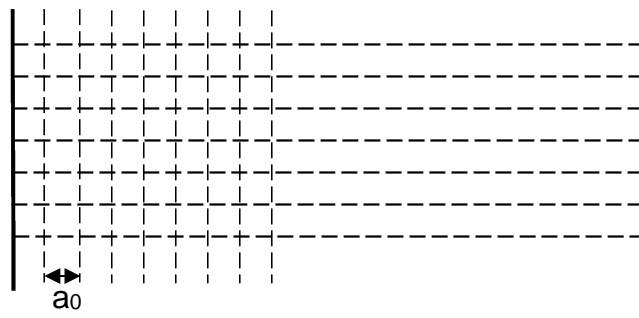


**Figure 2.3** Lattice model separating the space between two flat plates into basic cubes.

Each cell can be occupied by a solvent molecule, an ion, or a protein residue, but no site can remain empty. All of these components in the system are influence by the potential of mean force which is determined as a derivate of the free energy. This mean force is the result of averaged interactions experienced by any monomer, due to the presence of neighbouring residues. There are three major parts in the potential energy  $\psi^\alpha(z)$  for each item  $\alpha$  at layer  $z$ : the hard-cord term  $\psi_{hc}(z)$ , short-range interactions  $\psi_{int}^\alpha(z)$ , and the longer-ranged electrostatic interactions  $\psi_{el}^\alpha(z)$  (Akinshina et al., 2008).

$$\psi^\alpha(z) = \psi_{hc}(z) + \psi_{int}^\alpha(z) + \psi_{el}^\alpha(z)$$

The total volume fraction  $\varphi$  added together for all species has to be 1. The first item  $\psi_{hc}(z)$  in the above equation is the same for any type of species. This interaction enforces the incompressibility condition, i.e. total  $\varphi$  being equal to 1, in each layer. The second item  $\psi_{int}^\alpha(z)$  is the short-range interactions which can be calculated as follows:

$$\psi_{int}^\alpha(z) = \sum_{\beta=0}^N \chi_{\alpha\beta} (\langle \varphi^\beta(z) \rangle - \Phi^\beta) + (\delta_{z,1} + \delta_{z,r}) \chi_{\alpha S}$$

where  $\chi_{\alpha\beta}$  is the Flory-Huggins parameter between species of type  $\alpha$  and  $\beta$ , or for  $\chi_{\alpha S}$  the type  $\alpha$  and the surface (Ettelaie et al., 2014a). The quantity  $\Phi^\beta$

is the volume fraction of specie  $\beta$  in the bulk phase.  $\delta_{z,1}$  and  $\delta_{z,r}$  are the Kronecker symbols. When  $z = 1$  and  $z = r$ , the Kronecker numbers are 1. Since a monomer placed in layer  $z$ , interacts with neighbouring monomers in layer  $z + 1$  and  $z - 1$ , as well as  $z$ , for the purpose of calculating the interactions the volume fractions have to be suitably averaged over these layers.  $\langle \varphi^\beta(z) \rangle$  is denoted and given by

$$\langle \varphi^\beta(z) \rangle = \lambda_{-1}\varphi^\beta(z - 1) + \lambda_0\varphi^\beta(z) + \lambda_{+1}\varphi^\beta(z + 1)$$

In this cubic lattice model,  $\lambda$  is the fractions of neighbours in each adjacent layers,  $\lambda_{-1} = \lambda_{+1} = \frac{1}{6}$  and  $\lambda_0 = \frac{4}{6}$  because there are 4 neighbours at layer  $z$  while just one neighbour in each of the layers  $z - 1$  and  $z + 1$  (Ettelaie, et al., 2014a).

For the long-ranged electrostatic interactions,  $\psi_{el}^\alpha(z)$  is calculated by multiplying the charge of species  $\alpha$  and the electrostatic potential of mean force. The electrostatic potential has a relationship with the charge density  $\rho(z)$  as given by the Poisson equation:

$$\varepsilon_0\varepsilon_r\nabla^2\psi_{el}^\alpha(z) = -\rho(z)$$

where  $\varepsilon_0$  is the permittivity of vacuum;  $\varepsilon_r$  is the relative dielectric permittivity of solvent; and is the  $\nabla^2$  Laplacian operator (Ettelaie et al., 2014a).

In order to calculate the potential of mean force, it is essential to obtain the density profile  $\varphi^\alpha(z)$ , which itself is dependent on the potential of mean force  $\psi^\alpha(z)$ , for all the specie types in each layer. This then suggests an iterative process to solve the problem. Firstly, a rough guess of  $\varphi^\alpha(z)$  or  $\psi^\alpha(z)$  is made, as the starting point. This process is continued until convergence is obtained and the values of  $\varphi^\alpha(z)$  and  $\psi^\alpha(z)$  no longer change

substantially from one iteration step to the next. Then, iterations calculate  $\psi^\alpha(z)$  from  $\varphi^\alpha(z)$  and then  $\psi^\alpha(z)$  back from  $\varphi^\alpha(z)$ .

For a simple monomer, the starting point can be as follows:

$$G^\alpha(z) = e^{-\psi^\alpha(z)}$$

where  $G^\alpha(z)$  is the probability for the  $\alpha$  type monomer, in layer  $z$ . Following this starting point, the density profile  $\varphi_i(z)$  can be calculated by  $G_i(z)$  where  $i$  stands for different monomers such as solvent molecules or ions.

$$\varphi_i(z) = \Phi_i G_i(z)$$

When it comes to linear polymers consisting of  $N_i$  monomers, the probability  $G_i(z, s)$ , which is defined as the probability of  $s$ -mer ( $s$  from 2 to  $N_i$ ) of finishing in layer  $z$  the  $s^{\text{th}}$  monomer of our polymer, can be related to the probability of  $(s - 1)$ -mer  $G_i(z, s - 1)$  according to

$$G_i(z, s) = G_{ti(s)}(z) [\lambda_{-1} G_i(z - 1, s - 1) + \lambda_0 G_i(z, s - 1) + \lambda_{+1} G_i(z + 1, s - 1)]$$

where  $t_i(s)$  equals to the type  $\alpha$  of the  $s$ -th monomer, on backbone of polymer  $i$ . For example, the starting point of polymer  $i$ ,

$$G_i(z, 1) = G_{ti(1)}(z)$$

The equation connecting  $G_i(z, s)$  to  $G_i(z, s - 1)$  arises due to the connectivity of the polymer. If  $s^{\text{th}}$  monomer is in layer  $z$  then  $(s-1)^{\text{th}}$  monomer clearly has to be either in layer  $z - 1$ ,  $z$ , or  $z + 1$ .

Similarly, we denote the probabilities  $G'_i(z, s)$ , which begins from segment  $s = N_i$  to  $s = 1$  in polymer  $i$ , with the length of  $N_i$ . If the polymer is symmetric,  $G'_i(z, s) = G_i(z, s)$  since the first  $s$  monomers of the chain are

identical to the last  $s$  monomers (Ettelaie et al., 2014a). Polymers in real colloidal systems such as proteins rarely meet this requirement. Therefore, it is necessary to calculate the probabilities from first monomer to the end and also in reverse from the last monomer to the first one. When both values are obtained, the volume fraction  $\varphi_i^\alpha(z)$  of type  $\alpha$  belonging to polymer specie  $i$ , at certain layer  $z$ , is given as follows:

$$\varphi_i^\alpha(z) = \frac{\Phi_i^\alpha}{N_i} \sum_{s=1}^{N_i} \frac{G_i(z, s) G_i'(z, N_i - s + 1) \delta_{\alpha, ti(s)}}{G_{ti(s)}(z)}$$

Here  $\Phi_i^\alpha$  is the volume fraction of type  $\alpha$  monomers forming part of polymer specie  $i$ , in the bulk phase;  $\delta_{\alpha, ti(s)}$  is the Kronecker symbol (if  $\alpha = ti(s)$ ,  $\delta = 1$ ; for other conditions,  $\delta = 0$ ).

In this project, we focus on protein-polysaccharide conjugates which can be considered as a linear chain with one or more side chains. The presence of a side chain presents additional complication that needs to be included in the calculations above. Therefore, in order to account for these additional factors in SCF calculations, we have to generalize the calculations further. It is possible to do this for chains with a single branch point without too much difficulty.

After the self-consistent calculations of equations above, the potential  $\psi_\alpha(z)$  and density profiles  $\varphi_\alpha(z)$  can be reached. The iterative calculations will not be completed until the convergence is obtained with a certain accuracy. Based on the thermodynamic law, the system should stay at the minimum free energy state when it reaches the equilibrium state. Indeed it can be shown that this iterative process yields the potential and volume fraction profiles that minimize the free energy of the system.

Formally the free energy of the system for any density profile can be expressed in terms of  $\varphi^\alpha(z)$  and  $\Phi^\alpha(z)$  as follows (Ettelaie and Akinshina, 2014):

$$\begin{aligned}
 U(r) = & \sum_i \sum_\alpha \left[ - \sum_{z=0}^r \frac{1}{N_i} [\varphi_i^\alpha(z) - \Phi_i^\alpha] - \sum_{z=0}^r \varphi_i^\alpha(z) \psi^\alpha(z) \right] \\
 & + \sum_i \sum_\alpha \chi_{\alpha s} (\varphi_i^\alpha(0) - \varphi_i^\alpha(r)) \\
 & + \frac{1}{2} \sum_{ij} \sum_{\alpha\beta} \sum_{z=0}^r \chi_{\alpha\beta} (\varphi_i^\alpha(z) - \Phi_i^\alpha) (\varphi_j^\beta(z) - \Phi_j^\beta) + \frac{1}{2} \sum_z^r \sigma(z) \psi_{el}(z)
 \end{aligned}$$

Here the units of  $U(r)$  are  $k_B T$  per monomer area ( $a_0^2$ ), with  $r$  being the distance from the surface. All the components between the two surfaces and monomer types included in the above are summation to find the minimum free energy.

There are two major limitations of SCF calculations. First of all, the polymers in SCF model are star-like components with one possible branching point per each chain. However, the structure of protein-polysaccharide conjugates can be more complicated than polymers in the model used here in SCF calculations, because there are many available sites for the attachment of reducing polysaccharides in one protein molecule. Moreover, the model polymers in SCF are assumed to be disordered, such as caseins, without any secondary structure. In reality, secondary structures in whey proteins are quite common. Apart from the limitation of mimicking the structures for real globular protein molecules, SCF calculations concern solely the equilibrium state of the system. As such, any kinetic properties of the system cannot be predicted by the SCF model. Nonetheless, where the interest is on equilibrium properties,

and for denatured or disordered proteins, SCF has provided an excellent theoretical tool with which useful predictions can be made.

### 2.2.3 SCF calculation procedure

The iterative calculations in SCF model were mainly conducted by an in-house developed computer programme, “Betamo”. In order to obtain the potential and density profiles for each component in the system, it is important to input the information regarding all components in the system. Such data includes polymer lengths, monomer type, sequence, interaction parameters between all different residues and concentrations in the bulk. These input parameters are essential in order for the programme to calculate the density profile variation in the gap between two hydrophobic surfaces. For example, between two hydrophobic flat plates, there is a single type of linear polymer which contains 500 identical monomers having hydrophilic properties. The density profile for this model polymer can be obtained via SCF calculation and is presented in graph of Figure 2.4.

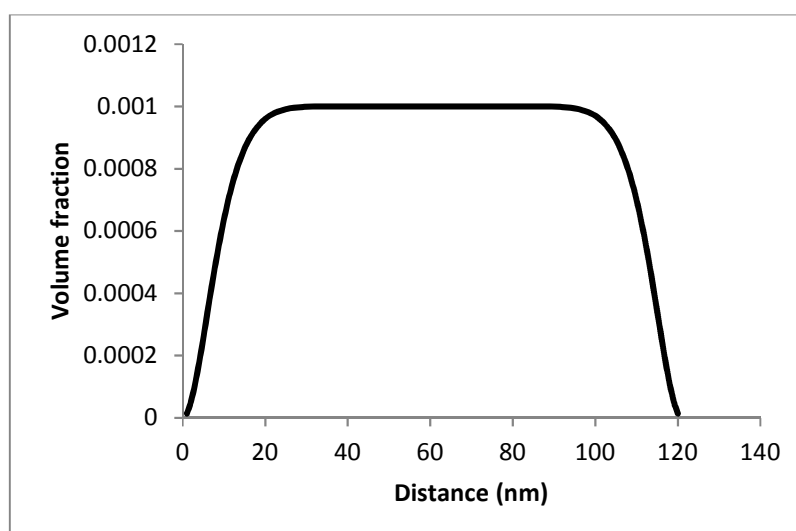


**Figure 2.4** Density profile of a hydrophilic model polymer (bulk volume fraction 0.001) between two hydrophobic surfaces calculated via SCF model.

The graph shows the concentration of the polymer in this example at different distances within the surface gap between the two surfaces. The gap was taken here at 120 nm. At the larger surfaces next to either distance 0 or 120 nm, there is no hydrophilic polymer present. When one moves away from the surface, the concentration of the hydrophilic polymer starts to increase until the bulk concentration 0.001 is attained in the middle of the gap, far from both surfaces. The results from SCF calculations are quite compatible with the experimental observations. Similarly, by calculating the value of free energy at different gap sites, one can determine the interaction potential, mediated by the presence of polymers, between the plates as function of plate-plate separation distance.

When the SCF model is applied to model “protein-polysaccharide conjugates” in O/W emulsion systems, the input file will be much longer than that in the above simple case. The details of SCF application in this PhD project will be described in Chapter 3.

## **2.3 Experimental Methods**

### **2.3.1 Introduction**

Experiments are major and reliable techniques to study the behaviour of food colloid systems. Predictions from theoretical models have to be verified by independent and carefully designed experiments. Results from experiments are not only used to develop theoretical models but also push forward the boundary of our knowledge. In this section, the key experimental methods adopted in this PhD project will be discussed.

### 2.3.2 Particle sizing methods

In order to fully investigate the properties of a colloidal system, determining the size distribution of dispersed particles is essential (Dickinson, 1982d). The particle-sizing methods for a colloidal system are often based on light-scattering behaviour of the particles. When light passes through a droplet in a dispersion, there are various interactions between the light waves and the droplet.

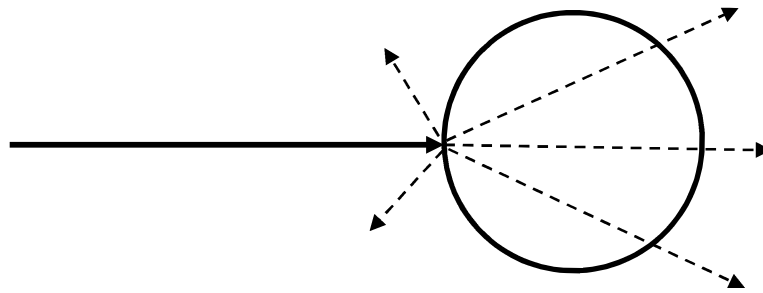


**Figure 2.5** Schematic illustration of light travelling from the homogeneous medium to a droplet.

In Figure 2.5, the light can be scattered on the surface of the droplet, or adsorbed by the droplet, or refracted, changing the direction of travel, as it passes through the droplet. When the environmental conditions, such as the material of the droplet, the intensity and direction of coming light, and the temperature, are fixed, the light-scattering profile of the system can be used to predict the size of the dispersed droplet.

In this project, the particle-sizing tasks were mainly conducted by the Mastersizer 3000 from Malvern Panalytical company. The basic mechanism of particle sizing by Mastersizer 3000 is presented in Figure 2.6.

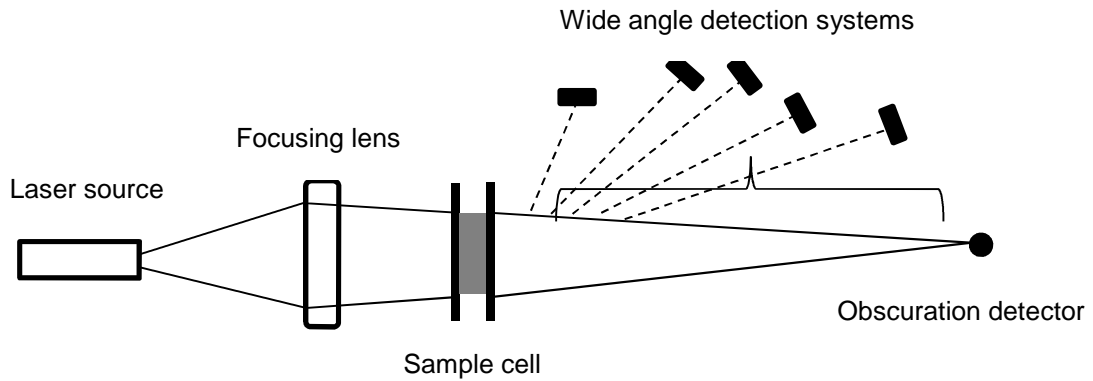


**Figure 2.6** Schematic illustration of Mastersizer 3000 for particle sizing.

There are two main parameters measured to predict the size of the particles in the sample: scattering angle and intensity. Generally, large particles have relatively small scattering angles with high scattering intensities, while small particles have larger scattering angles but with low scattering intensities (Dickinson, 1982d). In Figure 2.6, the system contains a laser source, to provide a consistent and intense light with fixed wavelength, and a group of detectors to measure the light pattern produced over a wide range of angles. The particle size distributions are then estimated by comparing a sample's scattering pattern with an appropriate optical model such as Fraunhofer and Mie Theory (Dickinson, 1982d).

The Fraunhofer theory assumes that the particles are opaque and scatter light at narrow angle. Therefore, it is only suitable for large particle sizes. Compared to the Fraunhofer model, Mie Theory predicts scattering intensities for all particles. It estimates the primary scattering from the surface of the particle with the intensity predicted by the refractive index difference between the particle and that of the dispersion medium. Furthermore, it also predicts the secondary scattering that results from the light refraction occurring within

the particle (Dickinson, 1982d). The instrument adopted in this project for particle size analysis (Mastersizer 3000) is based on Mie Theory.

For O/W emulsion systems in this project, the dispersed oil phase is sunflower oil with absorption parameter 0.001 and refractive index of 1.460. The average droplet size was calculated by volume moment mean  $d[4,3]$  defined by

$$d[4,3] = \frac{\sum_i n_i d_i^4}{\sum_i n_i d_i^3}$$

where  $n_i$  is the number of droplets with diameter  $d_i$ . The volume moment mean  $d[4,3]$  is a key indicator of the stability of an O/W emulsion at different storage times (Akhtar and Dickinson, 2003). Not only can the average droplet size be obtained via Mastersizer 3000, but also droplet size distribution can be measured. The distribution profile of particle sizes provides more information about the emulsion stability than the average of droplet size itself. For average droplet size, it simply uses one number to represent a group of droplets with various sizes. Compared to average droplet size, the distribution profile can show the full picture of the complicated system by estimating the volume density for each size class for all the droplets. Therefore, both mean droplet size and droplet size distributions are used in this project to estimate the stability of an emulsion system.

### **2.3.3 Rheological methods**

Rheology is the study of deformation of a material under an applied external force. The deformation is usually scaled in accordance to the size of the system and as such is called strain, while the force is divided by the surface area to which it is applied, which is named as stress. Therefore,

rheology is a subject to discover the relationship between the stress and the strain. Moreover, during experiments involving the shearing of certain colloidal systems, the relationship between shear stress  $\tau$  and shear strain  $\gamma$  can be presented as follows:

$$\tau = f(\gamma, \dot{\gamma}, T, p, \dots)$$

where  $\dot{\gamma}$  is shear rate;  $T$  is temperature;  $p$  is pressure (Dickinson, 1982f & 1992c).

For a simple relationship between shear rate and shear stress involving a linear relationship in a fluid, the sample is said to be a Newtonian liquid (Dickinson, 1992c). The viscosity  $\eta$  of the Newtonian liquid, which is constant under any shear rate, can be calculated as follows:

$$\eta = \frac{\tau}{\dot{\gamma}}$$

The common example of a Newtonian liquid in food is distilled water under room temperature. The Newtonian behaviour of distilled water indicates that complicated structures such as gel cannot be formed by water molecules under hydrogen bonding only (Dickinson, 1992c).

Compared to the Newtonian liquids, most food materials are shear-thinning systems, which means that the viscosity of the material declines when the shear rate increases. The decrease of viscosity under higher shear rate is mainly due to the breakdown of inner structure of the material as a result of the application of external stress. The other main type of non-Newtonian behaviour is named shear-thickening which is the opposite to shear-thinning behaviour. For a shear-thickening system such as corn flour dispersion, the increase of shear rate leads to an increase of the viscosity (Dickinson, 1992c).

The power law model is widely used to describe the relationship between shear stress and shear rate for both Newtonian and non-Newtonian fluids, more generally:

$$\tau = k\dot{\gamma}^n$$

where  $k$  is called the consistency index; and  $n$  the flow behaviour index which determines the type of fluid:  $n < 1$  for shear thinning;  $n = 1$  for Newtonian;  $n > 1$  for shear thickening (Dickinson, 1992c).

As we discussed above, there is a clear relationship between the flow behaviour and the inner structure of the colloidal system. For example, if an emulsion has Newtonian properties similar to distilled water, it suggests that there is few complicated structures such as flocculation and gelling. In other words, this indicates that this emulsion has a good level of colloidal stability. On the other hand, if the emulsion behaves as a shear-thinning liquid, then this suggests that certain degree of instability is occurring in the system, and that droplets are flocculating.

In this project, the rheological properties of emulsions were measured via Rheometer from Anton Paar. This Rheometer is a rotational shear equipment with cone and plate measuring geometries between which a sample of fluid is placed. The shear rate is controlled by the adjustable motor, and the shear stress is measured via a torque spring, accordingly. The basic mechanism on which a rheometer is based is presented in Figure 2.7.

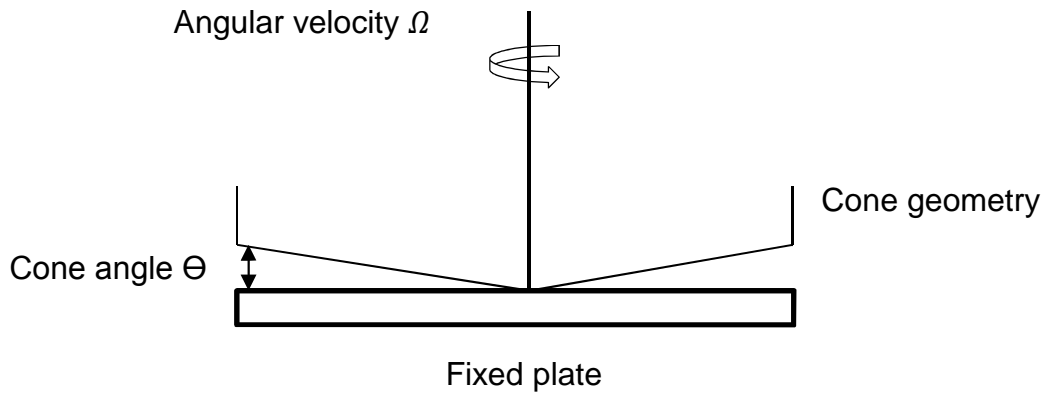


**Figure 2.7** Schematic illustration of Rheometer with cone geometry in shearing experiment.

In Figure 2.7, the cone angle is 2 degree. When cone angle ( $\Theta$ ) is small, the shear stress and the shear rate are constant throughout the sample, which means that every part of the sample experiences the same shearing force at the same time. The shear rate and shear stress are calculated as follows:

$$\dot{\gamma} = \frac{\Omega}{\theta}$$

$$\tau = \frac{3M}{2\pi\alpha^3}$$

where  $\Omega$  is angular velocity;  $M$  is the torque;  $\alpha$  is the radius of the cone geometry (Dickinson, 1982f). Based on these equations, the shear rate is only determined by the angular velocity and the cone angle while the shear stress is only dependent on the size of the geometry and the torque.

However, this rotational shear equipment has some disadvantages. First of all, it only can test low viscosity materials to avoid sticking between the upper cone and the fixed plate. Secondly, it is difficult to control the temperature during the experiment. Apart from these drawbacks, the evaporation of samples during the test cannot be entirely eliminated, because

of the relatively long experimental time needed. This is particularly an issue for samples that are sensitive to the volume fraction of water.

In this project, all tested emulsions are at low viscosities and not sensitive to the evaporation of water.

### 2.3.4 Interfacial tension methods

There are many experimental methods to measure the interfacial tension (see 1.5.2). In this project, the interfacial tension measurement was conducted by optical contact angle and contour analysis (OCA). The basic mechanism of OCA is presented in Figure 2.8.

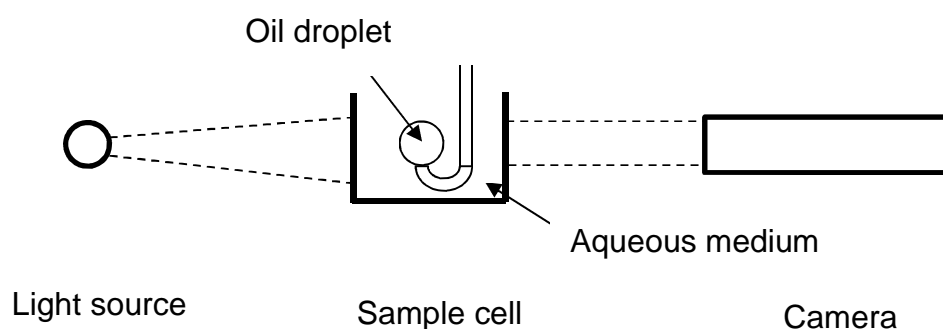


**Figure 2.8** Schematic illustration of OCA for interfacial tension analysis of oil-in-water system.

In Figure 2.8, the oil droplet is injected into the aqueous medium by a syringe with an upward bended needle. A light passes through the sample cell and is captured by the camera. The image of the oil droplet in the aqueous medium is obtained by the computer for interfacial tension calculations. The OCA can monitor the dynamic profile of interfacial tensions of the system over a long period of time. This is quite crucial for investigating the interfacial

behaviours of macromolecules such as proteins because large polymers take long time to reach their equilibrium adsorbed state.

However, there are several drawbacks of OCA tests for determination of interfacial tension. Firstly, it requires high standard of cleanness of the sample cell and syringe, because the interfacial tension is quite sensitive to the presence of surfactants or emulsifiers even at very low concentrations. Secondly, the evaporation of aqueous phase cannot be completely eliminated, which will influence the volume fraction of water in the aqueous medium. The last disadvantage is that OCA tests are relatively time consuming techniques.

### **2.3.5 Other experimental methods**

There are many other experimental methods adopted in this project apart from the one above. For protein-polysaccharide conjugates preparation, there are two categories: dry-heat and wet-heat preparation. The conjugates used in this project were mainly prepared by dry-heat Maillard reactions. The wet-heat treatment for conjugates preparation was also explored via the Spinning Disc Reactor (SDR) discussed in Chapter 5. The details of conjugate preparation (e.g. reaction time, temperature, and humidity etc.) will be discussed in Chapters 3, 4, and 5, respectively.

Following the conjugates preparations, it is essential to confirm the success and determine the degree of conjugation. Methods from other fields such as Biology and Food Chemistry are used. For example, electrophoresis (SDS-PAGE) was used to monitor the molecular weight change before and after heat treatment. Furthermore, results from HPLC also provided valuable information to support the formation of conjugates. The spectrophotometer is

another powerful tool to analyse the conjugates and determine the degree of conjugation.

The degree of conjugation is determined by analysing the reduction of free amino groups in proteins after conjugation because free amino groups are the major available sites for reducing polysaccharides attachment during the Maillard reactions.

There are, in general, two methods to determine free amino groups: 2,4,6-Trinitrobenzenesulfonic acid (TNBS) method (Nakamura et al., 1991; Kato et al., 1992; Shu et al., 1996; Jiménez-Castaño et al., 2007; Al-Hakkak and Al-Hakkak, 2010; Álvarez et al., 2012; Li et al., 2013) and the o-phthalaldehyde (OPA) test (Xu et al., 2010; Mu et al., 2011; Sun et al., 2011; Markman and Livney, 2012; Spotti et al., 2013). The chemical mechanism underlying the TNBS method is that the TNBS reagent reacts with the amino groups to form orange-coloured compound which can be analysed at a wavelength of 335nm via a spectrophotometer (Adlernissen, 1979). The reaction can be illustrated as follows (Figure 2.9):

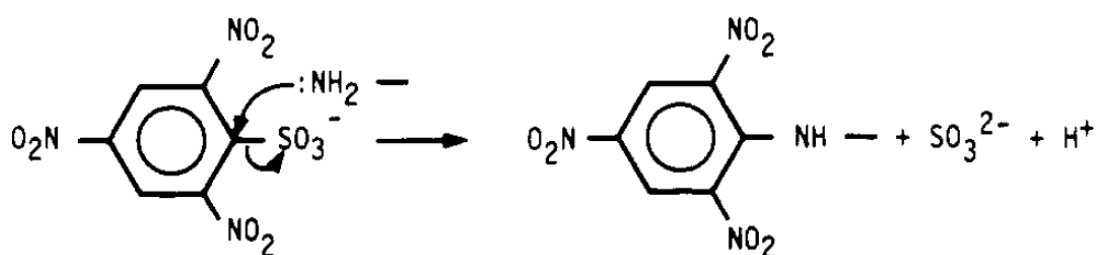


**Figure 2.9** A schematic illustration of reaction between TNBS and amino groups.

The TNBS method is well established and widely accepted for determination of free amino groups during protein hydrolysis. However, there

are several disadvantages of the TNBS method (Nielsen et al., 2001). Firstly, it is a time-consuming analysis, which takes one hour before measuring absorbance. Additionally, the TNBS reagent is toxic and difficult to handle because of the risk of explosion. Moreover, the TNBS reaction is sensitive to light, which develops a colour which disturbs measurements. Therefore, a new method using o-phthalaldehyde (OPA) was developed by Nielsen et al. (2001).

The OPA method was adopted to monitor the proteolysis of milk proteins in dairy science (Church et al., 1983), which can be summarized as in Figure 2.10 (Nielsen et al., 2001).

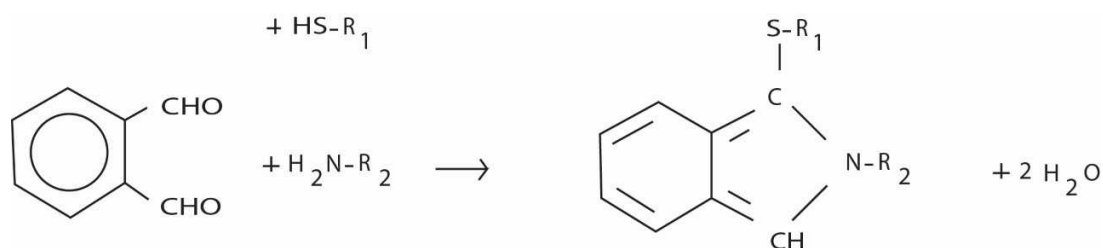


**Figure 2.10** A chemical reaction of OPA with SH- and NH<sub>2</sub>- groups to form detectable compound at 340nm.

OPA method is relatively easy and quicker than the TNBS reaction. Additionally, the OPA reagent is more stable and environmentally friendly than the TNBS reagent. Therefore, the OPA method was selected in this project to monitor the changes in the number of free amino groups in protein-polysaccharide conjugates. The calculations of degree of conjugation will be detailed in following chapters separately.

Imaging techniques are another group of methods used in support of the conclusions of this project, including pictures from digital cameras and confocal laser microscopy. Images can directly present the properties of

samples such as colour, shape, and size, which can also be used as evidence to support the argument arrived at by other techniques.

## **Chapter 3**

### **Competitive Adsorption and Stabilizing Properties of WPI and WPI-MD19 Conjugates on Oil-water Interface**

#### **3.1 Introduction**

Both proteins and protein-polysaccharide conjugates are surface active. Whey protein isolate (WPI) is an effective emulsifier by itself, particularly at pH values away from its isoelectric point, lower salt concentrations and in the absence of extensive heat treatment. When conjugates are prepared via Maillard reactions, it is inevitable to leave some unreacted WPI in the process. This is especially true if such preparation is carried out on large industrial scale. If it happens that the surface becomes dominated by unreacted WPI, while most of the conjugates remains in the aqueous phase, the enhanced steric stability from the conjugates will be significantly compromised. Therefore, it is crucial to investigate the competitive interfacial behaviour of WPI and conjugates in emulsion systems. In this chapter, both theoretical calculations and experiments were conducted to discover whether and to what extent the conjugates on the interface can be displaced by native proteins.

#### **3.2 Materials and Methods**

##### **3.2.1 Theoretical calculations**

Theoretical calculations were based on the SCF model and were carried out using an in-house developed programme available for both Linux and Windows based platforms. In this calculation, there are two proteins and two conjugates present in the system:  $\beta$ -lactoglobulin,  $\alpha$ -lactalbumin,  $\beta$ -lactoglobulin-MD19, and  $\alpha$ -lactalbumin-MD19.  $\beta$ -lactoglobulin and  $\alpha$ -

lactalbumin are the major components in WPI, and when they are modified by medium chain length maltodextrin with Dextrose Equivalent (DE) number 19 they lead to the protein-polysaccharide conjugates. Even though both proteins are globular proteins with a large degree of secondary structure, the higher level structures will be partially destroyed during Maillard reactions under heat treatment. Therefore, in the SCF model, the secondary structures of proteins and conjugates will not be considered, which means that we assume the proteins are linear polypeptide chains. Moreover, there is another assumption that the polysaccharide is attached at the first available amino acid lysine from the N-terminus because of the limitation in the complexity of polymer structures that can be tackled by the current implementation of SCF program in the in-house developed program.

Initially, the primary structures of the four polymers were keyed in the Input file. For example, the amino acids in  $\beta$ -lactoglobulin were categorized into five groups based on their physicochemical properties: hydrophobic, polar non-charge, positive charged, histidine, and negative charged. There are 162 amino acids in the primary structure of  $\beta$ -lactoglobulin (Figure 3.1) (Ettelaie et al., 2014a).



two monomers; and if  $\chi > 0$ , it means that these two types of monomers prefer not to be in contact, e. g.  $\chi_{1,3} = 2.5$ .

**Table 3.1** Flory-Huggins Interaction Parameters ( $K_B T$ ) between Monomer Types and  $pK_a$  Values for Charged Amino Acid Residues

Monomer type	0	1	2	3	4	5	6	7	Surface
0-Solvent	0	1	0	0	0	0	-1	-1	0
1-Hydrophobic residues	1	0	2.0	2.5	2.5	2.5	2.5	2.5	-2.0
2-Polar residues	0	2.0	0	0	0	0	0	0	0
3-Positive residues	0	2.5	0	0	0	0	0	0	0
4-Negative residues	0	2.5	0	0	0	0	0	0	0
5-Histidine	0	2.5	0	0	0	0	0	0	0
6-Positive charged ion	-1	2.5	0	0	0	0	0	0	0
7-Negative charged ion	-1	2.5	0	0	0	0	0	0	0
Surface	0	-2.0	0	0	0	0	0	0	0
$pK_a$	-	-	-	10	4.5	6.75	-	-	-

As can be seen in Table 3.1, the unfavourable interactions occur mainly between hydrophobic residues and other types of monomers, except for the interaction between the surface and hydrophobic residues (i.e.  $\chi = -2.0 K_B T$ ). A value of  $\chi \sim -1$  to  $-2 k_B T$  is typical of the hydrophobic interactions. As for charged ions, both of them show affinity for solvent molecules represent the tendency for such ions for hydration. The  $pK_a$  values are used to calculate the charge of both positively and negatively charged amino acids residues. Using the same calculations the pI of protein, i.e. pH when the net charge of the protein polymer is zero, can also be determined.

For protein-polysaccharide conjugates, the primary structure of protein is the same as unmodified proteins. The only difference is that there is a polysaccharide attachment (length = 77 monomer) at the 8<sup>th</sup> amino acid residues from the N-terminus side which is a lysine (Figure 3.1). The length of polysaccharide was estimated by the ratio between molecular weight and cubic unit ( $a_0$ ) in beta-lactoglobulin. For beta-lactoglobulin, it is approximately

8.8 kDa/a<sub>0</sub>. Therefore, the length of MD19 can be worked out around 77 a<sub>0</sub>. According to the hydrophilic properties of polysaccharide chains, the Flory-Huggins parameter between polysaccharide monomer and other types of monomer is zero except for hydrophobic residues (i.e.  $\chi_{1,PA} = 2.5$ ).

Systems containing various polymers were tested in the SCF model to obtain the potential energy of the colloidal system when two hydrophobic surfaces are approaching each other. The variation of the polymer volume fraction profiles can also be obtained. Results from individual polymers and polymer mixtures were generated via the SCF based program numerically. Experiments were designed and conducted to confirm or disprove the prediction of the SCF model.

### **3.2.2 Key materials for experiments**

After the theoretical calculations by SCF model, it is necessary to conduct experiments based on the theoretical estimations. The first experiment is the preparation of WPI-MD19 conjugates. The lactose-free whey protein isolate (WPI) powder was offered by Davisco Foods International (USA). The maltodextrin DE19 ( $M_w = 8.7$  kDa) (MD19) was purchased from the Roquette Ltd. (France) The sunflower oil was obtained from local supermarket Morrison (Leeds, UK). Other chemicals and reagents used in this project were of Analytical grade.

### **3.2.3 Preparation of WPI-MD19 conjugates**

The whey protein isolate (WPI) and maltodextrin DE19 (MD19) were fully dissolved in 100ml distilled water with gentle stirring under room temperature under the weight ratio of 1:2 (WPI : DE19). The solution was stored in the fridge (4 °C) overnight and frozen at – 30 °C for 3 hours. After the frozen

process, the solid solution was freeze dried for a period of 24 hours. The resulting powder of WPI and MD19 mixture was placed in a pre-heated desiccator under 80 °C for 3 hours, with relative humidity set to 79% controlled by saturated KBr solution. When the heat treatment was accomplished, the complex of WPI and MD19 was stored in a dark and dry place for further applications.

### **3.2.4 Confirmation of successful conjugation**

It is important to determine the attachment of polysaccharides to protein polymers after the Maillard reactions. There are two major methods to achieve this. The qualitative method involves the use of sodium dodecyl sulphate polyacrylamide gel electrophoresis (SDS-PAGE). Electrophoresis technique, especially SDS-PAGE, is widely applied to confirm the formation of protein-polysaccharide conjugates (Shu et al., 1996; Xu et al., 2010; Liu et al., 2012; Akhtar and Dickinson, 2003 & 2007). The pre-treatment of proteins by SDS before electrophoresis masks the native charge of proteins. Therefore, the mobility of proteins during electrophoresis is only dependent on the molecular weight of the proteins (Laemmli, 1970). The molecular weights of protein conjugates are higher than the native proteins when covalent bonding occurs between the proteins and the polysaccharides. The intensity band of protein conjugates, compared to pure proteins, will increase due to the formation of the conjugates.

However, only qualitative analysis is not sufficient to confirm the formation of conjugates between WPI and MD19. The quantitative method was also used to estimate the degree of conjugation (DC). It was determined by o-phthalaldehyde (OPA) tests of protein-polysaccharide conjugates

through monitoring the loss of free amino group after the Maillard reaction. The OPA reagent was prepared based on the previous literature (Nielsen et al., 2001). The WPI-ND19 conjugate was dissolved into distilled water with gentle stirring at a concentration corresponding to a WPI content of 1.0 mg/ml. For each prepared solution, 0.4 ml of the sample was added to 3 ml OPA reagent mixing on a Topmix at 1600 rpm for 5 seconds. The mixture was allowed to stand for exactly 2 mins at room temperature before its absorbance at a wavelength of 340 nm was measured using a spectrophotometer. The baseline was established by untreated pure WPI solution. The degree of conjugation for this complex can thus be calculated as follows:

$$\text{Degree of conjugation \%} = \frac{C_{WPI} - C_{nConj}}{C_{WPI}} \times 100\%$$

where  $C_{WPI}$  is the concentration of native WPI and  $C_{nConj}$  is the concentration of unreacted WPI in the conjugate sample. The analysis was carried out in triplicate.

### **3.2.5 Interfacial properties of WPI-MD19 conjugates**

After confirmation of the formation of WPI-MD19 conjugates, it is necessary to investigate the behaviours of WPI and WPI-MD19 conjugates on the oil-water interface. The capacity of WPI and WPI-MD19 in reducing the interfacial tension was measured by optical contact angle and contour analysis (OCA) (See Section 2.3.4). The oil phase was purified from sunflower with activated magnesium silicate (Florisil®, Fluka) to eliminate free fatty acids and surface active impurities at the weight ratio of 2:1 (oil : Florisil®). The mixture was stirred for 3 hours and centrifuged at 4000 rpm for 30min. For the aqueous phase, WPI or/and WPI-MD19 conjugates were mixed in distilled

water under gentle stirring at room temperature. The dynamic changes of interfacial tension at the oil-water interface were monitored. The plateau interfacial tensions at equilibrium states were also recorded.

### **3.2.6 O/W emulsion preparation**

Oil-in-water emulsions were prepared to test the stabilizing properties of WPI and WPI-MD19 mixtures at various weight ratios (Table 3.2). The aqueous buffer (500 ml) was prepared by mixing citric acid (3.125 g) and sodium chloride (2.920 g) into distilled water. Sodium azide was also added to the aqueous buffer at the concentration 0.1 % (w/v) as a preservative. The appropriate amount of protein-polysaccharide conjugates were dissolved into the aqueous buffer by gentle stirring at room temperature. The concentration was chosen so as to ensure a total protein (WPI) concentration of 1 % (w/v), including both unreacted and the protein in conjugated form. When the dissolution process was complete, the clear solution and sunflower oil were added to the mix by the high-speed blender at the volume ratio of 80 : 20 in order to prepare a coarse O/W emulsion. The coarse emulsion was passed through the Microfluidics M110P homogenizer under 1500 bar three times. The pH of fine emulsions after homogenization was adjusted to 4.6 by adding a few drops of 6 M NaOH, before these were stored quiescently at 30 °C.

**Table 3.2** Stabilizers of WPI and WPI-MD19 at Different Weight and Molar Ratios to be Utilized in O/W Emulsions

Conjugate weight percentages (%)	WPI (g)	WPI-MD19 (1:2 w/w) (g)	$\beta$ -LG : $\beta$ -LG-MD19* (Mole)
100	0	3 = 1 + 2 (WPI + MD19)	0
80	0.2	2.4 = 0.8 + 1.6	01:14.4
60	0.4	1.8 = 0.6 + 1.2	01:05.4
40	0.6	1.2 = 0.4 + 0.8	01:02.4
20	0.8	0.6 = 0.2 + 0.4	01:00.9
0	1	0	1

\*: Mw of  $\beta$ -LG is 18.4 kDa; Mw of  $\beta$ -LG-MD19 is 27.1 kDa (The assumption is that there is only one polysaccharide chain attached to each protein.)

In order to compare the theoretical results from SCF, the complicated structure of WPI-MD19 conjugate was simplified by the assumption that there is only one MD19 chain coupled with a single  $\beta$ -LG polymer which is the major component in WPI.

### 3.2.7 Emulsion stability monitoring

The emulsion stability can be a preliminary indication of the competitive adsorption of WPI and WPI-MD19 at the oil-water interface especially when the electrostatic effect is minimized i.e. pH = pI. If the oil droplet surfaces were dominated by WPI, the emulsion stability would be weak at this pH. However, if the native protein cannot fully displace WPI-MD19 on the interface, the emulsion will be stable. This is because the main component of repulsion force between droplets is electrostatic for former, while it is steric for latter. The emulsion stability was assessed under different stresses: pH, time, NaCl, and heat treatment. The major parameters to evaluate the emulsion stability are average droplet size (ADS) ( $d[4,3]$ ), droplet-size distributions (DSD) and flow behaviour of emulsions. The particle sizing of emulsions was performed using a Malvern Mastersizer 3000. The average droplet size  $d[4,3]$  is defined as

$$d[4,3] = \frac{\sum_i n_i d_i^4}{\sum_i n_i d_i^3}$$

where  $n_i$  is the number of droplets with diameter  $d_i$ . The droplet-size distributions can also be obtained from the same Mastersizer.

The flow behaviour of emulsions can also reflect the stabilizing properties of different stabilizers under various shear rates. In this study, emulsions were heated up to 85 °C in the water bath for 2 hours and cooled down to room temperature of around 25 °C. The relationships between viscosity of each sample and shear rate were recorded by the Rheometer (Discovery HR-2-TA), over shear rates from 0.001 to 1000 s<sup>-1</sup>.

### **3.2.8 Statistical analysis**

Data obtained from OPA analysis, interfacial tension measurements,  $d[4,3]$ , DSD and rheological measurements were analysed by using MS Excel<sup>®</sup> 2017 for the average values and their standard deviations of triplicates.

## **3.3 Results and Discussions**

In this section, all the results from theoretical calculations and experiments will be presented and discussed. The results will be shown according to the structure of section 3.2.

### **3.3.1 Predictions of theoretical model**

The theoretical calculations were conducted for various combinations of proteins and conjugates from a single type polymer systems to one containing four different kinds simultaneously. The environmental conditions such as pH and ionic strength were fixed at pH = 4.97 and [NaCl] = 0.01 (v/v) in order to minimize the electrostatic stabilizing effect and be close to the

cases where real protein stabilized emulsion become unstable. The interaction potential mediated between two colloidal particles were calculated within each type of solution, plotted as a function of particle-particle separation.

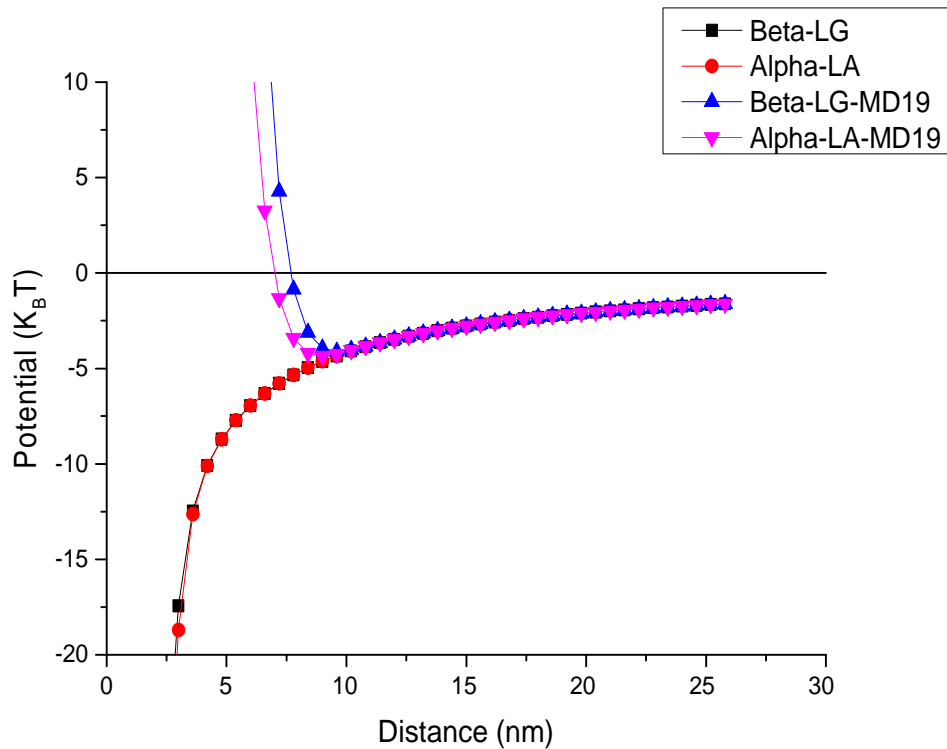
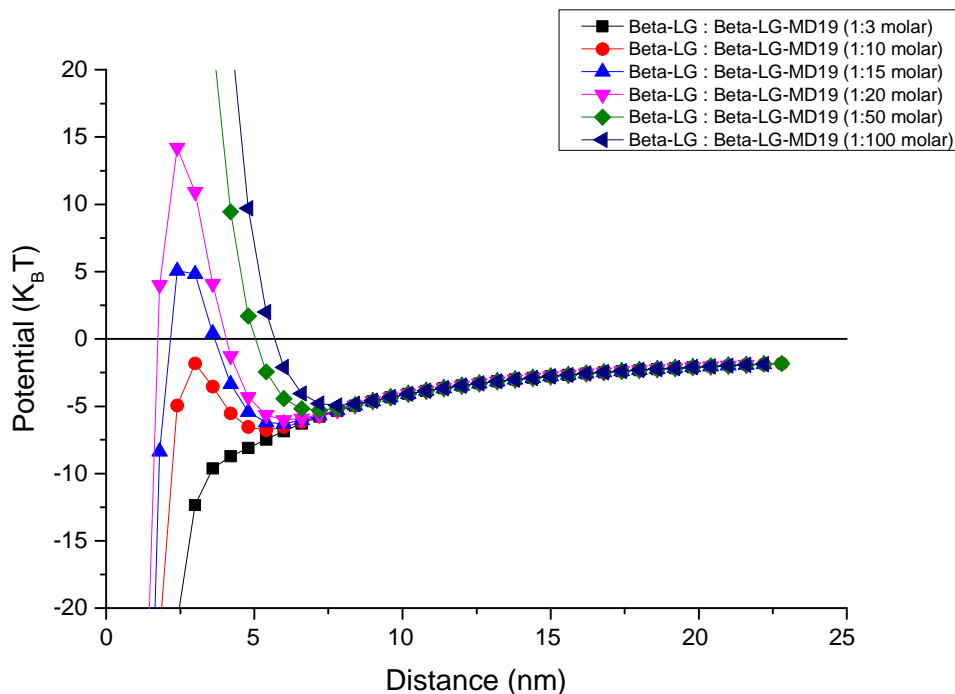


**Figure 3.2** Colloidal interaction potential between two droplets ( $d=1 \mu\text{m}$ ) mediated by systems consisting of a single type of polymer for  $\beta$ -lactoglobulin (Beta-LG),  $\alpha$ -lactalbumin (Alpha-LA),  $\beta$ -lactoglobulin-MD19 conjugate (Beta-LG-MD19) and  $\alpha$ -lactalbumin-MD19 (Alpha-LA-MD19) respectively.

It is seen from Figure 3.2 that unmodified proteins i.e. Beta-LG and Alpha-LA have clear attractive energy wells between two hydrophobic particles because of the negative values of total potentials from separation of 25 down to 3 nm. This also indicates that for conjugates Beta-LG-MD19 and Alpha-LA-MD19 there are strong repulsive effects when two surfaces are approaching each other at separation distances closer than 7nm. The strong

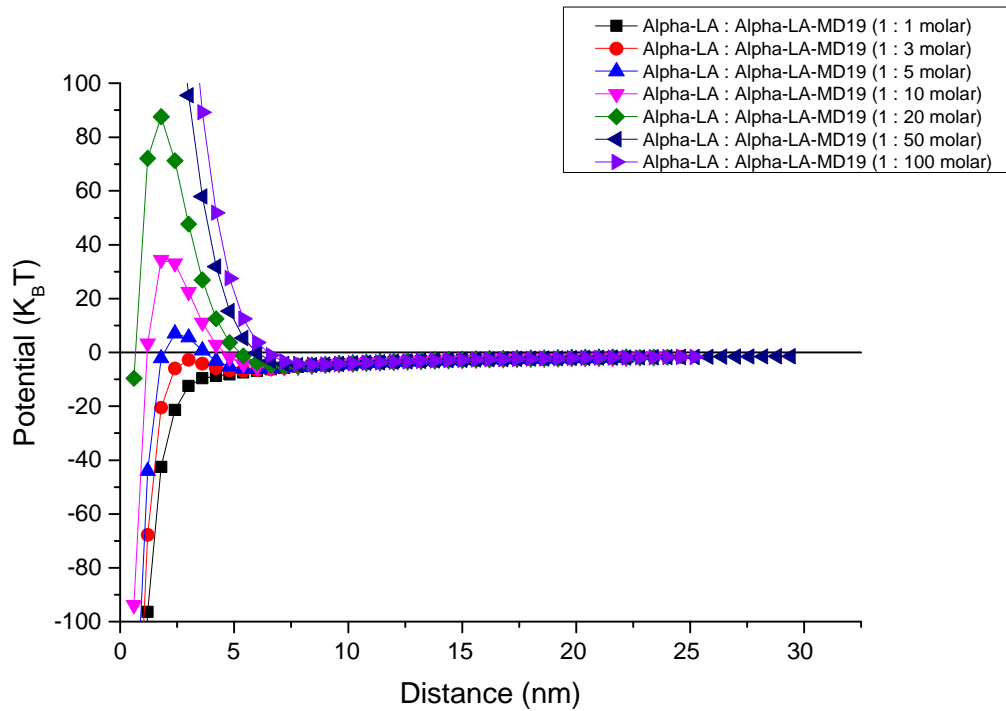
repulsions from conjugates are mainly from the steric effects of polysaccharide moieties because the electrostatic force is almost eliminated by adjusting pH to pI and strong screening effect of high salt content. This result is qualitatively in line with the experimental observations from many previous studies (Wooster and Augustin, 2006; Fan et al., 2006; Kika et al., 2007; Li et al., 2012; Xu et al., 2012; Chen et al., 2014; Tabatabaee Amid and Mirhosseini, 2014; Qiu et al., 2015; Yang et al., 2017). It indicates that conjugates can significantly improve the stabilizing properties of O/W emulsions.

The next step is to investigate the interaction potential in systems where one type of protein and one type of conjugates, at various molar ratios are both simultaneously present.



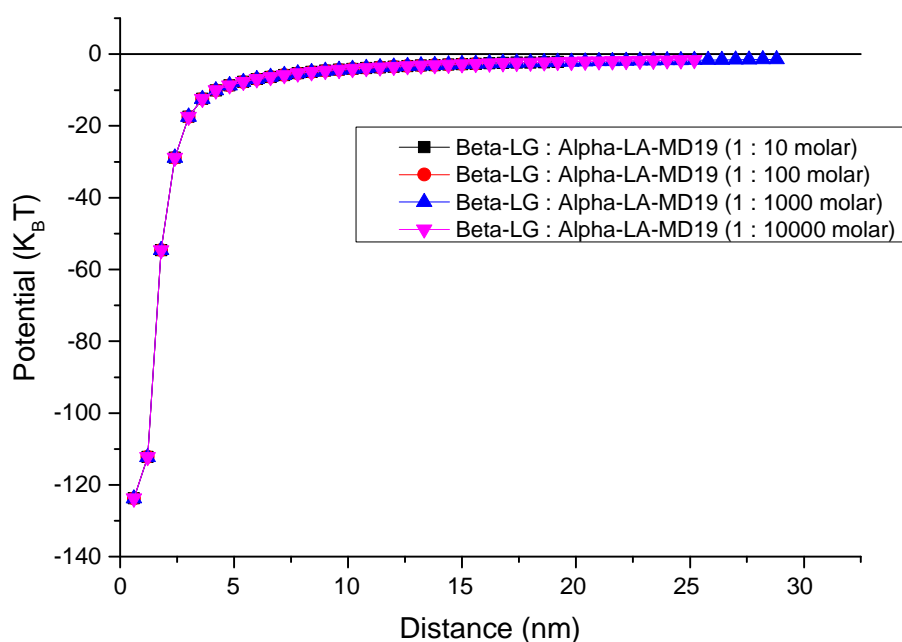
**Figure 3.3** Interactions induced between two droplets ( $d=1\ \mu\text{m}$ ) by polymers in a system containing both  $\beta$ -lactoglobulin (Beta-LG) and  $\beta$ -lactoglobulin-MD19 conjugate (Beta-LG-MD19).

Figure 3.3 displays the total interaction potential energy of the systems containing one protein, i.e.  $\beta$ -lactoglobulin, and one conjugate which is  $\beta$ -lactoglobulin-MD19, studied under various molar ratios, plotted as a function of separation distance between a pair of droplets. at different distances. When the proportion of conjugate increases, the steric repulsion becomes stronger and occurs at longer distances. However, if the percentage of conjugate in the system is not sufficiently high, such as molar ratios at 1:3 and 1:10, the total potential energy predominately indicates attraction. For example, at the molar ratio of 1:3 (Beta-LG : Beta-LG-MD19), the interaction potential curve is similar to that seen for a single type polymer system (Beta-LG) as shown in Figure 3.2. As the molar fraction of conjugate in the system is increased, the repulsive effect becomes stronger due to the enhancement of steric repulsions from attached polysaccharide moieties. When the molar conjugate ratio is increased to 1:50 and 1:100, there is no significant difference in the interaction potential curves between the mixed protein + conjugate system and conjugate-only one (see Figure 3.2). Furthermore, not only is the steric repulsion increased, but also the repulsive force takes effect at large separation distances, suggesting less likelihood of two surfaces closely approaching each other. Therefore, it is clear that the existence of conjugate in the emulsion system can improve the stability over certain percentages. This also indicates that, provided the molar fraction of conjugate is not too low, that conjugates compete favourably with the unreacted/unmodified protein for adsorption onto the surface of the droplets.



**Figure 3.4** Interaction potential between two droplets mediated by polymers in a mixed system of  $\alpha$ -lactalbumin (Alpha-LA) and  $\alpha$ -lactalbumin-MD19 conjugate (Alpha-LA-MD19).

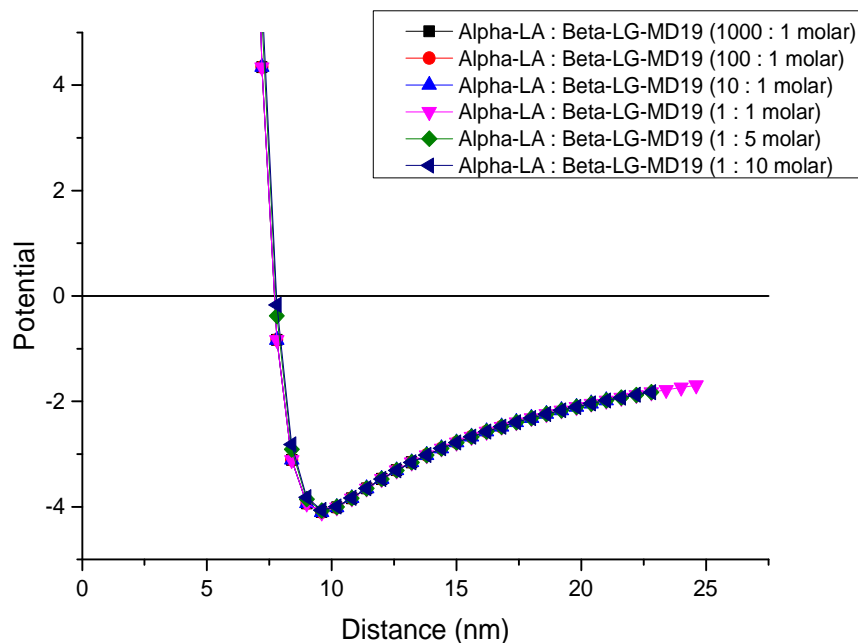
For Figure 3.4 we present the potential energy profiles of  $\alpha$ -lactalbumin and  $\alpha$ -lactalbumin-MD19 conjugate between two hydrophobic surfaces. Similar to Figure 3.3, the steric repulsion increases as the percentages of conjugate become higher. However, the repulsive effect is more clearly displayed from a molar ratio 1:5 onwards. This means that a lower proportion of conjugate in this system are still able to provide good steric stability, when compared with the  $\beta$ -LG and  $\beta$ -LG-MD19 mixed system, based on results of Figure 3.3. When the proportion of conjugates is increased reaching 1:50 and 1:100 (molar ratio), the steric repulsion is enhanced considerably. These results also suggest that conjugates can improve the stability, even though there is still unmodified protein in the system competing for adsorption.



**Figure 3.5** Interaction potential between two droplets mediated by polymers in a mixed system of  $\beta$ -lactoglobulin (Beta-LG) and  $\alpha$ -lactalbumin-MD19 conjugate (Alpha-LA-MD19).

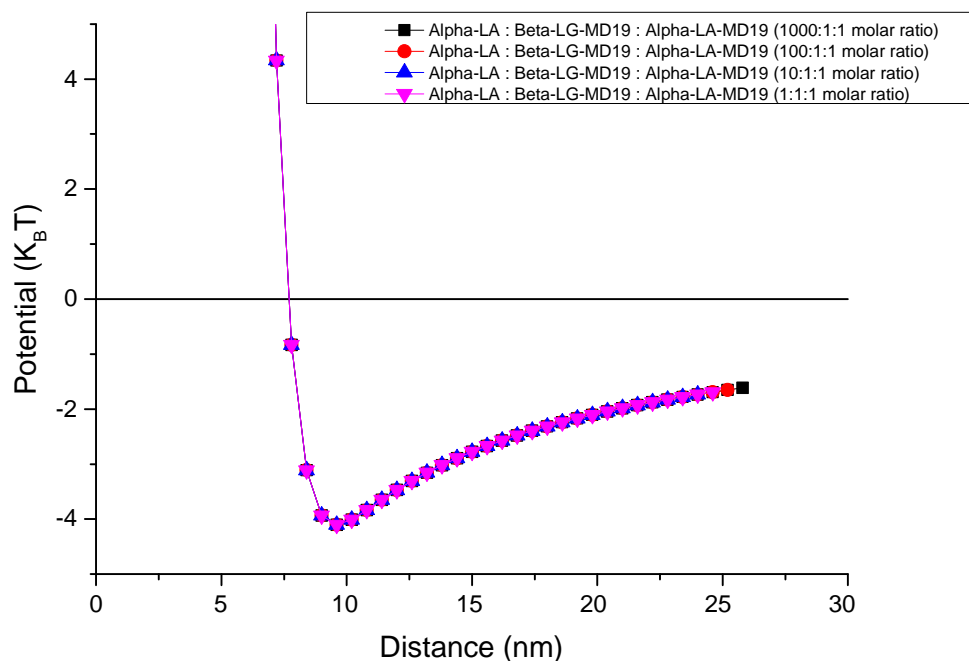
The interaction potential curves for two droplets in the system containing mixtures of  $\beta$ -LG and  $\alpha$ -LA-MD19 are shown in Figure 3.5. These results are quite different from the estimations in Figure 3.3 and Figure 3.4. In this two-polymer system, no matter how large the proportion of Alpha-LA-MD19 conjugate is made, no clear repulsion interactions between droplets develop there is no clear repulsion observed. Even when the conjugate to Beta-LG in molar ratio is more than 10000, the steric effect is not observed. The reason for this prediction could be that the hydrophobic surface is very strongly dominated by Beta-LG which cannot be easily displaced by the conjugate Alpha-LA-MD19. When the conjugate cannot compete successfully for the oil-water interface, it will obviously not be able to provide the required steric repulsions. Although the predictions may exaggerate the strong affinity

of Beta-LG compared to Alpha-LA, it nonetheless shows that such a mixture will not be favourable as a good steric stabilizer.



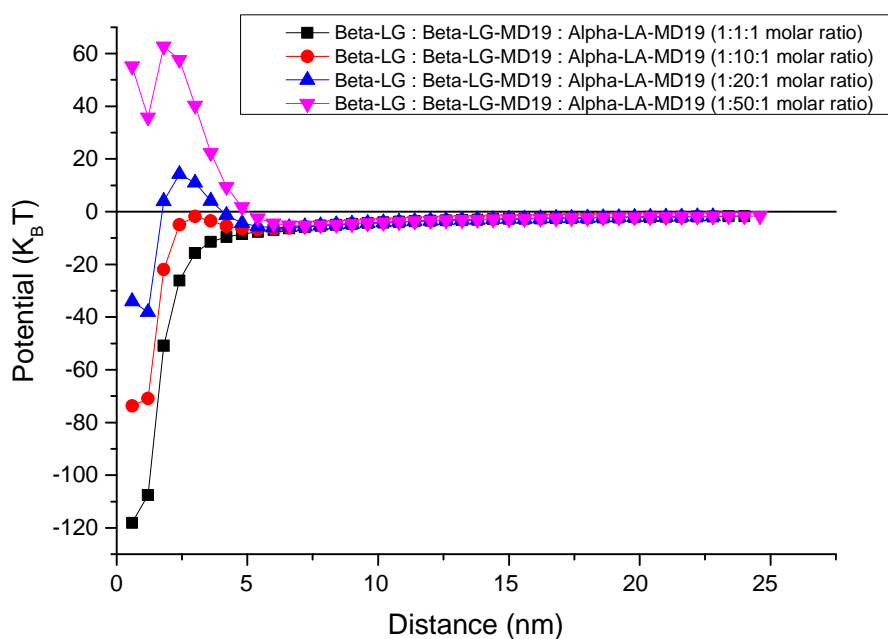
**Figure 3.6** Interaction potential between two droplets mediated by polymers in a mixed system of  $\alpha$ -lactalbumin (Alpha-LA) and  $\beta$ -lactoglobulin-MD19 conjugate (Beta-LG-MD19).

Figure 3.6 shows the interaction potential induced in solutions containing of Alpha-LA and Beta-LG-MD19, between a pair of droplets. Compared to Figure 3.3, 3.4 and 3.5, there is strong repulsion when the gap between droplets is smaller than 7 nm. This is different from other two-polymer systems shown previously. In this system, only a small fraction of conjugate (e.g. molar ratio of 1000 : 1) is sufficient to provide strong steric repulsion between two particles. This result indicates that Beta-LG-MD19 conjugate can easily attach to the oil-water interface even when a large amount of unmodified Alpha-LA is present to compete with it for the surface of droplets.



**Figure 3.7** Interaction potential curve for forces induced in a mixed three-polymer system containing  $\alpha$ -lactalbumin (Alpha-LA),  $\beta$ -lactoglobulin-MD19 conjugate (Beta-LG-MD19) and  $\alpha$ -lactalbumin-MD19 conjugate (Alpha-LA-MD19).

It has been shown in Figure 3.7 that there is strong steric repulsion in the system containing all three polymers: Alpha-LA, Beta-LG-MD19 and Alpha-LA-MD19. The energy profiles in this figure is quite similar to the results in Figure 3.6. If there are two conjugates existing in the system, the steric repulsion is clearly shown even when the protein Alpha-LA is much higher in volume fractions than other polymers (e.g. molar ratio 1000 : 1 :1). These results suggest that the surface is dominated by conjugates instead of native protein Alpha-LA. The results suggest that Beta-LG has a stronger affinity for the surface than Alpha-LA in general, and that even when conjugated with a polysaccharide chain, this strong tendency is still present.



**Figure 3.8** Colloidal interaction potential plotted as a function of particle-particle separation distance, induced between droplets in mixed solutions of  $\beta$ -lactoglobulin (Beta-LG) +  $\beta$ -lactoglobulin-MD19 conjugate (Beta-LG-MD19) +  $\alpha$ -lactalbumin-MD19 conjugate (Alpha-LA-MD19).

In Figure 3.8, the interaction potential curves between droplets in systems containing Beta-LG and two conjugates i.e. Beta-LG-MD19 and Alpha-LA-MD19 at various molar mix ratios are presented. Once the protein is changed from Alpha-LA to Beta-LG, the total free energy profiles of three-polymer system are similar to that forward in Figure 3.3, where there were only a mixture of Beta-LG and its conjugate Beta-LG-MD19 present. When the proportion of Beta-LG-MD19 increases, the steric repulsion starts to be exhibited and becomes stronger until the molar ratio reaches 1: 20 : 1 (Beta-LG : Beta-LG-MD19 : Alpha-LA-MD19). Compare to the results in Figure 4.7, it can be seen that Beta-LG is more capable of displacing the conjugates from the oil-water interface than Alpha-LA, which in turn reduces the steric

repulsion significantly when the native protein in the system is changed from Alpha-LA to Beta-LG in this protein + two conjugates mixture. In the three-polymer type systems, there are two more combinations we can consider, involving a combination of two native proteins and only one type of conjugate.

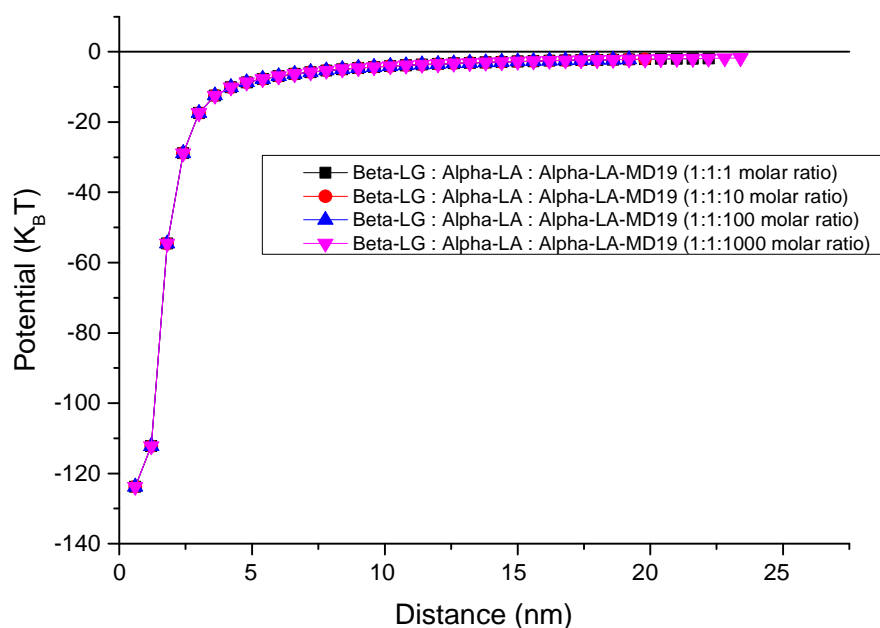


**Figure 3.9** Interaction potential between two droplets mediated by polymers in a system containing  $\beta$ -lactoglobulin (Beta-LG),  $\alpha$ -lactalbumin (Alpha-LA), and  $\alpha$ -lactalbumin-MD19 conjugate (Alpha-LA-MD19).

In Figure 3.9 we display the calculated interaction potential between droplets when two proteins i.e. Beta-LG and Alpha-LA and one conjugate (Alpha-LA-MD19) are all present in the system. These results are similar to the profiles presented in Figure 3.5 where the system contained a mixture of Beta-LG and Alpha-LA-MD19 only. It is clear that the existence of Alpha-LA-MD19 conjugate in the system has no impact on the strength of steric repulsions, even when included at much higher volume fractions (1000 times) than the other two proteins. It once again suggests that Alpha-LA-MD19 is

less surface active than the native proteins especially Beta-LG. That is why the steric repulsive effect of Alpha-LA-MD19 cannot be exhibited if there is Beta-LG in the system, where this latter displaces Alpha-LA-MD19 from the interface.

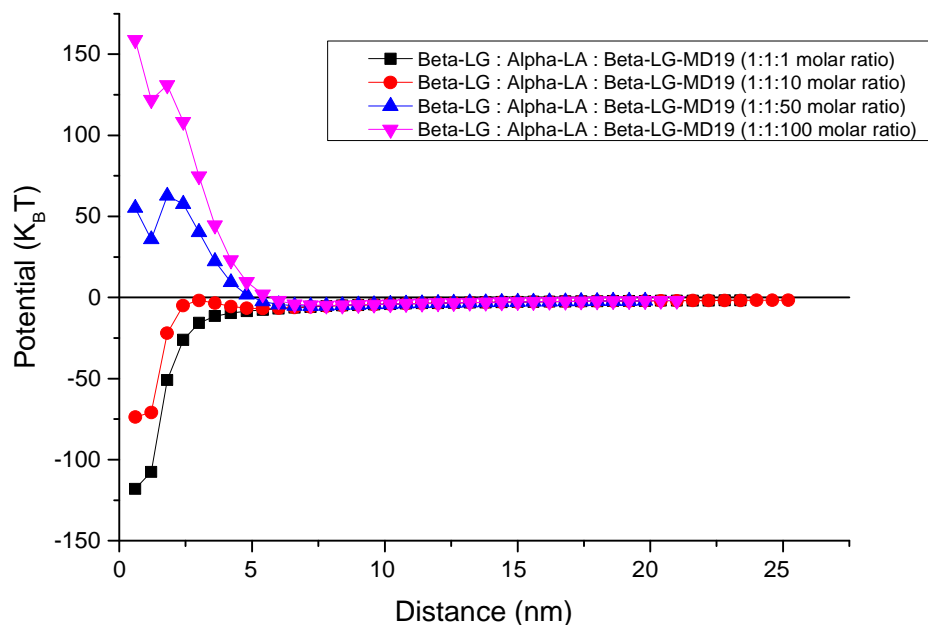


**Figure 3.10** Interaction potential graph in a mixed three-polymer system involving  $\beta$ -lactoglobulin (Beta-LG) +  $\alpha$ -lactalbumin (Alpha-LA) +  $\beta$ -lactoglobulin-MD19 conjugate (Beta-LG-MD19).

It has been shown in Figure 3.10 that the steric repulsion occurs when the conjugate is changed from Alpha-LA-MD19 to Beta-LG-MD19. Similarly, in Figure 3.3 and 3.8, the repulsion becomes more significant as the proportion of Beta-LG-MD19 conjugate increases in the system. However, the total energy profiles are quite different from the results in Figure 3.9 showing the system contained Alpha-LA-MD19 conjugate only. This difference indicates that Beta-LG-MD19 can indeed compete successfully with the mixture of other two native proteins in the interfacial adsorption process and

anchor to the oil-water interface. It is critical to provide sufficient steric stability between two hydrophobic surfaces that the conjugate is sufficiently surface active.

In the real emulsion systems, it is highly possible to have a mixture of two proteins and two conjugates in the system given that WPI used to produce the conjugates will most certainly include both  $\beta$ -LG and  $\alpha$ -LA. In Figure 3.11, we present our predicted results for the most complicated systems containing all of these four polymers.

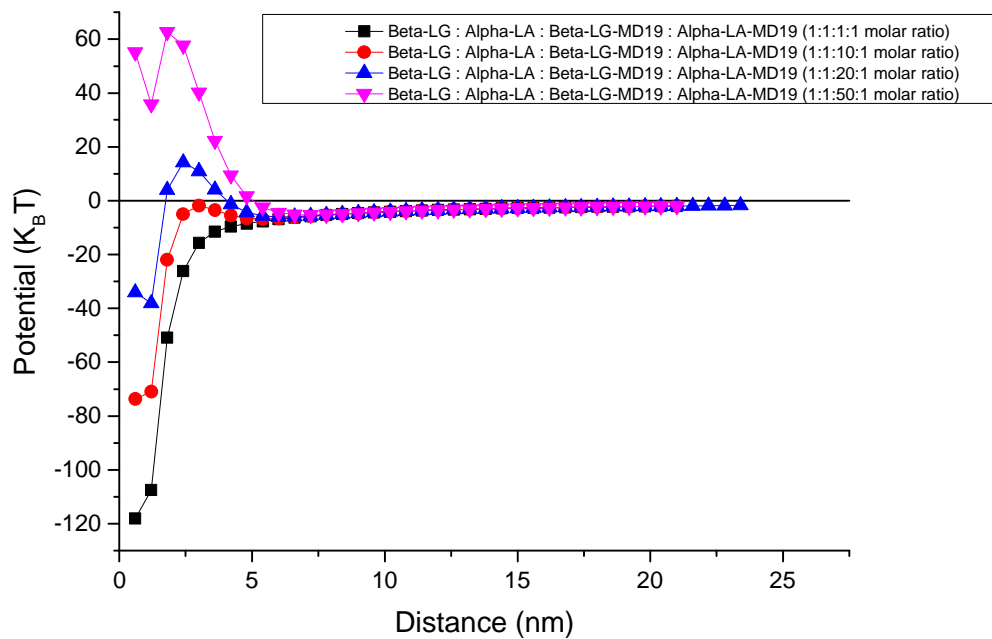


**Figure 3.11** Colloidal interaction induced between a pair of droplets in systems consisting of four types of polymer:  $\beta$ -lactoglobulin (Beta-LG),  $\alpha$ -lactalbumin (Alpha-LA),  $\beta$ -lactoglobulin-MD19 conjugate (Beta-LG-MD19), and  $\alpha$ -lactalbumin-MD19 conjugate (Alpha-LA-MD19).

In this diagram (Figure 3.11), it shows the free energy profiles of systems with four types of polymers all present in the mix: two kinds of native proteins and two conjugates. The variation of the interaction potential with

separate distance in this figure is similar to that of Figure 3.3 where a bi-polymeric system containing Beta-LG and Beta-LG-MD19 was considered. As can be seen in this figure, the repulsion occurs when the proportion of Beta-LG-MD19 increases to certain threshold (1: 1: 20: 1 Beta-LG : Alpha-LA : Beta-LG-MD19 : Alpha-LA-MD19 molar ratio) leading to the appearance of an energy barrier at a separation distance of around 5nm (shown in the curve with blue triangles). If the percentage of Beta-LG-MD19 decreases in this four-polymer system, the repulsive effect is significantly reduced. The curves in Figure 3.11 suggest that the conjugate Beta-LG-MD19 plays a critical role on provision of steric repulsion between two hydrophobic surfaces in this four-polymer type system.

The results from all the theoretical calculations suggest that the four polymers have different affinity to the hydrophobic surface. The denatured protein  $\beta$ -lactoglobulin has the strongest adsorption to the surface while  $\alpha$ -lactalbumin-MD19 conjugate has the weakest affinity for the hydrophobic interfaces. Furthermore, the attachment of polysaccharides MD19 to proteins can reduce the affinity of the proteins owing to the decreased level of hydrophobicity of the resulting bi-polymer. In terms of the stabilizing properties of the polymers under the unfavourable environmental conditions (i.e. pH close to pI and high ionic strength), the systems containing the conjugate of  $\beta$ -lactoglobulin will continue to exhibit the steric repulsion between droplets if the proportion of the  $\beta$ -lactoglobulin-MD19 is sufficiently high. In contrast, the  $\alpha$ -lactalbumin-MD19 conjugate may not be able to compete with unreacted proteins and provide the desired repulsive effect between droplets, especially when  $\beta$ -lactoglobulin is also present in the system. Therefore, it can be concluded from the results and discussions above that the protein-

polysaccharide conjugates can improve the stability of O/W emulsions under harsh environmental conditions if the conjugates can be adsorbed onto the oil-water interface strongly, which means that the conjugates should not be easily displaced by other surface-active components such as unreacted proteins. The similar enhancing steric stability of this kind of polymer (e.g. modified  $\alpha_{s1}$ -casein) predicted from SCF calculations was also reported by other researchers (Parkinson et al., 2005; Akinshina et al., 2008; Ettelaie et al., 2008; Ettelaie and Akinshina, 2014).

Theoretical calculations provide valuable insights in the O/W emulsions stabilized by proteins and their conjugates. It helps us to design the experiments to determine the critical proportion of conjugates needed relative to unreacted protein in stabilizing emulsion droplets and to achieve acceptable lifetime for O/W emulsions. The next section will present the experimental results.

### **3.3.2 Appearance of WPI-MD19 conjugates after the Maillard reactions**

After the heat treatment of the mixture WPI and MD19, a pleasant smell was detected immediately once the desiccator was opened. The conjugates are shown in Figure 3.12.

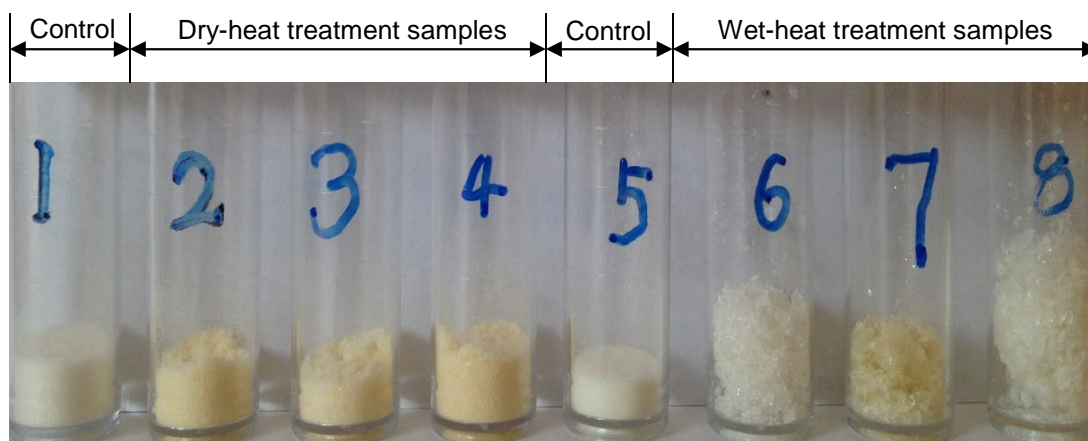


**Figure 3.12** Appearance of WPI-MD19 conjugates prepared via dry-heat treatments (sample 2, 3, 4) and wet-heat treatments (sample 6, 7, 8); sample 1 and 5 are controls (heated WPI only).

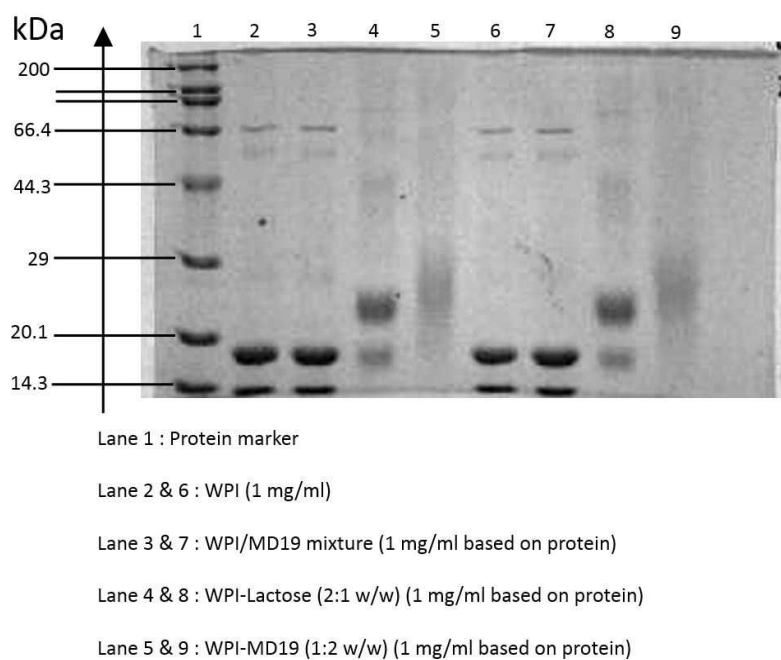
In Figure 3.12, WPI-MD19 conjugates prepared via the Maillard reactions are shown. Conjugates (sample 2, 3, and 4) from the dry-heating method are yellow compared to the control sample 1 which is WPI under the same treatment as conjugates. The yellow colour of the conjugates is from the browning effects of the Maillard reactions which develops only in the middle stages of the reaction, as there is no clear brown or black colour observed in the products which often are produced at later stages (Maillard, 1912; Walker, 1972). However, the WPI-MD19 conjugates (sample 6, 7, and 8) prepared via wet-heating route exhibit a lighter yellow colour than those from traditional dry heating treatment. The colour changes in samples 6, 7, and 8 also suggest that the Maillard reactions can occur in aqueous medium, but to a less advanced stage than the reactions in samples 2, 3, and 4. The preparation details for samples 6, 7, and 8 will be discussed further in Chapter 5.

The appearance of WPI-MD19 conjugates suggests that the Maillard reactions occur during heating process. It is important to confirm the

successful formation of covalent bond between WPI and MD19 by other independent methods.

### 3.3.3 Confirmation of conjugates by SDS-PAGE and OPA tests

A significant alteration of protein molecular weight upwards is a direct evidence confirming that the conjugation is successful and the attachment to polysaccharides has been made. The protein separation technique from SDS-PAGE can show the change of protein molecular weights both before and after conjugation (Figure 3.13).



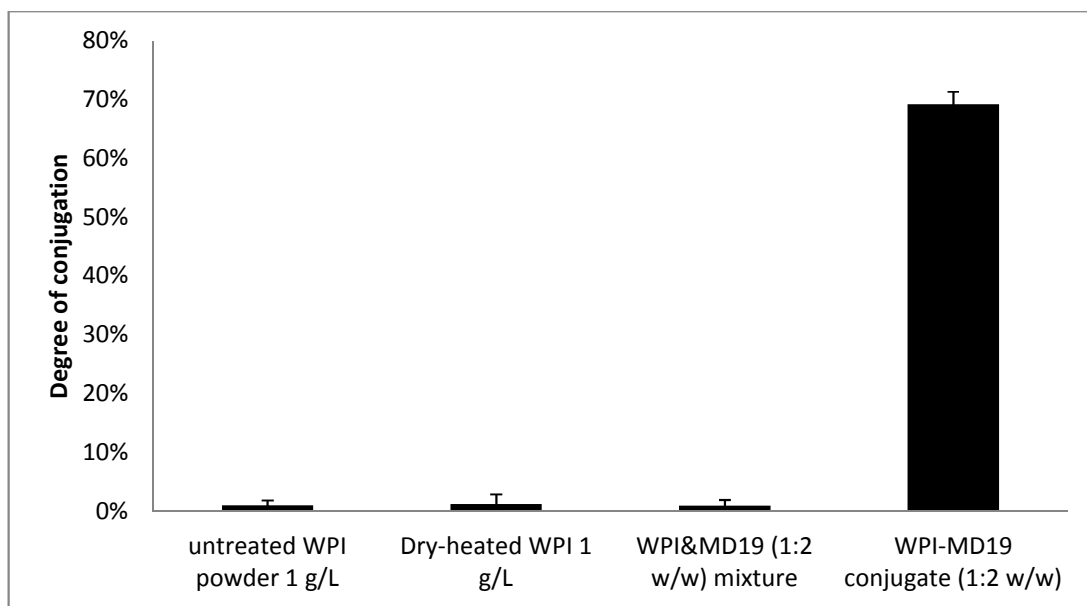
**Figure 3.13** SDS-PAGE results of WPI, WPI-lactose conjugates, and WPI-MD19 conjugates prepared via dry-heat treatments.

Figure 3.13 shows the result from SDS-PAGE analysis conducted by the candidate in Zhejiang Gongshang University. There are four samples analyzed by the standard procedure and repeated twice. The repeatability of results is quite high, which can be seen from Figure 3.13 above. For the control (Lane 2), there are three clear bands which represent three major

proteins in WPI: BSA (~ 66 kDa),  $\beta$ -lg (~ 18 kDa), and  $\alpha$ -lactalbumin (~ 14 kDa) from the top to the bottom, respectively. Furthermore, the darkness of each band suggests the weight percentage of each protein in WPI. Therefore, it can be seen that  $\beta$ -lactoglobulin dominates WPI about 50 % (w/w) while  $\alpha$ -lactalbumin and BSA only account for 20 % and 10 % of WPI protein. This result agrees with the information from textbook regarding composition of WPI (Fox et al., 2015).

Lane 3 shows a similar pattern to Lane 2, suggesting that the presence of unattached MD19 has little influence on WPI. However, Lane 4 is quite different from Lane 2 and 3. Firstly, the top band and bottom band (representing BSA and  $\alpha$ -lactalbumin) disappears. Secondly, the middle band representing  $\beta$ -lactoglobulin becomes lighter, and a new band which is the darkest amongst others is Lane 4 in the range between 21 and 25 kDa. These suggest that the molecular weight of proteins increased after heat treatment generally but not significantly, due to the low molecular weight of lactose (as opposed to MD) included in these systems. Moreover, the  $\beta$ -lactoglobulin band still exists after glycation, suggesting that there are quite a large amount of unreacted  $\beta$ -lactoglobulin still remaining in the system, in this case.

For Lane 5, there is no clear band visible on the gel except a light dark one extending from 20 to 29 kDa. This suggests that the molecular weight of the WPI-MD19 conjugates is higher than 200 kDa in majority, and only a few fractions of unreacted WPI are left in the final product. This observation agrees with the result from OPA tests in the quantitative analysis of conjugation, which indicates the degree of conjugation of WPI-MD19 is around 70 %.



**Figure 3.14** Degree of conjugation analysis of different protein and protein/polysaccharide systems via OPA tests.

Figure 3.14 shows four samples that were analyzed through the OPA tests. These include native WPI powder, dry-heated WPI powder, mixture of WPI and MD19 (1:2 w/w) without any heating treatment, and WPI-MD19 conjugates (1:2 w/w) formed post heat treatment. There is no significant difference amongst the systems containing only WPI and the mixture of protein and polysaccharide. Moreover, these systems exhibit little loss of free amino groups in protein chains as the degree of conjugation in these samples is around 0%. In contrast, the WPI-MD19 conjugates show dramatic increase of degree of conjugation (~ 70%) owing to the considerable reduction of free amino groups in WPI. These results suggest that dry-heating treatment and the existence of reducing polysaccharide MD19 are two essential conditions for successful conjugation.

According to the results from SDS-PAGE and OPA tests, it can be confirmed that the WPI-MD19 conjugates can be formed through the Maillard

reactions. Once the conjugates are successfully prepared, it is possible to further the investigation on the interfacial and emulsion stabilizing properties of the WPI-MD19.

### 3.3.4 Interfacial properties of dry-heating WPI-MD19 conjugates

Before investigating the stabilizing property of WPI-MD19, it is necessary to study and compare the interfacial behaviours of WPI and WPI-MD19 on the oil-water interface.

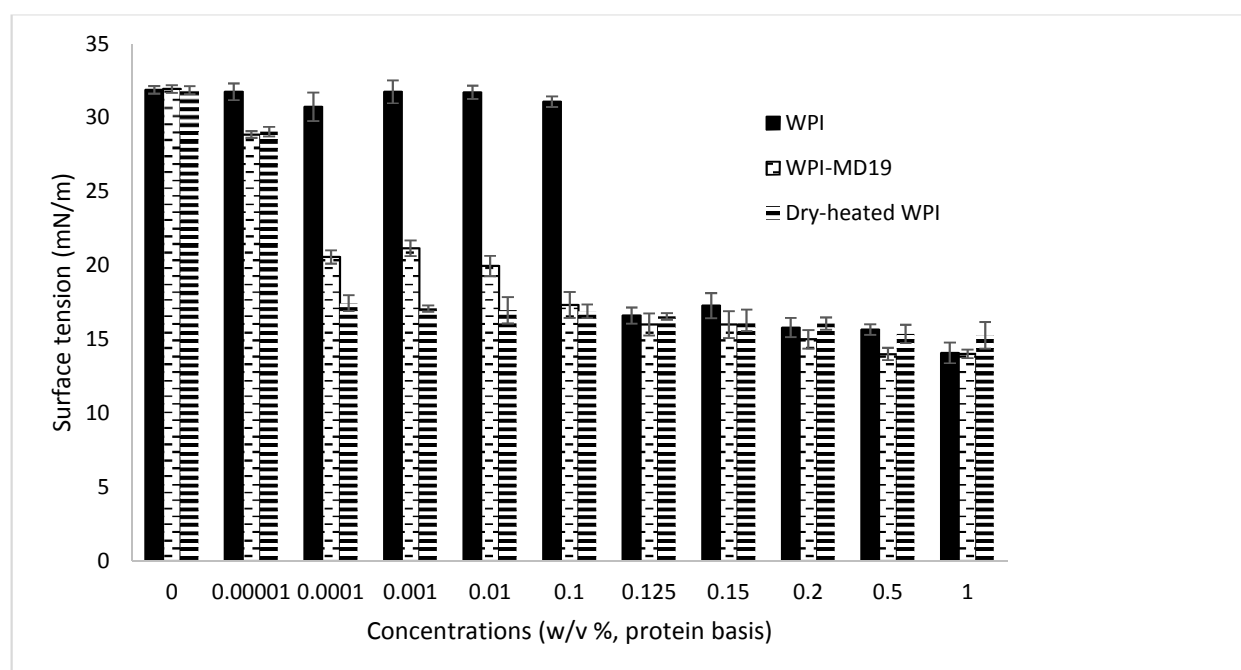


**Figure 3.15** Interfacial tensions of WPI, dry-heated WPI, and WPI-MD19 conjugates at various protein concentrations, measured for oil-water interfaces.

In Figure 3.15, the oil-water interfacial tensions of systems containing WPI, dry-heated WPI, and WPI-MD19 conjugates at different protein concentrations are shown. The oil-water interfacial tension is around 31 mN·m<sup>-1</sup> when the surface is devoid from any surfactant. Once the protein or

protein-polysaccharide conjugates are introduced into the aqueous phase, the surface tension begins to drop. For WPI, the change of surface tension is not significant until the protein concentration reaches 0.1%. However, the interfacial tension starts to decrease as the concentration of WPI-MD19 increases from very diluted status i.e. 0.00001%. However, if the concentration of WPI-MD19 is increased further, the oil-water surface tension will not dramatically decrease showing only a slight reduction as a high concentration, say around 1% is reached. Compared to WPI-MD19, WPI shows significant capacity to reduce surface tension when the concentration is higher than 0.1%, becoming similar to the behaviors of conjugates at the same concentrations once above this value. Interestingly, for the sample of dry-heated WPI without any polysaccharide, the pattern is quite similar to that of conjugates with only minor difference. In the diluted systems, such as concentrations 0.0001, 0.001, and 0.01%, the dry-heated WPI exhibits noticeably stronger capacity for reducing surface tensions, than the conjugates. However, when the concentration increases to higher levels, the difference amongst the three samples disappears within experimental accuracy.

The experimental results in Figure 3.15 suggest the different behaviors of native protein, denatured protein, and protein-polysaccharide conjugates during the adsorption process to the oil-water interface. From the prospective of protein structure, native protein has more secondary structures than the other samples which have been denatured by the heating treatment. That is the reason why WPI shows little surface activities when the concentration of protein is extremely low ( $< 0.01\%$ ). It is more difficult for globular proteins to rearrange at the oil-water interface than the already denatured WPI and WPI-

MD19 (See 1.5.3). Additionally, there is another reason to explain the phenomenon. The experiments were allowed to continue for only 3000 s, which may not be long enough for globular proteins to be fully unfolded on the oil-water interface, especially when the bulk concentrations are relatively low according to the results from other similar interfacial tension experiments (Dickinson, 1982e). In other words, the equilibrium surface tension values are only achieved over much longer time periods for such cases. However, when the protein concentration is sufficiently high, there is no significant difference between WPI, dry-heated WPI and WPI-MD19 owing to the similar structure of adsorbed protein part.

Apart from the final interfacial tensions of systems with various surfactants, it is important to observe the change of interfacial pressures for each system over a time period, here from 0 to 3000 s. The interfacial pressure  $\pi$  is defined as follows:

$$\pi = \gamma_c - \gamma$$

where  $\gamma_c$  is the interfacial tension between oil and water without any surfactant;  $\gamma$  is the interfacial tension of the system at different times. In the dynamic adsorption to the oil-water interface experiments, various mixed combinations of WPI and WPI-MD19 conjugates were tested, based on the ratios shown in Table 3.2. In all cases though, the total protein concentration in each system was limited to 0.1% (w/v).

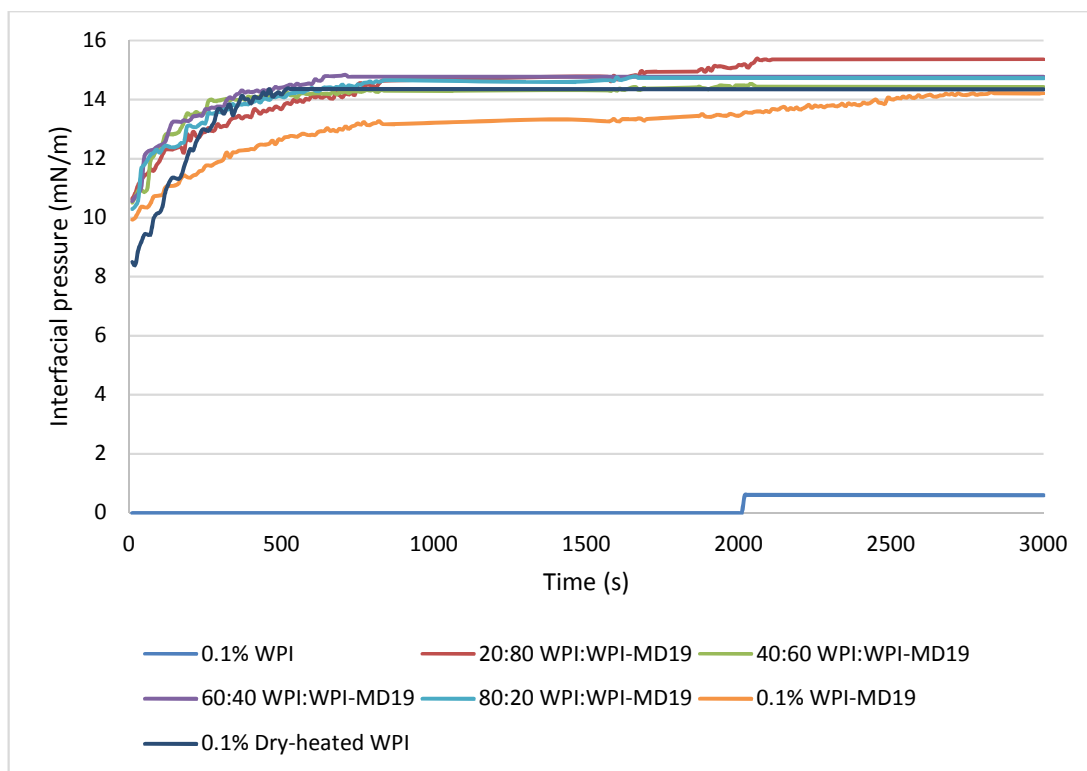


**Figure 3.16** Interfacial pressures of WPI, dry-heated WPI, and WPI-MD19 conjugates at different adsorption time on the oil-water interface. Total protein content was the same for all systems at 0.1 w/v %.

Results presented in Figure 3.16 show the variation in interfacial pressures vs. time for mixed WPI and WPI-MD19 conjugates systems, at various combinations. Generally, the interfacial pressures increase for most of the systems during the observation period except the system with native WPI with a slightly higher value of interfacial pressure about  $0.6 \text{ mN}\cdot\text{m}^{-1}$  after a period of 2000s compared to other systems. For the mixtures of WPI and WPI-MD19 at various weight ratios, there is no significant difference in the observed dynamic interfacial pressures, no matter what ratio was between the protein and the conjugates. Similarly, the adsorption behaviours of dry-heated WPI and pure WPI-MD19 conjugates are not considerably different to each

other. After duration of 1000s, the interfacial pressures for each system plateau out to around  $14 \text{ mN}\cdot\text{m}^{-1}$ .

The results from interfacial behaviours of the protein and conjugates suggest that unreacted protein WPI, whether is native or denatured form, cannot displace the WPI-MD19 conjugates once they are adsorbed onto the oil-water interface given that all these molecules have roughly the same surface pressure. These experimental results agree with the theoretical calculations via the SCF model. Moreover, all the results from theoretical calculations and experiments suggest that it is possible to improve the stability of an emulsion under harsh environmental conditions such as pH values close to pI, and at high ionic strength by a mixture of WPI and WPI-MD19 conjugates, as well as just WPI-MD19 alone.

In the next step of experiments, it is important to determine the threshold weight ratio between WPI and WPI-MD19 conjugates in the stabilizing mixture which can still provide acceptable stabilizing properties in O/W emulsions after at least 28 days of storage.

### **3.3.5 Stability analysis of O/W emulsions with the mixture of WPI and WPI-MD19**

The stability of O/W emulsions can be assessed through various techniques and standards. For example, particle sizing is a common technique to monitor the stability of emulsions during storage. Moreover, the rheological properties of emulsions can be also used to evaluate the stability of emulsions. Apart from these two techniques, the visual assessment of creaming and confocal imaging can offer more evidence on the stability of emulsions.

For particle sizing analysis, there are two major parameters used to measure the size of oil droplets in emulsions: average droplet size usually presented via  $d[4,3]$  and droplet size distribution which shows the proportion of oil droplets under various size classes in the whole emulsion system.

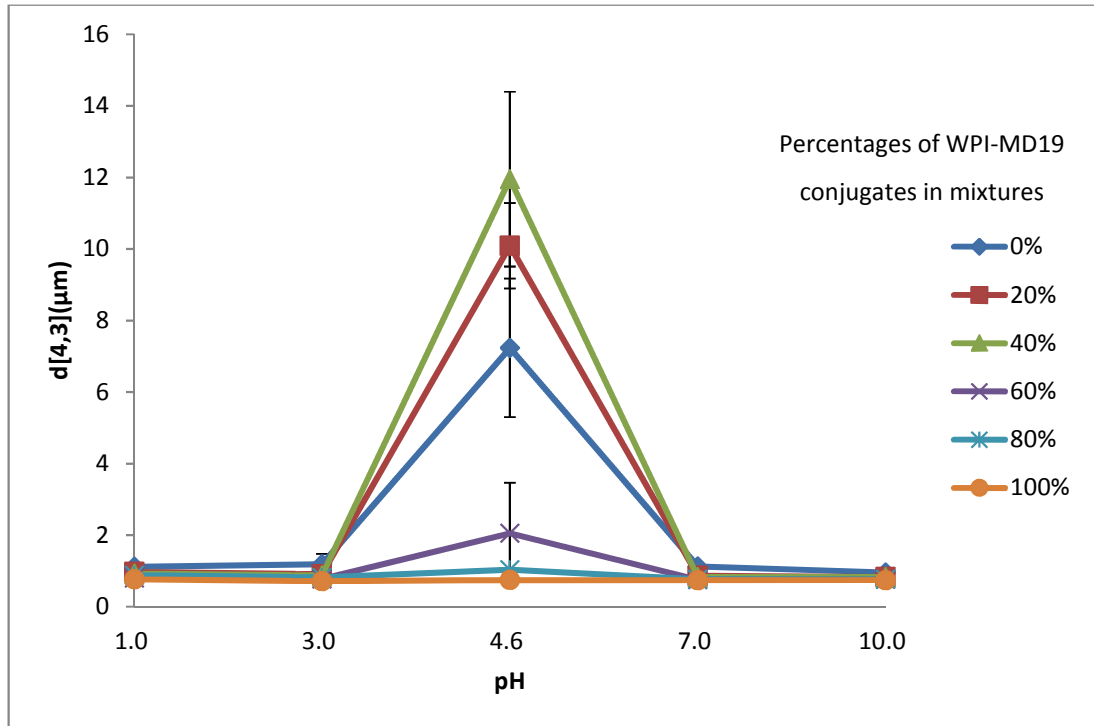


**Figure 3.17** Average droplet size (ADS) of O/W emulsions stabilized by the mixture of WPI and WPI-MD19 conjugates at various weight ratios under different environmental pH.

In Figure 3.17, we show the way that pH can affect the average droplet size (ADS) of O/W emulsions stabilized by the mixture of WPI and WPI-MD19. First considering the two controls (i.e. 0% and 100% WPI-MD19), the average droplet size is significantly increased to around 7  $\mu\text{m}$  when pH is at 4.6 when the emulsion is stabilized by native WPI (0% WPI-MD19). In contrast, at the same pH, the ADS of the emulsion stabilized by WPI-MD19 conjugates stays at 1  $\mu\text{m}$ . This result suggest that WPI-MD19 conjugates have much better stabilizing properties than native WPI, particularly when pH is close to pl of

WPI, around 4.6. The improved stabilizing properties of conjugates mainly arise from the steric stability of attached polysaccharide moieties, present even when the electrostatic repulsion is considerably reduced at pH 4.6. As for the mixture of WPI and WPI-MD19 conjugates, the percentage of WPI-MD19 in the mixture is a key parameter for providing sufficient stabilizing properties, particularly at pI (i.e. pH 4.6). When pH is far from pI, the ADS of all emulsions were comparable, remaining close to the baseline of  $\sim 1 \mu\text{m}$ . At pH values away from pI, for all emulsions there are the strong electrostatic repulsions to ensure stability. However, at pH close to 4.6, the emulsions stabilized by mixtures containing less than 60% WPI-MD19 conjugates become destabilized as observed by the significant increase of ADS values. On the other hand, when the percentages of WPI-MD19 conjugates are higher than 60% (w/w), the ADS values do not change considerably from  $1 \mu\text{m}$ , thus suggesting that these emulsions are sufficiently stable under the more severe conditions, pH 4.6.

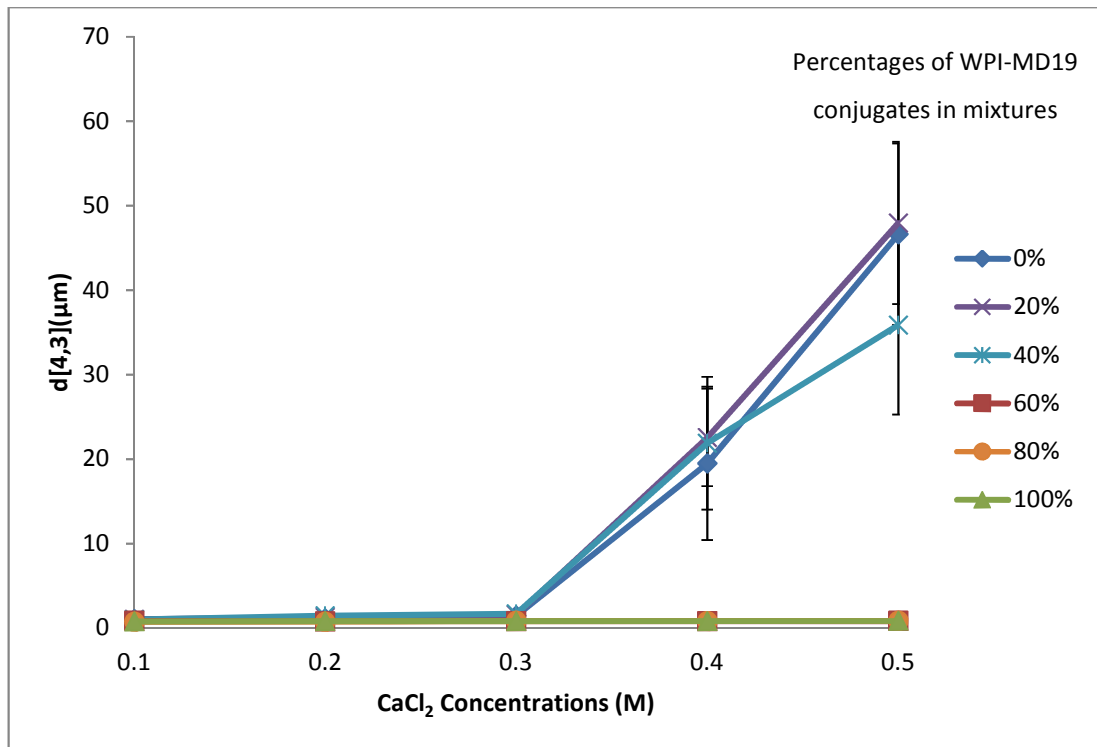


**Figure 3.18** Average droplet size (ADS) of O/W emulsions stabilized by the mixture of WPI and WPI-MD19 conjugates at various weight ratios under different concentrations of CaCl<sub>2</sub>.

The average droplet size (ADS) of emulsions stabilized by the mixture of WPI and WPI-MD19 conjugates under various concentrations of CaCl<sub>2</sub>, from 0.1 to 0.5 mol/L, is displayed in Figure 3.18. When the concentration of CaCl<sub>2</sub> is lower than 0.4 mol/L, there are no significant differences in ADS values, which all remain close to 1 μm irrespective of whether droplets are stabilized by WPI or/and WPI-MD19 at any weight ratio. However, emulsions stabilized solely by WPI and those with mixtures having the percentage of WPI-MD19 lower than 60% (w/w) start to be destabilized as reflected in the significant increase of ADS values at the CaCl<sub>2</sub> concentrations over 0.4 mol/L (see Figure 4.18). In terms of emulsions with conjugates or the mixtures with proportion of WPI-MD19 conjugates higher than 60% (w/w), no instability of emulsions occur according to the ADS values, even when the concentration

of  $\text{CaCl}_2$  is higher than 0.4 mol/L. There are two major reasons why electrolytes in the aqueous phase can cause instability of emulsions: depression of electronic double layers and the promotion of bridging flocculation. In this experiment, as the ionic strength increases it reduces the electrostatic repulsion between two oil droplets. If the concentration of  $\text{CaCl}_2$  in the aqueous phase is sufficiently high, such as 0.4 mol/L, it is likely to result in flocculation of droplets which considerably affects the  $d[4,3]$  values in emulsions. However, in emulsions mainly stabilized by conjugates, there is another more major stabilizing mechanism namely, steric stability, apart from the electrostatic. The steric stability is only moderately affected by the increase of ionic strength in the environment. This explanation can be used to understand the insignificant change of average droplet sizes in emulsions that are stabilized by conjugates or in mixtures where conjugates dominate. The existence of  $\text{Ca}^{2+}$  in the aqueous phase may lead to bridging effects due to the divalence nature of  $\text{Ca}^{2+}$ . However, if the surface of oil droplets are mainly covered by uncharged non-ionic polysaccharide moieties, then this kind of bridging flocculation is unlikely to occur.

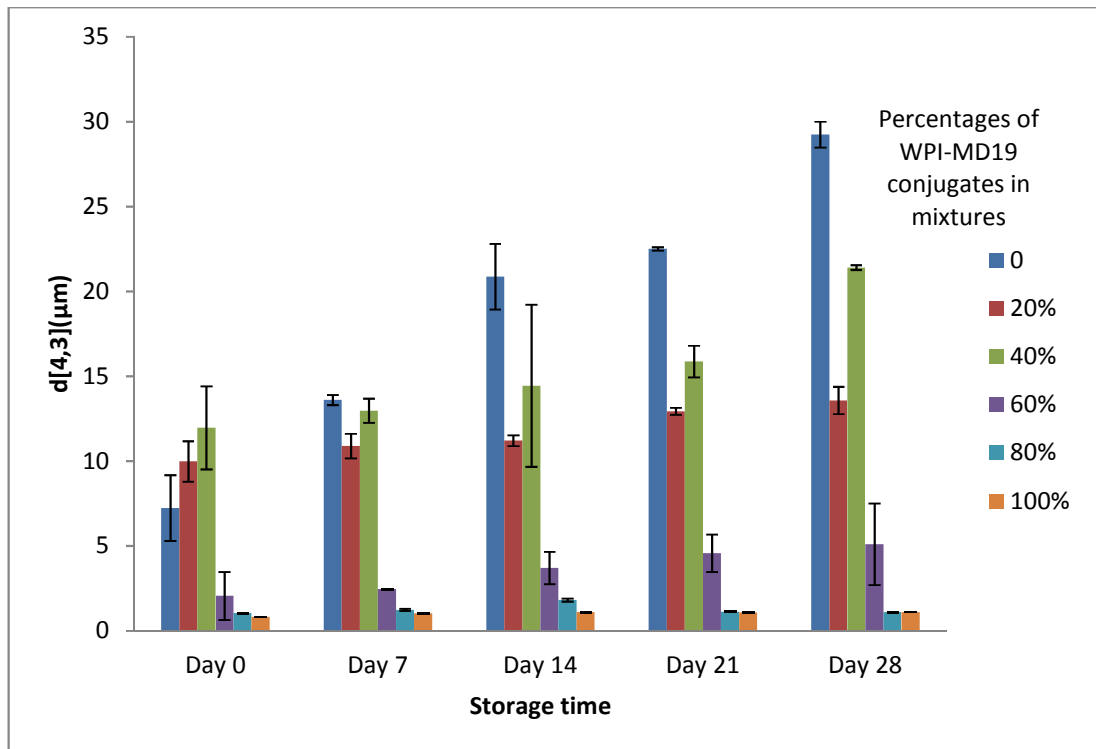
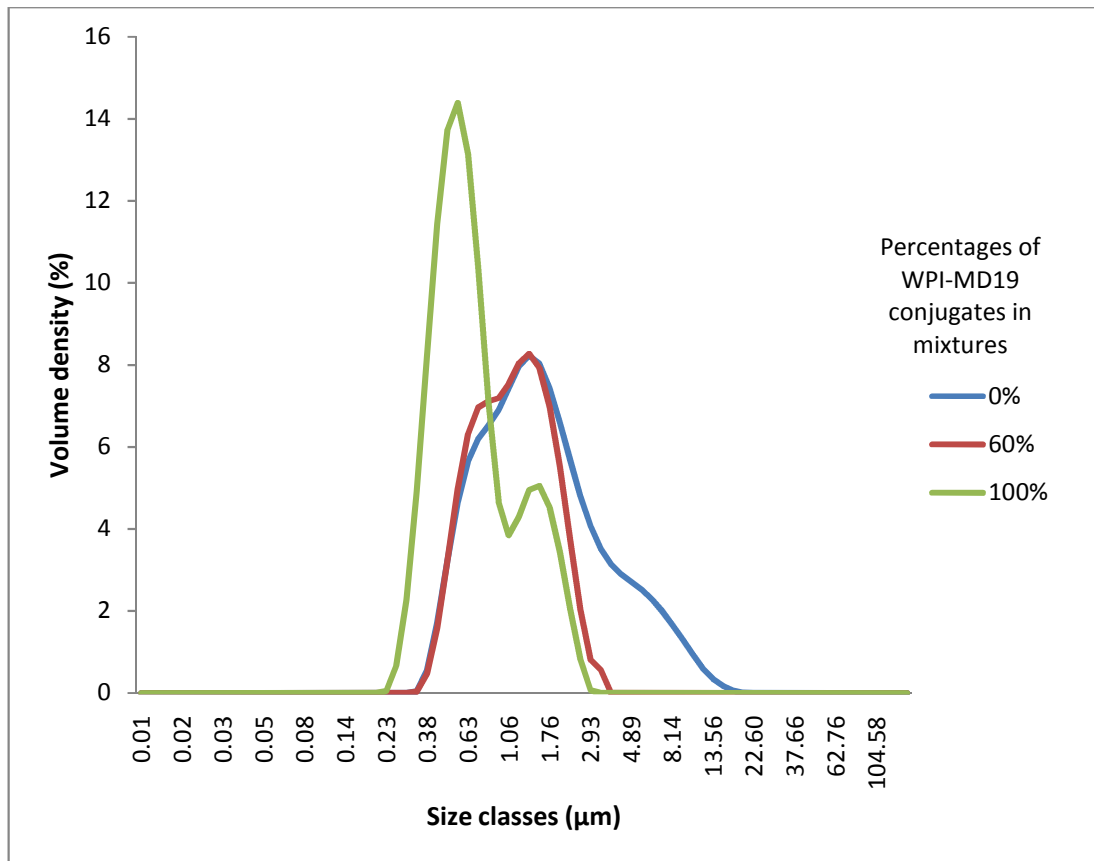


**Figure 3.19** Average droplet size  $d[4,3]$  of O/W emulsions (pH 4.6) stabilized by the mixture of WPI and WPI-MD19 conjugates at various mix weight ratios, following different storage time.

In Figure 3.19, one can see that the stability of emulsions with different stabilizers varies during 28-day storage. There were six O/W emulsion systems tested, categorized into two groups according to their stabilizing performances. The first group contains 0, 20, and, 40% conjugates in the mixtures used for stabilizing the droplets. The ADS values from these three groups are much higher than those for the other group where the ratio of conjugates in the mix are 60, 80, and 100%, increasing much more rapidly from d 0 to d 28. This observation agrees with the result from the  $d[4,3]$  values in Figure 3.17. When pH is close to 4.6, the stabilizing ability of WPI is dramatically reduced owing to the decreased electrostatic repulsion between the oil droplets. However, the ADS values from the sample 20% and 40%, while initially starting as relatively high, do not significantly increase further

during the 28-day storage as compared to results from Day 0. In contrast, if there were no conjugates in the system, the ADS values increase considerably throughout the 28 days. This suggests that it is possible to somewhat improve the stabilizing property with the presence of WPI-MD19 conjugates even though the stabilizing mixtures is mostly dominated by native WPI. Similarly, even more significant improvement is observed when the proportion of conjugates in the stabilizing mixtures is higher than 50%. In such systems the emulsifying and stabilizing properties are remarkably enhanced as suggested by the results of Figure 4.19. For example, in the emulsion stabilized by the mixture containing 80% WPI-MD19, the ADS values stay at around 1  $\mu\text{m}$  from Day 0 through to Day 28, with very little fluctuation. All these observations from Figure 4.19 indicate that the stabilizing mixture of WPI and WPI-MD19 conjugates can provide just as sufficient stability in O/W emulsions under harsh environmental conditions if the weight ratio of conjugates is higher than 60%.

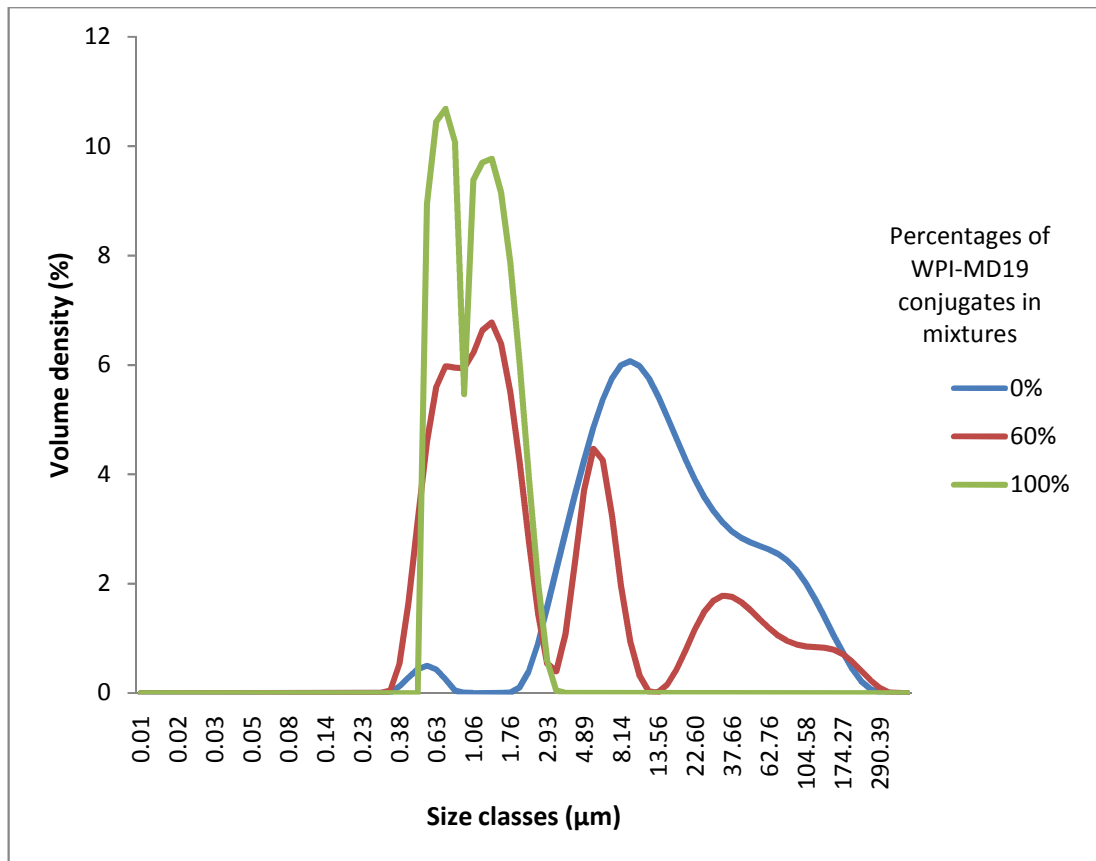
Apart from the ADS values of emulsions to estimate the stability during storage, the droplet size distribution is another parameter useful for monitoring the stability of emulsions. The droplet size distributions were recorded at the same frequency as the  $d[4,3]$ , every 7 days, through the whole storage period. Based on the observations from  $d[4,3]$  values, it is not necessary to present the whole profile of droplet size distributions for every emulsion samples, not least due to the limitation of the space in this thesis. Instead the key results of distributions are selected and presented as follows.



**Figure 3.20** Droplet size distribution (DSD) of O/W emulsions (pH 4.6) stabilized by the mixture of WPI and WPI-MD19 conjugates at three weight ratios (0, 60, and 100%) at storage time Day 0.

It is shown in Figure 3.20 that the O/W emulsions stabilized by different systems have different patterns of droplet size distributions when they were freshly prepared. For the control (i.e. emulsion consisting of 100% conjugates), the majority of oil droplets in the emulsion are less than 1 µm in size. The largest droplets are no more than 3 µm, which is less than 1% of the total oil droplets in the tested emulsion (the columns in green). Similarly, the distribution profile of the emulsion stabilized by 60% WPI-MD19 conjugates mixed with 40% WPI lies mainly in the range from 1 µm to 1.76 µm. The maximum size of droplets in this emulsion was also around 3 µm. Compared to the distribution of the control (100% conjugate), the droplet size of these

emulsions (60% conjugate) is marginally larger. However, if the emulsion is stabilized by native WPI only, the droplet size distribution is quite different from these two samples containing WPI-MD19 conjugates. There are still a large amount of small droplets, less than 2  $\mu\text{m}$ , when the emulsion was freshly prepared. At the same time, the large droplets, with size larger than 3  $\mu\text{m}$ , constitute a considerable fraction of the whole emulsions, as seen by the blue column in Figure 4.20. Moreover, the largest droplet can be more than 10  $\mu\text{m}$ . Droplets as large as these are not observed in emulsions stabilized by conjugates, or ones containing 60% conjugates. All the distribution profiles from Figure 4.20 suggest that the native protein and protein-polysaccharide conjugates have comparable emulsifying properties, with pure conjugate systems having better stabilizing properties, especially in emulsions where pH is close to pI. The next figure will present how the distribution profiles of these three emulsions change after 28-day of storage.



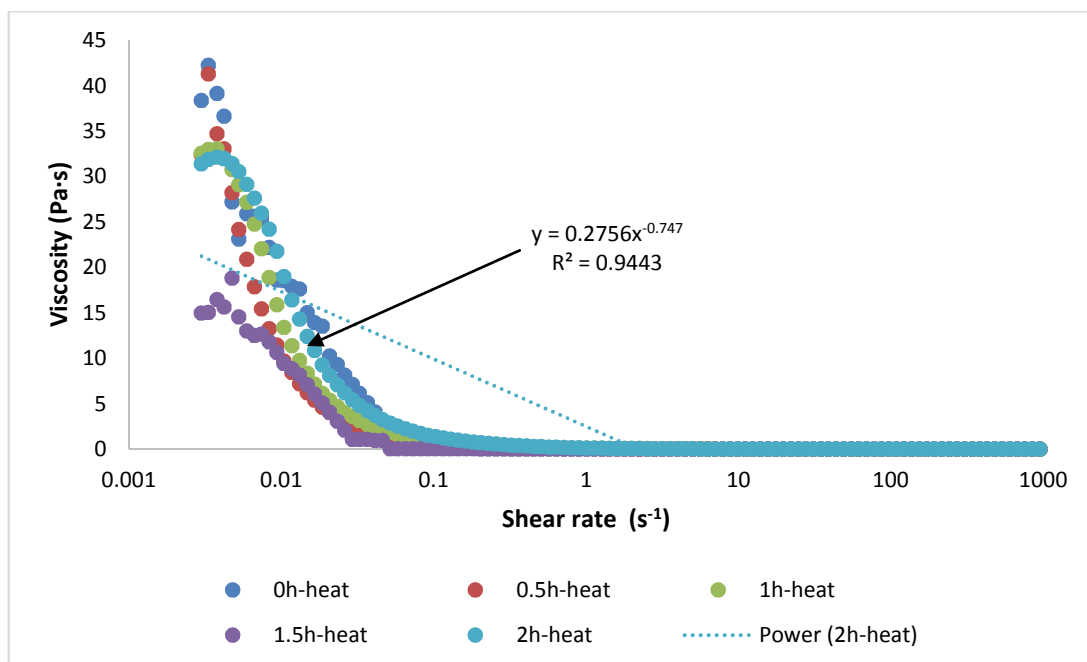
**Figure 3.21** Droplet size distribution (DSD) of O/W emulsions (pH 4.6) stabilized by the mixture of WPI and WPI-MD19 conjugates at three weight ratios (0, 60, and 100%) at storage time Day 28.

Figure 3.21 exhibits the final distribution profiles of three emulsions at the end of the observation period. It is clear that the droplet sizes are mainly around 1 µm in the control (100% conjugate) emulsion, not significantly different from the DSD of the same emulsion at Day 0 (see Figure 3.20). However, at the large size tail of the distribution, 2.93 µm, the percentage is higher than that in the emulsion at the initial stage of storage. It suggests that conjugates can provide excellent stabilizing properties in emulsions with few droplets flocculating with time. Similar observations have also been reported by other researchers (Sato et al., 2003; Maitena et al., 2004; Diftis and

Kiosseoglou, 2006; Wooster and Augustin, 2006; Yang et al., 2015; Zhang et al., 2017).

When it comes to the emulsion prepared with mixtures containing 60% conjugates, the instability of the droplets can be observed by the change in distribution profile. There are two peaks appearing at size values 4.89 and 37.66  $\mu\text{m}$ , seen in Figure 3.21, which are not present in the DSD profile when the emulsion was freshly prepared. Nevertheless, the majority of droplets are still in a range from 0.63 to 1.76  $\mu\text{m}$ . For the emulsion without any conjugate, the peak of DSD dramatically shift from 1.73 to 8.14  $\mu\text{m}$ , clearly visible in Figures 3.20 and 3.21. Furthermore, the droplets in the small size classes (< 1  $\mu\text{m}$ ) almost flocculate in this emulsion after 28-day of storage. At the same time, a great number of large droplets (> 100  $\mu\text{m}$ ) are also formed. Therefore, the stability of the emulsion with native WPI is not acceptable under more severe environmental conditions.

Emulsion stability can also be tested to some extent via its flow behaviours under different shear rates. The next section will present the rheological properties of emulsions stabilized by WPI-MD19 conjugates, mixture of WPI-MD19 conjugates + WPI, at 60 % to 40 % weight ratios, as well as the native WPI.



**Figure 3.22** Viscosity profiles of the emulsion stabilized by WPI-MD19 conjugates only in 85 °C water bath for 2 hours and gradually cooled down to room temperature under different shear rates.

In Figure 3.22, it shows how the viscosity of the emulsion with 100 % conjugates changes under constant thermal treatments for 2 hours and cooled down to room temperature gradually. As can be seen from this figure that the emulsion at different heating stages exhibits similar shear-thinning properties especially when the shear rate is in the range between 0.001 and 0.1 s<sup>-1</sup>. As the shear rate increases from 0.1 s<sup>-1</sup>, there is few change of viscosities even though the shear rate arrive at 1000 s<sup>-1</sup>. For the emulsion in water bath for 2 hours, the relationship between shear rate and viscosity is quite well fitted into the power law ( $R^2 = 0.9443$ ) ( $y = 0.2765x^{-0.747}$ ). The  $n$  value is  $-0.747 (< 1)$ , which indicates that the emulsion stabilized by WPI-MD19 conjugate after 2-hour water bath and cooling downing process exhibited shear-thinning behaviour (see 2.3.3 ). A similar pattern was also observed for the emulsion under other heating times in water bath. This observation suggests that heat

treatment has insignificant influence on the flow behaviour of the emulsion stabilized by WPI-MD19 conjugates (100 %).

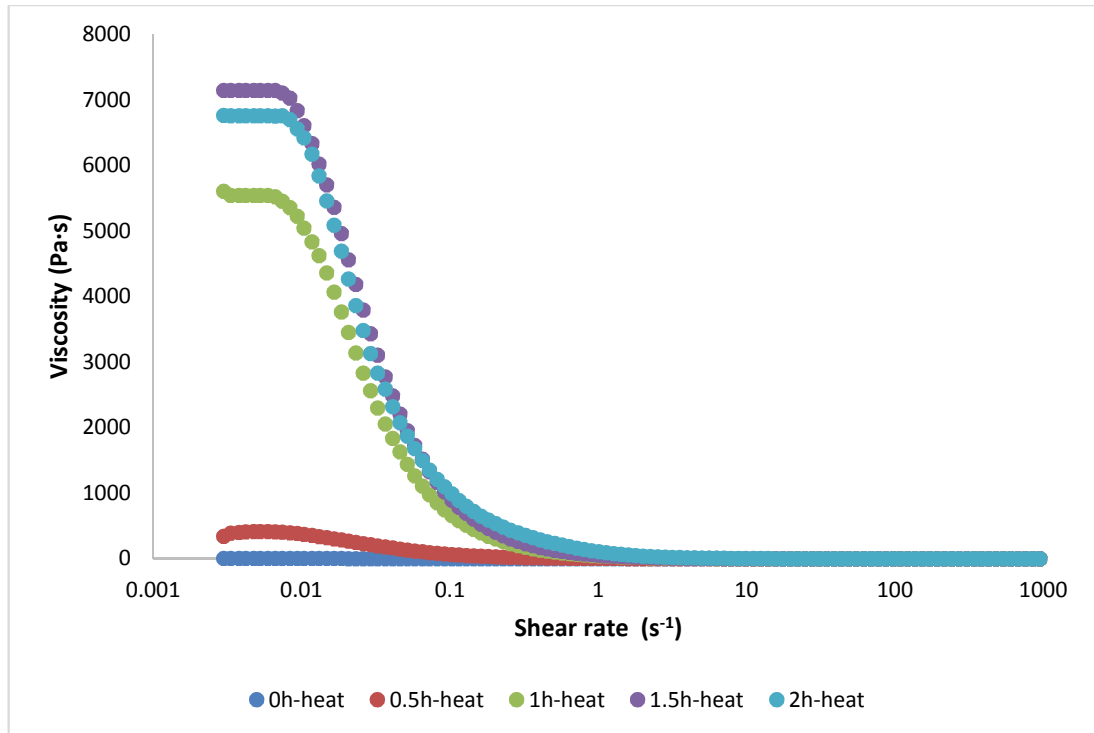


**Figure 3.23** Viscosity profiles of the emulsion stabilized by native WPI only in 85 °C water bath for 2 hours and gradually cooled down to room temperature under different shear rates.

Figure 3.23 exhibits the viscosity of the emulsion stabilized by native WPI only, following up to 2-hour of heat treatment, with slow-cooling-down process, plotted against shear rate. At the initial stage of water bath heating for around 0.5 h, the viscosity of the emulsion only slightly increases. With longer heating time to about 2 h, the viscosity of this emulsion shoots up dramatically to values more than 5000 Pa·s which is 100 times higher than the viscosity of the emulsion with conjugates under the same shear rate conditions, as seen in Figure 3.22. If we take the emulsion with 2-hour heat in

water bath as an example, the relationship between shear rate and viscosity is close to Cross model (Dickinson, 1982f & 1992c). When shear rate was less than  $0.01 \text{ s}^{-1}$ , the viscosity of emulsion stayed around  $7000 \text{ Pa}\cdot\text{s}$ . A significant decrease of viscosity from  $7000$  to  $1000 \text{ Pa}\cdot\text{s}$  occurred from shear rate  $0.01$  to  $0.1 \text{ s}^{-1}$ . At the third stage, if shear rate was higher than  $0.1 \text{ s}^{-1}$ , the viscosity hardly changed according to Figure 3.23. The emulsion under heat treatment in water bath over 1 hour showed the similar pattern.

For the emulsion stabilized by native WPI alone, the significant difference of rheological behaviours at various heating times in water bath was observed. The considerable increase in viscosity of this emulsion could be the formation of 3D network gels incorporating oil droplets. In comparison, the performance of the emulsion stabilized with WPI-MD19 conjugate only involves shear-thinning behaviour at shear rates less than  $0.1 \text{ s}^{-1}$ , which suggests less 3D structures were formed during heating process than that of the emulsion stabilized by WPI alone (see Figure 3.22). Therefore, it can be concluded that emulsions stabilized by conjugates have better rheological stability than those stabilized by native WPI only under heating-cooling process.

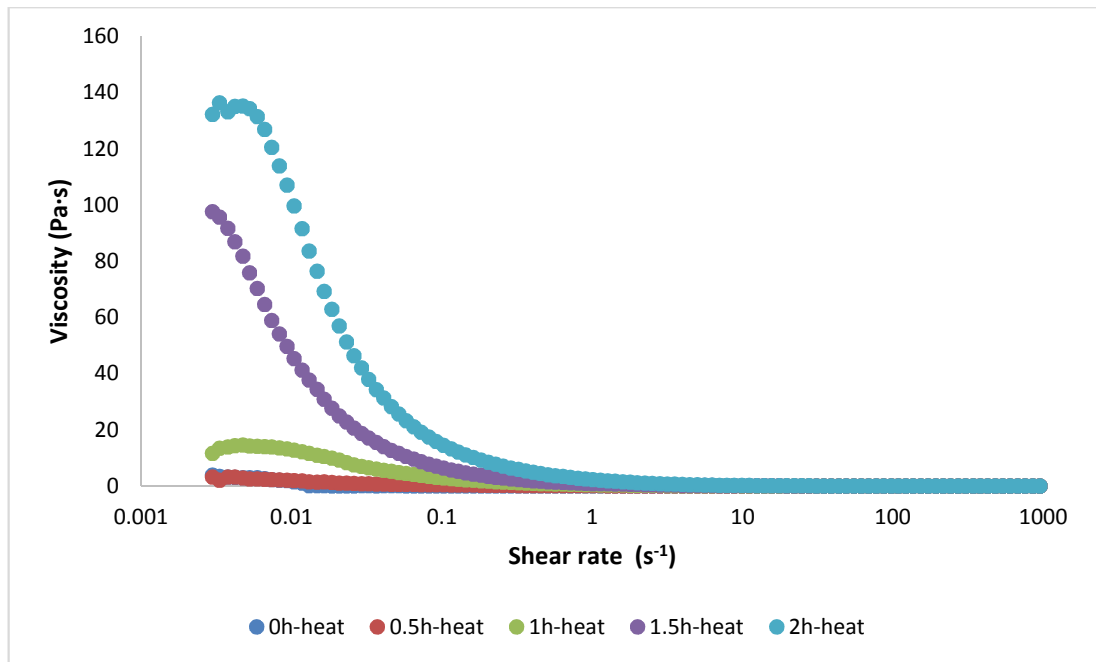


**Figure 3.24** Viscosity profiles of the emulsion stabilized by the mixture of WPI-MD19 conjugates (60 w/w %) and WPI (40 w/w %) in 85 °C water bath for 2 hours and gradually cooled down to room temperature under different shear rates.

The viscosity profiles of the emulsion stabilized by the mixture of WPI-MD19 and WPI at the weight ratio of 60 : 40 w/w are shown in Figure 3.24. It can be seen that this emulsion demonstrates shear-thinning behaviour under low shear rates ( $< 0.1 s^{-1}$ ) especially when the heating time is over 1h. Similar to samples in Figure 3.22 and 3.23, at the high shear rates, the viscosity plateaus out and becomes constant even at a shear rate up to  $1000 s^{-1}$ . The maximum viscosity of this emulsion is around 140 Pa·s, a value that is intermediate between that seen for emulsions stabilized with WPI-MD19 conjugate (around 45 Pa·s) and that of for the emulsions stabilized solely by native WPI ( $> 5000 Pa·s$ ), under the same shear rate conditions (See Figures 3.22 and 3.23). This observation suggest that the existence of WPI-MD19

conjugates, even in a mixture of WPI + conjugates, can considerably improve the thermal stability of emulsions.

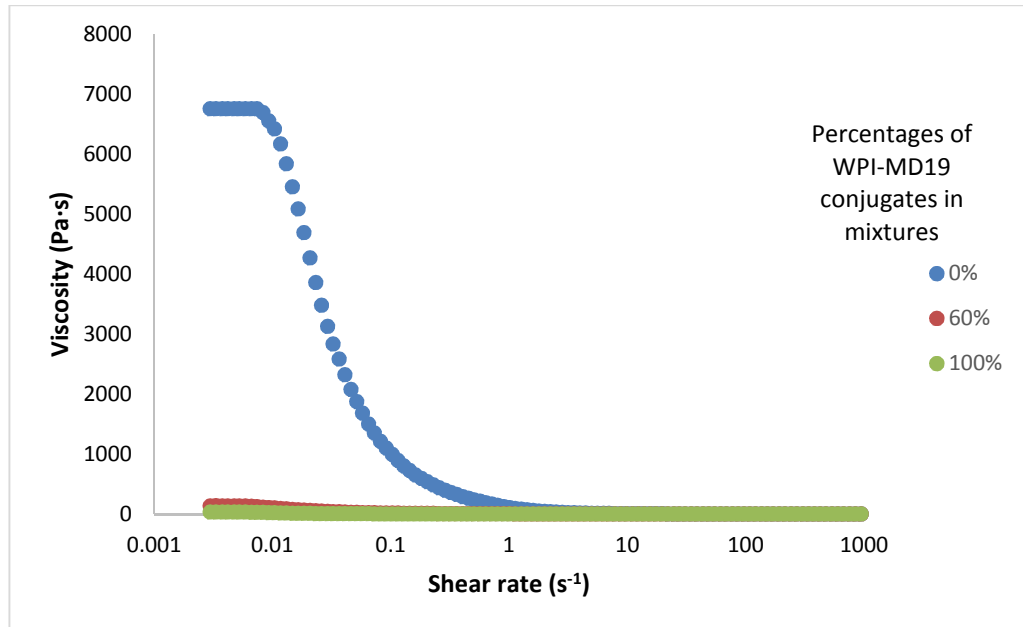


**Figure 3.25** Viscosity profiles of the emulsions stabilized by different systems in 85 °C water bath after 2 hours and gradually cooled down to room temperature under different shear rates.

Figure 3.25 shows the flow properties of emulsions stabilized by the mixture of WPI-MD19 and WPI at 0, 60, and 100 w/w % mix ratios after 2 hours of constant heating, at 85 °C. It can be seen that the viscosities are not significantly altered, throughout the entire thermal treatment for the 60 % and 100 % sample as compared to the 0 % sample. The viscosity of the emulsion without any conjugates dramatically increases after the heating, which means that this sample is not stable following the heat treatment. These results suggest that presence of 60 w/w % conjugates, in a mixture of WPI-MD19 and WPI, is sufficient to provide acceptable thermal stability for the O/W emulsion systems.

To sum up the thermal stability of the emulsions with the mixture of WPI-MD19 and WPI, conjugates can remarkably increase the emulsion stability through the thermal treatment applied for relatively long durations. The existence of native WPI in emulsions may not drastically influence the thermal stability of the whole system if the weight proportion of WPI in the stabilizers is less than 40 %. This result is significant since the thermal stability of emulsions is critical in food manufacturing, due to common food processing techniques such as sterilization.

### **3.4 Conclusions**

In this chapter, the properties of the mixtures of WPI-MD19 conjugates and WPI were investigated through both theoretical calculations and experiments. It is almost inevitable that any large scale production of conjugates will lead to such mixtures, as it is unlikely that all WPI will react in such a process. From the theoretical results obtained via the SCF calculations, it can be concluded that WPI-MD19 conjugates have significantly enhanced stabilizing properties, especially at pH values close to pI when compared to native WPI stabilized systems. Furthermore, the conjugates at a sufficient mix ratio, can adsorb to the oil-water interface even in the presence of WPI in the bulk phase, the conjugates having a lower surface affinity than native protein ( $\beta$ -LG). These predictions seem to agree with our experimental results. In the examination of their interfacial properties, the conjugates have similar capacities to reduce the oil-water interfacial tension as the WPI, meaning that conjugates will not be displaced from the interface by WPI, once they are adsorbed. Therefore, it is possible to stabilize O/W emulsions by a

mixture of WPI-MD19 and WPI under unfavourable pH and other environmental conditions.

Based on these findings, emulsions stabilized by the WPI-MD19 and WPI mixtures, at various weight ratios, were tested under different conditions such as pH, concentrations of CaCl<sub>2</sub>, and thermal treatment in order to determine the critical ratio of acceptable emulsion stabilizing properties between these two bio-polymers at which the emulsion stability is still comparable to that observed for systems stabilized by pure conjugates. All the results suggest that 60 w/w % conjugates in the mixture is sufficient to provide acceptable stability close to the performance of pure conjugates.

Both theoretical and experimental results suggest that the mixture of protein and its conjugates has a great potential to lower the cost of applying conjugates to food industry as novel emulsifiers and stabilizers. In the next chapter, the influence of the presence of lactose impurity on the conjugates during preparation will be studied to explore another potential issue in large scale manufacturing of conjugates.

## **Chapter 4**

### **Influence of Reducing Polysaccharides on Protein-polysaccharide Conjugates via the Maillard Reactions**

#### **4.1 Introduction**

The characteristics of polysaccharides play an important role in the emulsifying and stabilizing properties of protein-polysaccharide conjugates prepared through Maillard reactions. For example, the length of polysaccharide chains coupled with protein backbones can influence the steric stability of the conjugates adsorbed onto the oil-water interface. Generally, it is thought that the longer is the polysaccharide chain, the better is its steric stabilizing performance (Shu et al., 1996; Kato, 2002; Dunlap and Cote, 2005). Moreover, the attachment sites of polysaccharides to the protein can also be critical for the stabilizing properties of the conjugates, as demonstrated by theoretical calculations (Ettelaie et al., 2005 & 2008; Parkinson et al., 2005; Akinshina et al., 2008; Ettelaie and Akinshina, 2014). Furthermore, the competitive attachments to proteins between different polysaccharides during heat treatments may affect the functional properties of the final conjugates (Ding et al., 2017).

In this chapter, the influence of reducing polysaccharides on the conjugates will be investigated including the influence of the weight ratio of native proteins to polysaccharides prior to Maillard reactions, length of polysaccharides chains, and different molar ratios between short chain reducing sugars and longer chain polysaccharides, both competing to react with proteins. The effects of different types of sugars can be demonstrated through the stability of O/W emulsions. This type of research can help us to

understand in more detail the stabilizing properties of conjugates and to show the potential for the large scale use of Maillard-type conjugates in food industry.

## **4.2 Materials and Methods**

The major materials in this study are whey protein isolate and maltodextrins chosen with various chain lengths. The whey protein, which was manufactured to be homogeneous and lactose-free white powder by concentrating and spray drying from fresh whey, was purchased from Sigma-Aldrich (St Louis, MO, USA) and Davisco Foods International (USA). For polysaccharides, maltodextrins (MD2, MD19, and MD47) were provided by Roquette (UK) Ltd.. Apart from long-chain saccharides, the disaccharide lactose (DE ~2) was obtained from Fisher Scientific (Loughborough, LE11 5RG, UK).

There are other materials used in this research such as sunflower oil which was purchased from local supermarket Morrison (Leeds, UK) for emulsion preparation. Common chemicals and reagents are Analytical grade.

### **4.2.1 Preparation of WPI-MD conjugates**

Whey protein isolate and maltodextrin with various Dextrose Equivalent (DE) values (2, 19, 47) were dissolved in 100 ml distilled water according to the weight ratios in Table 4.1.

**Table 4.1** Conjugates WPI-MD Prepared with Different DE Values at Various WPI to MD Ratios

Conjugates	WPI (g)	MD (g)
WPI-MD2 (2:1 w/w)	2	1
WPI-MD2 (1:1 w/w)	1	1
WPI-MD2 (1:2 w/w)	1	2
WPI-MD2 (1:3 w/w)	1	3
WPI-MD2 (1:4 w/w)	1	4
WPI-MD19 (2:1 w/w)	2	1
WPI-MD19 (1:1 w/w)	1	1
WPI-MD19 (1:2 w/w)	1	2
WPI-MD19 (1:3 w/w)	1	3
WPI-MD19 (1:4 w/w)	1	4
WPI-MD47 (2:1 w/w)	2	1
WPI-MD47 (1:1 w/w)	1	1
WPI-MD47 (1:2 w/w)	1	2

The solution of protein and polysaccharide was put in the fridge and stored at a temperature of 4 °C overnight allowing for better mixing of WPI and maltodextrins. Next the solution was completely frozen at -30 °C for 3 hours and then freeze-dried at -50 °C under pressure of 0.04 mbar for 24 hours. This removed the water molecules preparing the samples for Maillard reactions.

Before the heat treatment, it is necessary to preheat the desiccator which provides a stable environment for reactions at relative humidity of 79% controlled by the saturated potassium bromide solution. The preheating was carried out for 2 hours in a fan oven at 80 °C, before the dry powder containing the mixture of WPI and MD was placed in it. The dry-heating process lasts for

3 hours in total, and the products were gradually cooled down under room temperature. When the samples were collected from the desiccator, they were placed in sealed plastic bags and stored in dry and dark cupboards for further applications.

#### 4.2.2 Preparation of WPI-MD19 conjugates with lactose

Similar to the preparation of WPI-MD in section 4.2.1, proteins and disaccharides were mixed into 100 ml distilled water to form a solution. However, in the method here, the weight ratio between WPI and MD19 is fixed to 1:2 with different levels of lactose introduced as impurity into the system prior to the Maillard reactions (Table 4.2).

**Table 4.2** Conjugates WPI-MD with Different DE Values at Various Ratios of MD19 to Lactose

WPI (g)	MD19 (g)	Lactose (g)	MD19:lactose (molar)*
1	2	0.0787	1:1
1	2	0.1574	1:2
1	2	0.3135	1:4
1	2	0.4703	1:6
1	2	0.7839	1:10

\*MD19 ( $M_w = 8.7$  kDa); lactose ( $M_w = 342.3$  g/mol)

Once the solution was prepared, based on the recipe in Table 4.2, it was stored overnight at 4 °C in a fridge. The rest of the preparation is identical to the procedure described in 4.2.1.

#### **4.2.3 Degree of conjugation**

The conjugates prepared through the Maillard reactions were confirmed by the OPA tests which can also estimate the degree of conjugation (DC) of each sample. The details of OPA tests and calculations of the DC are the same as those described in section 3.2.4.

#### **4.2.4 Preparation of emulsions**

The first step to make an O/W emulsion is to prepare the aqueous solution containing citric acid and salt. For 500 ml aqueous buffer, citric acid (3.125 g) and sodium chloride (2.920 g) were dissolved into 100 ml distilled water. Sodium azide was also added to the solution at the concentration 0.1 w/v % as the preservative. The solution was finalised to 500 ml by distilled water.

The dry conjugates were then dissolved in the aqueous buffer based on overall protein concentration of 2 w/v % by gentle stirring under room temperature. When the clear conjugates solution was ready, it was passed through the jet homogenizer at 350 bar with sunflower oil at a volume ratio of 80 : 20 solution to oil. After the emulsification, the pH of the emulsion was adjusted to 4.6 (isoelectric point of WPI) by adding several drops of 6 M NaOH in order to eliminate the electrostatic effects between the oil droplets. All the emulsions were stored quiescently at 30 °C.

#### **4.2.5 Emulsion stability monitoring**

The stability of emulsions during any given storage time is a critical feature to ascertain the stabilizing properties of the stabilizers. There are three techniques used to analyse the emulsion stability in this study: particle sizing by the Mastersizer 3000, flowing behaviours by the Rheometer, and micro-

images by confocal laser scanning microscopy (CLSM). For particle sizing and flowing behaviours, the methods are similar to these already described in Chapter 3. The details can be found in section 3.2.7. In the CLSM, the emulsion samples (2.5 g) were stained by Nile red (25  $\mu$ l of 0.01 w/v % dye in polyethylene glycol) with gentle mixing under room temperature. The stained samples were then placed in a plastic cell and covered with a cover slip. A Leica microsystem was used to observe and record the images.

#### **4.2.6 Statistic analysis**

All the data generated from OPA tests, particle sizing, and rheological measurements were collected and processed through MS Excel<sup>®</sup> 2013. The results were presented as the average values with standard deviations of triplicates.

### **4.3 Results and Discussions**

#### **4.3.1 Appearance of conjugates**

The protein-polysaccharide conjugates were prepared by non-enzymatic browning process. The change of colour is a direct evidence for the occurrence of Maillard reactions.



**Figure 4.1** Appearance of the whey protein isolate and maltodextrin mixture in the dry state before (Left) and after (Right) following heat treatments at 80 °C for 3 hours.

Figure 4.1 shows the appearance of dry mixture of WPI and MD before and after dry-heating treatment. After freeze drying, the mixture displays a white colour with fluffy texture, which indicates that there is no significant browning process occurring before heating. However, the colour of the product changes from white to yellow and to brown after the heating at 80 °C for 3 hours owing to the Maillard reactions. This observation can be used as a preliminary evidence to support the formation of conjugates. Moreover, it can be seen from Figure 4.1 (Right) that the yellow colour is quite evenly distributed amongst the products, which suggests that the Maillard reactions happened throughout the whole system during heating, because of good mixing and contact between proteins and polysaccharides. The evenness of final products is critical for the further application of conjugates to preparation of emulsions.

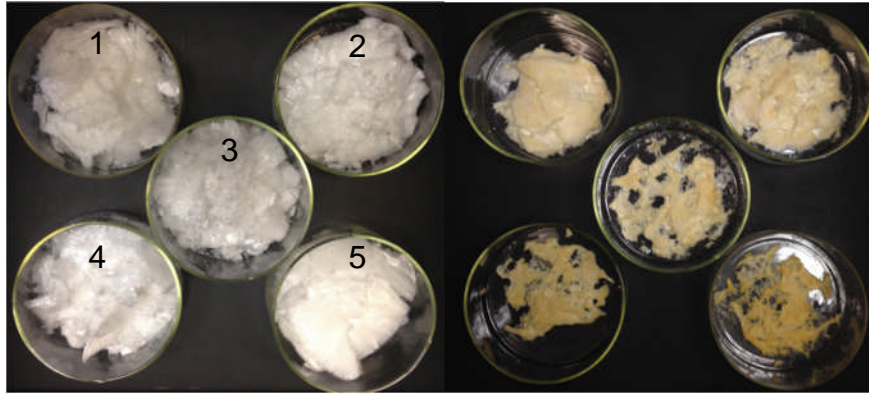


**Figure 4.2** An illustration of WPI and MD19 mixture combining various proportions of lactose before (Left) and after (Right) the Maillard reactions; (1) MD19 : lactose (molar) = 1:1; (2) MD19 : lactose (molar) = 1:2; (3) MD19 : lactose (molar) = 1:4; (4) MD19 : lactose (molar) = 1:6; (5) MD19 : lactose (molar) = 1:10.

It is shown in Figure 4.2 that the appearance of WPI and MD19 mixture containing different levels of lactose is dramatically altered after the heat treatments. Similar to Figure 4.1, the yellow colour is also observed in the final products. As for the texture of conjugates, it has a relatively loose and porous structure at lower lactose ratio ( $< 1:6$ ), while it becomes rigid and hard when the molar ratio of lactose is increased above 1:6 and beyond to 1:10. This observation indicates that the presence of lactose impurity in the mixture of WPI and MD19 may affect the Maillard reactions and further influence the properties of the final products.

#### 4.3.2 Solubility of conjugates

Solubility is one of the key physicochemical property of a good emulsifier and stabilizer, especially for food industrial formulations. Therefore, it is essential to compare the solubility between the native protein on one hand and the conjugates on the other, under different environmental conditions.

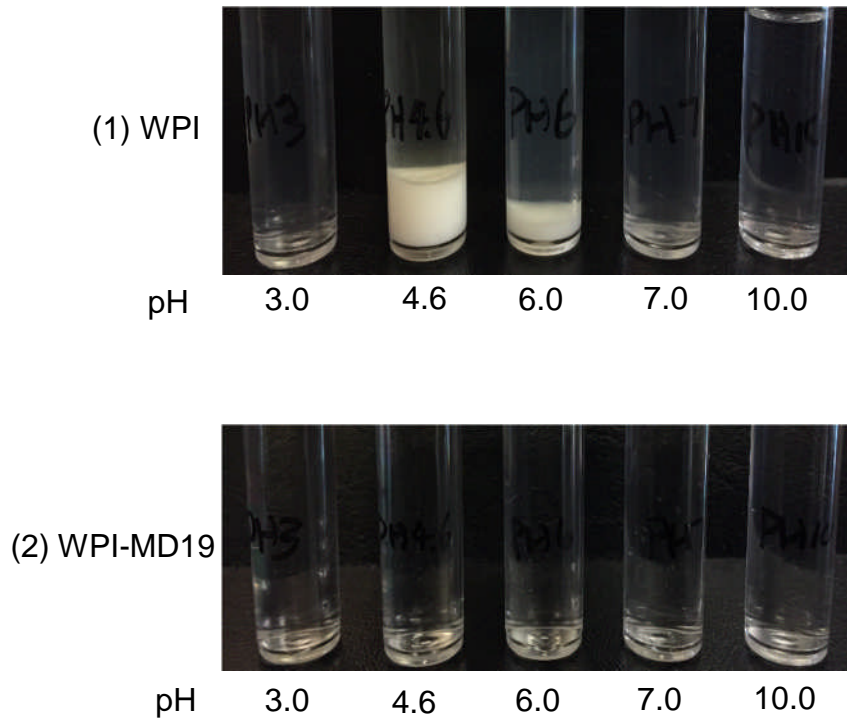


**Figure 4.3** Solubility tests of WPI and WPI-MD19 conjugates at different pH values from 3 to 10, including the pI of WPI pH 4.6; (1) 1 w/v % WPI at pH 3, 4.6, 6, 7, and 10; (2) 1 w/v % (on protein basis) WPI-MD19 at pH 3, 4.6, 6, 7, and 10.

In Figure 4.3, we exhibit the solubility of WPI and WPI-MD19 in aqueous solutions at pH range from 3 to 10. For WPI as seen in Figure 4.3 (a), the solubility is quite high when pH is far from pI 4.6. However, when pH is 6, WPI starts to precipitate. The solubility reaches its lowest point if pH is 4.6 as expected. On the contrary, there is no noticeable precipitation of conjugates for the whole pH range at the same proportion of proteins (1 w/v %), in any of the system according to Figure 4.3 (b).

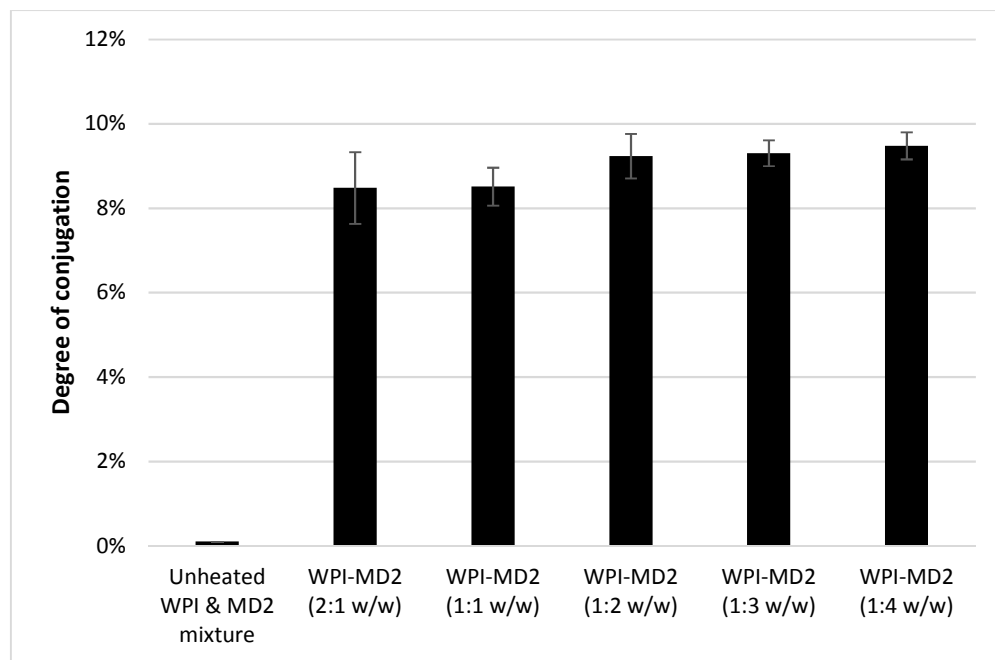
Apart from the solubility difference between native protein and conjugates, the easiness of dissolving is also considerably different. It took more than half an hour to fully dissolve WPI in 100 ml distilled water at the

ambient temperature while it took less than 1 min to prepare a clear solution with conjugates at the same conditions.

All these results and observations from solubility tests, suggest that the attachment of polysaccharides can remarkably enhance the solubility of native proteins and be more resilient against unfavourable environmental conditions.

### 4.3.3 Degree of conjugation

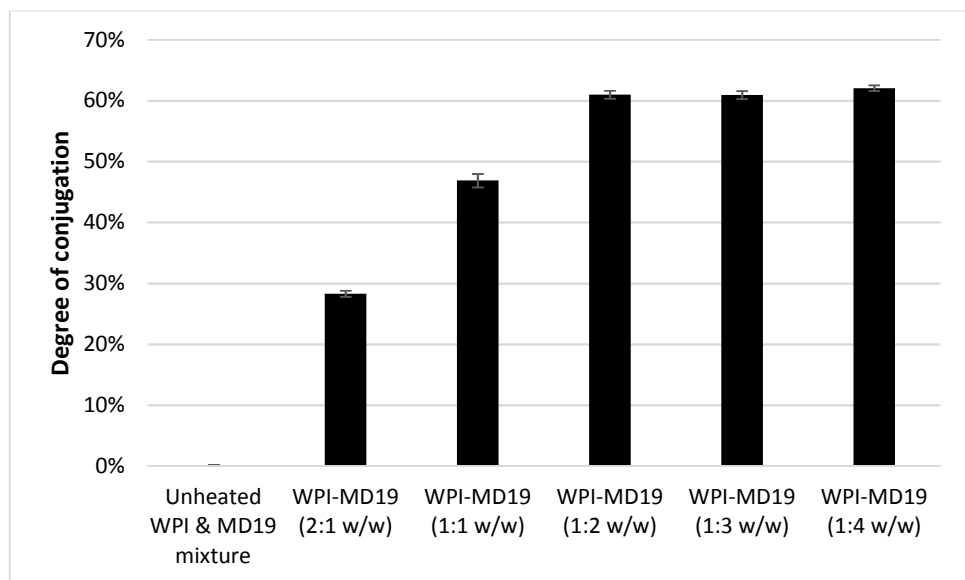
After the Maillard reactions, it is important to analyse the degree of conjugation for all types of conjugates.



**Figure 4.4** Degree of conjugation for WPI and maltodextrin (DE 2) at various weight ratios between WPI and maltodextrin based on the protein concentration 1 w/v %.

Figure 4.4 shows the results of the analysis of the degree of conjugation using the method described in 3.2.4. It can be seen that WPI and maltodextrin (DE 2) (MD2) can have various degrees of conjugation as the

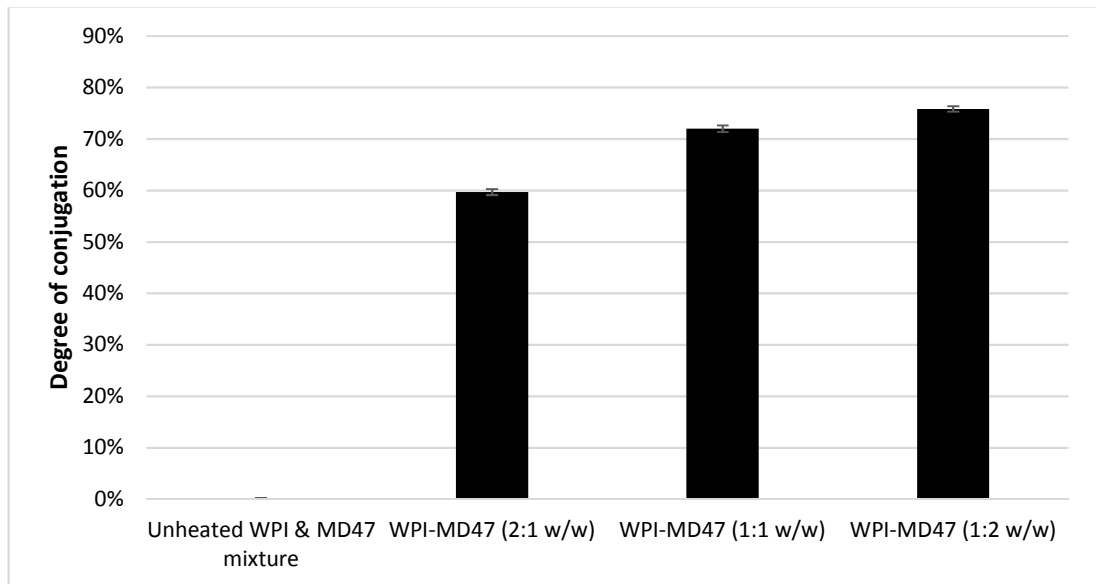
weight ratios of the two components is altered. When compared to the mixture of WPI and MD2 without the Maillard reactions, the conjugation between WPI and MD2 at all weight ratios is found to proceed successfully. The degrees of conjugation is quite similar around 9 % for all the samples. This result suggests that there is no significant influence of weight ratios of MD2 during the Maillard reactions on the actual degree of conjugation.



**Figure 4.5** Degree of conjugation for WPI and maltodextrin (DE 19), at various weight ratios between WPI and maltodextrin, based on the protein concentration of 1 w/v %.

It is demonstrated in Figure 4.5 that, at different weight ratios between WPI and MD19, there are different conjugation behaviours. When the polysaccharide is changed to MD19, the relationship between the weight proportion of polysaccharides and the degree of conjugation shows a positive correlation. When the MD weight ratio is lower than 1:2 (WPI : MD19), the degree of conjugation is generally less than 50 %. As the MD weight ratio in reactants is increased, until reaching 1:4, the degree of conjugation also

become larger, attaining a value of 60 %. However, higher MD weigh ratio than 1:2 will not result in the higher degree of conjugation. Compared to the result in Figure 4.4, the degree of conjugation is dramatically increased at all MD weight ratios, from around 9 % to around 60 %, especially when the weight ratio between WPI and MD19 is higher than 1 : 1, under the same reaction conditions. It suggests that shorter chain polysaccharides, which have higher DE values, may have a better chance to react and attach to the protein molecules during heating.



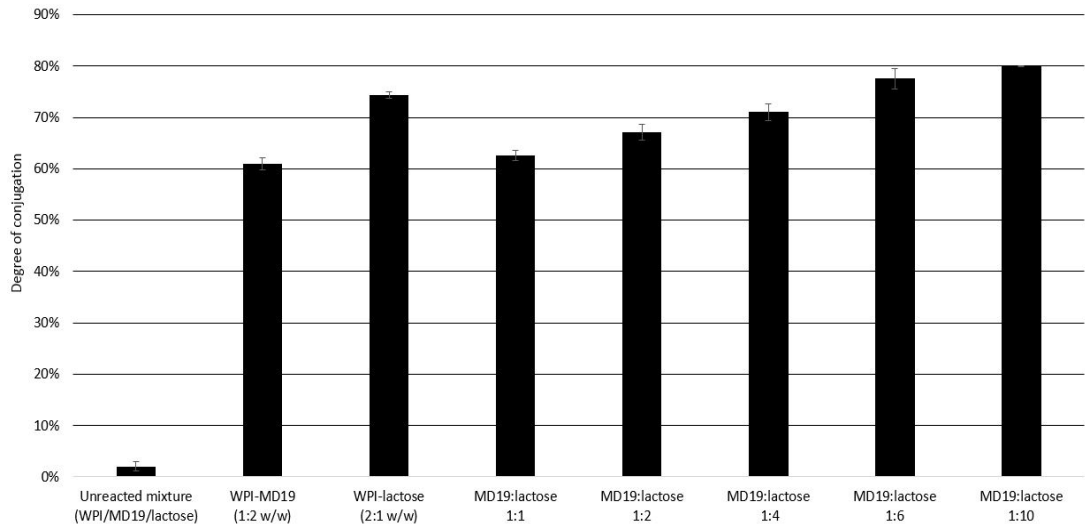
**Figure 4.6** Degree of conjugation for WPI and maltodextrin (DE 47) at various weight ratios between WPI and maltodextrin based on the protein concentration 1 w/v %.

Figure 4.6 exhibits the degrees of conjugation for conjugate complexes of WPI with MD47, at different weight ratios. It is clear that the degree of conjugation is relatively high, even at low MD weight ratios such as DC 60% at 2:1 (WPI : MD). When the proportion of MD increases to 1:2, the degree of

conjugation also goes up to 75 %. It is difficult to collect the products if the MD47 weight ratio is higher than 1:2 because the polysaccharides would be solidified and will stick strongly to the container.

It can be seen from Figure 4.4, 4.5 and 4.6 that the chain length of polysaccharides and weight ratios of polysaccharides in reactants can affect the degree of conjugation which may in turn influence the stabilizing properties of the conjugates in emulsions. Generally, higher sugar weight ratios involving shorter chain length of sugars can enhance the degree of conjugation. However, the stabilizing properties of conjugates will not only be determined by the degree of conjugation. Therefore, it is critical to consider the influence of polysaccharides on the conjugates during the preparation.

In the study concerning the influence of lactose on the WPI-MD19 conjugation system, the weight ratio between WPI and MD19 was chosen to be 1:2. Lactose was then intentionally added to the mixture as an impurity to compete with MD19 for reacting and attachment to proteins, at various levels of molar ratios to MD19. The degree of conjugation for this complicated system is presented in Figure 4.7 as follows.



**Figure 4.7** Degree of conjugation for WPI and maltodextrin (DE 19) at weight ratio of 1:2 with different molar ratios of MD19 to lactose during the Maillard reactions based on the protein concentration 1 w/v %.

As can be seen from Figure 4.7, the degree of conjugation is positively correlated to the increase of lactose percentage in reactants, which is similar to the trend we observed in Figure 4.5 and 4.6. The total DC value increases only marginally from 60 % to 80 %, while the molar ratio of lactose to MD19 was made 10 times higher from 1 : 1 to 1:10. This observation indicates that lactose can react with WPI in the mixture of WPI and MD19 system during dry heating process but is not able to maximize the DC to complete 100 % reaction. This incomplete conjugation may result from the globular structure of  $\beta$ -lactoglobulin, which is the major protein in WPI which prevents access to some of the potential reactant sites of the protein. Similarly, possible caramelisation among lactose under the heat treatment, will considerably reduce the amount of sugar (on a molar ratio basis) available for conjugation. The hard and rigid structure of conjugates arising from sugar-sugar reactions were also observed during the preparation of WPI-MD47.

To summarize the influence of polysaccharides on the degree of conjugation, there is a clear negative relationship between the chain length of the polysaccharides and the DC values. For the proportion of polysaccharides in the reactants, it depends on the nature of polysaccharides. Generally, higher percentages of polysaccharides can lead to higher degree of conjugation in a certain range. Beyond this range, DC does not increase correspondingly, owing to the sugar-sugar reactions. In the next part, the stabilizing properties of all the above conjugates will be tested by producing O/W emulsions stabilized by each group of these complex macromolecules. In doing so we wish to further investigate the impact of different polysaccharides on such stabilizing properties.

#### **4.3.4 Emulsion stability by visual assessment**

Emulsions stabilized by different conjugates were stored for 28 days at 30 °C. The creaming process for each sample is visualized by the following photographs.

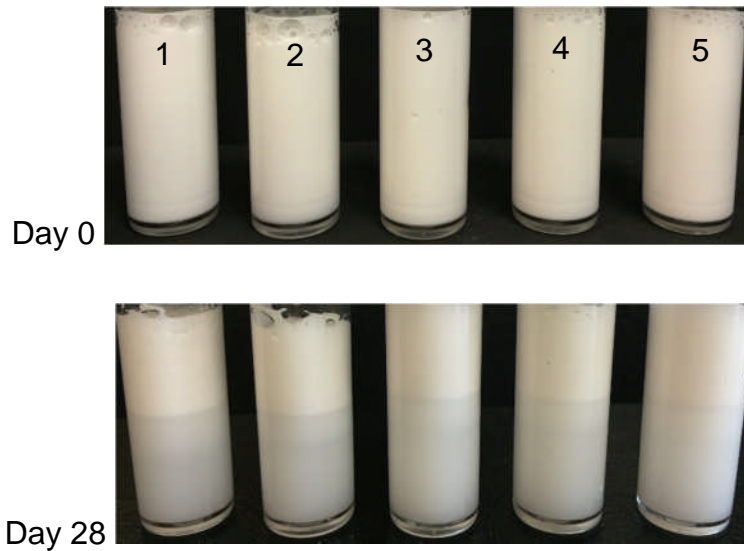


**Figure 4.8** Photograph of O/W emulsions stabilized by WPI-MD2 at different weight ratios between WPI and MD2 from storage day 0 to day 28; (1) WPI : MD2 = 2:1; (2) WPI : MD2 = 1:1; (3) WPI : MD2 = 1:2; (4) WPI : MD2 = 1:3; (5) WPI : MD2 = 1:4.

Figure 4.8 shows the creaming process of emulsions stabilized by WPI-MD2 prepared at various weight ratios between WPI and MD2, after 28-day of storage. There is no obvious creaming for all the samples when they were freshly prepared. However, after the storage, all these emulsions exhibited some degree of creaming, as displayed in photograph above (Figure 4.8). The creaming process is more obvious when the weight ratio of MD2 is lower than 1:2 ( WPI : MD2) than that in the other three emulsions having higher MD2 percentages. Even for the emulsion with the highest MD2 proportion (sample 5), the creaming is still noticeable compared to its original state at day 0. From these pictures, it is clear that the WPI-MD2 conjugates cannot successfully stabilize the O/W emulsions for 28 days. The major reason for this instability of emulsions can be the low degree of conjugations (~ 9 %) in WPI-MD2 for all MD2 weight ratios (see 4.3.3). The low DC values in WPI-MD2 suggests that there is a small amount of polysaccharides attached to WPI, which may

not provide sufficient steric stability when the electrostatic repulsion is also minimized as for example close to pI. More evidence from other techniques, such as particle sizing, to further investigate the emulsion stability is also possible and will be discussed in this chapter latter.

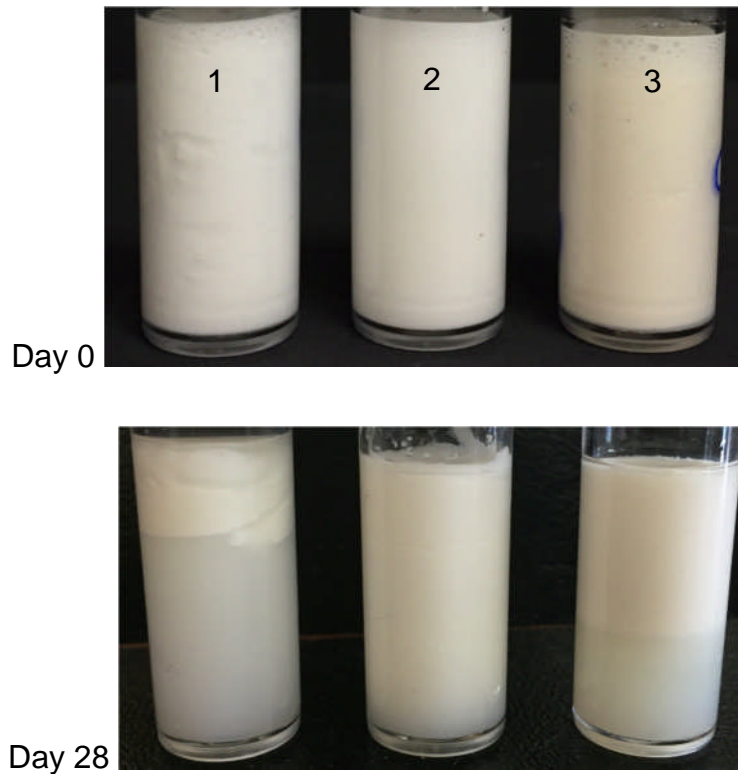


**Figure 4.9** Photograph of O/W emulsions stabilized by WPI-MD47 at three different weight ratios between WPI and MD47 from storage day 0 to day 28; (1) WPI : MD47 = 2:1; (2) WPI : MD47 = 1:1; (3) WPI : MD47 = 1:2.

Figure 4.9 presents photographs of emulsions stabilized by WPI-MD47 at three weight ratios between WPI and MD47, at 2:1, 1:1, and 1:2, on day 0 and day 28 of storage post preparation. The three emulsions were quite homogenous after preparation at day 0 whilst they became unstable after 28 days due to the clear creaming phenomenon. For sample 1 and 3, the creaming is more obvious than that in sample 2 which has the medium level

of MD47 in the conjugates. As can be seen from Figure 4.9 that the emulsion stabilized by WPI-MD47 at WPI : MD47 = 1 : 1 (w/w) has the best stability amongst the three samples. Compared to the result in Figure 4.8, the creaming processes of these three emulsions occurs more gradually than those in the samples stabilized by WPI-MD2. First of all, the DC values (> 60 %) of WPI-MD47 are much higher than those of WPI-MD2 (see 4.3.3), which indicates that more polysaccharides are attached to proteins in the case of MD47. It reduces the creaming by preventing the formation of droplet clusters, due to the steric forces between the droplets. Nevertheless, too much unattached polysaccharides in the bulk phase could stimulate the creaming process by the process of depletion flocculation (see 1.3.3). It can explain the more advanced creaming seen in sample 3, which has a similar DC value as sample 2 but extra MD47 left unreacted in the emulsion system.

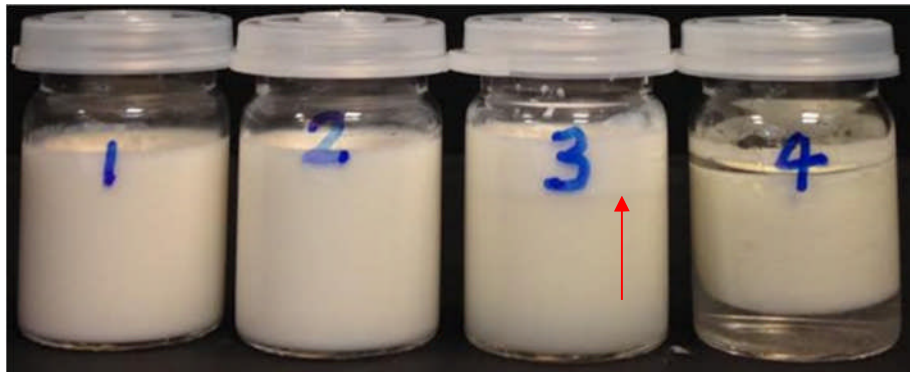


**Figure 4.10** Photograph of O/W emulsions stabilized by different complexes after 28 days; in each case the emulsifier was synthesized as follows: (1) WPI-MD19 (1: 2 w/w) without lactose contamination; (2) WPI-MD19 with lactose impurity present at the molar ratio of 1:10 (MD19 : lactose); (3) WPI-lactose (2:1 w/w) with no maltodextrin present; (4) a mixture of WPI and MD19 (1:2 w/w) without any heat treatment; in sample 3, the position of cream layer is indicated by an arrow.

Figure 4.10 shows a photo of emulsions stabilized by WPI-MD19 (1:2 w/w) with high molar ratio of lactose contamination, after 28-days of storage. It can be seen from this photograph that sample 1, stabilized by WPI-MD19, exhibits no noticeable creaming during storage. In contrast, there is a clear aqueous phase separated from the emulsion in sample 4, which is stabilized by the WPI and MD19 mixture not having undergone Maillard reactions. Compared to sample 1 and 4, sample 2, which is stabilized by WPI-MD19 with the lactose impurity at a molar ratio of 1:10 (MD19 : lactose), is quite homogenous and similar to sample 1, whilst the cream layer can be observed in sample 3 stabilized by the conjugates of WPI and lactose at the weight ratio of 2:1. From these observations, it is suggested that the lactose impurity, present during the heat treatment and synthesis of WPI-MD19 conjugates system, has no significant influence on the stabilizing properties of the final product in the O/W emulsion. Further characterisation of these emulsions by other methods is described below.

#### **4.3.5 Emulsion stability by average droplet size**

Average droplet size obtained from particle sizing technique is a key parameter to analyse the stability properties of emulsions.

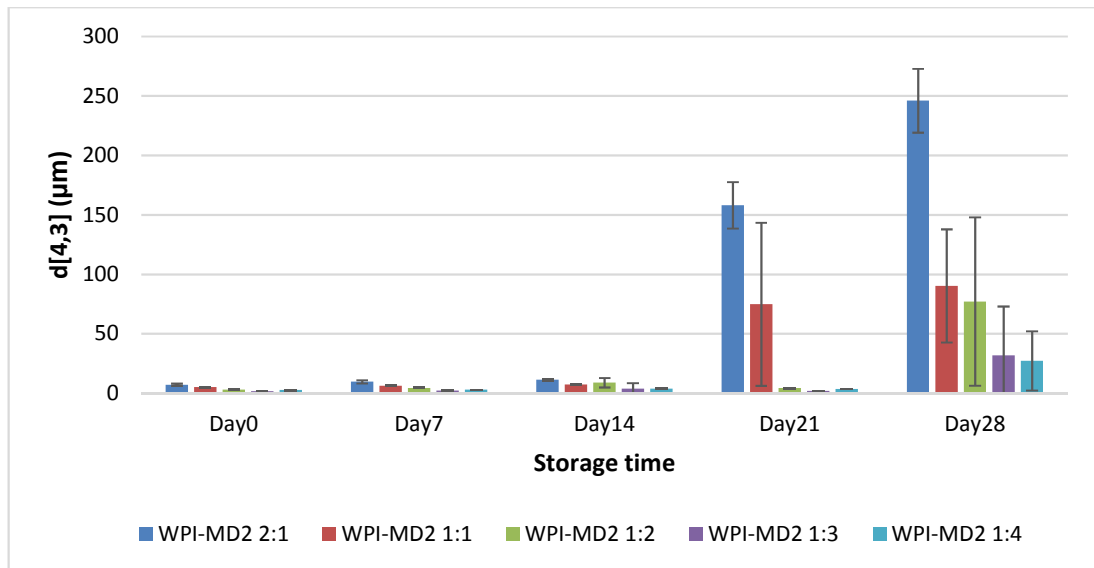


**Figure 4.11** Average droplet size of emulsions stabilized by WPI-MD2 at different weight ratios between WPI and MD2 from storage day 0 to day 28.

It is shown in Figure 4.11 that the average droplet size of each emulsion stabilized by WPI-MD2 alters during the storage. The samples were at pH value 4.6 and 0.1 mol/L NaCl. As can be seen from this figure, during the first two weeks, the average droplet size of all the samples barely change. However, the emulsions become unstable from the third week onward, especially for the samples stabilized by WPI-MD2 with lower proportion of MD2 in the conjugates i. e. WPI-MD2 (1:2 w/w) and WPI-MD2 (1:1 w/w). After 21 days of storage, the average droplet sizes of the other three emulsions are still as low as those on day 0. However, at the end of the observation, all of the emulsions exhibit some degree of instability reflected by the dramatic increase of average droplet size. This result is quite agreeable with the visual assessment observations (see 4.3.4). After 28 days, all the samples exhibited various degrees of creaming. However, the WPI-MD2 has certain level of stabilizing ability especially for the first two weeks, as indicated by the average droplet size values of Figure 4.11. This indicates that conjugation between

WPI and MD2 improves the emulsion stabilizing properties, even though the degree of conjugation of WPI-MD2 is not as high as the other conjugates in this study.

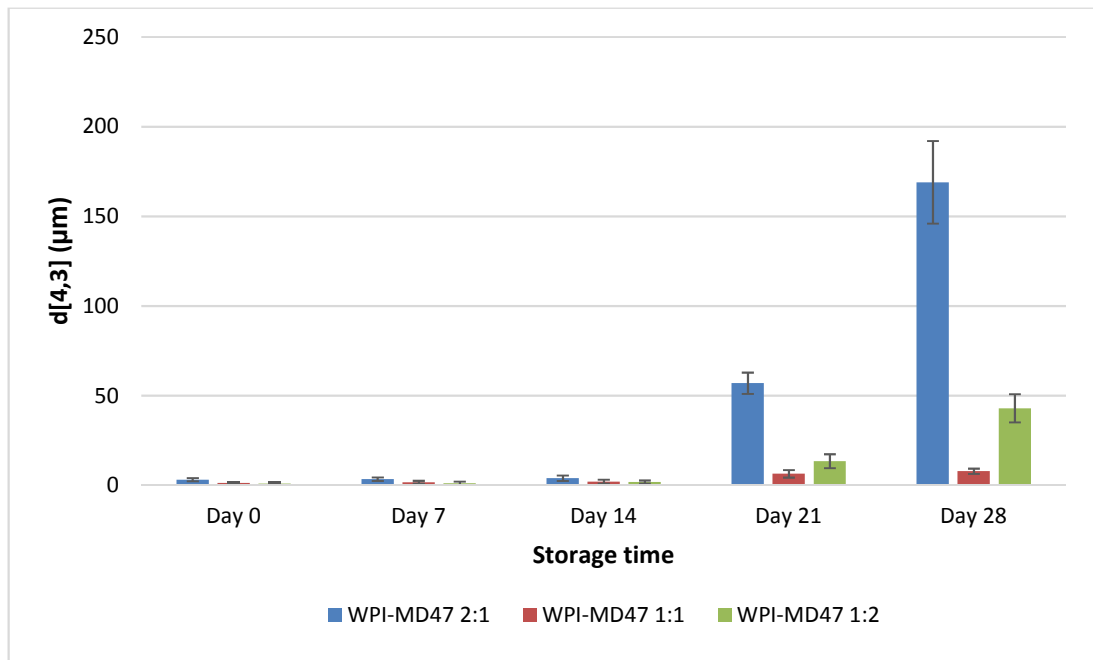


**Figure 4.12** Average droplet size of emulsions stabilized by WPI-MD47, synthesized at different weight ratios between WPI and MD47, throughout storage from day 0 to day 28.

In Figure 4.12, the average droplet sizes of emulsions stabilized by WPI-MD47, synthesized at different weight ratios, are shown. As can be seen, all the emulsions are stable for the initial 14 days, with  $d[4,3]$  around 1  $\mu\text{m}$ . This is quite similar to the results observed for the emulsions stabilized by WPI-MD2 (see Figure 4.11). The average droplet size of the emulsion containing WPI-MD47 (2:1 w/w) considerably increases by a factor of 50 times, and 100 times, at days 21 and 28, respectively. Compared to the emulsion with WPI-MD47 (2:1 w/w), the other two samples in Figure 4.12 are

found to be more stable, because the average droplet sizes are much smaller than that of WPI-MD47 (2:1 w/w). However, at the last day of observation (i.e. day 28), the ADS of emulsion stabilized by WPI-MD47 (1:2 w/w) has shown a significant increase from 1 to approximately 50  $\mu\text{m}$ . These results are in line with the observations on creaming process seen from visual assessment of the samples (see 4.3.4). Moreover, the trend of changing average droplet size with storage time for these emulsions is quite similar to those in Figure 4.11. The WPI-MD47 can provide some degree of stabilizing ability for a certain period of time (about 14 days). All these results suggest that the chain length of polysaccharides and their weight ratios to proteins, during formation of the conjugates have a critical impact on their stabilizing properties in O/W emulsions.

When we come to consider the influence of lactose as a contaminate in the WPI-MD19 (1:2 w/w) system, the impact on the stabilizing properties of the final product is surprisingly low, even at relatively high molar ratio of lactose during the synthesis of the conjugate chains. The following figure shows the change in average droplet size for emulsions stabilized by WPI-MD19, with different molar ratios of lactose in the conjugation system at the time of heat treatment.

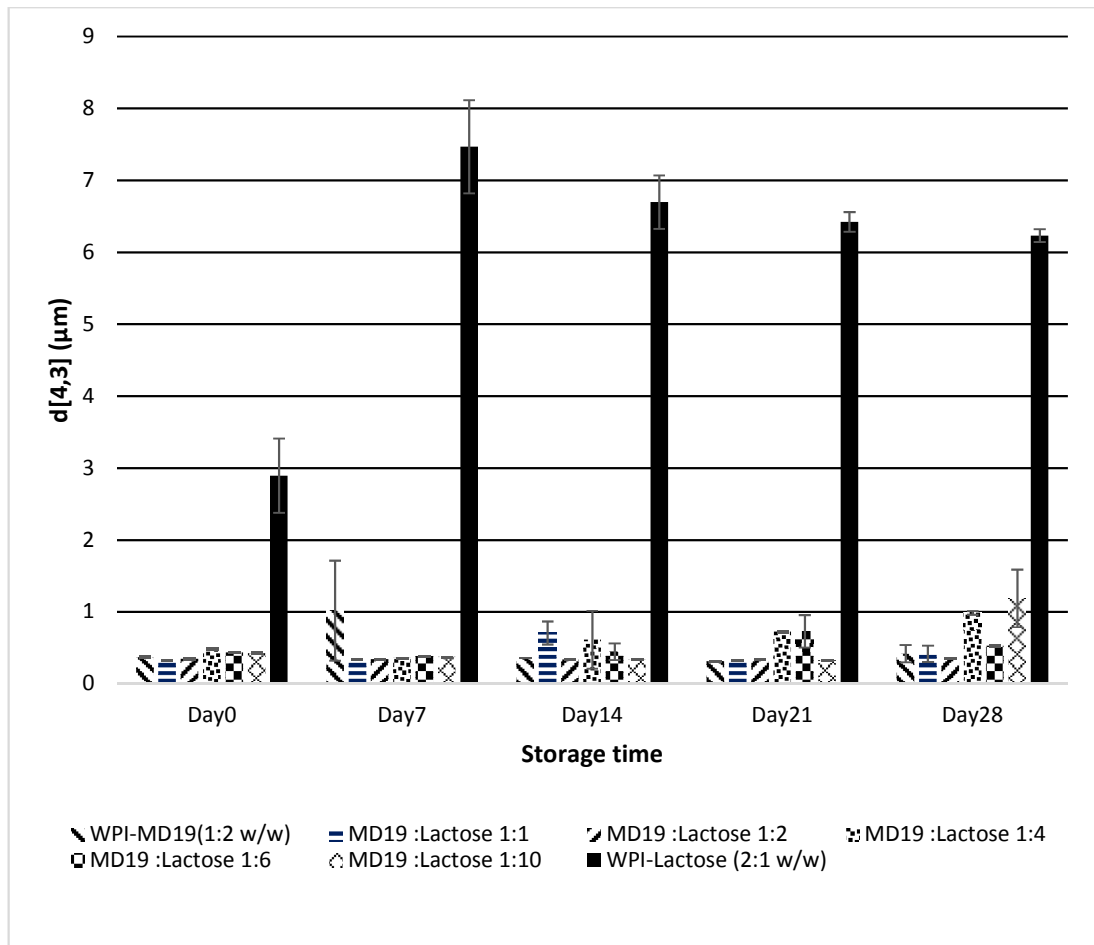


**Figure 4.13** Average droplet size of emulsions stabilized by WPI-MD19 containing lactose as impurity at different molar ratios between MD19 and lactose for 28 days.

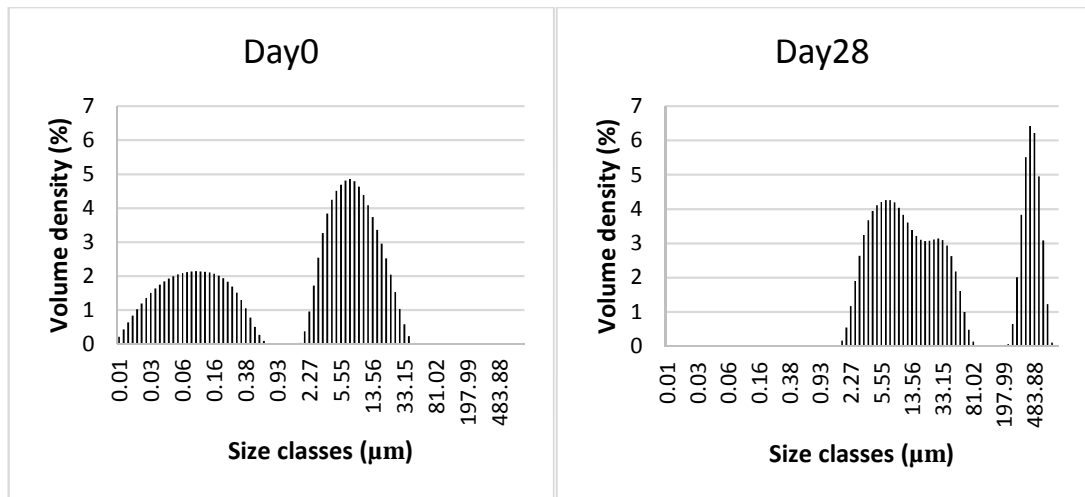
It can be seen from Figure 4.13 that the average droplet size of each emulsion stabilized by various complexes changes during the period of 28 days of storage. If there was no lactose present during the WPI-MD19 conjugates synthesis period, the emulsion exhibits excellent stability throughout the observation with average droplet size remaining constant around 0.5 µm. By contrast, when the MD19 is completely replaced by lactose in the conjugates, the emulsifying and stabilizing properties are dramatically compromised starting from day 0 throughout to day 28. These two emulsions are chosen as extremes. As can be seen in the other five samples of Figure

4.13, all of the average droplet size generally remain less than 1  $\mu\text{m}$  for the whole storage time. This is quite similar to the behaviours of the emulsion stabilized by WPI-MD19 only (i.e. no lactose). Surprisingly then, the average droplet size is not drastically increased when the WPI-MD19 conjugation system is heavily contaminated by lactose at molar ratio of 1:10 (MD19 : lactose) at the time of formation of the conjugates. This observation suggests that the presence of lactose, in the mixture of WPI and MD19 during heat treatment, will not significantly affect the stabilizing properties of the final conjugates.

Apart from the  $d[4,3]$  values, there is another key set of measurements, also resulting from particle sizing technique, to reflect the properties of emulsions: droplet size distribution.

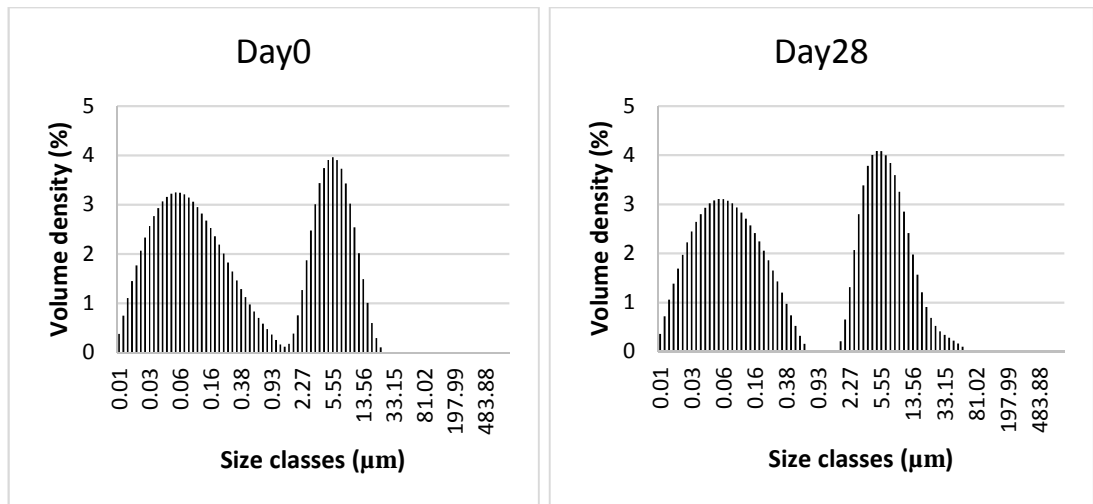
#### **4.3.6 Emulsion stability by droplet size distribution**

Droplet size distribution can be used as another indicator of the stability of emulsion samples. In this section, the distribution profiles of emulsions at various storage times will be presented.



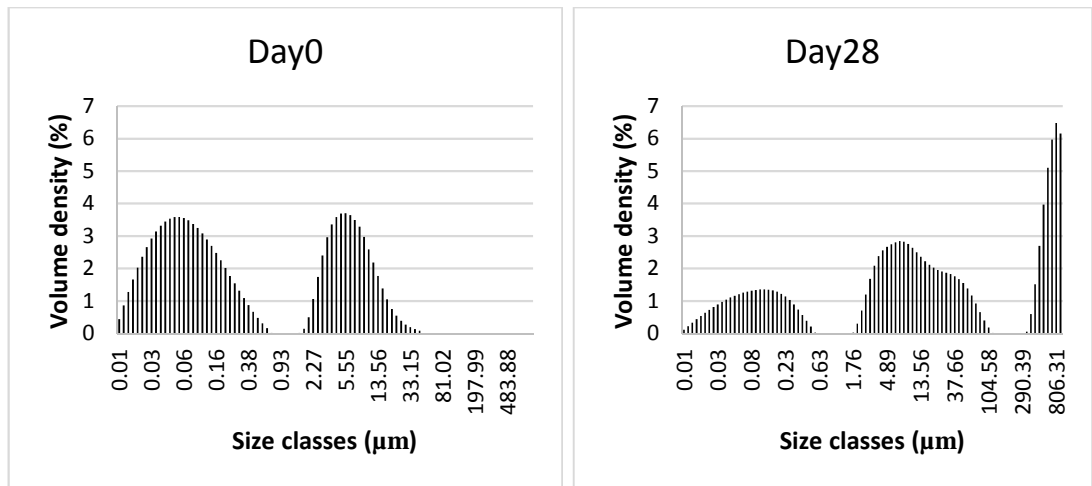
**Figure 4.14** Droplet size distribution of the emulsion stabilized by WPI-MD2, formed at a weight ratio of 2:1, on day 0 and day 28.

The droplet size distributions of the emulsion stabilized by WPI-MD2 (2:1 w/w) at the first and last day of storage are shown in Figure 4.14. When the emulsion was freshly prepared, most of the oil droplets are smaller than 10  $\mu\text{m}$ . There are two peaks in the size distribution at day 0: at size classes 0.11  $\mu\text{m}$  and 6  $\mu\text{m}$ , which means that there are a large number of oil droplets in this emulsion with the size around 0.11  $\mu\text{m}$  and 6  $\mu\text{m}$ . After 28-day storage, the distribution profile of the emulsion has a significant change. The distribution lying in the size classes under 1  $\mu\text{m}$  completely disappears. Furthermore, there is a new peak at the size class 483  $\mu\text{m}$ . For the size range from 2 to 81  $\mu\text{m}$ , a clear right shift of distribution is observed indicating that most of the oil droplets become larger than these at day 0. The results from distribution profiles of the emulsion agree with other results from visual assessment and  $d[4,3]$  values.



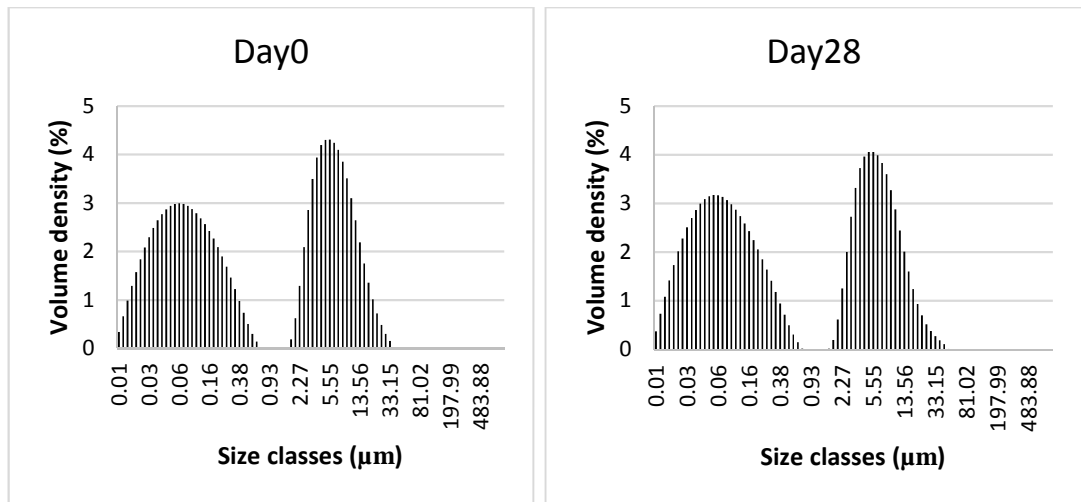
**Figure 4.15** Droplet size distribution of the emulsion stabilized by WPI-MD2 at the weight ratio of 1:4 at day 0 and day 28.

In Figure 4.15, the droplet distribution profiles of the emulsion stabilized by WPI-MD2 (1:4 w/w) at day 0 and 28 is presented. Generally, there are no significant differences between the two distribution profiles with both showing two main peaks at sizes less than 1  $\mu\text{m}$  and 5  $\mu\text{m}$ , respectively. However, there is a slight increase of droplet size at the large size classes from 33 to 81  $\mu\text{m}$  after 28 days storage. It means that WPI-MD2 (1:4 w/w) has an acceptable stabilizing properties for around 28 days of storage, which is also supported by previous evidence from  $d[4,3]$  values. Comparing these results to those of Figure 4.14, the distribution profile is similar to that of the emulsion stabilized by the same conjugates produced with a weight ratio of 2:1 (WPI : MD2) at day 0, whilst the distribution pattern is considerably altered after 28 days of storage for the emulsion with WPI-MD2 (2:1 w/w). This suggests that increasing the weight ratio of MD2 during synthesis of the conjugates can improve their stabilizing properties.



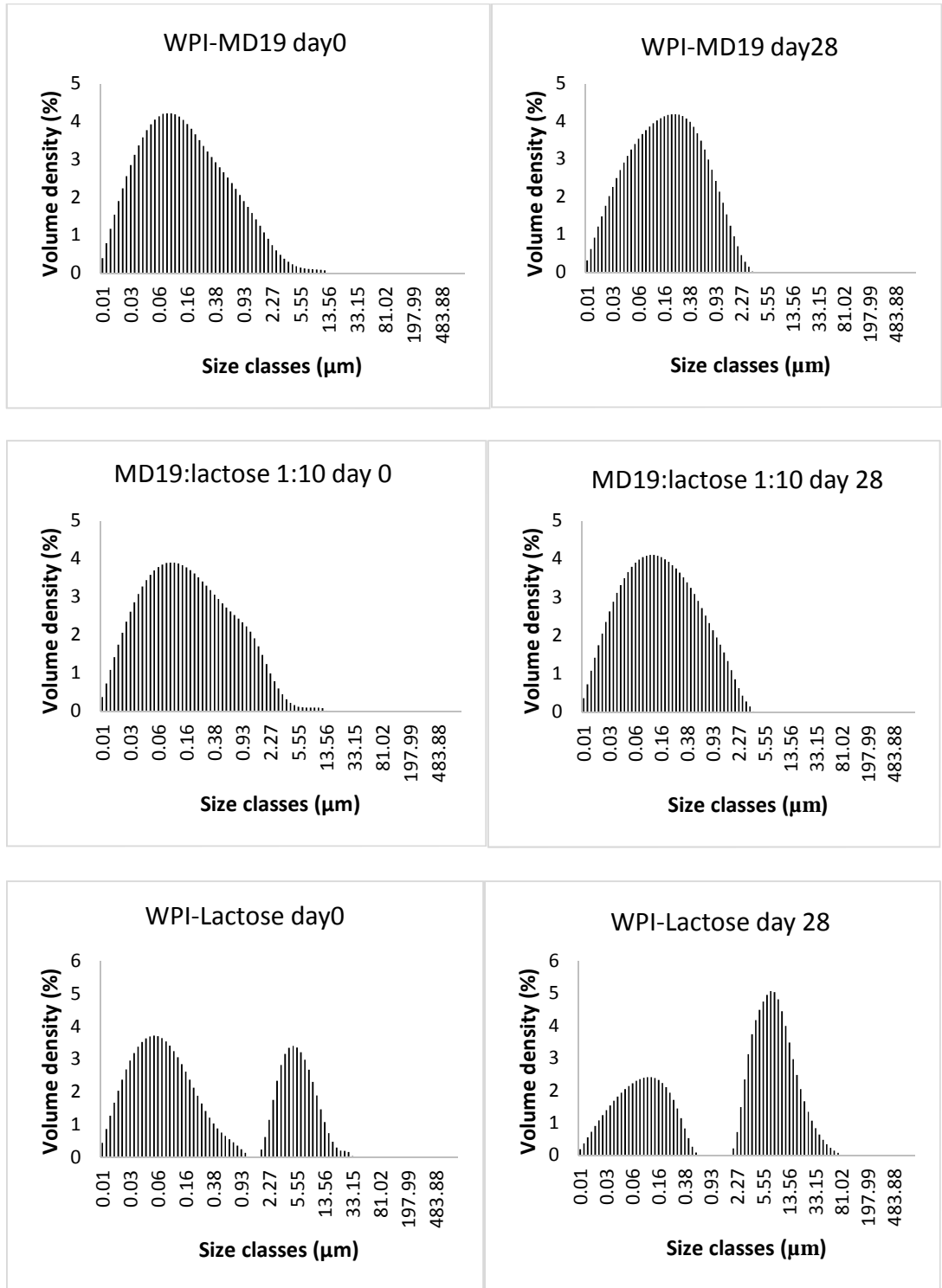
**Figure 4.16** Droplet size distribution of the emulsion stabilized by WPI-MD47 at the weight ratio of 2:1 at day 0 and day 28.

Figure 4.16 exhibits the droplet size distribution of the emulsion stabilized by WPI-MD47 (2:1 w/w) immediately after preparation and on day 28 of storage. There are two major size classes at day 0 peaking around: 0.06 and 5  $\mu\text{m}$  while three peaks at size classes 0.2, 6.0, and 806  $\mu\text{m}$ , are observed in the DSD profile following 28 days. This indicates that WPI-MD47 (2:1 w/w) cannot properly stabilize the emulsions for 28 days, with extremely large droplets appearing in the system. This instability is also observed during the creaming process (see 4.3.4). Nevertheless, at the same weight ratio of WPI to MD (2:1), the WPI-MD47 shows better stabilizing properties than that for WPI-MD2, according to the DSD profile in Figure 4.14. This suggests that the degree of conjugation plays a critical role in its ability to stabilize an emulsion, being even more important than the chain length of polysaccharides.



**Figure 4.17** Droplet size distribution of the emulsion stabilized by WPI-MD47 at the weight ratio of 1:2 at day 0 and day 28.

The droplet size distribution of the emulsion stabilized by WPI-MD47 (1:2 w/w), at day 0 and 28 are shown in Figure 4.17. The DSD profile of this sample barely alters through the whole of the 28 days of storage period. Most of the oil droplets are in the size classes with peaks at around 0.1 and 5  $\mu\text{m}$ , both on the first and last day of testing. Thus, the WPI-MD47 (1:2 w/w) can be seen to efficiently stabilize the O/W emulsion, even under unfavourable environmental conditions. Different from the DSD profile of the emulsion with WPI-MD47 (2:1 w/w), in this latter case there are no large oil droplets formed at any stage during the storage. This may be due to the higher degree of conjugation in WPI-MD47 (1:2 w/w) than that in WPI-MD47 (2:1 w/w) (see 4.3.3), which as we mentioned seem to be rather important factor in determining the stabilizing ability of the conjugates.



**Figure 4.18** The comparison of droplet size distribution (DSD) of the emulsions stabilized by WPI-MD19 with the impurity of lactose at molar ratio of 1:10 (MD19 : lactose) at day 0 and day 28.

In Figure 4.18, different distribution profiles of emulsions with WPI-polysaccharide conjugates are compared on days 0 and 28. With regards to

the system containing WPI-MD19, this exhibits excellent emulsion stability, based on the non-altered size distribution from day 0 to day 28. The majority of oil droplets in this emulsion are smaller than 0.5  $\mu\text{m}$ . In contrast, the emulsion stabilized by WPI-lactose conjugate, without any MD19 during its synthesis, exhibits a dramatically reduced stability, with large droplets appearing in the emulsion immediately from day 0. Moreover, the number of large oil droplets grows, with a reduction in the proportion of small droplets, after 28 days. This indicates that WPI-MD19 has significantly better stabilizing properties than that of WPI-lactose. When it comes to the emulsion stabilized by WPI-MD19, but contaminated with lactose at molar ratio 1:10 (MD19 : lactose) during the production of the conjugates, the distribution profile is similar to that of WPI-MD19 stabilized droplets, once again showing that most of the droplets are smaller than 5  $\mu\text{m}$  through the whole observation period. This result is in agreement with the findings by visual assessment and with monitoring of average droplet size (see 4.3.4 and 4.3.5). It suggests that the presence of lactose during Maillard reactions has insignificant influence on the stabilizing properties of resulting WPI-MD19 conjugates. More evidence to support this hypothesis is coming from the rheological properties of these emulsions, discussed in section 4.3.7.

Particle sizing technique is a convincing method to monitor the stability of emulsions during storage. However, there is a major drawback to this method during testing: dilution. In order to estimate the droplet size of emulsions, the samples have to be diluted dramatically before they are introduced into the glass cell. The dilution can greatly affect instability of emulsions such as those involving depletion flocculation. This type of flocculation arises from the high osmosis pressure difference between the

bulk phase and the gap between two approaching droplets. Therefore, it is useful to also analyse the emulsion stability via the rheological technique which requires no dilution of samples. The following section will present the flow behaviours of emulsions stabilized by different complexes.

#### 4.3.7 Emulsion stability studied via rheological properties

Emulsion stability can be reflected by its rheological properties under different shear rates. Generally, if the emulsion behaves in a manner similar to Newtonian fluids, it indicates lack of formation of complex structures in the system, showing a well dispersed ensemble of droplets in the sample. On the contrary, when the emulsion is a shear-thinning fluid and becoming more viscous during quiescent storage, the emulsion is likely to be suffering from possible colloidal instability.

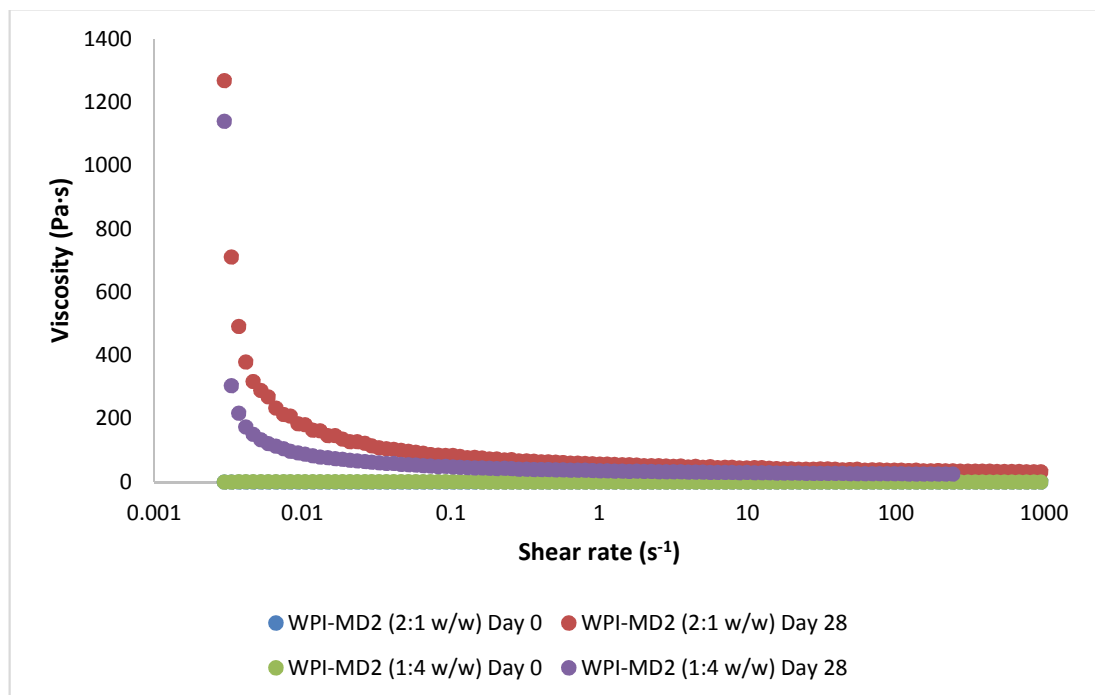


**Figure 4.19** The relationship between viscosities and shear rates for two emulsions stabilized by WPI-MD2 (2:1 w/w) and WPI-MD2 (1:4 w/w), immediately after preparation and after 28 days of storage.

Figure 4.19 shows the viscosity variation with shear rate for two emulsions stabilized by conjugates WPI-MD2 (2:1 w/w) and WPI-MD2 (1:4 w/w), at initial time following preparation and after 28 days of storage. It can be seen that the viscosities of both samples are quite low under different shear rates on day 0. Moreover, there is no significant change of viscosities for these two emulsions at various shear rates when they were prepared freshly (The line with blue dots are completely covered by the line with green dots in Figure 4.19.), which indicates that both samples are close in behaviour to Newtonian fluid. This observation suggests that the two emulsions are quite stable when freshly prepared. However, the shear-thinning behaviour is seen to develop for both sets of emulsions after storage, especially noticeable at shear rates lower than  $0.1 \text{ s}^{-1}$ . In this range of shear rates, the viscosity of the emulsion stabilized by WPI-MD2 (1:4 w/w) is lower than that of the sample with WPI-MD2 (2:1 w/w) at the same corresponding shear rate. This indicates that the emulsion with less proportion of MD2 during Maillard reactions to prepare the conjugates, has weaker stability than that of emulsion stabilized by protein-polysaccharide complexes made with a higher percentage of polysaccharides during their synthesis. These results suggest that increasing the proportion of MD2 in the conjugates could improve the stabilizing properties of WPI-MD2 in O/W emulsions. This is in line with other results obtained from a study of creaming process and from particle sizing (see 4.3.4, 4.3.5 and 4.3.6).

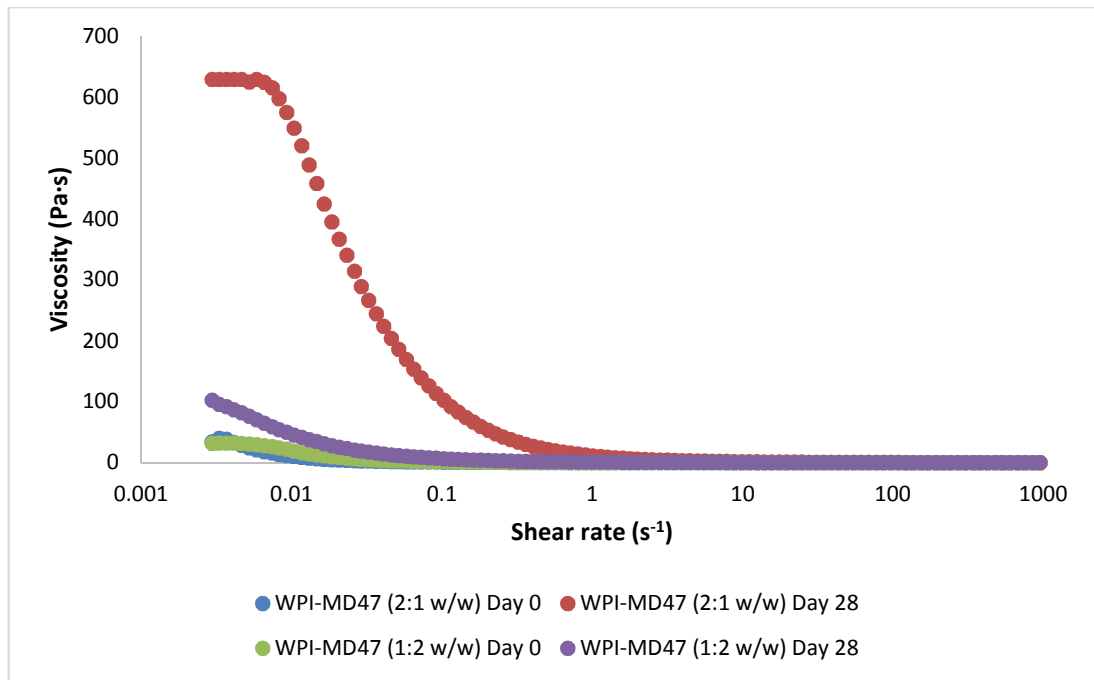


**Figure 4.20** The relationship between viscosities and shear rates for two emulsions stabilized by WPI-MD47 (2:1 w/w) and WPI-MD47 (1:2 w/w), at day 0 and day 28 following emulsion preparation.

Figure 4.20 displays the change of flow behaviours of two emulsions stabilized by WPI-MD47 (2:1 w/w) and WPI-MD47 (1:2 w/w), with shear rate post 28 days storage. At day 0, there is no significant differences of viscosities of the two samples. Both emulsions show a slight decrease in viscosity, observed when the shear rate increases from 0.001 to 0.01  $s^{-1}$ . The viscosity profile of the emulsion stabilized by WPI-MD47 (2:1 w/w) is significantly altered at day 28. The viscosity is now hundreds of times higher than what it was at the initial day of observation, at shear rates  $< 0.1 s^{-1}$  and below. The emulsion exhibits clear shear-thinning behaviour developed during storage. Compared to this, the sample with WPI-MD47 (1:2 w/w) has not changed considerably during the 28 days, with only a slight increase of viscosity at low shear rates ( $< 0.01 s^{-1}$ ). The rheological properties of these two emulsions suggest that increasing the percentage of MD47 during complex preparation

can improve the stabilizing properties of WPI-MD47 conjugates. These results further support the conclusions arrived at from other analytical measurements, previously discussed in section 4.3.5 and 4.3.6.

If we compare the viscosities in both Figure 4.19 and 4.20 at day 28, it can be seen that the viscosities of the emulsions stabilized with WPI-MD47 (maximum 650 Pa·s) are much lower than those of emulsions prepared with WPI-MD2 (maximum 1300 Pa·s), in the same low shear rate range. This observation indicates that WPI-MD47 has a better stabilizing properties than WPI-MD2, most likely because of the higher degree of conjugation in WPI-MD47 than that of WPI-MD2 (see 4.3.3).

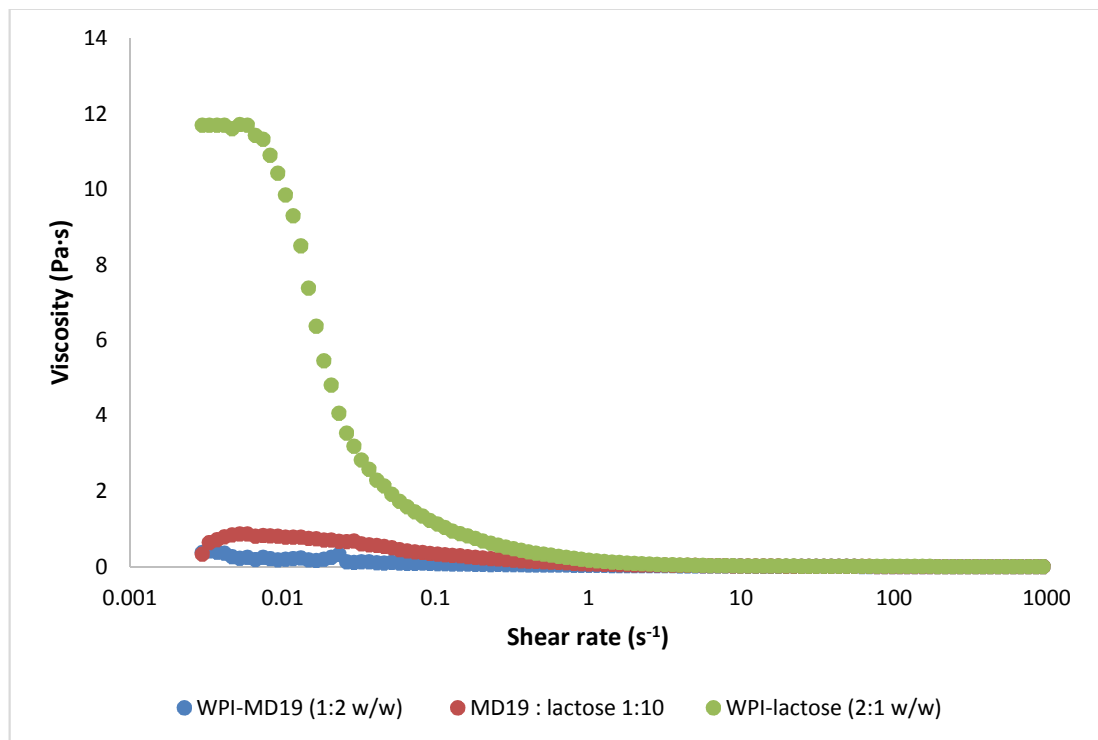


**Figure 4.21** The relationship between viscosities and shear rates for two emulsions stabilized by WPI-MD19 (1:2 w/w), WPI-MD19 (1:2 w/w) with lactose at molar ratio 1:10 (MD19 : lactose) and WPI-lactose (2:1 w/w).

The rheological properties of emulsions stabilized by several different complexes are presented in Figure 4.21. As a control, WPI-MD19 (1:2 w/w) shows excellent emulsion stabilizing properties, showing no changes of viscosity with time under the full range of shear rates. On the contrary, if the sample is stabilized by WPI-lactose, the viscosity increases dramatically to 10 Pa·s when shear rate is around  $0.01 \text{ s}^{-1}$ , considerably higher than emulsion prepared with WPI-MD19. Between these two samples in its behaviour, it is the case where the lactose is mixed with the WPI and MD19 combination during the Maillard reactions at the molar ratio of 1:10 (MD19 : lactose). For emulsions stabilized by these conjugates, the flow behaviour is quite similar to that with WPI-MD19, and unlike WPI-lactose complexes. The conclusion seem to be that the presence of lactose during Maillard reactions does not affect the stabilizing properties of resulting WPI-MD19 conjugate even when mixed in at a very high molar ratio. This finding has a promising implication for production of WPI-MD19 complexes as novel more efficient stabilizer in food industry, by using low cost whey proteins which very likely will be containing lactose. Furthermore, evidence from other techniques also point in the same direction supporting the conclusions drawn from the rheological measurements of emulsions.

Apart from the rheological assessments of emulsions, the images from confocal laser scanning microscopy (CLSM) can be used as direct evidence to monitor the emulsion stability.

#### **4.3.8 Emulsion stability by images from CLSM**

A view of oil droplet size can be formed directly from the images obtained by CLSM, which facilitates the monitoring emulsion stability during

storage. The emulsion was gently shaken before sampling at the depth around 2 cm below the emulsion surface. After sampling, it was stained by Nile red (25  $\mu$ l of 0.01% w/v dye in polyethylene glycol) and gently mixed with a glass rod at room temperature. Then the stained samples were placed in a plastic cell covered with a cover slip. In order to balance the details and image resolutions, the dimension of chosen images is 70  $\mu$ m in reality. The following part of this section will present the images of various emulsions at different storage days.

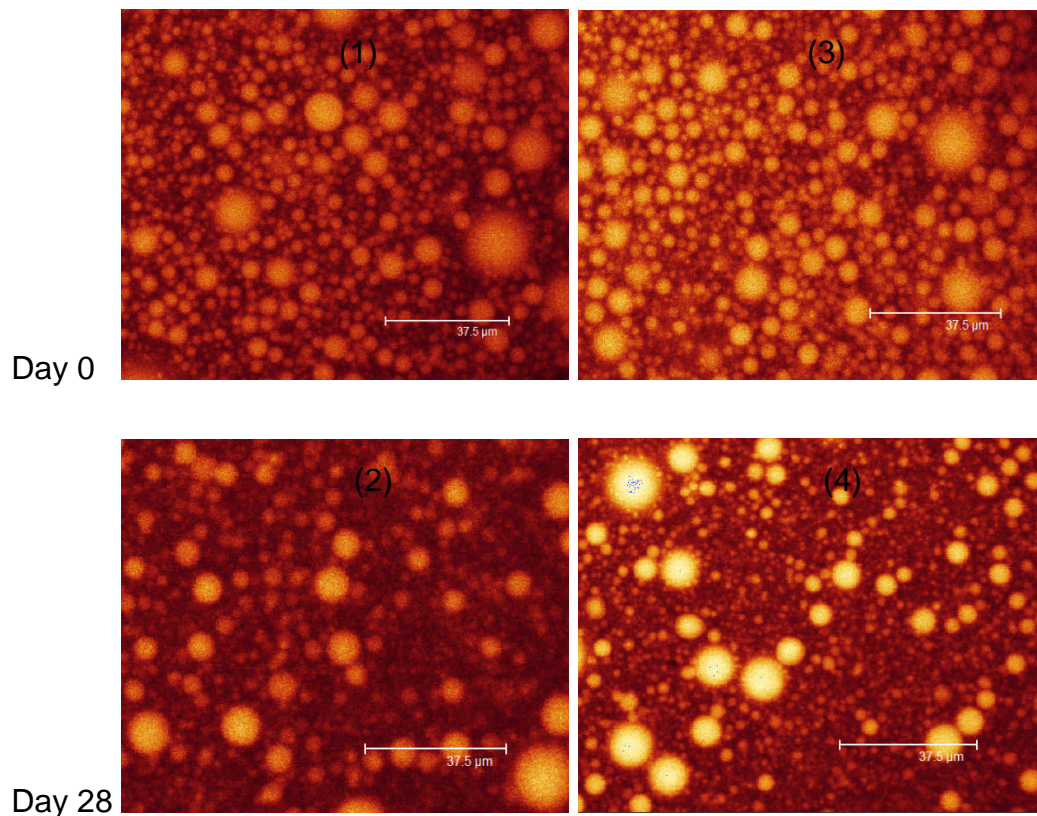


**Figure 4.22** Images obtained from CLSM of emulsions stabilized by WPI-MD2 (2:1 w/w): (1) & (2) and WPI-MD2 (1:4 w/w): (3) & (4), respectively at day 0 and day 28, post preparation of emulsions.

It is illustrated in Figure 4.22 that oil droplets stabilized by WPI-MD2 at two weight ratios are distributed in emulsions at day 0 and day 28 post emulsion preparation. When the emulsions were freshly prepared, both set of samples have small droplets which are smaller than 10  $\mu\text{m}$ , with only a few large droplets with diameters higher than 15  $\mu\text{m}$  visible. Moreover, the distance between droplets is relatively large, which indicates that the emulsion are reasonably well dispersed. After 28-day storage, it can be seen that the proportion of small oil droplets decreases whilst more large droplets are observed in the system. This phenomenon is true for both sets of the emulsions. Furthermore, the distance between droplets becomes small, as flocculation occurs to form small clusters. It is clear that WPI-MD2 cannot fully stabilize the system for periods as long as 28 days, according to these images. However, it is difficult to distinguish the stabilizing properties of the conjugates for these two samples with different levels of MD2 contents used at the time of the synthesis of the protein-polysaccharide complex.

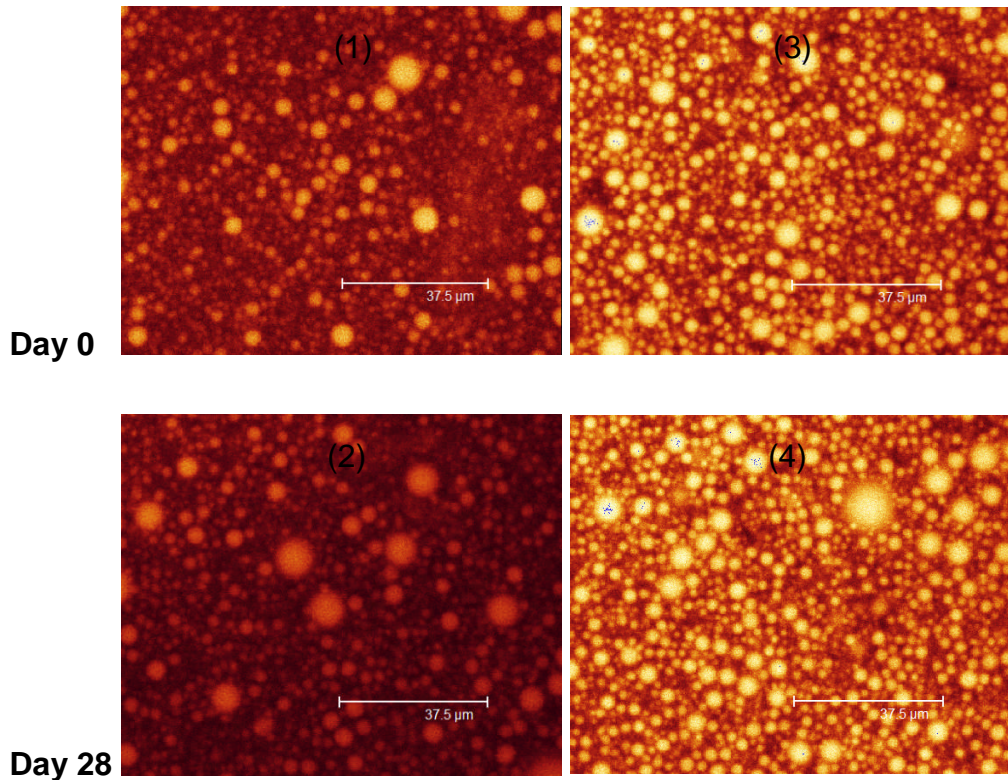
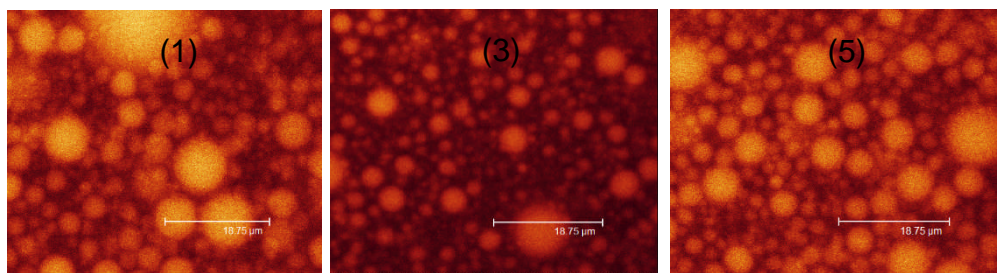


**Figure 4.23** Images from CLSM of emulsions stabilized by WPI-MD47 (2:1 w/w): (1) & (2) and WPI-MD47 (1:2 w/w): (3) & (4) initially and following 28 days of storage.

In Figure 4.23, the oil droplets in two emulsions stabilized by WPI-MD47 immediately after preparation and after 28 days of storage, are shown. Generally, there is no significant difference in droplet size between the two samples initially. The diameters of most oil droplets are much smaller than 5 μm according to the Figure 4.23 (1) & (3). Furthermore, the fine droplets are nicely separated and distributed in the emulsion without any evidence for flocculation. Nevertheless, the droplets in the emulsion stabilized by WPI-MD47 (2:1 w/w) become larger after 28 days than those at first day post preparation (Figure 4.23 (2)). For the other sample (i.e. WPI-MD47 1:2 w/w), it is difficult to see any growth in the size of oil droplets after 28 days (Figure

4.23 (4) compared to 4.23(3)). This indicates that the emulsion stabilized by WPI-MD47 (1:2 w/w) is more stable than that formed with complexes containing a smaller proportion of MD47, during Maillard preparation of WPI-MD47 conjugates. The conclusion agrees well with the findings in rheological tests and the particle sizing of previous sections (see 4.3.7 and 4.3.6).

### Day 0



### Day 28

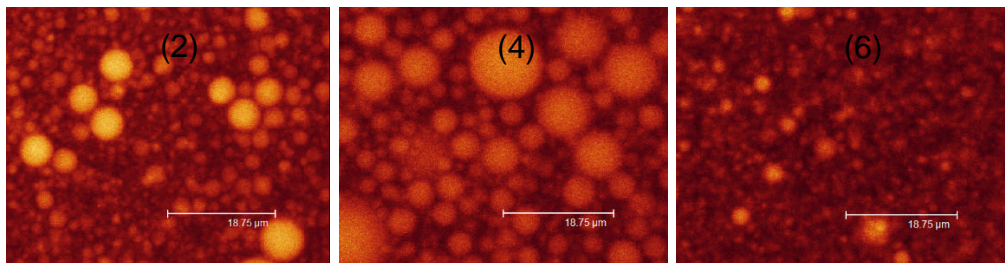


**Figure 4.24** Images from CLSM of emulsions stabilized by WPI-MD19 (1:2 w/w): (1) & (2), WPI-MD19 (1:2 w/w), formed in the presence of lactose contamination, at the molar ratio of 1:10 (MD : lactose): (3) & (4), and WPI-lactose (2:1 w/w): (5) & (6), immediately post emulsion preparation and after 28 days of storage.

Figure 4.24 illustrates the sizes of oil droplets in emulsions with different protein-polysaccharide complex stabilizers initially after emulsion preparation and after 28 days. For the system with the WPI-MD19 (1:2 w/w) stabilizer, there is no significant change in droplet size, from day 0 to day 28.

The majority of droplets are smaller than 5  $\mu\text{m}$  with a couple of exceptions according to Figures 4.24 (1) & (2). On the other hand, the emulsion cannot be stabilized by WPI-lactose for 28 days because of the clear changes occurring in oil droplets as seen in Figures 4.24 (5) and (6). At day 0, the round shape of droplets can be observed, possibly due to their aggregation, whilst most of the droplets disappear with a couple of large ones left in the system at day 28. Most of the oil phase in this emulsion has been separated by creaming. As confirmed by the formation of a cream layer in the sample observed by visual assessment (see 4.3.4). If WPI and MD19 are mixed with lactose, at a relatively high molar ratio say 1:10 (MD19 : lactose) at the time of synthesis of the conjugate, the resulting complex can stabilize the emulsion for 28 days with the image for the sample similar to the emulsion with WPI-MD19 (1:2 w/w), as displayed in Figure 4.24 (4). Generally, the droplet size increases when compared to day 0, but the oil droplets are still nicely distributed in the emulsion. This is clearly not the case for the system with WPI-lactose (Figure 4.24 (4) & (6)).

#### **4.4 Conclusions**

Protein-polysaccharide conjugates prepared via Maillard reactions can enhance the colloidal stability properties in O/W emulsions, compared to native proteins especially under unfavourable environmental conditions (pH close to pI and high salt concentrations). Both the nature of saccharides and preparation conditions significantly affect the properties of the final conjugates such as the length of sugar polymers and the weight ratios between proteins and polysaccharides during heating treatment.

Generally, the longer is the polysaccharide chain in conjugates, the better is the stabilizing properties owing to stronger steric repulsions between oil droplets, if the degree of conjugation is sufficiently high. However, the long chain polysaccharides can cause low degree of conjugation because of the decline of reducing ends which are the key functional groups to be attached to protein backbones. Based on the theoretical calculations, the position of polysaccharides attachment also influence on the stabilizing properties of the conjugates (Ettelaie et al., 2008). If sugar moieties are linked to the N terminus side of proteins, the conjugates perform better than the polymers attached by polysaccharides in the middle of the polypeptide chain. However, it is extremely challenging to control the attachment position of polysaccharides during Maillard reactions. In future, if the site-specified modification of protein becomes possible, these theoretical predictions can be verified by experiments.

In terms of lactose as impurity in WPI + MD19 system during dry heating, the results in this Chapter indicate insignificant influence on the stabilizing properties of the final product. This is somewhat surprising since lactose competes with MD19 during Maillard reactions. For the same weight percentage, due to its much smaller size, lactose is much more reactive. This finding suggests that the purity of whey protein does not need to be particularly high during conjugates preparation, which means that it is possible to manufacture acceptable whey protein – maltodextrin conjugates by using commercial whey proteins containing lactose. For industrial applications of conjugates in future, it can help to reduce the total expenditure of preparation by lowering the cost of raw materials.

## **Chapter 5**

### **A Novel Approach for Preparing Protein-polysaccharide Conjugates via Spinning Disc Reactor (SDR)**

#### **5.1 Introduction**

Previous studies have shown that proteins after glycation via the Maillard reactions significantly improve the emulsifying and stabilizing properties compared to the unmodified proteins especially under unfavourable environmental conditions (Kato and Kobayashi, 1991; Dickinson and Semenova, 1992; Kato et al., 1993; Nakamura et al., 1994; Nagasawa et al., 1996; Fujiwara et al., 1998; Aoki et al., 1999; Tanaka et al., 1999; Ho et al., 2000; Akhtar and Dickinson, 2003; Xu et al., 2010; Zhu et al., 2010; Tian et al., 2011; Wang et al., 2013; Zhang et al., 2014; Zhang et al., 2015a; Bi et al., 2017). In these studies, the protein-polysaccharide conjugates were mainly prepared via dry-heating treatment in controlled humidity. The incubation periods were from several hours to a couple of weeks (Kato et al., 1988; Saeki, 1997; Laneville et al., 2000; Wooster and Augustin, 2006; O'Regan and Mulvihill, 2009 & 2010). The long preparation cycle of protein-based conjugates is the major hurdle for large-scale manufacturing in food industry. Therefore, some researchers conducted experiments to investigate the possibility to prepare conjugates in aqueous medium (Zhang et al., 2012; Chen et al., 2013; Luo et al., 2013; Pirestani et al., 2017a & b). If the Maillard reactions can occur in aqueous solution, it is likely to shorten the preparation time because the solutions are much easier to handle than dry powders. In 2008, a study was conducted by Zhu et al. about the coupling between proteins and polysaccharides in aqueous solution through Maillard reaction. Following this research, three more papers have been published using similar

wet-heating method to synthesize protein-polysaccharide conjugates (Zhu et al., 2010; Mu et al., 2011; Niu et al., 2011). These studies indicate that it is possible to prepare protein-polysaccharide conjugates in aqueous medium under certain conditions such as pH and temperature.

It is important to compare the two preparation methods of conjugates: dry-heating and wet-heating treatments which are illustrated in Figure 1.11 (See 1.6.3). According to this Figure, the freeze-drying process is eliminated in the wet-heating treatment. It can significantly reduce time and energy before the heating as in freeze-drying it usually takes 24 hours to remove water from the solutions completely under vacuum. However, some researchers argued that dry-heating method is more desirable, from an industrial point of view, than the wet method because of the ease of handling and long-term storage in dry reactions (Oliver et al., 2006). Alternatively, it was suggested that other drying techniques such as spray drying and roller drying can be considered to replace the freeze-drying (Oliver et al., 2006).

Based on the discussion above, a novel preparation method of protein-polysaccharide conjugates was explored and developed which involved the wet-heating method utilizing a Spinning Disc Reactor (SDR).

SDR is a system to make various products via controlled temperature, spinning speed and the flow rate (Akhtar et al., 2011). It has been utilised in chemical engineering but rarely in food production (Akhtar et al., 2011 & 2014; Khan and Rathod, 2014; de Caprariis et al., 2015; Haseidl et al., 2015; van Eeten et al., 2015; Kleiner et al., 2017; Ahoba-Sam et al., 2018). For example, it has been reported recently that SDR was used to concentrate apple juice

by a group of researchers at University of Leeds (Akhtar et al., 2011). The schematic diagram of the SDR is presented in Figure 5.2.

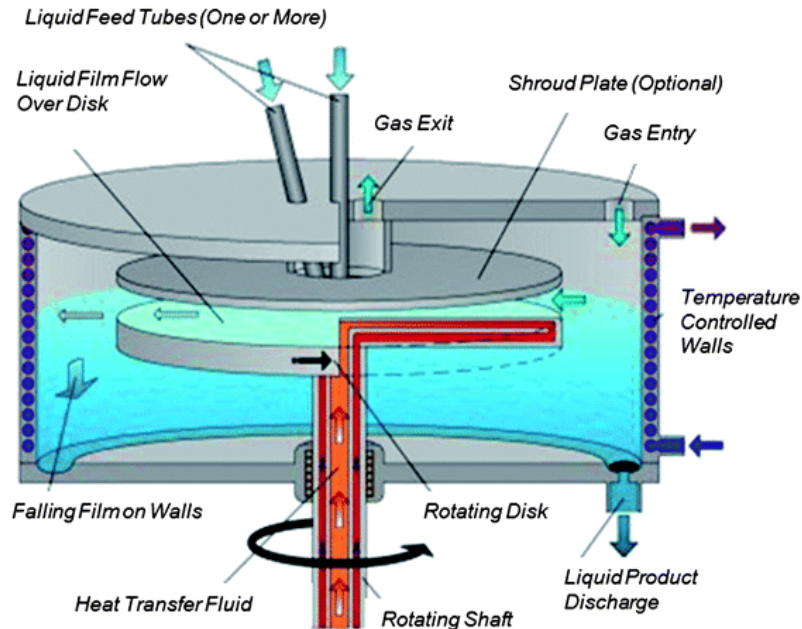


**Figure 5.1** A schematic diagram of main reactor showing various components in SDR during process.

Figure 5.1 shows the main reactor in the SDR system when the aqueous medium is introduced from the top of liquid-feed tubes. The liquid is fed into the centre of a high-speed rotating disc. A thin liquid film is formed due to centrifugal force. The disc is heated using the heat transfer fluid. The liquid sample is then transferred to the temperature controlled walls. When the liquid reaches the bottom of the main reactor, the liquid product is collected from the outlet.

The main advantage of SDR is the excellent efficiency of heat transfer. When the liquid is introduced to the spinning disc, a very thin layer of fluid is formed due to the centrifugal force provided by the high-speed rotation. At the same time, the temperature of the disc can be stabilised at the set point, say,

120°C. When the liquid leaves the spinning disc, it can be collected or circulated via different pathways. Therefore, it is possible to reduce the reaction time compared to classic dry-heating method by adopting the SDR system. Furthermore, the freeze-drying step which is generally used in preparing conjugates could be removed by using the SDR. However, the optimum reaction conditions (spinning speed, disc and jacket temperatures, and flow rate) of SDR for synthesizing protein-polysaccharide conjugates need to be determined. The SDR system used at Leeds is presented as follows (Figure 5.2):

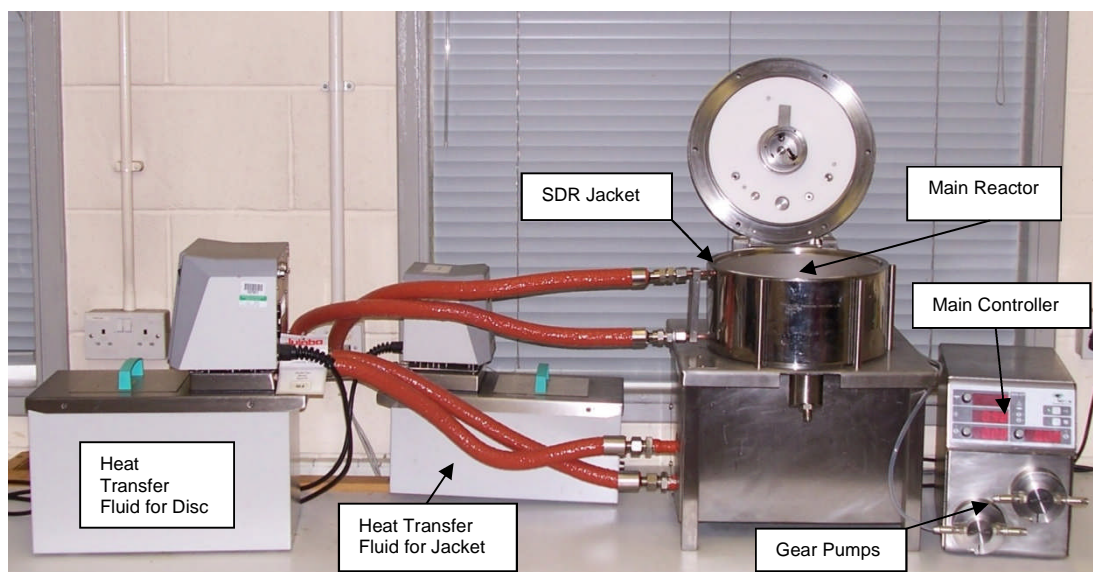


**Figure 5.2** The SDR system in the School of Food Science and Nutrition University of Leeds.

In Figure 5.2, there are two temperature control systems for rotating disc and the wall jacket separately. Therefore, the temperature for the whole process can be adjusted by these two systems. The basic structure and mechanism of fluid circulation through the main reactor has been demonstrated in Figure 5.1. The flow rate of inlet solution is controlled by a

gear pump via the main controller. Additionally, the main controller is also used to manage and monitor the speed of rotating disc in the main reactor. In the preparation of conjugates, only one cycle of heating from the main reactor is not sufficient to couple the polysaccharides to proteins to the acceptable degree of conjugation. Therefore, at the end of each heating cycle, the solution is re-introduced into the main reactor. This cycling process is also controlled by the gear pump. After the whole heating process, the final product is collected from the outlet at the bottom of the main reactor.

The use of SDR method appears to be a promising approach for preparing protein-polysaccharide conjugates, which could enhance their industrial applications. In this chapter, the possibility of preparing WPI-MD conjugates by using the SDR will be explored. Furthermore, the emulsifying and stabilizing properties of the SDR-processed conjugates are compared with the conjugates prepared by dry-heating treatment.

## **5.2 Materials and Methods**

Whey protein isolate was purchased from Sigma-Aldrich (St Louis, MO, USA). It is homogenous white powder without any lactose. Maltodextrins (DE 19) were provided by Roquette Ltd. (France), as used in the previous chapters (see Chapter 4). In terms of emulsion preparation, the sunflower oil was purchased from local supermarket Morrisons (Leeds, UK). The general chemicals such as NaOH for pH adjustment were Analytical grade.

### **5.2.1 Preparation of WPI-MD conjugates**

Whey protein isolate and maltodextrin (DE 12 or 19) were mixed at various weight ratios 1:2 or 1:3 (WPI : MD) and dissolved into 400 ml distilled

water with gentle stirring at room temperature. The pH of the solution was adjusted to 11 by adding several drops of 6 M NaOH, and the solution was stored at 4 °C in a refrigerator overnight. Before introducing the solution of WPI and MD into the main reactor of SDR, via the feeding tube, it is important to preheat the rotating disc at 110 °C and the jacket at 90 °C. Furthermore, the speed of the rotating disc was set at 2000 rpm, and the circulation flow was maintained at 7 ml/s. These parameters can be adjusted through the main controller (Figure 5.2).

Initially, distilled water was used to calibrate all these conditions for reactions between WPI and MD. The distilled water was then drained completely from the main reactor, and WPI/MD solution was introduced through the inlet tube at 7 ml/s and circulated for 20 mins. The product was collected and placed in an ice bath immediately after heating treatment to stop further reactions. Once the product was fully cooled down, it was stored in a dark and dry cupboard for further analysis and characterisations.

### **5.2.2 Confirmation of successful conjugation**

In order to confirm the formation of SDR-processed conjugates, several methods have been used. First of all, browning process could be a direct evidence to support the occurrence of Maillard reactions. The samples at different reaction time were collected to monitor the progress of browning by visual assessments. A 5 ml of sample was collected from the discharged outlet every 2 mins, and put in an ice bath immediately to cease the browning process. The total processing and observation time of browning process was 14 mins. These liquid products were further diluted by using distilled water to

give a protein concentration of 1 w/v%. A photograph was taken against a white background.

The OPA test is another method to determine the degree of conjugation of SDR-processed products. There are three combinations of WPI and MD passing through the SDR for 20 mins: 1) WPI and MD19 at weight ratio 1:3; 2) WPI and MD19 at weight ratio 1:6; 3) WPI and MD12 at weight ratio 1:3. When the liquid products were collected from the discharged outlet and cooled down to room temperature, they were freeze dried for 24 hours before any further application. The dry-heated conjugate WPI-MD19 (1:2 w/w) was selected as the control for OPA test. The rest procedure of OPA is the same as described in Section 3.2.4.

Furthermore, a spectrophotometer was used to confirm the conjugation between WPI and MD. For spectra scanning, a solution of WPI and MD12 (1:3 w/w) at protein concentration 10 g/l in 400 ml distilled water was passed through the SDR heated at 110 °C for 10 mins. After the SDR process, the liquid product was diluted back to 400 ml with distilled water and further diluted 100 times before scanning in the spectrophotometer (Cecil CE3200). The solution of WPI and MD12 alone were selected as the controls. The samples were scanned from 250 nm to 400 nm wavelength at the frequency of 10 nm/min. The absorbance for each sample was recorded accordingly.

Based on the results from spectra scanning, 280 nm was chosen to detect WPI or WPI-MD conjugates for HPLC analysing (O'Regan and Mulvihill, 2009). The samples were prepared at protein concentration 1 w/v%. For the reversed HPLC system, the separation column was XBridge™ Amide 3.5 µm 4.6X150 mm (Part No. 186004869) (Waters, USA) with an introducing

program of a linear gradient from 0.1% TCA in water to 0.1% trichloroacetic acid (TCA) in acetonitrile/water mixture (60/40 v/v) at a flow rate of 2 ml/min. The absorbance of the components washed by this mobile phase was detected at 280 nm and recorded every 24 secs for 4 hours (Hattori et al., 1994).

### **5.2.3 Preparation of emulsions**

In order to test the emulsifying properties of SDR-processed conjugates of WPI-MD19, the oil-in-water emulsions were prepared using a lab blender at 10,000 rpm for 5 mins. The volume ratio between oil phase and aqueous phase was still 20 : 80. The coarse emulsions were stored at 4 °C in a Fridge for further analysis such as particle sizing and centrifugation.

In emulsion stability experiments, the SDR-processed liquid products (WPI/MD19 1:3 w/w) or (WPI/MD19 1:6 w/w) were diluted to 100 ml with aqueous buffer (see Section 3.2.6) at the protein concentration of 2 w/v%. 20 vol% sunflower oil was homogenized in the aqueous phase (80 vol%) using a jet-homogenizer at 350 bar. The pH of freshly prepared emulsion was adjusted to 4.6. The emulsions were stored quietly at 30 °C for 28 days. The control emulsion was stabilized by WPI-MD19 (dry-heated, DH) (1:2 w/w) at the same environmental conditions.

### **5.2.4 Interfacial properties of SDR-processed WPI-MD19 conjugates**

Prepared emulsions were centrifuged using an ultracentrifuge (BECKMAN COULTER, USA) at 10,000 rpm for 1 hour at the room temperature to separate the emulsion into the cream and serum layers. After the centrifugation, the serum layer was extracted using a long-needle syringe.

1 ml of serum phase was added into standard Biuret reagent for 5 mins, and the absorbance was measured at 540 nm in the spectrophotometer (Cecil CE3200) (Gornall et al., 1949). The concentration of WPI-MD19 conjugates can be calculated using the standard curve of the Biuret method (Gornall et al., 1949).

In order to produce the standard curve of the Biuret method for WPI-MD19 conjugates, several standard concentrations 1 mg/ml to 10 mg/ml (WPI basis) of conjugate samples were prepared. Moreover, the Biuret reagent was prepared by mixing 1.5 g  $\text{CuSO}_4 \cdot 5\text{H}_2\text{O}$  with 6.0 g  $\text{NaKC}_4\text{H}_4\text{O}_6 \cdot 4\text{H}_2\text{O}$  and 3.0 g NaOH in 1000 ml distilled water. The Biuret reagent was stored at room temperature in a dark cupboard. 1 ml conjugate sample was mixed with 3 ml of the reagent for 5 mins at room temperature. After the reaction, the absorbance of the mixture was read in the spectrophotometer at wavelength 540 nm.

The interfacial adsorption of WPI-MD19 conjugates can be calculated from results obtained from the Biuret method, in the formation of percentage according to the following equations

$$\text{Interfacial adsorption (\%)} = \frac{W_{total} - W_{aqu}}{W_{total}} \times 100\%$$

where is  $W_{total}$  the total weight of WPI-MD19 conjugates used in the emulsion;  $W_{aqu}$  is the weight of WPI-MD19 left in the aqueous phase after centrifugation.

In order to obtain the surface concentration of WPI-MD19, the total surface areas of oil phase was measured using the Mastersizer 3000 (Malvern, UK). The surface concentration can be calculated as follows:

$$\text{Surface concentration } \left( \frac{mg}{m^2} \right) = \frac{W_{ads} (mg)}{A_{sur} (m^2)}$$

where  $W_{ads}$  is the weight of adsorbed WPI-MD19 conjugates;  $A_{sur}$  is the total surface area of oil droplets.

### **5.2.5 Stabilizing properties of SDR-processed WPI-MD19 conjugates**

The emulsions stabilized by SDR-processed WPI-MD19 (1:3 w/w) or WPI-MD19 (1:6 w/w) were analysed using the Mastersizer 3000 (Malvern, UK) for 28 days storage at 7-day interval. The control emulsion was stabilized by WPI-MD19 (1:2 w/w) (Dry Heat / DH) under the same conditions. The average droplet size and droplet size distribution for each emulsion sample were recorded.

### **5.2.6 Statistic analysis**

All the data generated from OPA tests, particle sizing, and rheological measurements were collected and processed through MS Excel® 2013. The results were presented as the average values of triplicates with standard deviations.

## **5.3 Results and Discussions**

### **5.3.1 Visual assessment of SDR-processed conjugates**

Browning of food is a key indicator for the Maillard reactions when proteins and reducing sugars are present in the system. The following picture shows the development of browning process of the solution containing WPI and MD12 at various stages of reactions.



**Figure 5.3** Photographs of WPI-MD12 (1:3 w/w) conjugates prepared by using the SDR at different reaction time for 14 mins.

Figure 5.3 shows the visual appearance of the conjugates prepared by wet-heating method using the SDR at initial pH 11.0. The photograph shows that the browning process occurred at very early stage of reaction (2 mins) and developed significantly after 8 mins and remained the intensity of browning at a stable level till the end of 14-min heating treatment. This observation supports that the SDR has the ability to produce protein-polysaccharide conjugates via wet-heating treatment. Similarly, the browning process in wet-heating treatment was also observed in other studies (Zhu et al., 2008 & 2010). However, further characterisation was necessary to confirm the formation of protein-polysaccharide conjugates in the aqueous condition.

### **5.3.2 Degree of conjugation for SDR-processed conjugates**

Apart from visually observed browning in Figure 5.3, the degree of conjugation for SDR-processed conjugates is a critical evidence to confirm the success of conjugation and estimates the proportion of total attachments of polysaccharides. The results are presented in Figure 5.4.

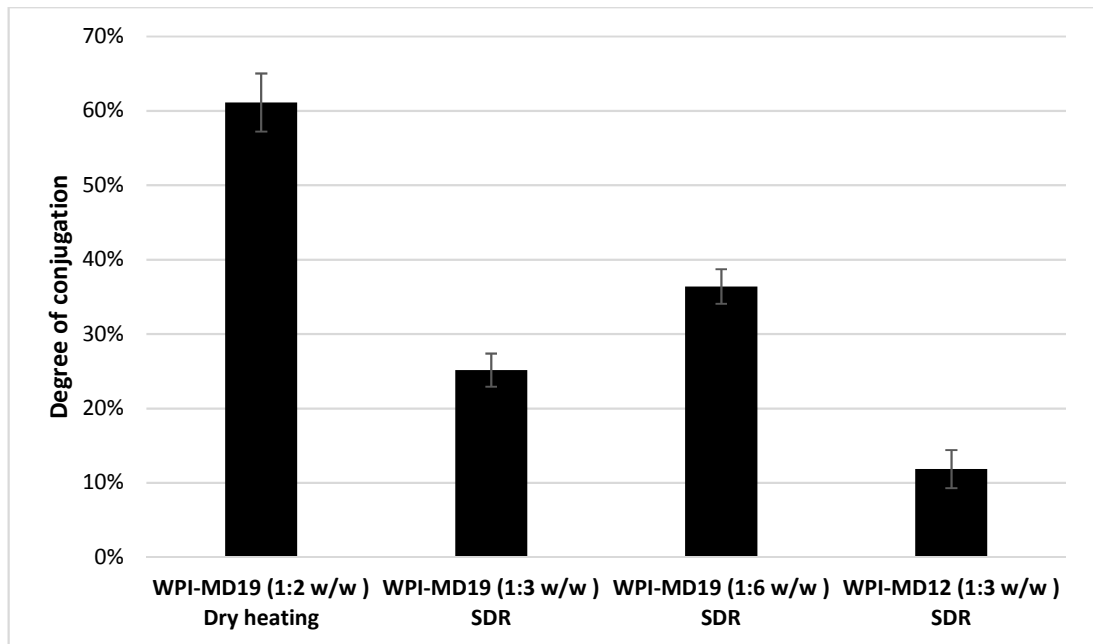


**Figure 5.4** Degree of conjugations for WPI-MD conjugates with different chain length of MD prepared via dry-heating method and SDR processing (10 mins).

It can be seen from Figure 5.4 that the degree of conjugation between WPI and MD varies significantly for dry-heating and SDR-processed conjugates. Generally, the degree of conjugation for the product of dry-heating treatment is around 60%, which is almost double than the SDR-processed WPI-MD19 (1:6 w/w) conjugates, even though the weight proportion of MD19 is three times higher than the sample passing through the dry-heating route. Under similar preparation conditions as WPI-MD19 (1:6 w/w), the degree of conjugation significantly decreases about 10% when less MD19 was present in the system. It indicates that the weight proportion of MD in preparation system can considerably affect the conjugation. Furthermore, when the chain length of maltodextrin was changed from DE19 to DE12 at the same weight ratio (1:3 WPI : MD), the degree of conjugation continues decreasing to around 10%. This observation suggests that at the same weight ratio between WPI and MD shorter chain length MD has higher DC values than the longer

chain length MD. Based on these results, it is clear that conjugation between WPI and MD can occur in aqueous phase via SDR-processing method. However, the degree of conjugation of SDR-processed conjugates is not as high as the dry-heating conjugates. The results show that the weight ratio between WPI and MD and the chain length of MD can influence the degree of conjugation. In order to improve the degree of conjugation for the SDR-processed conjugates, it is important to adjust these two parameters.

The processing time for the SDR is another factor that affects the degree of conjugation.

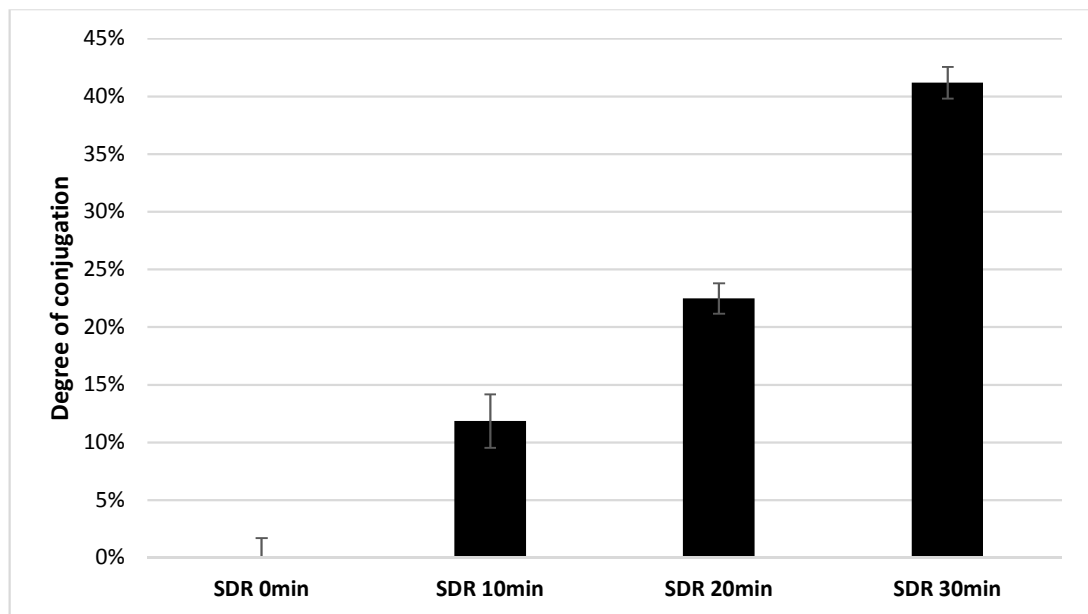


**Figure 5.5** Degree of conjugations for WPI-MD12 (1:3 w/w) prepared via SDR at different process time.

In Figure 5.5, it shows how the SDR-processing time affects the conjugation between WPI and MD12 at weight ratio of 1:3. It can be seen that the DC values increased considerably with increasing the processing time

from 0 to 30 mins. Initially, when WPI/MD12 solution was introduced into the SDR, there was negligible conjugation in the system. After 10 mins, the DC increased to around 10% and for 30 mins the DC was more than 40%. At the same time, the colour of solution became darker and darker from colourless state at the initial stage. This result demonstrates that it is possible to enhance the DC value by increasing treating time. However, the longer is processing time, the darker is the colour of solution, which is not favourable for further applications such as emulsion preparations.

### 5.3.3 Spectra scanning of SDR-processed conjugates

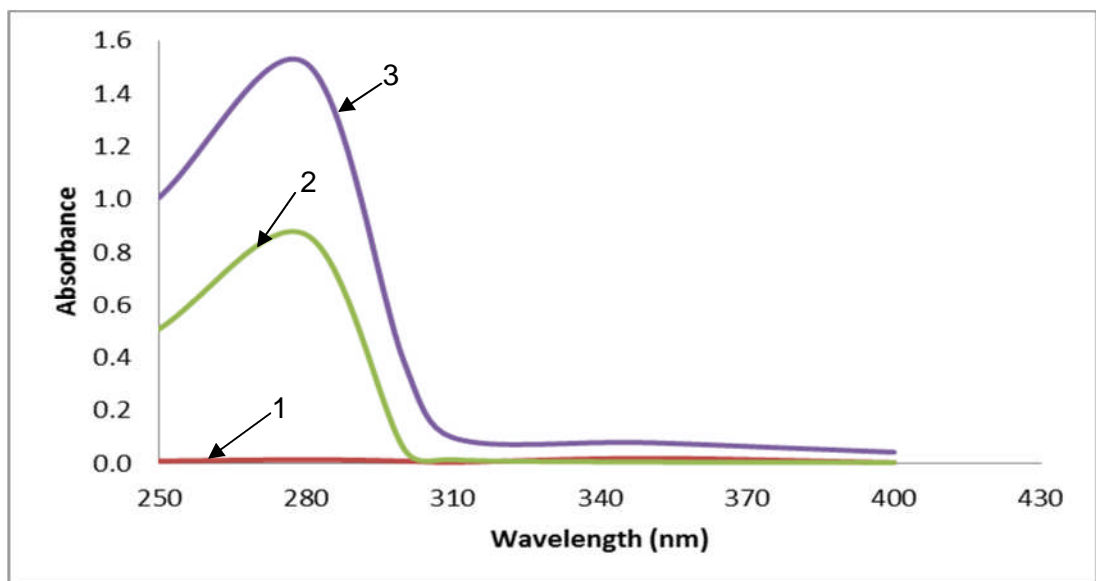


**Figure 5.6** Absorbance spectra of WPI-MD12 conjugates prepared by SDR (110 °C for 10 minutes): (1) 10 g/L MD12; (2) 10 g/L WPI alone; (3) 10 g/L WPI-MD12 (1:3 w/w) mixture.

As shown in Figure 5.6, the absorbance spectra of sample WPI-MD12 SDR-processed conjugates is compared to the controls of MD and WPI alone from wavelength 250 nm to 400 nm. In order to maintain the concentration at the same level for conjugates and control samples, each sample and control was made up to 400 ml by distilled water after 10-min SDR circulation and

then diluted 100 times for the spectra scanning. It can be seen that the interaction between WPI and MD12 (WPI-MD12, line 3) resulted in the increase of maximum absorbance at 280 nm compared to the control (WPI alone, line 2). Moreover, polysaccharide (MD12) solution does not show the absorbance maximum in the whole scanning wavelength range. Therefore, the increased absorbance maximum at 280 nm suggests the formation of the Maillard reaction products. Similarly, it has been proposed by Zhu et al. (2008, 2010) that the WPI and WPI-Dextran conjugates prepared by wet-heating method have the maximum absorbance at 304nm, suggesting the formation of Schiff base. In Figure 5.6, there is no distinct absorbance peak at 304 nm, however, the heated WPI-MD12 conjugate sample and the control do have some absorbance (~0.4 and 0.2, respectively) at 304nm. This suggests the formation of protein-polysaccharide conjugates at relatively low concentration. In summary, the characterising wavelength range for detecting WPI-polysaccharide conjugates can be narrowed between 280 and 304 nm. The absorbance maximum at 280 nm is important to monitor when the conjugates are formed during the SDR process.

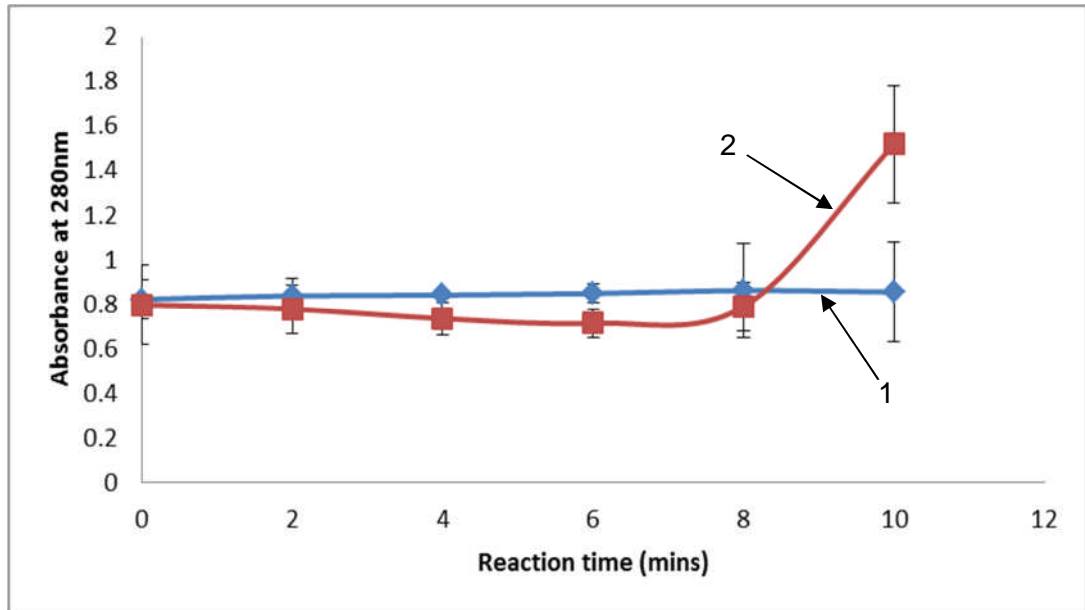


**Figure 5.7** Absorbance at 280 nm of WPI-MD12 mixture subjected to wet-heating method using the SDR (110 °C) at various reaction time: (1) 10 g/L WPI alone; (2) 10 g/L WPI-MD12 (1:3 w/w).

As presented in Figure 5.7, the absorbance of WPI-MD12 and WPI alone was recorded at wavelength 280 nm for 0 – 10 mins. There is no considerable change of absorbance was observed at 280 nm for both the control (WPI) and WPI-MD12 mixture for the initial 8 minutes of reaction in the SDR process. However, after 8-min reaction, the absorbance of WPI-MD12 mixture was increased significantly, whereas no change was observed in the control. This suggests that the concentration of conjugates resulted from the interactions between WPI and MD12 were sufficient to be detected by the spectrophotometer. Similar reaction time (8 mins) in the SDR was also observed in visual assessment (Figure 5.3). These results show that the browning process developed considerably after 8 mins reaction for SDR process.

The spectra scanning results provide further evidence to support the formation of protein-polysaccharide conjugates prepared by wet-heating

method using the SDR. Moreover, a critical reaction time (> 8 mins) for synthesising conjugates via wet-heating preparation in the SDR is established.

#### **5.3.4 Hydrophobicity change of WPI-MD19 from SDR by HPLC**

Apart from the evidence from OPA tests and spectra scanning, there is another method to confirm the formation of conjugates by analysing the change of hydrophobicity of proteins before and after heating treatment. HPLC is a well-established separation technique that is used to detect the composition of a sample mixture. The key part of HPLC is the separation column which is designed according to the different physicochemical properties of ingredients such as polarity, size, and hydrophobicity. In this project, the column was chosen by differentiating the hydrophobicity of each component because the attachment of hydrophilic polysaccharides to native proteins can reduce the total hydrophobicity of proteins. Therefore, it can be predicted that WPI-MD19 conjugates are more hydrophilic than WPI. In other words, if the hydrophobicity of WPI significantly decreases after heating treatment, it suggests the formation of WPI-MD19 conjugates.

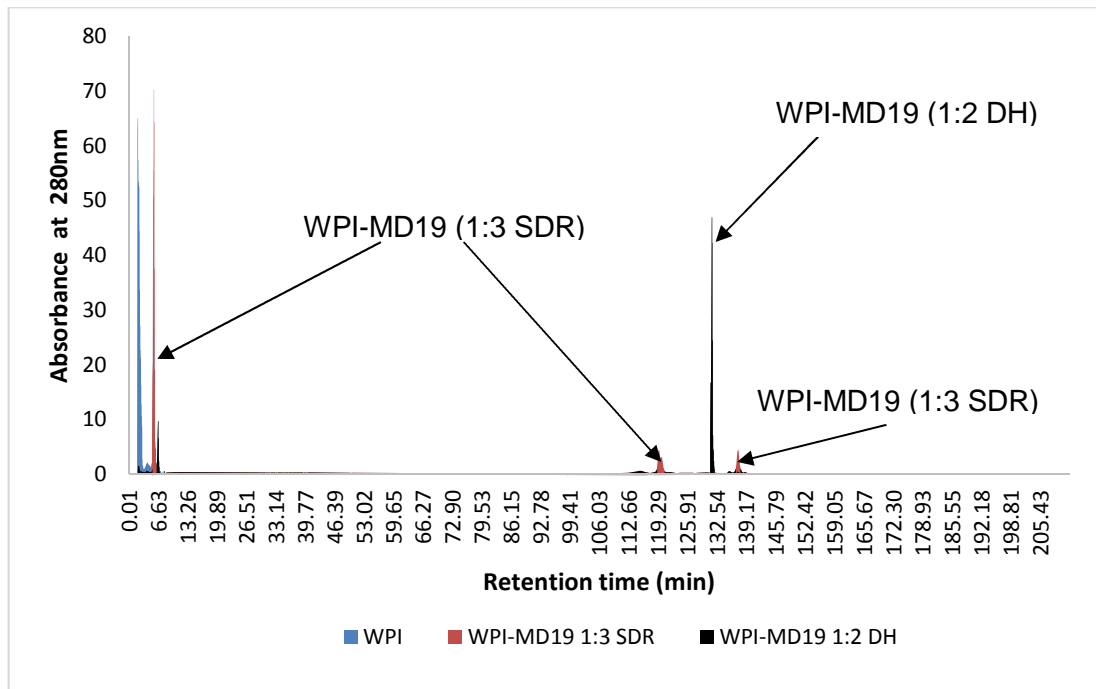


**Figure 5.8** The relationship between retention time and absorbance at wavelength 280 nm of WPI and WPI-MD19 prepared by SDR or dry-heating (DH) method.

An HPLC diagram of WPI and WPI-MD19 conjugates is shown in Figure 5.8. The results show that conjugates prepared by dry-heating and SDR-processing methods have different absorbance peaks and retention time. For WPI, most of the components have a relatively short retention time (less than 7 mins), which means that the major components in WPI have a weak affinity to the hydrophilic column and can be detected shortly after passing through the column. On the other hand, the absorbance peak for WPI-MD19 (dry-heating DH) appears at the retention time around 130 mins, which is much later than that of WPI. When it comes to the SDR product, the absorbance pattern is quite similar to WPI, which indicates that the majority of WPI-MD19 SDR is hydrophobic. However, there are two small peaks around 119 and 139 mins for SDR-processed product which has a similar retention time as WPI-MD19 (DH) suggesting that some of hydrophilic components

were formed during the SDR process. These results correlate well with the degree of conjugation shown in Figure 5.4. Therefore, it can be concluded that dry-heating conjugates are more hydrophilic than SDR-processed conjugates owing to the high degree of conjugation in WPI-MD19 (1:2 w/w, DH).

Visual assessment, OPA analysis, spectra scanning and HPLC results suggest that conjugation between WPI and MD can occur in aqueous medium via SDR-processing when the processing conditions are carefully established, such as weight ratio, pH, and reaction time. The following sections will present the performance of SDR-processed conjugates for making stable O/W emulsions, such as interfacial adsorption and stabilizing properties during storage.

### **5.3.5 Adsorption behaviour of SDR-processed WPI-MD19 conjugates**

In order to estimate the amount of conjugates adsorbed at the oil-water interface, it is necessary to determine the contents of conjugates in the serum phase when the O/W emulsion was destabilized using centrifugation. Therefore, the Biuret method was adopted (Gornall et al., 1949).

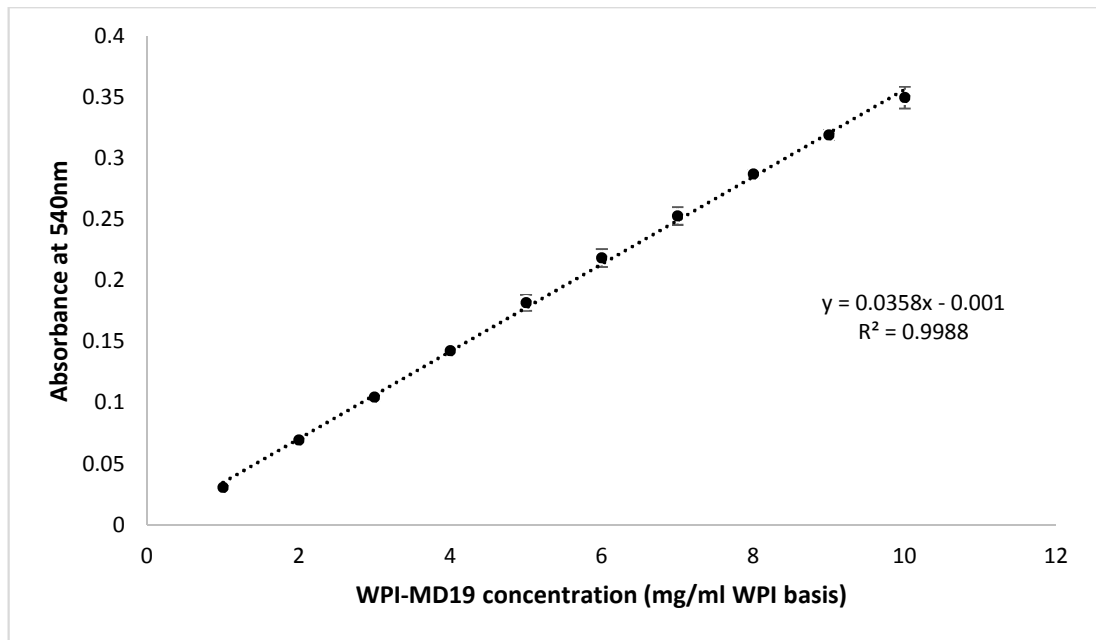


**Figure 5.9** The relationship between the concentration of WPI-MD19 in serum layer and the absorbance of complex formed via the Biuret method at wavelength 540nm.

Figure 5.9 shows a linear relationship between the concentration of WPI-MD19 (protein basis) and the absorbance of complex formed at wavelength 540nm during Biuret analysis. As can be seen that the absorbance increases with the increase of conjugates concentrations from 1 to 10 mg/ml. The  $R^2$  value (0.9988) indicates that the experimental results agree very well with the linear model at this concentrations range for the conjugates. Moreover, the error bar for each data point, which represent the standard deviation of three individual results, is also insignificant suggesting the accuracy of each number. Therefore, the Biuret method is a reliable tool to determine the conjugate contents left in the serum phase. After centrifugation of emulsions, it is possible to estimate the contents of protein or protein conjugates left in the aqueous phase and to calculate the percentages of adsorbed proteins.

The following graph exhibits the adsorption of WPI-MD19 conjugates at the oil-water interface of O/W emulsions.

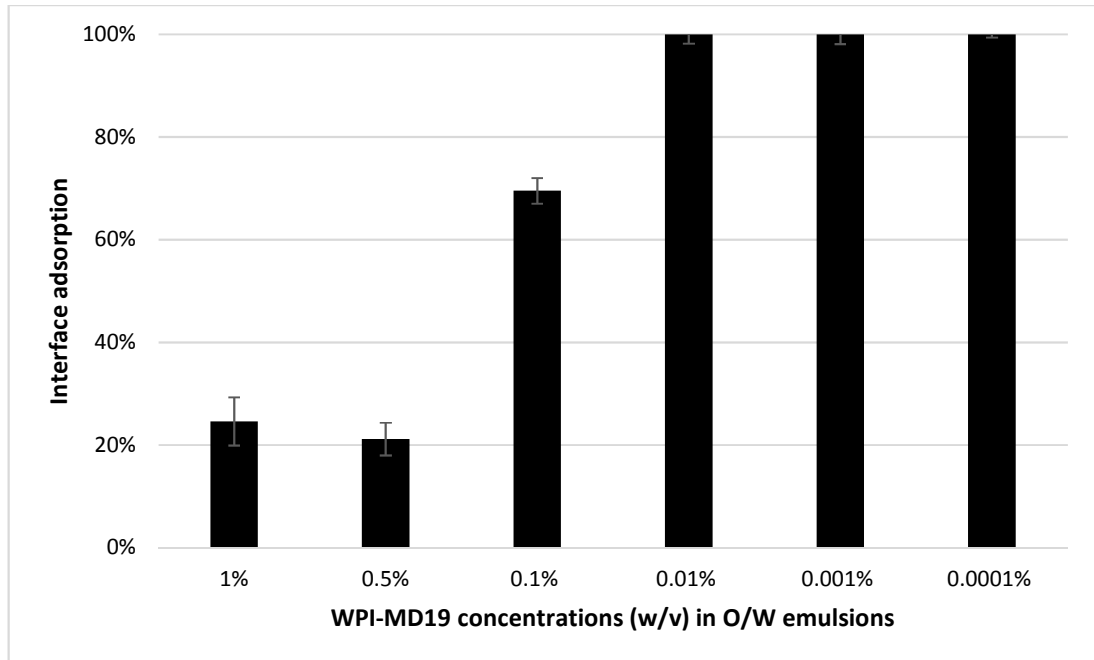


**Figure 5.10** The adsorption of WPI-MD19 at the oil-water interface in emulsions (O/W 20:80 v/v) at various concentrations.

It is shown in Figure 5.10 that the interfacial adsorption varies at different WPI-MD19 conjugate concentrations. When the concentration of WPI-MD19 is higher than 0.01 w/v%, not all the conjugates are adsorbed at the oil-water interface. Furthermore, if the WPI-MD19 concentration is higher than 0.5 w/v%, only 20% of the conjugates are adsorbed at the interface. This observation demonstrates that the oil-water interfaces have been fully covered (saturated) by WPI-MD19 conjugates when the concentration of WPI-MD19 is higher than 0.01 w/v%. In other words, there were considerable amount of conjugates left in the aqueous phase when the emulsion was prepared at high concentrations (> 0.01 %). However, if the WPI-MD19 concentration is around

0.01 w/v% or lower, the adsorption is 100%, which means that there are few conjugates left in the aqueous phase.

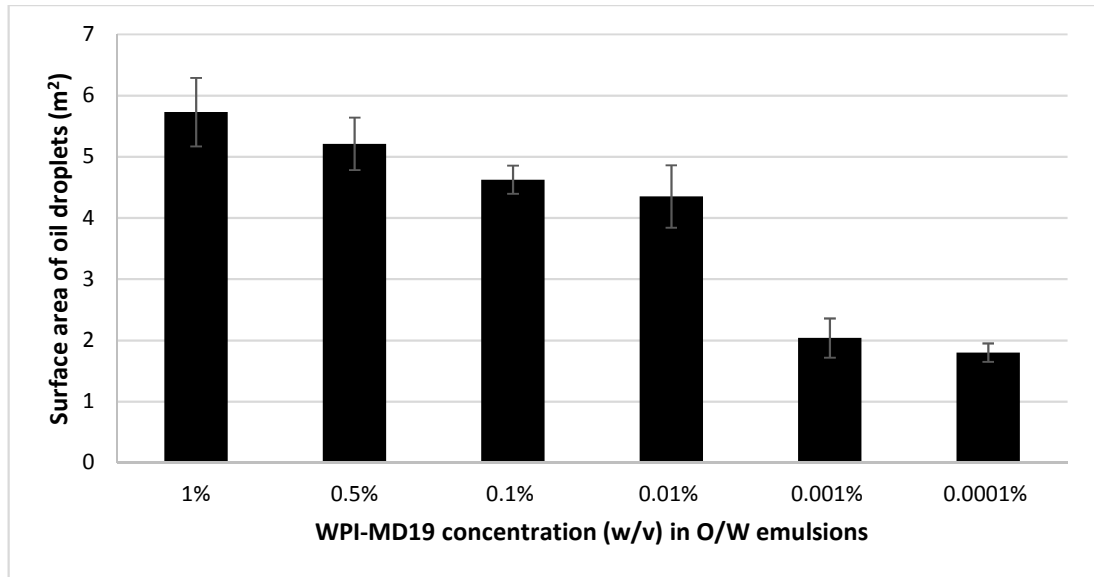


**Figure 5.11** The surface area of oil droplets of oil-in-water emulsions containing various WPI-MD19 concentrations.

Figure 5.11 shows the total surface area of oil phase in emulsions prepared at different concentrations of WPI-MD19. It is clear that the surface area of oil droplets decreases when lower the concentration of WPI-MD19 in the aqueous phase. When the concentration is around 0.001 w/v% or less, the surface area is around 2 m<sup>2</sup>. For a high WPI-MD19 concentration (1 w/v%), the surface area is no more than 6 m<sup>2</sup>. It is possible to estimate the surface concentrations of WPI-MD19 for each emulsion by using the results from Figures 5.10 and 5.11.

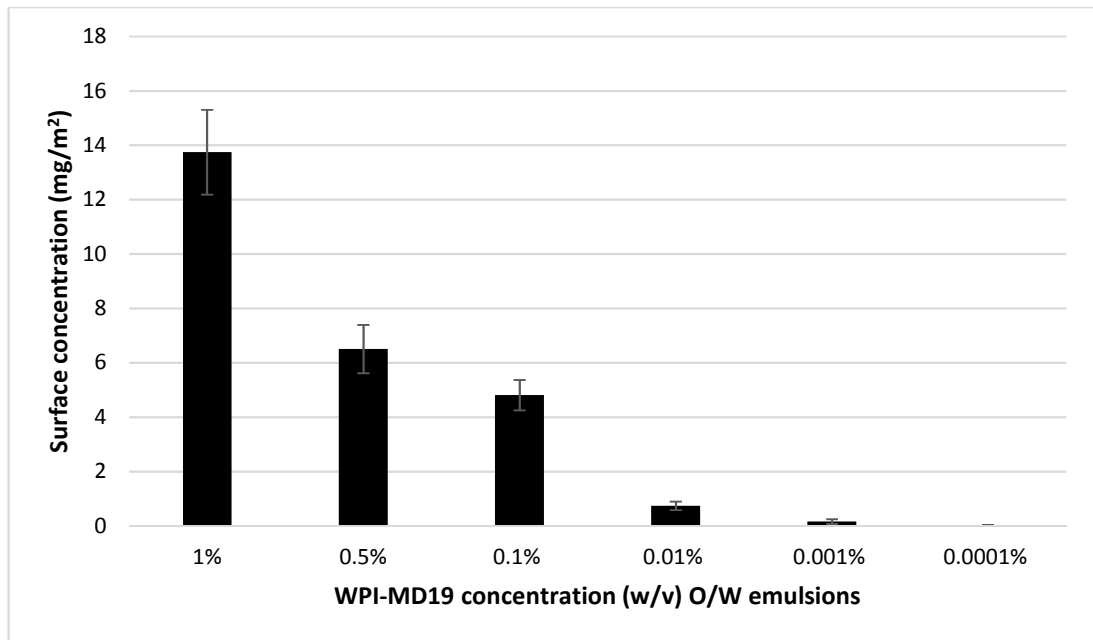


**Figure 5.12** The surface concentration of WPI-MD19 in emulsions with different total conjugates concentrations.

It can be seen from Figure 5.12 that WPI-MD19 has different surface concentrations when the bulk concentration varies. As the concentration of bulk phase increases from 0.0001 w/v% to 1 w/v%, the surface concentration increases significantly, from almost 0 mg/m<sup>2</sup> to around 14 mg/m<sup>2</sup>. Compared to the sample with 0.5 w/v% WPI-MD19, the emulsion which has 1 w/v% conjugates is twice concentrated on the interface. According to the results from Figures 5.10 and 5.11, the emulsion stabilized by WPI-MD19 conjugates at bulk concentration 1 w/v% and 0.5 w/v% have similar adsorption percentage around 20% (see Figure 5.10) and surface area of oil droplets about 5.5 m<sup>2</sup> (see Figure 5.11). These results suggest that a second layer of conjugates may have been formed around the oil droplets via hydrophobic interactions between the protein backbones when the oil-water interface has already fully covered by conjugates.

Analysis of results of WPI-MD19 conjugate adsorption at the oil-water interface suggests that the conjugates prepared in aqueous medium via SDR process can be used as emulsifiers and stabilizers for making emulsions. In order to test the stabilizing properties of SDR-processed WPI-MD19 stabilized emulsions, the dry-heated WPI-MD19 conjugates were chosen as a reference.

### 5.3.6 Stabilizing properties of SDR-processed WPI-MD19 conjugates

The stabilizing properties of WPI-MD19 in O/W emulsions were tested by average droplet size and droplet size distribution at day 0 and 28.

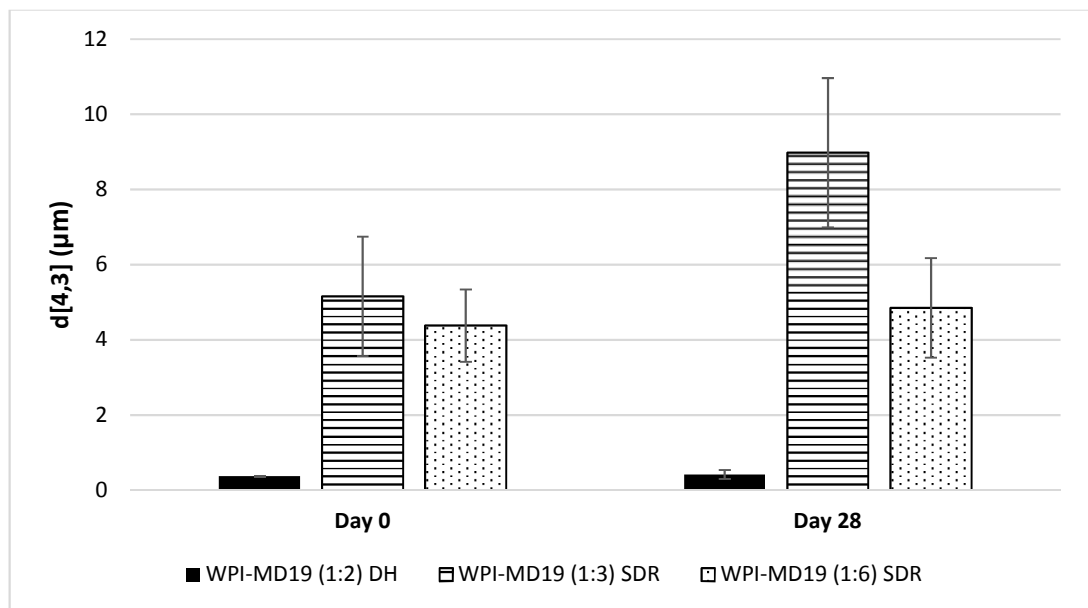


**Figure 5.13** Average droplet size,  $d[4,3]$ , of emulsions stabilized by WPI-MD19 conjugates prepared by dry heating (DH) and SDR processing at different weight ratios for a storage period of 28 days.

The average droplet size of emulsions stabilized by various conjugates during 28-day storage is presented in Figure 5.13. It can be seen that the

emulsion stabilized by the conjugates prepared by dry-heating treatment has smaller droplet size, which is less than 1  $\mu\text{m}$  throughout the whole observation period even though the percentage of polysaccharide is relatively low. However,  $d[4,3]$  values for the freshly made emulsions stabilized by SDR-processed conjugates are around 5  $\mu\text{m}$ . After 28 days, there was a significant increase of droplet size (9  $\mu\text{m}$ ) in the emulsion stabilized by SDR-processed WPI-MD19 (1:3 w/w) conjugates. Nevertheless, the other emulsion with higher weight ratio of MD19 (WPI-MD19 1:6 w/w) exhibits certain stability during 28-day storage. A slight increase of average droplet size ( $\sim 0.5 \mu\text{m}$ ) can be observed in Figure 5.13. These results indicate that SDR-processed WPI-MD19 conjugate can stabilize O/W emulsion to a certain extent but not as good as the conjugates prepared via dry-heating method. Moreover, a higher proportion of MD19 in conjugates can improve the stabilizing properties of the conjugates.

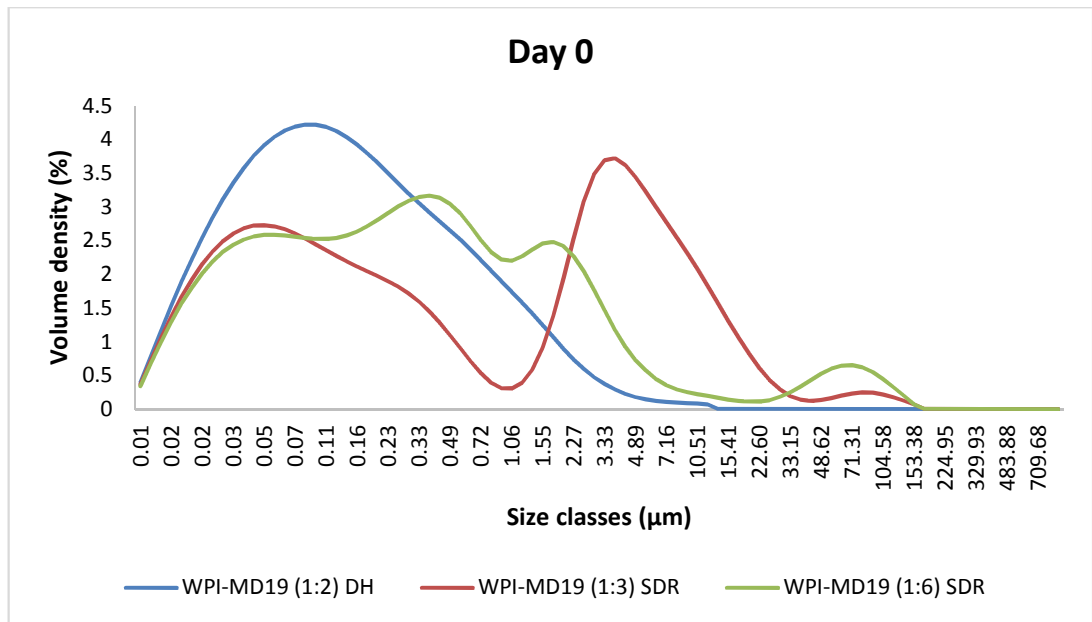


**Figure 5.14** Droplet size distribution of freshly made emulsions stabilized by WPI-MD19 prepared by dry heating (DH) and SDR processing at different weight ratios.

Figure 5.14 shows the droplet size distributions of freshly made emulsions stabilized by conjugates prepared via dry-heating method and SDR processing. For the control (WPI-MD19 DH), the majority of oil droplets are around 0.1 µm. It also contains a small proportion of large droplets (>1 µm). On the other hand, WPI-MD19 SDR-processed conjugates stabilized emulsions have a high percentage of large droplets that are over 1 µm. However, the average droplet size of oil droplets is about 100 µm for SDR-processed conjugates.

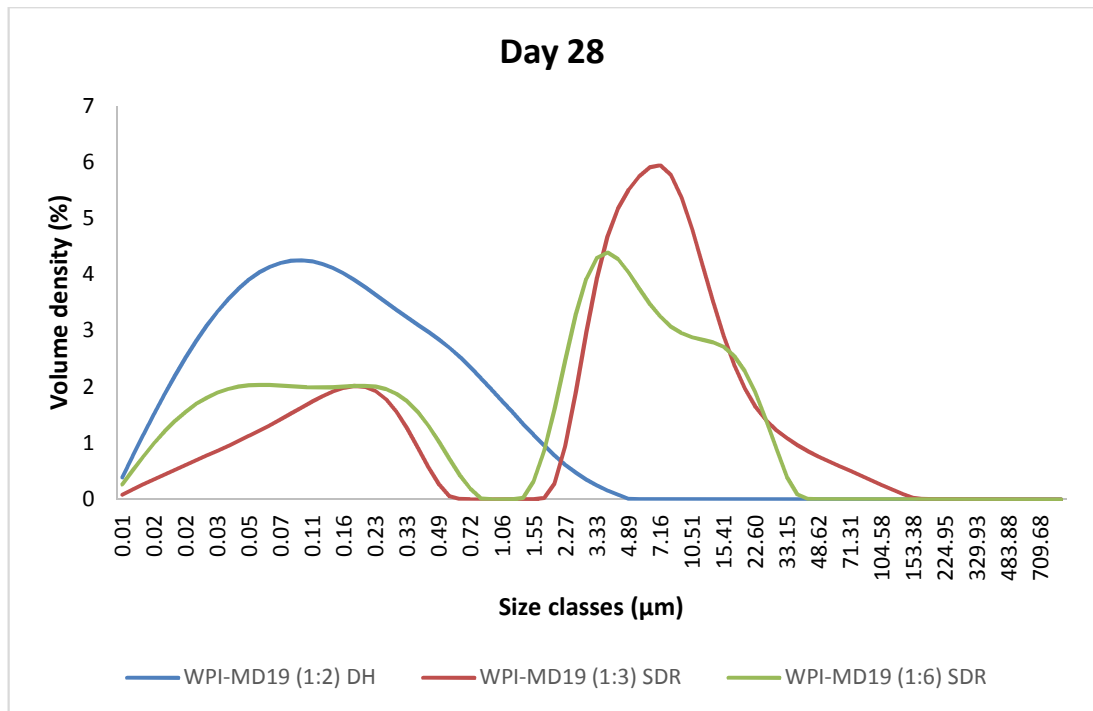


**Figure 5.15** Droplet size distribution of emulsions stabilized by WPI-MD19 prepared by dry heating (DH) and SDR at different weight ratios at storage day 28.

The droplet size distributions of three emulsions stored for 28 days are shown in Figure 5.15. There is no noticeable change in the size distribution of the control emulsion whilst a shift of the distribution towards larger droplet size can be observed for SDR-processed WPI-MD19 (1:3) conjugate stabilized emulsions. At the size classes less than 1 µm, there is a considerable decrease compared to that in the same size range according to Figure 5.15. When it comes to the emulsion with higher MD19 content (1:6 WPI : MD19), the increase of large droplets is also clear. However, the small droplets in emulsion (1:6 WPI : MD19) have higher proportion than that in the other SDR-processed sample. The results suggest that the conjugates with higher amount of MD19 have better stabilizing properties. Based on the degree of conjugation results in Section 5.3.2, there is a positive relationship between the degree of conjugation and the stabilizing properties, suggesting that the

higher is the degree of conjugation, the better is the stabilizing properties of conjugates. A similar relationship is also reported in Chapter 4.

It can be concluded from the stabilizing properties of WPI-MD19 from SDR processing that conjugates can be prepared using the SDR and improve stabilizing properties of O/W emulsions. However, the stabilizing properties of SDR-processed conjugates are not as good as those from dry-heating method under similar environmental conditions.

## **5.4 Conclusions**

In this chapter, a novel approach utilizing the SDR for preparing protein-polysaccharide conjugates has been explored. The main advantage of this method is to improve the efficiency of preparation of conjugates by shortening the reaction time. However, there are many challenges in this method. The major one is to ensure a successful conjugation of protein-polysaccharide in an aqueous medium which is unfavourable condition for the Maillard reactions because the Maillard reactions are mainly dehydrated processes. Another challenge is to improve the degree of conjugation. Even though the Maillard reactions can occur in protein and polysaccharide, the functional properties of protein especially stabilizing properties may not be significantly enhanced if the degree of conjugation is relatively low.

According to the experimental results, several achievements can be confirmed. First of all, the preparation time of conjugates is remarkably reduced by using the SDR, from more than one day (See 3.2.3) to a couple of hours due to the elimination of freeze drying and 3 hours incubation time. Secondly, the results from visual assessment, OPA analysis, and spectra

scanning suggest that the Maillard reactions can occur in aqueous medium. Furthermore, the SDR-processed products can adsorb onto the oil-water interface and offer certain emulsifying and stabilizing properties of OW emulsions.

However, more further experiments are necessary especially in the area of improving the degree of conjugation of SDR-processed products. In this project, increasing the weight ratio of polysaccharides for preparing conjugates has also been tested. Increasing the weight ratio improves the degree of conjugation at limited level even if the amount of polysaccharide is doubled, which suggests that the low degree of conjugation may be resulted from the structure of native proteins.

In future, it is possible to improve the stabilizing properties of conjugates prepared via SDR processing by optimizing the processing conditions such as the heating temperature, circulation time, and speed of the spinning disc. Moreover, it is worth exploring some pre-treatments of native proteins before processing through the SDR in order to facilitate the attachment of reducing polysaccharides. For example, hydrolysing proteins by enzymes can reduce the complexity of natural protein structures.

## **Chapter 6**

### **General Discussion and Conclusions**

#### **6.1 Introduction**

Protein-polysaccharide conjugates prepared from Maillard reactions have interesting functional properties. Many scientists have spent almost three decades studying this type of polymers and have tried to apply the conjugates as useful functional ingredients in food industry, based on the understanding of their properties. With regards to the discoveries of this PhD project, there are several issues which can be summarized in this chapter.

#### **6.2 Improved colloidal stability by protein-polysaccharide conjugates**

The most important feature of protein-polysaccharide conjugates is the enhanced stabilizing properties in O/W emulsions, especially under unfavourable environmental conditions (i.e. pH value close to pI and high ionic strength). This finding is also confirmed by the results from our studies (see Chapter 3). Similarly, other studies have also reported recently that covalent bonding between protein and polysaccharides can improve the stabilizing properties of the formed complex (Inada et al., 2015; Liu et al., 2015; Zhang et al., 2015b; Kim and Shin, 2016; Mulcahy et al., 2016; Wefers et al., 2018). Moreover, previous investigations of protein-polysaccharide conjugates, based on different combinations of proteins and polysaccharides, show improving physicochemical properties, as well (see Appendix A). More details can be found in Section 1.6.4. The main reason of this improvement in functional properties of conjugates is likely to be the provision of much enhanced steric repulsion resulting from sugar moieties attached to protein

(see Figure 1.10). This explanation is also supported by a study from Wooster and Augustin (2006), showing that  $\beta$ -lactoglobulin-dextran conjugate forms a thicker layer than that of  $\beta$ -lactoglobulin alone, once adsorbed onto latex spheres. The steric layer from the attached polysaccharide chains in conjugate is the main factor preventing flocculation between droplets.

### **6.3 Interfacial properties of protein-polysaccharide conjugates**

Apart from the improved stabilizing properties, the protein-polysaccharide conjugates have different interfacial properties from the native proteins. It has been reported that protein experiences a great conformational change during surface adsorption (Zhai et al., 2013). The re-arrangement of protein on oil-water interface is highly dependent on the flexibility of protein polymer chain, distribution of hydrophobic/hydrophilic domains in the chain, and the hydrophobicity of oil phase (Zhai et al., 2013). These adsorption properties of protein can significantly influence the emulsifying and stabilizing effect on an emulsion. However, there are not many studies on the interfacial behaviours of conjugates especially on competitive adsorption between conjugate and native protein. In Chapter 3, we investigated such competitive adsorption of WPI and WPI-MD19 on oil-water interface by using theoretical calculations from SCF and experiments. These results suggest that conjugates can adsorb to the oil-water interface in the presence of unreacted proteins. In other words, once the conjugates adsorb on the interface, they cannot be easily displaced by unreacted proteins. A similar finding was reported that whey protein after glycation becomes more resistant to other surfactants in the competition of adsorption than unmodified whey protein on

air-water interface (Cai and Ikeda, 2016). Another report about competitive adsorption on oil-water interface between soy-protein-dextran conjugates and small molecule surfactants such as Tween 40 or bovine serum albumin (BSA) suggests that conjugates cannot be completely displaced by surfactants or BSA (Diftis and Kiosseoglou, 2004). Although the interface in that study is not as the same as ours, nonetheless the adsorption ability of conjugates are evident in both systems. Once the interfacial behaviour of conjugates is discovered, it is possible to apply this novel biopolymer to different systems for colloidal stability.

#### **6.4 Influence of polysaccharides on the properties of protein-polysaccharide conjugates**

In Chapter 4, we focused on the influence of polysaccharides on the stabilizing properties of conjugates including the effect of sugar chain length and lactose as impurity for competitive reaction during heat treatment. Results from Chapter 4 suggest that longer sugar chain has better stabilizing property than shorter chain. However, if the chain length is too small, such as just lactose, the enhanced stabilizing property is insignificant. Our findings agree with other research studies on the effect of polysaccharide length on stabilizing properties of various protein-polysaccharide conjugates (Kato, 1995; Shu et al., 1996; Li et al., 2016). Based on the model in Figure 1.10, we can predict that longer polysaccharide chains on the surface can provide stronger steric repulsion at longer distance between two droplets due to the increase of thickness of steric layer. This prediction is supported by the results also from the study of Wooster and Augustin (2006). When higher molecular weight of dextran (440 kDa) was attached, the thickness of adsorbed layer is

20 nm while the thickness reduced to 5 nm for lower molecular weight dextran (18.5 kDa) attached (The thickness of adsorbed layer with  $\beta$ -lactoglobulin alone is 3 nm).

When it comes to the influence of lactose on the stabilizing properties of WPI-MD19 conjugates during heat treatment, the presence of lactose in the mixture of WPI and MD19 has insignificant influence on the stabilizing properties of WPI-MD19 conjugates even the molar ratio between MD19 and lactose is 1:10 (Ding et al., 2017). It suggests that a small fraction of MD19 attached to protein is sufficient to impart acceptable steric stability. This finding exhibits a potential to use lower purity whey protein, containing a high proportion of lactose, to prepare acceptable stabilizers. This is likely to be an important consideration in large scale manufacturing.

## **6.5 Novel preparation method of protein-polysaccharide conjugates**

The traditional preparation method for protein-polysaccharide conjugates is by dry-heating treatment, with controlled humidity for a relatively long period. There are a few published papers attempting to form conjugates in an aqueous medium (i.e. wet-heating treatment) (Zhang et al., 2014; Wang et al., 2016; Pirestani et al., 2017a). All these studies show that it is possible to prepare protein-polysaccharide conjugates via wet-heating treatment. This is also observed in our study on SDR-processed conjugates (see Chapter 5). The Spinning Disc Reactor (SDR) can prepare protein-polysaccharide conjugates with enhanced stabilizing property. However, the stabilizing properties of SDR-processed conjugates are still not as good as these from dry-heating treatment. The optimum condition for the progress of Maillard

reactions is a water activity of around 6.5 (Maillard, 1912). The main reason for less efficient production of conjugates in the SDR system could therefore be the presence of aqueous medium which is unfavourable to Maillard reactions.

## **6.6 Conclusions and outlook**

Protein-polysaccharide conjugates are proteins chemically modified by attachment of reducing polysaccharides through Maillard reactions. This modification significantly change the functional properties of native protein. In the world of food colloids, proteins play an important role in emulsifying and stabilizing oil/water mixtures such as emulsions. Many scientists devoted themselves to understand the behaviours of proteins in a complicated colloidal system.

This PhD project is based on the solid foundation of colloid science and attempts to further the understanding of protein-polysaccharide conjugates in emulsion systems. It is confirmed that protein-polysaccharide conjugates have improved physicochemical properties than unmodified proteins especially in stabilizing O/W emulsions. Moreover, conjugated proteins can adsorb onto oil-water interface and not be displaced by unreacted proteins when both of them are present in bulk phase.

The length of polysaccharide chain is critical for the final properties of Maillard-type conjugates. If the chain is too short, it cannot provide sufficient steric repulsion between two approaching droplets. However, once long polysaccharides are attached to proteins, the steric repulsion is considerably

increased, even when only a small molar fraction of long polysaccharides is successfully attached.

Based on these findings, it is possible to prepare protein-polysaccharide conjugates in large scale in food industry to replace expensive emulsifiers and stabilizers such as Gum Arabic (Akhtar and Dickinson, 2007). Firstly, the raw materials for conjugates preparation can be from by-products. For example, whey protein is a by-product from cheese manufacturing. Furthermore, the work of this project has shown that there is no need for extensive separating of lactose from whey protein, because lactose has insignificant influence on the stabilizing properties of final products from heat treatment. Secondly, the application of SDR in conjugates preparation can considerably reduce the processing time and provide continuous manufacturing instead of batch-by-batch production.

For further research, a large number of unknown questions relating to production and use of conjugates are still waiting to be explored. For example, it is not entirely clear what conformation and re-arrangement the conjugates and unreacted proteins in mixed layers adopt on the oil-water interface. Moreover, one can ask whether it is possible to hydrolyse proteins and separate the hydrophobic segments before Maillard reactions. The aim of this process is trying to prepare di-block bio-polymers with stronger surface activity and stabilizing properties. Moreover, site-specified modification of protein could be another method to prepare novel emulsifiers and stabilizers by allowing a more selective site for binding of polysaccharides with proteins (e.g. in middle, at N-terminus side, at C-terminus side, etc.). For the application of conjugates in food emulsions during digestion, there are many undiscovered

areas such as bioavailability of conjugate-based system in oral processing, stomach, and small intestine digestion (Liu et al., 2017).

For industrial application, it is important to optimize the process conditions such as the process time and temperature in SDR preparation of conjugates. More importantly, the safety of this new polymers needs to be verified and approved by food safety authorities before wide-spread applied to food.

In conclusion, protein-polysaccharide conjugates are promising emulsifiers and stabilizers in future, offering a rich oven of both academic and applied industrial research.

## Bibliography

- Adlernissen, J. 1979. Determination of the degree of hydrolysis of food protein hydrolysates by trinitrobenzenesulfonic acid. *Journal of Agricultural and Food Chemistry*. **27**(6), pp.1256-1262.
- Ahoba-Sam, C., Boodhoo, K.V.K., Olsbye, U. and Jens, K.J. 2018. Tailoring Cu Nanoparticle Catalyst for Methanol Synthesis Using the Spinning Disk Reactor. *Materials*. **11**(1), [no pagination].
- Akhtar, M., Chan, P., Safriani, N., Murray, B.S. and Clayton, G. 2011. Concentration of apple juice using spinning disc reactor technology. *Journal of Food Processing & Technology*. **2**(108), [no pagination].
- Akhtar, M. and Dickinson, E. 2003. Emulsifying properties of whey protein-dextran conjugates at low pH and different salt concentrations. *Colloids and Surfaces B-Biointerfaces*. **31**(1-4), pp.125-132.
- Akhtar, M. and Dickinson, E. 2007. Whey protein-maltodextrin conjugates as emulsifying agents: An alternative to gum arabic. *Food Hydrocolloids*. **21**(4), pp.607-616.
- Akhtar, M., Murray, B.S., and Dowu, S. 2014. A novel continuous process for making mayonnaise and salad cream using the spinning disc reactor: effect of heat treatment. *Food Hydrocolloids*. **42**(1), pp.223-228.
- Akinshina, A., Ettelaie, R., Dickinson, E. and Smyth, G. 2008. Interactions between adsorbed layers of alpha(S1)-casein with covalently bound side chains: A Self-Consistent Field Study. *Biomacromolecules*. **9**(11), pp.3188-3200.
- Al-Hakkak, J. and Al-Hakkak, F. 2010. Functional egg white-pectin conjugates prepared by controlled Maillard reaction. *Journal of Food Engineering*. **100**(1), pp.152-159.
- Álvarez, C., Garcia, V., Rendueles, M. and Diaz, M. 2012. Functional properties of isolated porcine blood proteins modified by Maillard's reaction. *Food Hydrocolloids*. **28**(2), pp.267-274.
- Aoki, T., Hiidome, Y., Kitahata, K., Sugimoto, Y., Ibrahim, H.R. and Kato, Y. 1999. Improvement of heat stability and emulsifying activity of ovalbumin by conjugation with glucuronic acid through the Maillard reaction. *Food Research International*. **32**(2), pp.129-133.
- Belitz, H.D. 2004. Milk and Dairy Products. In: Belitz, H.D., Grosch, W. and Schieberle P. ed. *Food Chemistry*. 3<sup>rd</sup> Edition. New York: Springer, pp.505-549.
- Bi, B.W., Yang, H., Fang, Y.P., Nishinari, K. and Phillips, G.O. 2017. Characterization and emulsifying properties of beta-lactoglobulin-gum Acacia Seyal conjugates prepared via the Maillard reaction. *Food Chemistry*. **214**(1), pp.614-621.
- Cai, B. and Ikeda, S. 2016. Effects of the conjugation of whey proteins with gellan polysaccharides on surfactant-induced competitive displacement from the air-water interface. *Journal of Dairy Science*. **99**(8), pp.6026-6035.
- Chen, H.Y., Jin, Y.M., Ding, X.L., Wu, F.F., Bashari, M. Chen, F., Cui, Z.W. and Xu, X.M. 2014. Improved the emulsion stability of phosvitin from hen egg yolk against different pH by the covalent attachment with dextran. *Food Hydrocolloids*. **39**(0), pp.104-112.
- Chen, H.Y., Wang, P., Wu, F.F., Xu, J. Tian, Y.Q., Yang, N. Cissouma, A.I. Jin, Z.Y. and Xu, X.M. 2013. Preparation of phosvitin-dextran

- conjugates under high temperature in a liquid system. *International Journal of Biological Macromolecules*. **55**(1), pp.258-263.
- Church, F.C., Swaisgood, H.E., Porter, D.H., and Catignani, G.L. 1983. Spectrophotometric assay using ortho-phthaldialdehyde for determination of proteolysis in milk and isolated milk-proteins. *Journal of Dairy Science*. **66**(6), pp.1219-1227.
- Dickinson, E. 1982a. Basic concepts. In: Dickinson, E. and Stainsby, G. ed. *Colloids in Food*. Essex: Applied Science Publishers LTD., pp.1-25.
- Dickinson, E. 1982b. Macromolecular adsorption and colloid stability. In: Dickinson, E. and Stainsby, G. ed. *Colloids in Food*. Essex: Applied Science Publishers LTD., pp.67-100.
- Dickinson, E. 1982c. The oil-water interface and emulsion stability. In: Dickinson, E. and Stainsby, G. ed. *Colloids in Food*. Essex: Applied Science Publishers LTD., pp.107-189.
- Dickinson, E. 1982d. Experimental methods. In: Dickinson, E. and Stainsby, G. ed. *Colloids in Food*. Essex: Applied Science Publishers LTD., pp.196-246.
- Dickinson, E. 1982e. Adsorption of proteins. In: Dickinson, E. and Stainsby, G. ed. *Colloids in Food*. Essex: Applied Science Publishers LTD., pp.285-318.
- Dickinson, E. 1982f. Rheology. In: Dickinson, E. and Stainsby, G. ed. *Colloids in Food*. Essex: Applied Science Publishers LTD., pp.331-384.
- Dickinson, E. 1982g. Colloids in food processing. In: Dickinson, E. and Stainsby, G. ed. *Colloids in Food*. Essex: Applied Science Publishers LTD., pp.67-100.
- Dickinson, E. 1992a. The field of study. In: Dickinson, E. ed. *An Introduction to Food Colloids*. New York: Oxford University Press, pp.1-8.
- Dickinson, E. 1992b. Surface activity. In: Dickinson, E. ed. *An Introduction to Food Colloids*. New York: Oxford University Press, pp.30-47.
- Dickinson, E. 1992c. Rheology. In: Dickinson, E. ed. *An Introduction to Food Colloids*. New York: Oxford University Press, pp.51-70.
- Dickinson, E. and Izgi, E. 1996. Foam stabilization by protein-polysaccharide complexes. *Colloids and Surfaces a-Physicochemical and Engineering Aspects*. **113**(1-2), pp.191-201.
- Dickinson, E. and Semenova, M.G. 1992. Emulsifying properties of covalent protein dextran hybrids. *Colloids and Surfaces*. **64**(3-4), pp.299-310.
- Diftis, N. and Kiosseoglou, V. 2004. Competitive adsorption between a dry-heated soy protein–dextran mixture and surface-active materials in oil-in-water emulsions. *Food Hydrocolloids*. **18**(4), pp.639-646.
- Diftis, N. and Kiosseoglou, V. 2006. Stability against heat-induced aggregation of emulsions prepared with a dry-heated soy protein isolate–dextran mixture. *Food Hydrocolloids*. **20**(6), pp.787-792.
- Ding, R., Valicka, E., Akhtar, M. and Ettelaie, R. 2017. Insignificant impact of the presence of lactose impurity on formation and colloid stabilizing properties of whey protein-maltodextrin conjugates prepared via Millard reactions. *Food Structure*. **12**(1), pp.43-53.
- Dunlap, C.A. and Cote, G.L. 2005. beta-lactoglobulin-dextran conjugates: Effect of polysaccharide size on emulsion stability. *Journal of Agricultural and Food Chemistry*. **53**(2), pp.419-423.

- Edwards, S.F. 1965. Statistical Mechanics of polymers with excluded volume. *Proceedings of the Physical Society of London*. **85**(546), pp.613-618.
- Ettelaie, R. 2003. Computer simulation and modeling of food colloids. *Current Opinion in Colloid & Interface Science*. **8**(4-5), pp.415-421.
- Ettelaie, R. and Akinshina, A. 2014. Colloidal interactions induced by overlap of mixed protein plus polysaccharide interfacial layers. *Food Hydrocolloids*. **42**(1), pp.106-117.
- Ettelaie, R., Akinshina, A. and Dickinson, E. 2008. Mixed protein-polysaccharide interfacial layers: a self consistent field calculation study. *Faraday Discussions*. **139**(1), pp.161-178.
- Ettelaie, R., Khandelwal, N. and Wilkinson, R. 2014a. Interactions between casein layers adsorbed on hydrophobic surfaces from self consistent field theory: kappa-casein versus para-kappa-casein. *Food Hydrocolloids*. **34**(1), pp.236-246.
- Ettelaie, R., Zengin, A. and Lee, H. 2014b. Fragmented Proteins as Food Emulsion Stabilizers: A Theoretical Study. *Biopolymers*. **101**(9), pp.945-958.
- Everett, D.H. 1988a. What are colloids? In: Everett, D.H. ed. *Basic Principles of colloid science*. London: the Royal Society of Chemistry, pp.1-8.
- Everett, D.H. 1988b. Why are colloidal dispersions stable? II Interparticle forces. In: Everett, D.H. ed. *Basic Principles of colloid science*. London: the Royal Society of Chemistry, pp.30-51.
- Everett, D.H. 1988c. How are colloidal dispersions prepared? In: Everett, D.H. ed. *Basic Principles of colloid science*. London: the Royal Society of Chemistry, pp.54-60.
- Everett, D.H. 1988d. Some Important properties of colloids II Scattering of radiation. In: Everett, D.H. ed. *Basic Principles of colloid science*. London: the Royal Society of Chemistry, pp.95-104.
- Everett, D.H. 1988e. How are colloidal dispersions destroyed? I aggregation processes. In: Everett, D.H. ed. *Basic Principles of colloid science*. London: the Royal Society of Chemistry, pp.127-140.
- Fan, J.F., Zhang, Y.Y., Szesze, T., Li, F.J., Zhou, M.Y., Saito, M., Tatsumi, E. and Li, L.T. 2006. Improving functional properties of soy protein hydrolysate by conjugation with curdlan. *Journal of Food Science*. **71**(5), pp.285-291.
- Flory, P.J. 1985. Citation classic – thermodynamics of high polymer-solutions. *Current Contents/Engineering Technology & Applied Sciences*. **18**(1), pp.3-18.
- Fox, P.F. 2015. Milk proteins. In: Fox, P.F., Lowe, T.U., McSweeney, P.L.H. and O'Mahony, J.A. ed. *Dairy Chemistry and Biochemistry*. New York: Springer International Publishing, pp.145-239.
- Fujiwara, K., Oosawa, T. and Saeki, H. 1998. Improved thermal stability and emulsifying properties of carp myofibrillar proteins by conjugation with dextran. *Journal of Agricultural and Food Chemistry*. **46**(4), pp.1257-1261.
- Golkar, A., Nasirpour, A. and Keramat, J. 2017. Improving the emulsifying properties of -lactoglobulin-wild almond gum (*Amygdalus scoparia* Spach) exudate complexes by heat. *Journal of the Science of Food and Agriculture*. **97**(1), pp.341-349.

- Gornall, A.G., Bardawill, C.J. and David, M.M. 1949. Determination of serum proteins by means of the Biuret reaction. *Journal of Biological Chemistry*. **177**(2), pp.751-766.
- Gu, F.L., Kim, J.M., Abbas, S., Zhang, X.M., Xia, S.Q. and Chen, Z.X. 2010. Structure and antioxidant activity of high molecular weight Maillard reaction products from casein-glucose. *Food Chemistry*. **120**(2), pp.505-511.
- Halling, P.J. 1981. Protein-stabilized foams and emulsions. *Crc Critical Reviews in Food Science and Nutrition*. **15**(2), pp.155-203.
- Haseidl, F., Schuh, P. and Hinrichsen, K.O. 2015. Further Development and Characterization of a Rotor-Stator Spinning Disc Reactor. *Chemie Ingenieur Technik*. **87**(6), pp.830-836.
- Hattori, M., Nagasawa, K., Ametani, A., Kaminogawa, S. and Takahashi, K. 1994. Functional-changes in beta-lactoglobulin by conjugation with carboxymethyl dextran. *Journal of Agricultural and Food Chemistry*. **42**(10), pp.2120-2125.
- Ho, Y.T., Ishizaki, S. and Tanaka, M. 2000. Improving emulsifying activity of epsilon-polylysine by conjugation with dextran through the Maillard reaction. *Food Chemistry*. **68**(4), pp.449-455.
- Huggins, M.L. 1941. Solutions of long chain compounds. *Journal of Chemical Physics*. **9**(5), pp.440-440.
- Hunter, R.J. 2001. Nature of colloidal dispersions. In: Hunter, R.J. ed. *Foundations of Colloid Science*. United States: Oxford University Press, pp.1-6.
- Inada, N., Hayashi, M., Yoshida, T. and Hattori, M. 2015. Functional improvements in beta-lactoglobulin by conjugating with soybean soluble polysaccharide. *Bioscience Biotechnology and Biochemistry*. **79**(1), pp.97-102.
- Jimenez-Castano, L., Villamiel, M. and Lopez-Fandino, R. 2007. Glycosylation of individual whey proteins by Maillard reaction using dextran of different molecular mass. *Food Hydrocolloids*. **21**(3), pp.433-443.
- Kasran, M., Cui, S.W. and Goff, H.D. 2013. Covalent attachment of fenugreek gum to soy whey protein isolate through natural Maillard reaction for improved emulsion stability. *Food Hydrocolloids*. **30**(2), pp.552-558.
- Kato, A. 1995. Effects of the length of polysaccharide chain on the functional-properties of Maillard-type protein-polysaccharide conjugates. *Abstracts of Papers of the American Chemical Society*. **209**(1), pp.2-10.
- Kato, A. 2002. Industrial applications of Maillard-type protein-polysaccharide conjugates. *Food Science and Technology Research*. **8**(3), pp.193-199.
- Kato, A. and Kobayashi, K. 1991. Excellent emulsifying properties of protein dextran conjugates. In: Elnokaly, M. and Cornell, D. ed. *Microemulsions and Emulsions in Foods*. [no place]: [no publisher], pp.213-229.
- Kato, A., Mifuru, R., Matsudomi, N. and Kobayashi, K. 1992. Functional casein-polysaccharide conjugates prepared by controlled dry heating. *Bioscience Biotechnology and Biochemistry*. **56**(4), pp.567-571.

- Kato, A., Minaki, K. and Kobayashi, K. 1993. Improvement of emulsifying properties of egg-white proteins by the attachment of polysaccharide through Maillard reaction in a dry state. *Journal of Agricultural and Food Chemistry*. **41**(4), pp.540-543.
- Kato, A., Murata, K. and Kobayashi, K. 1988. Preparation and characterization of ovalbumin-dextran conjugate having excellent emulsifying properties. *Journal of Agricultural and Food Chemistry*. **36**(3), pp.421-425.
- Kato, A., Sasaki, Y., Furuta, R. and Kobayashi, K. 1990. Functional protein polysaccharide conjugate prepared by controlled dry-heating of ovalbumin dextran mixtures. *Agricultural and Biological Chemistry*. **54**(1), pp.107-112.
- Khan, W.H. and Rathod, V.K. 2014. Process intensification approach for preparation of curcumin nanoparticles via solvent-nonsolvent nanoprecipitation using spinning disc reactor. *Chemical Engineering and Processing*. **80**(1), pp.1-10.
- Kika, K., Korlos, F. and Kiosseoglou, V. 2007. Improvement, by dry-heating, of the emulsion-stabilizing properties of a whey protein concentrate obtained through carboxymethylcellulose complexation. *Food Chemistry*. **104**(3), pp.153-1159.
- Kim, D.Y. and Shin, W.S. 2016. Functional improvements in bovine serum albumin-fucoidan conjugate through the Maillard reaction. *Food Chemistry*. **190**(1), pp.974-981.
- Kittel, C. 1980a. States of a model system. In: Kittel, C. and Kroemer, H. ed. *Thermal Physics*. 2<sup>nd</sup> Edition. New York: W.H. Freeman and Company, pp.5-23.
- Kittel, C. 1980b. Entropy and temperature. In: Kittel, C. and Kroemer, H. ed. *Thermal Physics*. 2<sup>nd</sup> Edition. New York: W.H. Freeman and Company, pp.27-50.
- Kittel, C. 1980c. Gibbs free energy and chemical reactions. In: Kittel, C. and Kroemer, H. ed. *Thermal Physics*. 2<sup>nd</sup> Edition. New York: W.H. Freeman and Company, pp.261-270.
- Kleiner, J., Haseidl, F. and Hinrichsen, O. 2017. Rotor-Stator Spinning Disc Reactor: Characterization of the Single-Phase Stator-Side Heat Transfer. *Chemical Engineering & Technology*. **40**(11), pp.2123-2133.
- Laemmli, U.K. 1970. Cleavage of structural proteins during assembly of head of bacteriophage-T4. *Nature*. **227**(5259), pp.680-682.
- Lam, R.S.H. and Nickerson, M.T. 2013. Food proteins: A review on their emulsifying properties using a structure-function approach. *Food Chemistry*. **141**(2), pp.975-984.
- Laneuville, S.I., Paquin, P. and Turgeon, S.L. 2000. Effect of preparation conditions on the characteristics of whey protein—xanthan gum complexes. *Food Hydrocolloids*. **14**(4), pp.305-314.
- Li, C., Zhu, B., Xue, H.R., Chen, Z.Y., Ding, Q. and Wang, X.G. 2013. Physicochemical Properties of Dry-Heated Peanut Protein Isolate Conjugated with Dextran or Gum Arabic. *Journal of the American Oil Chemists Society*. **90**(12), pp.1801-1807.
- Li, J.L., Cheng, Y.Q., Wang, P., Zhao, W.T., Yin, L.J. and Saito, M. 2012. A novel improvement in whey protein isolate emulsion stability: Generation of an enzymatically cross-linked beet pectin layer using horseradish peroxidase. *Food Hydrocolloids*. **26**(2), pp.448-455.

- Li, W.W., Zhao, H.B., He, Z.Y., Zeng, M.M., Qin, F. and Chen, J. 2016. Modification of soy protein hydrolysates by Maillard reaction: Effects of carbohydrate chain length on structural and interfacial properties. *Colloids and Surfaces B-Biointerfaces*. **138**(1), pp.70-77.
- Li, Y., Zhong, F., Ji, W., Yokoyama, W., Shoemaker, C.F., Zhu, S. and Xia, W.S. 2013. Functional properties of Maillard reaction products of rice protein hydrolysates with mono-, oligo- and polysaccharides. *Food Hydrocolloids*. **30**(1), pp.53-60.
- Li, Z., Luo, Y.K. and Feng, L.G. 2011. Effects of Maillard reaction conditions on the antigenicity of alpha-lactalbumin and beta-lactoglobulin in whey protein conjugated with maltose. *European Food Research and Technology*. **233**(3), pp.387-394.
- Liu, F.G., Sun, C.X., Wang, D., Yuan, F. and Gao, Y.X. 2015. Glycosylation improves the functional characteristics of chlorogenic acid-lactoferrin conjugate. *Rsc Advances*. **5**(95), pp.78215-78228.
- Liu, F.G., Ma, C.C., Gao, Y.X. and McClements, D.J. 2017. Food-Grade Covalent Complexes and Their Application as Nutraceutical Delivery Systems: A Review. *Comprehensive Reviews in Food Science and Food Safety*. **16**(1), pp.76-95.
- Liu, J.H., Ru, Q.M. and Ding, Y.T. 2012. Glycation a promising method for food protein modification: Physicochemical properties and structure, a review. *Food Research International*. **49**(1), pp.170-183.
- Luo, Y.Q., Ling, Y.Z., Wang, X.Y., Han, Y., Zeng, X.J. and Sun, R.C. 2013. Maillard reaction products from chitosan-xylan ionic liquid solution. *Carbohydrate Polymers*. **98**(1), pp.835-841.
- Maillard, L.C. 1912. The action of amino acids on sugar: the formation of melanoidin by a methodic route. *Comptes Rendus Hebdomadaires Des Seances De L Academie Des Sciences*. **154**(1), pp.66-68.
- Maitena, U., Katayama, S., Sato, R. and Saeki, H. 2004. Improved solubility and stability of carp myosin by conjugation with alginate oligosaccharide. *Fisheries Science*. **70**(5), pp.896-902.
- Markman, G. and Livney, Y.D. 2012. Maillard-conjugate based core-shell co-assemblies for nanoencapsulation of hydrophobic nutraceuticals in clear beverages. *Food & Function*. **3**(3), pp.262-270.
- Matsudomi, N., Nakano, K., Soma, A. and Ochi, A. 2002. Improvement of gel properties of dried egg white by modification with galactomannan through the Maillard reaction. *Journal of Agricultural and Food Chemistry*. **50**(14), pp.4113-4118.
- Medrano, A., Abirached, C., Panizzolo, L., Moyna, P. and Anon, M.C. 2009. The effect of glycation on foam and structural properties of beta-lactoglobulin. *Food Chemistry*. **113**(1), pp.127-133.
- Mu, L.X., Zhao, H.F., Zhao, M.M., Cui, C. and Liu, L.Y. 2011. Physicochemical Properties of Soy Protein Isolates-Acacia Gum Conjugates. *Czech Journal of Food Sciences*. **29**(2), pp.129-136.
- Mulcahy, E.M., Mulvihill, D.M. and O'Mahony, J.A. 2016. Physicochemical properties of whey protein conjugated with starch hydrolysis products of different dextrose equivalent values. *International Dairy Journal*. **53**(1), pp.20-28.
- Nagasawa, K., Takahashi, K. and Hattori, M. 1996. Improved emulsifying properties of beta-lactoglobulin by conjugating with carboxymethyl dextran. *Food Hydrocolloids*. **10**(1), pp.63-67.

- Nakamura, S., Kato, A. and Kobayashi, K. 1991. New antimicrobial characteristics of lysozyme dextran conjugate. *Journal of Agricultural and Food Chemistry*. **39**(4), pp.647-650.
- Nakamura, S., Kobayashi, K. and Kato, A. 1994. Role of positive charge of lysozyme in the excellent emulsifying properties of Maillard-type lysozyme polysaccharide conjugate. *Journal of Agricultural and Food Chemistry*. **42**(12), pp.2688-2691.
- Nielsen, P.M., Petersen, D. and Dambmann, C. 2001. Improved method for determining food protein degree of hydrolysis. *Journal of Food Science*. **66**(5), pp.642-646.
- Niu, L.Y., Jiang, S.T., Pan, L.J. and Zhai, Y.S. 2011. Characteristics and functional properties of wheat germ protein glycosylated with saccharides through Maillard reaction. *International Journal of Food Science and Technology*. **46**(10), pp.2197-2203.
- O'Regan, J. and Mulvihill, D.M. 2009. Preparation, characterisation and selected functional properties of sodium caseinate-maltodextrin conjugates. *Food Chemistry*. **115**(4), pp.1257-1267.
- O'Regan, J. and Mulvihill, D.M. 2010. Sodium caseinate-maltodextrin conjugate stabilized double emulsions: Encapsulation and stability. *Food Research International*. **43**(1), pp.224-231.
- Oliver, C.M. 2011. Insight into the Glycation of Milk Proteins: An ESI- and MALDI-MS Perspective (Review). *Critical Reviews in Food Science and Nutrition*. **51**(5), pp.410-431.
- Oliver, C.M., Melton, L.D. and Stanley, R.A. 2006. Creating proteins with novel functionality via the Maillard reaction: A review. *Critical Reviews in Food Science and Nutrition*. **46**(4), pp.337-350.
- Parkinson, E.L., Ettelaie, R. and Dickinson, E. 2005. Using self-consistent-field theory to understand enhanced steric stabilization by casein-like copolymers at low surface coverage in mixed protein layers. *Biomacromolecules*. **6**(6), pp.3018-3029.
- Pirestani, S., Nasirpour, A., Keramat, J. and Desobry, S. 2017a. Preparation of chemically modified canola protein isolate with gum Arabic by means of Maillard reaction under wet-heating conditions. *Carbohydrate Polymers*. **155**(1), pp.201-207.
- Pirestani, S., Nasirpour, A., Keramat, J. and Desobry, S. 2017b. Effect of glycosylation with gum Arabic by Maillard reaction in a liquid system on the emulsifying properties of canola protein isolate. *Carbohydrate Polymers*. **157**(1), pp.1620-1627.
- Qi, J.R., Yang, X.Q. and Liao, J.S. 2009. Improvement of functional properties of acid-precipitated soy protein by the attachment of dextran through Maillard reaction. *International Journal of Food Science and Technology*. **44**(11), pp.2296-2302.
- Qiu, C.Y., Zhao, M.M. and McClements, D.J. 2015. Improving the stability of wheat protein-stabilized emulsions: Effect of pectin and xanthan gum addition. *Food Hydrocolloids*. **43**(0), pp.377-387.
- Saeki, H. 1997. Preparation of neoglycoprotein from carp myofibrillar protein by Maillard reaction with glucose: Biochemical properties and emulsifying properties. *Journal of Agricultural and Food Chemistry*. **45**(3), pp.680-684.
- Sato, R., Katayama, S., Sawabe, T. and Saeki, H. 2003. Stability and emulsion-forming ability of water-soluble fish myofibrillar protein

- prepared by conjugation with alginate oligosaccharide. *Journal of Agricultural and Food Chemistry*. **51**(15), pp.4376-4381.
- Scheutjens, J. and Fleer, G.J. 1979. Statistical-theory of the adsorption of interacting chain molecules. 1. Partition-function, segment density distribution, and adsorption-isotherms. *Journal of Physical Chemistry*, **83**(12), pp.1619-1635.
- Scheutjens, J. and Fleer, G.J. 1980. Statistical-theory of the adsorption of interacting chain molecules. 2. Train, loop, and tail size distribution. *Journal of Physical Chemistry*. **84**(2), pp.178-190.
- Shaw, D.J. 1991a. The colloidal state. In: Shaw, D.J. ed. *Introduction to Colloid and Surface Chemistry*. 4<sup>th</sup> Edition. Oxford: Butterworth-Heinemann Ltd., pp.1-10.
- Shaw, D.J. 1991b. Liquid-gas and liquid-liquid interfaces. In: Shaw, D.J. ed. *Introduction to Colloid and Surface Chemistry*. 4<sup>th</sup> Edition. Oxford: Butterworth-Heinemann Ltd., pp.64-84.
- Shu, Y.W., Sahara, S., Nakamura, S. and Kato, A. 1996. Effects of the length of polysaccharide chains on the functional properties of the Maillard-type lysozyme-polysaccharide conjugate. *Journal of Agricultural and Food Chemistry*. **44**(9), pp.2544-2548.
- Spotti, M.J., Perduca, M.J., Piagentini, A., Santiago, L.G., Rubiolo, A.C. and Carrara, C.R. 2013. Gel mechanical properties of milk whey protein-dextran conjugates obtained by Maillard reaction. *Food Hydrocolloids*. **31**(1), pp.26-32.
- Sun, W.W., Yu, S.J., Yang, X.Q., Wang, J.M., Zhang, J.B., Zhang, Y. and Zheng, E.L. 2011. Study on the rheological properties of heat-induced whey protein isolate-dextran conjugate gel. *Food Research International*. **44**(10), pp.3259-3263.
- Tabatabaee Amid, B. and Mirhosseini, H. 2014. Stabilization of water in oil in water (W/O/W) emulsion using whey protein isolate-conjugated durian seed gum: enhancement of interfacial activity through conjugation process. *Colloids and surfaces. B, Biointerfaces*. **113**(1), pp.107-14.
- Tanaka, M., Kunisaki, N. and Ishizaki, S. 1999. Improvement of emulsifying and antibacterial properties of salmine by the Maillard reaction with dextran. *Fisheries Science*. **65**(4), pp.623-628.
- Tian, S.J., Chen, J. and Small, D.M. 2011. Enhancement of solubility and emulsifying properties of soy protein isolates by glucose conjugation. *Journal of Food Processing and Preservation*. **35**(1), pp.80-95.
- Usui, M., Tamura, H., Nakamura, K., Ogawa, T., Muroshita, M., Azakami, H., Kanuma, S. and Kato, A. 2004. Enhanced bactericidal action and masking of allergen structure of soy protein by attachment of chitosan through Maillard-type protein-polysaccharide conjugation. *Nahrung-Food*. **48**(1), pp.69-72.
- van Eeten, K.M.P., Verzicco, R., van der Schaaf, J., van Heijst, G.J.F. and Schouten, J.C. 2015. A numerical study on gas-liquid mass transfer in the rotor-stator spinning disc reactor. *Chemical Engineering Science*. **129**(1), pp.14-24.
- Walker, N.J. 1972. Flavor defects in edible casein and skim-milk powder. 1. Role of Maillard browning. *Journal of Dairy Research*. **39**(2), pp.231-238.
- Wang, Z.J., Han, F.F., Sui, X.N., Qi, B.K., Yang, Y., Zhang, H., Wang, R., Li, Y. and Jiang, L.Z. 2016. Effect of ultrasound treatment on the wet

- heating Maillard reaction between mung bean *Vigna radiata* (L.) protein isolates and glucose and on structural and physico-chemical properties of conjugates. *Journal of the Science of Food and Agriculture*. **96**(5), pp.1532-1540.
- Wefers, D., Bindereif, B., Karbstein, H.P. and van der Schaaf, U.S. 2018. Whey protein-pectin conjugates: Linking the improved emulsifying properties to molecular and physico-chemical characteristics. *Food Hydrocolloids*. **85**(1), pp.257-266.
- Wong, B.T., Day, L., McNaughton, D. and Augustin, M.A. 2009. The Effect of Maillard Conjugation of Deamidated Wheat Proteins with Low Molecular Weight Carbohydrates on the Secondary Structure of the Protein. *Food Biophysics*. **4**(1), pp.1-12.
- Wooster, T.J. and Augustin, M.A. 2006. beta-Lactoglobulin-dextran Maillard conjugates: Their effect on interfacial thickness and emulsion stability. *Journal of Colloid and Interface Science*. **303**(2), pp.564-572.
- Xu, D.X., Wang, X.Y., Jiang, J.P., Yuan, F. and Gao, Y.X. 2012. Impact of whey protein - Beet pectin conjugation on the physicochemical stability of beta-carotene emulsions. *Food Hydrocolloids*. **28**(2), pp.258-266.
- Yang, S.Y., Lee, S., Pyo, M.C., Jeon, H., Kim, Y. and Lee, K.W. 2017. Improved physicochemical properties and hepatic protection of Maillard reaction products derived from fish protein hydrolysates and ribose. *Food Chemistry*. **221**(1), pp.1979-1988.
- Yang, Y.X., Cui, S.W., Gong, J.H., Guo, Q., Wang, Q. and Hua, Y.F. 2015. A soy protein-polysaccharides Maillard reaction product enhanced the physical stability of oil-in-water emulsions containing citral. *Food Hydrocolloids*. **48**(1), pp.155-164.
- Zhai, J.L., Day, L., Aguilar, M.I. and Wooster, T.J. 2013. Protein folding at emulsion oil/water interfaces. *Current Opinion in Colloid & Interface Science*. **18**(4), pp.257-271.
- Zhang, B., Chi, Y.J. and Li, B. 2014. Effect of ultrasound treatment on the wet heating Maillard reaction between beta-conglycinin and maltodextrin and on the emulsifying properties of conjugates. *European Food Research and Technology*. **238**(1), pp.129-138.
- Zhang, B., Guo, X.N., Zhu, K.X., Peng, W. and Zhou, H.M. 2015a. Improvement of emulsifying properties of oat protein isolate-dextran conjugates by glycation. *Carbohydrate Polymers*. **127**(1), pp.168-175.
- Zhang, X., Qi, J.R., Li, K.K., Yin, S.W., Wang, J.M., Zhu, J.H. and Yang, X.Q. 2012. Characterization of soy beta-conglycinin-dextran conjugate prepared by Maillard reaction in crowded liquid system. *Food Research International*. **49**(2), pp.648-654.
- Zhang, Y.T., Tan, C., Abbas, S., Eric, K., Xia, S.Q., and Zhang, X.M. 2015b. Modified SPI improves the emulsion properties and oxidative stability of fish oil microcapsules. *Food Hydrocolloids*. **51**(1), pp.108-117.
- Zhang, Z.Y., Wang, X.B., Yu, J., Chen, S., Ge, H.R. and Jiang, L.Z. 2017. Freeze-thaw stability of oil-in-water emulsions stabilized by soy protein isolate-dextran conjugates. *Lwt-Food Science and Technology*. **78**(1), pp.241-249.
- Zhu, D., Damodaran, S. and Lucey, J.A. 2008. Formation of whey protein isolate (WPI)-dextran conjugates in aqueous solutions. *Journal of Agricultural and Food Chemistry*. **56**(16), pp.7113-7118.

Zhu, D., Damodaran, S. and Lucey, J.A. 2010. Physicochemical and emulsifying properties of Whey Protein Isolate (WPI)-Dextran conjugates produced in aqueous solution. *Journal of Agricultural and Food Chemistry*. **58**(5), pp.2988-2994.

## List of Abbreviations

Abs: absorbance

DC: degree of conjugation

DE: dextrose equivalent

DH: drying heating

DX: dextran

EP: emulsifying property

GM: galactomannan

MALDI: matrix-assisted laser desorption

MD: maltodextrin

Mins: minutes

O/W: oil in water

OPA: o-phthaldialdehyde

pI: isoelectric point

pK<sub>a</sub>: acid dissociation constant

RH: relative humidity

SDR: spinning disc reactor

SDS-PAGE: sodium dodecyl sulphate polyacrylamide gel electrophoresis

SPI: soy protein isolate

TNBS: trinitrobenzenesulfonic acid

TS: thermal stability

WKS: weeks

W/O: water in oil

WPI: whey protein isolate

WPI-MD19: whey protein isolate and maltodextrin (DE19) conjugate

WPI/MD19 mixture: whey protein isolate and maltodextrin (DE19) without Maillard reactions

## Appendix A

### Previous Studies on Protein-polysaccharide Conjugates

Proteins	Poly-saccharides	Reacting conditions	Characterization techniques	Main findings	References
Lysozyme	dextran(DX)	Dry heating (DH). 1:5(w/w); pH7, lyophilized. Incubation 60°C, 79%RH, 3wks	Determination of free amino group (TNBS method)	Increased emulsifying properties (EP) and antimicrobial properties compared to pure protein	(Nakamura et al., 1991)
	galactomannan (GM)	DH; 1:4(molar); lyophilized; incubation 60°C, 79%RH, 2wks	TNBS & SDS-PAGE	EP increase proportionately to the size of polysaccharide ; thermal stability (TS) increase regardless of saccharide molar mass.	(Shu et al., 1996)
	xyloglucan				
Casein	DX	Dry heating (DH). 1:3(w/w); lyophilized. Incubation 60°C, 79%RH, 24h	TNBS & SDS-PAGE	Increased EP compared to pure protein	(Kato et al., 1992)
	GM				
	glucose	Heating in solution. 1:2mass. pH12.the solution was heated to 100°C for 130min	size-exclusion chromatography. SDS-PAGE, reversed-phase chromatography and infrared	Increased antioxidant capacity	(Gu et al., 2010)
	maltodextrin	DH; freeze-dried solutions of caseinate and maltodextrin at different molar ratios. 60°C, 79%RH, for 4, 6 and 8 hours	OPA, SDS-PAGE	Used in nano-encapsulation of hydrophobic nutraceuticals to enrich clear beverages	(Markman and Livney, 2012)
Soy protein	chitosan	Dry heating (DH). 1:1(w/w); lyophilized. Incubation 60°C, 65%RH, 14days	SDS-PAGE	Increased EP and antimicrobial property compared to pure protein; allergens were reduced	(Usui et al., 2004)

		Dry heating (DH). 1:1(w/w); lyophilized. Incubation 60°C, 79%RH, 1day to 7days	fluorescence absorbance at 470nm & SDS-PAGE	Increased TS and EP	(Qi et al., 2009)
Whey	DX	Dry heating (DH). 1:2 & 1:6(w/w); lyophilized. Incubation 60°C, a <sub>w</sub> 0.44; and 55°C, a <sub>w</sub> 0.65; 14days	TNBS at 420nm	Increase EP and TS at acidic pH; increase solubility	(Jiménez-Castaño et al., 2007)
De-aminated wheat protein	glucose	DH; 2:1(molar); pH6.5; lyophilized; incubation 60°C, 75%RH, 24hrs	SDS-PAGE; amino acid composition analysis; Size-exclusion chromatography; ATR-FTIR; circular dichroism	The study evaluated the impact of glycosylation on protein secondary structure.	(Wong et al., 2009)
	maltodextrin				
β-Ig	lactose	DH; 1:10 & 1:100 (molar); pH7.0; lyophilized; incubation 50°C, 65%RH, 96hrs	MALDI-TOF mass spectrometry, fluorescence measurement, SDS-PAGE, colourimetry	Increase EP, Foaming properties were more stable in the protein glycosylated with lactose than the protein glycosylated with glucose.	(Medrano et al., 2009)
	glucose				
Egg white protein	pectin	DH; 1:1(mass); lyophilized; incubation 60°C, 79%RH, 6 to 18 hrs	SDS-PAGE, TNBS	Increase EP and decrease solubility	(Al-Hakkak and Al-Hakkak, 2010)
WPI	DX	Heating in solution. 10%WPI, 30%DX (w/w). pH6.5. The solution was heated to 60°C for 48hrs	SDS-PAGE, size exclusion chromatography multi-angle laser light scatter. Protein analysis by BCA method.	Increase EP, solubility, and TS	(Zhu et al., 2010)
	maltose	DH. Various proportions; lyophilised; incubation at various temperatures and times at 79%RH	SDS-PAGE, TNBS, absorbance at 420nm	Diminished antigenicity of α-lactalbumin and β-LG	(Li et al., 2011)

	DX (15-25kDa)	DH; Mixed solutions of WPI (12% w/w) and DX (3.6 to 10.8% w/w), pH 7.0; lyophilised. Incubation 60°C, 63%RH, for 2,5,9 days	colour measurement, OPA	Preventing fracture, significantly modified mechanical properties of conjugates gels	(Sun et al., 2011)
Soy protein isolate	acacia gum	heating in solution. 1:1mass. 80°C for 48hrs	SDS-PAGE, free amino acid group determination by OPA test	Increase solubility and EP	(Mu et al., 2011)
Wheat germ protein	xylose	heating in solution. 1:1mass.pH11 ; 90°C for 90hrs	absorbance measurement at 420nm, TNBS, fluorescence measurement, scanning electron microscopy, circular dichroism and amino acid analysis	Increase EP, carbohydrate size is important for conjugate functional properties	(Niu et al., 2011)
	glucose				
	galactose				
Protein isolated from porcine blood	DX	DH; 1:3(mass); lyophilized; incubation at 70,75,80°C	SDS-PAGE, TNBS	Decrease solubility, increase TS, EP, and gelling ability	(Álvarez et al., 2012)
Soy whey protein	fenugreek gum	DH; various mass ratios, lyophilised. Incubation 60°C, 79%RH, for 3days	SDS-PAGE, high performance size exclusion chromatography	Increase EP	(Kasran et al., 2013)